

Resistance to Targeted Anti-Cancer Therapeutics 18

*Series Editor:* Benjamin Bonavida

Makoto Hosono · Jean-François Chatal  
*Editors*

# Resistance to Ibritumomab in Lymphoma

 Springer

# **Resistance to Targeted Anti-Cancer Therapeutics**

Volume 18

**Series Editor:**

Benjamin Bonavida

More information about this series at <http://www.springer.com/series/11727>

Makoto Hosono • Jean-François Chatal  
Editors

# Resistance to Ibritumomab in Lymphoma

 Springer

*Editors*

Makoto Hosono  
Institute of Advanced Clinical Medicine  
Kindai University Faculty of Medicine  
Osaka, Japan

Jean-François Chatal  
GIP Arronax  
Nantes-Saint-Herblain, France

ISSN 2196-5501

ISSN 2196-551X (electronic)

Resistance to Targeted Anti-Cancer Therapeutics

ISBN 978-3-319-78237-9

ISBN 978-3-319-78238-6 (eBook)

<https://doi.org/10.1007/978-3-319-78238-6>

Library of Congress Control Number: 2018937356

© Springer International Publishing AG, part of Springer Nature 2018

This work is subject to copyright. All rights are reserved by the Publisher, whether the whole or part of the material is concerned, specifically the rights of translation, reprinting, reuse of illustrations, recitation, broadcasting, reproduction on microfilms or in any other physical way, and transmission or information storage and retrieval, electronic adaptation, computer software, or by similar or dissimilar methodology now known or hereafter developed.

The use of general descriptive names, registered names, trademarks, service marks, etc. in this publication does not imply, even in the absence of a specific statement, that such names are exempt from the relevant protective laws and regulations and therefore free for general use.

The publisher, the authors and the editors are safe to assume that the advice and information in this book are believed to be true and accurate at the date of publication. Neither the publisher nor the authors or the editors give a warranty, express or implied, with respect to the material contained herein or for any errors or omissions that may have been made. The publisher remains neutral with regard to jurisdictional claims in published maps and institutional affiliations.

Printed on acid-free paper

This Springer imprint is published by the registered company Springer International Publishing AG part of Springer Nature.

The registered company address is: Gewerbestrasse 11, 6330 Cham, Switzerland

# “Resistance to Targeted Anti-Cancer Therapeutics”: Aims and Scope

Published by Springer Inc.

For several decades, treatment of cancer consisted of chemotherapeutic drugs, radiation, and hormonal therapies. These treatment regimens were not tumor specific and exhibited several toxicities. During the last several years, targeted cancer therapies (molecularly targeted drugs) have been developed and consisting of immunotherapies (cell mediated and antibody), drugs, or biologicals that can block the growth and spread of cancer by interfering with surface receptors and with specific dysregulated gene products that control tumor cell growth and progression. These include several FDA-approved drugs/antibodies/inhibitors that interfere with cell growth signaling or tumor blood vessel development, promote the cell death of cancer cells, stimulate the immune system to destroy specific cancer cells, and deliver toxic drugs to cancer cells. Targeted cancer therapies are being used alone or in combination with conventional drugs and other targeted therapies.

One of the major problems that arise following treatment with both conventional therapies and targeted cancer therapies is the development of resistance, preexisting in a subset of cancer cells or cancer stem cells and/or induced by the treatments. Tumor cell resistance to targeted therapies remains a major hurdle, and, therefore, several strategies are being considered in delineating the underlining molecular mechanisms of resistance and the development of novel drugs to reverse both the innate and acquired resistance to various targeted therapeutic regimens.

The new series *Resistance to Targeted Anti-Cancer Therapeutics* was inaugurated and focuses on the clinical application of targeted cancer therapies (either approved by the FDA or in clinical trials) and the resistance observed by these therapies. Each book will consist of updated reviews on a specific target therapeutic and strategies to overcome resistance at the biochemical, molecular, and both genetic and epigenetic levels. This new series is timely and should be of significant interest to clinicians, scientists, trainees, students, and pharmaceutical companies.

Benjamin Bonavida  
David Geffen School of Medicine at UCLA  
University of California, Los Angeles  
Los Angeles, CA, USA

## Biography of Series Editor



Dr. Benjamin Bonavida, Ph.D. (Series Editor) is currently Distinguished Research Professor at the University of California, Los Angeles (UCLA). His research career, thus far, has focused on basic immunochemistry and cancer immunobiology. His research investigations have ranged from the mechanisms of cell-mediated killing, sensitization of resistant tumor cells to chemo-/immunotherapy, characterization of resistant factors in cancer cells, cell-signaling pathways mediated by therapeutic anticancer antibodies, and characterization of a dysregulated NF- $\kappa$ B/Snail/YY1/RKIP/PTEN loop in many cancers that regulate cell survival, proliferation, invasion, metastasis, and resistance. He has also investigated the role of nitric oxide in cancer and its potential antitumor activity. Many of the above studies are centered on the clinical challenging features of cancer patients' failure to respond to both conventional and targeted therapies. The development and activity of various targeting agents, their modes of action, and resistance are highlighted in many refereed publications.

### Acknowledgments

The Series Editor acknowledges the various assistants who have diligently worked in both the editing and formatting of the various manuscripts in each volume, especially Leah Moyal and Kevin Li.

# Preface

Ibritumomab labeled with yttrium-90 is a CD20-directed antibody agent for radionuclide therapy (RNT), recently also designated as molecular radiotherapy (MRT), of patients with relapsed or refractory, low-grade, or follicular B-cell non-Hodgkin's lymphoma (NHL). This pharmaceutical has unique features as it came up as the first radioimmunotherapy (RIT) agent to be approved by healthcare authorities and is now the only RIT agent that has commercial availability. Ibritumomab provides an overall response rate of about 80% in relapsed or refractory, low-grade, or follicular B-cell NHL. Long-term follow-up proved that ibritumomab was safe and effective, and early use could deliver good, sustained effects with low toxicity for long periods and adequate quality of life. It has also an established role as a consolidation therapy agent after first-line chemotherapy. Some factors associated with better or poor outcomes were reported. Treatment with ibritumomab at earlier stages may lead to better outcome and bulky disease, and extended stages were negative predictors of long-term response.

Yet resistance to ibritumomab may compromise therapeutic efficacy and affect outcomes of patients, and such resistance may deeply be related with the characteristics of patients and the biological behaviors of tumors. To discuss resistance to ibritumomab, this volume focuses on the mechanism, hematological aspects, radiological and nuclear medicine aspects, and medical physics that deals with radiation dosimetry, and proposes future prospects for overcoming resistance and enhancing the efficacy of ibritumomab.

Among them, new technologies such as pretargeting methods and the use of  $\alpha$ -emitting nuclides seem promising in breaking through resistance. One of the pretargeting methods consists of a primary injection of an unlabeled bispecific monoclonal antibody, followed by a second injection of a radiolabeled bivalent hapten-peptide. Using this strategy, higher radioactivity can be delivered to the targets while reducing radioactivity in normal tissues. Lately, studies on RNT or MRT have been focused on  $\alpha$ -emitting nuclides. Due to their high linear energy transfer,  $\alpha$ -particles deliver a high fraction of their energy inside the targeted cells leading to highly efficient killing, making them particularly suited for targeting of isolated tumor cells and minimal residual disease.

Theranostic approaches, that is, the combination of therapeutics and diagnostics, are also a key issue in enhancing the efficacy of RIT. Imaging of radiolabeled antibodies, positron emission tomography (PET), single photon emission computed tomography (SPECT), and hybrid imaging PET/CT, PET/MR, and SPECT/CT are indispensable in order to improve therapeutic procedures through the precise assessment of tumors and through dosimetry-guided individualized RIT.

Combinations of all possible new developments, including new antibody specificities, pretargeting methods, and the use of  $\alpha$ -emitters, will improve their efficacy in tumors resistant to them and will change the whole game in RIT.

Osaka, Japan  
Nantes-Saint-Herblain, France

Makoto Hosono  
Jean-François Chatal



# Acknowledgments

I am grateful to my wife Masako Hosono for her constant support to my work in this volume. Also, I am grateful to Professor Jean-François Chatal for his extensive support to me in this volume as well as in academic activities for decades. Together with Professor Jean-Francois Chatal, I wish to thank Dhayanidhi Karunanidhi, Sheik Kaja Mohideen, Christina Jebamalar Oliver, and Benjamin Bonavida for their friendly help and encouragement in this volume.

Makoto Hosono

I am grateful to Professor Makoto Hosono for his kind invitation to contribute to this textbook as a coeditor. A long time ago, I spent some time with his wife Masako in my research group in Nantes, France, and I am very proud to collaborate with him 25 years later as a Professor in Kindai University.

I am also grateful to my previous research group in Nantes for their excellent contribution to this textbook particularly in reporting on their experience on the future Association of Immunotherapy with Radioimmunotherapy for an improved clinical efficacy.

Jean-François Chatal

# Contents

<b>Clinical Use and Efficacy of Ibritumomab in B Cell Lymphoma . . . . .</b>	<b>1</b>
Ilseung Choi and Naokuni Uike	
<b>Biology and Pathology of B-Cell Lymphoma . . . . .</b>	<b>9</b>
Yoichi Tatsumi	
<b>Resistance to Y-90 Ibritumomab Tiuxetan Therapy . . . . .</b>	<b>33</b>
Koichiro Abe	
<b>Features of Ibritumomab as Radionuclide Therapy . . . . .</b>	<b>59</b>
Makoto Hosono	
<b>Radiological Evaluation of Response and Resistance of Ibritumomab . . .</b>	<b>67</b>
Takayoshi Ishimori and Koya Nakatani	
<b>Characteristics of Ibritumomab as Radionuclide Therapy Agent . . . . .</b>	<b>79</b>
Hidekazu Kawashima	
<b>Resistance and Heterogeneity of Intratumoral Antibody Distribution . . .</b>	<b>99</b>
Kohei Hanaoka and Makoto Hosono	
<b>Radiation Dosimetry in Ibritumomab Therapy . . . . .</b>	<b>105</b>
Gerhard Glatting	
<b>Combining RAIT and Immune-Based Therapies to Overcome Resistance in Cancer? . . . . .</b>	<b>119</b>
Jean-Baptiste Gorin, Jérémie Ménager, Yannick Guilloux, Jean-François Chatal, Joëlle Gaschet, and Michel Chérel	
<b>Prospects for Enhancing Efficacy of Radioimmunotherapy . . . . .</b>	<b>139</b>
Clément Bailly, Caroline Bodet-Milin, François Guérard, Caroline Rousseau, Michel Chérel, Françoise Kraeber-Bodéré, and Jean-François Chatal	
<b>Index . . . . .</b>	<b>155</b>

# Clinical Use and Efficacy of Ibritumomab in B Cell Lymphoma



Ilseung Choi and Naokuni Uike

**Abstract** Ibritumomab tiuxetan labeled with yttrium-90 ( $^{90}\text{Y}$ ) is one of the excellent therapeutic options for patients with low-grade B cell non-Hodgkin lymphoma (NHL) who have relapsed disease after first-line chemotherapy regimens and are reluctant to the precedent therapy. The overall response rate (ORR) of 80–90% and the complete response rate (CR) of 30–69% have been reported for patients with relapsed or refractory low-grade B cell NHL. It has also an established role as a consolidation therapy agent after first-line chemotherapy. Ibritumomab tiuxetan has also proved to be an efficient and feasible treatment option as first-line therapy. The short-term toxicity associated with ibritumomab tiuxetan is mainly reversible bone marrow suppression. For diffuse large B cell lymphoma, which is the most frequent NHL subtype, ibritumomab tiuxetan has been also introduced as conditioning therapy added to conventional conditioning regimens before stem cell transplantation.

**Keywords** Low-grade B cell non-Hodgkin lymphoma · CD20 · Ibritumomab tiuxetan · Yttrium-90 · Crossfire effect · Bystander effect · Frontline therapy · Consolidation therapy · Conditioning therapy

## Abbreviations

G-CSF	Granulocyte colony-stimulating factor
R-CHOP	Rituximab, cyclophosphamide, doxorubicin hydrochloride, vincristine (oncovin), prednisolone
R-CVP	Cyclophosphamide, vincristine, prednisolone

---

I. Choi (✉)

Department of Hematology, National Kyushu Cancer Center, Fukuoka, Japan

Department of Hematology, National Hospital Organization Kyushu Cancer Center, Fukuoka, Japan

e-mail: [ilchoi@nk-cc.go.jp](mailto:ilchoi@nk-cc.go.jp)

N. Uike

Palliative Care Unit, Saga-ken Medical Centre Koseikan, Saga, Japan

## 1 Introduction

Although chemotherapy results in high remission rates for most patients with low-grade B cell non-Hodgkin lymphoma (NHL) [1], recurrences are frequently recognized even in the era of the therapeutic monoclonal antibody, rituximab [2]. Patients who repeat recurrence have several therapeutic options such as the purine analog fludarabine or cladribine, bendamustine, local radiation, and stem cell transplantation, but the optimal treatment that should be applied at each relapse has not been established. Furthermore, most of relapsed patients who have experienced combination chemotherapy such as R-CHOP [3] or R-CVP [4] are reluctant to undergo repeat therapy with the same types of agents because of adverse effects such as cardiac limitation, vomiting, alopecia, and peripheral neuropathy.

Zevalin is one of an excellent alternative salvage therapy for such patients [5–8], because the a major toxicity is transient myelosuppression essentially without severe nonhematological toxicity [6].

## 2 Characteristics of Zevalin

Ibritumomab is an antihuman CD20 murine IgG1 kappa monoclonal antibody, and Zevalin (IDEC-Y2B8) is a conjugate of ibritumomab labeled with radioisotope, yttrium-90 ( $^{90}\text{Y}$ ) or indium-111 ( $^{111}\text{In}$ ) chelated by tiuxetan [9].  $^{90}\text{Y}$ -Zevalin is the first radioimmunoconjugate to be approved for the treatment of cancer [10]. The biological half-life elimination of  $^{90}\text{Y}$ -Zevalin is 30 h [11].  $^{90}\text{Y}$  delivers pure beta-emitting energy (2.3 MeV) with a half-life of 64 h [12] and has a path length of 5–10 mm, resulting in the improved ability to kill both targeted and neighboring cells (crossfire or bystander effect) [11]. Because of the stable link between the antibody and the radioisotope, clearance rates are minimal and predictable, with  $7.3\% \pm 3.2\%$  of the radiolabeled activity being excreted in the urine over 7 days [11]. Thus, patients can be treated as outpatients [13].  $^{111}\text{In}$ -Zevalin is used for imaging that detects altered distribution.

## 3 Treatment Schedule and Dosage of Zevalin

Radioimmunotherapy with Zevalin is completed within about 1 week and consists of a single dose of the therapeutic  $^{90}\text{Y}$ -Zevalin. Patients receive rituximab 250 mg/m<sup>2</sup> before administration of Zevalin, at a slightly lower than the commonly applied therapeutic dose to improve the biodistribution of the radionuclide and targeting of the tumor [13]. Rituximab pretreatment is administered to reduce the nonmalignant CD20 binding that occurs with circulating B cells and within the spleen [11]. Seven days before the administration of therapeutic  $^{90}\text{Y}$ -Zevalin,  $^{111}\text{In}$ -Zevalin is used for imaging that detects altered distribution. At 48–72 h after administration of  $^{111}\text{In}$ -Zevalin, the biodistribution is checked by gamma camera. If there is no altered distribution, such

as massive bone marrow involvement or abnormal up take of the small intestine, 7–9 days after first rituximab, patients can receive  $^{90}\text{Y}$ -Zevalin for 10 min push inter-venously within 4 h after the second administration of rituximab. Within the European Union, such imaging study is not required [14].  $^{90}\text{Y}$ -Zevalin dosage is recommended either at 14.8 MBq/kg (to a maximum of 1184 MBq/body) or at 11.1 MBq/kg according to the platelet counts of  $\geq 150,000/\mu\text{L}$  or 100–150,000/ $\mu\text{L}$ , respectively [11].

## 4 Patient Eligibility

For patients with increased development of hematological toxicities, the following criteria should be excluded from the treatment: (1) the presence of >25% infiltration of lymphoma cells within the bone marrow, (2) the prior history of external beam radiation therapy to >25% of the bone marrow, and (3) the baseline platelet count <100,000/ $\mu\text{L}$  or neutrophil count <1200/ $\mu\text{L}$ .

## 5 Zevalin in Relapse or Refractory Patients

High efficacy of Zevalin has been demonstrated in various clinical trials, mostly in the patients with relapse or refractory CD20 positive indolent B cell lymphomas [13, 15–18]. A randomized phase III trial including 143 patients with relapsed or refractory low-grade, follicular, or transformed NHL compared the efficacy of a single dose of Zevalin with rituximab once weekly for 4 weeks [16]. The response rates were significantly higher in the Zevalin arm, with an overall response rate (ORR) of 80% versus 56% and a complete response rate (CR) of 30% versus 16%. The overall time to progression was, however, not different in both treatment groups, but patients treated with Zevalin showed a trend toward a longer median duration of response.

According to our retrospective data analysis of 94 patients who were treated with Zevalin for relapse or refractory low-grade B cell NHL, in a single institution experience, the overall and complete response rates of all 94 treated patients were 90% and 69%, respectively. The median overall survival (OS) was not reached, and 2-year OS was 78.0%. The median and 2-year progression-free survival (PFS) were 26 months and 50.8%, respectively [19].

## 6 Zevalin in Frontline Therapy

Zevalin as consolidation after induction therapy could improve PFS. The randomized phase III trial [5, 20] proved a benefit for Zevalin as consolidation in previously untreated follicular lymphoma patients. After completing induction therapy of the investigator's choice, patients in CR or partial response (PR) were randomized to receive either a single dose of Zevalin or no further treatment.

After induction chemotherapy, the CR rate was similar in both arms. After Zevalin, almost three-quarters of the patients in PR converted to CR. This response improvement led to a significant PFS prolongation of more than 2 years in the Zevalin consolidation arm as compared to the control arm. Despite these promising results, their value for the current clinical routine is limited since almost all patients nowadays receive rituximab in first line, while in the trial approximately only 14% underwent rituximab containing chemotherapy. This was because, at the time, the study was designed when rituximab was not yet a standard agent for frontline therapy involved in the trial. The use of Zevalin as first-line consolidation might also allow for the reduction of the number of immunochemotherapy cycles [21–23].

Zevalin has also proved to be an efficient and feasible treatment option as first-line therapy [24]. Zevalin as first-line treatment has shown high ORR with minimal toxicities. The favorable efficacy of Zevalin was also confirmed in a fractionated administration of Zevalin (11.1 MBq/kg given 8–12 weeks apart) [25].

Zevalin has an important part in the frontline setting, either as single agent or a consolidation following standard chemoimmunotherapy [26].

## 7 Toxicities and Safety Profile

The short-term toxicity associated with Zevalin is mainly reversible bone marrow suppression. Serious infusion reactions, prolonged and severe cytopenias, and severe cutaneous and mucocutaneous reactions may require the discontinuation of Zevalin [27]. According to our retrospective data, the most common adverse event was also reversible hematological toxicity [19]. The nadir of platelet and neutrophil counts and hemoglobin levels appeared at about 5, 6, and 8 weeks after <sup>90</sup>Y-Zevalin, respectively. Around this time, 43 (46%), 10 (11%), and 39 (42%) patients of the 94 patients had received transfusions with platelets or red blood cells and had been administered with G-CSF, respectively. On the other hand, nonhematological toxicities were generally mild to moderate in severity. Nausea (grades 1–2) was the most frequent (17%; 16/94 patients) nonhematological toxicity. Concerning severe (grade  $\geq 3$ ) nonhematological toxicities, there were eight events (9%; 8/94 patients) as follows: two jaundice, one febrile neutropenias, one pneumonia, one phlegmon, one liver injury, one empyema, and one ileus. No other types of severe toxicity were evident including late infections such as herpes virus, cytomegalovirus, and pneumocystis [19].

Second primary malignancies after Zevalin were also discussed [5, 28, 29]. In our experience, at a median follow-up of 46.5 months, two patients (2.1%), one each of who had previously been treated with four and one regimens of R-CHOP (R-fludarabine, radiation therapy, rituximab), developed secondary malignancies comprising pancreatic cancer and chronic myelogenous leukemia at 3.5 and 10.5 months, respectively, after Zevalin. It might be considered of the possibilities of second primary malignancy after Zevalin.

## 8 Factor Associated with Effects of Zevalin

Some factors associated with better outcome after Zevalin were reported. The number of prior treatment regimens [8] and the response to Zevalin significantly affected PFS [19]. Bulky disease and extended stage at the time of Zevalin were negative predictors of long-term responders [30].

## 9 Future Aspects

Now Zevalin is widely used as consolidation therapy after chemoimmunotherapy, as frontline therapy [24] (even with fractionated RIT [25]) or salvage therapy [31] and as a part of conditioning regimens for stem cell transplantation [32, 33]. For diffuse large B cell lymphoma, which is the most frequent NHL subtype, Zevalin has been also introduced as consolidation chemotherapy for patients who are newly diagnosed with this disease [34] or as conditioning therapy added to conventional conditioning regimens before stem cell transplantation [35].

In conclusion, Zevalin is highly effective in the treatment of low-grade CD20 positive B cell NHL with acceptable toxicity. Further studies are warranted for optimal benefits of the patients.

**Conflict of Interest** No conflict statement: No potential conflicts of interest were disclosed.

## References

1. Witzig TE, Vukov AM, Habermann TM, Geyer S, Kurtin PJ, Friedenberg WR, White WL, Chalhchal HI, Flynn PJ, Fitch TR, Welker DA. Rituximab therapy for patients with newly diagnosed, advanced-stage, follicular grade I non-Hodgkin's lymphoma: a phase II trial in the North Central Cancer Treatment Group. *J Clin Oncol.* 2005;23:1103–8.
2. Colombat P, Salles G, Brousse N, Eftekhari P, Soubeyran P, Delwail V, Deconinck E, Haioun C, Foussard C, Sebban C, Stamatoullas A, Milpied N, Boué F, Taillan B, Lederlin P, Najman A, Thièblemont C, Montestruc F, Mathieu-Boué A, Benzohra A, Solal-Céligny P. Rituximab (anti-CD20 monoclonal antibody) as single first-line therapy for patients with follicular lymphoma with a low tumor burden: clinical and molecular evaluation. *Blood.* 2001;97:101–6.
3. Hiddemann W, Kneba M, Dreyling M, Schmitz N, Lengfelder E, Schmits R, Reiser M, Metzner B, Harder H, Hegewisch-Becker S, Fischer T, Kropff M, Reis HE, Freund M, Wörmann B, Fuchs R, Planker M, Schimke J, Eimermacher H, Trümper L, Aldaoud A, Parwaresch R, Unterhalt M. Frontline therapy with rituximab added to the combination of cyclophosphamide, doxorubicin, vincristine, and prednisone (CHOP) significantly improves the outcome for patients with advanced-stage follicular lymphoma compared with therapy with CHOP alone: results of a prospective randomized study of the German Low-Grade Lymphoma Study Group. *Blood.* 2005;106:3725–32.
4. Marcus R, Imrie K, Belch A, Cunningham D, Flores E, Catalano J, Solal-Celigny P, Offner F, Walewski J, Raposo J, Jack A, Smith P. CVP chemotherapy plus rituximab compared with CVP as first-line treatment for advanced follicular lymphoma. *Blood.* 2005;105:1417–23.

5. Morschhauser F, Radford J, Van Hoof A, Botto B, Rohatiner AZ, Salles G, Soubeyran P, Tilly H, Bischof-Delaloye A, van Putten WL, Kylstra JW, Hagenbeek A. 90Yttrium-ibritumomab tiuxetan consolidation of first remission in advanced-stage follicular non-Hodgkin lymphoma: updated results after a median follow-up of 7.3 years from the International, Randomized, Phase III First-Line Indolent trial. *J Clin Oncol.* 2013;31:1977–83.
6. Witzig TE. Efficacy and safety of 90Y ibritumomab tiuxetan (Zevalin) radioimmunotherapy for non-Hodgkin's lymphoma. *Semin Oncol.* 2003;30:11–6.
7. Watanabe T, Terui S, Itoh K, Terauchi T, Igarashi T, Usubuchi N, Nakata M, Nawano S, Sekiguchi N, Kusumoto S, Tanimoto K, Kobayashi Y, Endo K, Seriu T, Hayashi M, Tobinai K. Phase I study of radioimmunotherapy with an anti-CD20 murine radioimmun-conjugate ((90)Y-ibritumomab tiuxetan) in relapsed or refractory indolent B-cell lymphoma. *Cancer Sci.* 2005;96:903–10.
8. Tobinai K, Watanabe T, Ogura M, Morishima Y, Hotta T, Ishizawa K, Itoh K, Okamoto S, Taniwaki M, Tsukamoto N, Okumura H, Terauchi T, Nawano S, Matsusako M, Matsuno Y, Nakamura S, Mori S, Ohashi Y, Hayashi M, Endo K. Japanese phase II study of 90Y-ibritumomab tiuxetan in patients with relapsed or refractory indolent B-cell lymphoma. *Cancer Sci.* 2009;100:158–64.
9. Krasner C, Joyce RM. Zevalin: 90yttrium labeled anti-CD20 (ibritumomab tiuxetan), a new treatment for non-Hodgkin's lymphoma. *Curr Pharm Biotechnol.* 2001;2:341–9.
10. Ibritumomab tiuxetan (Zevalin) for non-Hodgkin's lymphoma. *Med Lett Drugs Ther.* 2002;44:101–102.
11. Weigert O, Illidge T, Hiddemann W, Dreyling M. Recommendations for the use of yttrium-90 ibritumomab tiuxetan in malignant lymphoma. *Cancer.* 2006;107:686–95.
12. Wagner HN Jr, Wiseman GA, Marcus CS, Nabi HA, Nagle CE, Fink-Bennett DM, Lamonica DM, Conti PS. Administration guidelines for radioimmunotherapy of non-Hodgkin's lymphoma with (90)Y-labeled anti-CD20 monoclonal antibody. *J Nucl Med.* 2002;43:267–72.
13. Witzig TE, White CA, Wiseman GA, Gordon LI, Emmanouilides C, Raubitschek A, Janakiraman N, Gutheil J, Schilder RJ, Spies S, Silverman DH, Parker E, Grillo-López AJ. Phase I/II trial of IDEC-Y2B8 radioimmunotherapy for treatment of relapsed or refractory CD20+ B-cell non-Hodgkin's lymphoma. *J Clin Oncol.* 1999;17:3793–803.
14. Wiseman GA, Kornmehl E, Leigh B, Erwin WD, Podoloff DA, Spies S, Sparks RB, Stabin MG, Witzig T, White CA. Radiation dosimetry results and safety correlations from 90Y-ibritumomab tiuxetan radioimmunotherapy for relapsed or refractory non-Hodgkin's lymphoma: combined data from 4 clinical trials. *J Nucl Med.* 2003;44:465–74.
15. Witzig TE, Flinn IW, Gordon LI, Emmanouilides C, Czuczman MS, Saleh MN, Cripe L, Wiseman G, Olejnik T, Multani PS, White CA. Treatment with ibritumomab tiuxetan radioimmunotherapy in patients with rituximab-refractory follicular non-Hodgkin's lymphoma. *J Clin Oncol.* 2002;20:3262–9.
16. Witzig TE, Gordon LI, Cabanillas F, Czuczman MS, Emmanouilides C, Joyce R, Pohlman BL, Bartlett NL, Wiseman GA, Padre N, Grillo-López AJ, Multani P, White CA. Randomized controlled trial of yttrium-90-labeled ibritumomab tiuxetan radioimmunotherapy versus rituximab immunotherapy for patients with relapsed or refractory low-grade, follicular, or transformed B-cell non-Hodgkin's lymphoma. *J Clin Oncol.* 2002;20:2453–63.
17. Wiseman GA, Gordon LI, Multani PS, Witzig TE, Spies S, Bartlett NL, Schilder RJ, Murray JL, Saleh M, Allen RS, Grillo-López AJ, White CA. Ibritumomab tiuxetan radioimmunotherapy for patients with relapsed or refractory non-Hodgkin lymphoma and mild thrombocytopenia: a phase II multicenter trial. *Blood.* 2002;99:4336–42.
18. Morschhauser F, Illidge T, Huglo D, Martinelli G, Paganelli G, Zinzani PL, Rule S, Liberati AM, Milpied N, Hess G, Stein H, Kalmus J, Marcus R. Efficacy and safety of yttrium-90 ibritumomab tiuxetan in patients with relapsed or refractory diffuse large B-cell lymphoma not appropriate for autologous stem-cell transplantation. *Blood.* 2007;110:54–8.



19. Uike N, Choi I, Tsuda M, Haji S, Toyoda K, Suehiro Y, Abe Y, Hayashi T, Sawamoto H, Kaneko K, Shimokawa M, Nakagawa M. Factors associated with effects of 90Y-ibritumomab tiuxetan in patients with relapsed or refractory low-grade B cell non-Hodgkin lymphoma: single-institution experience with 94 Japanese patients in rituximab era. *Int J Hematol.* 2014;100:386–92.
20. Morschhauser F, Radford J, Van Hoof A, Vitolo U, Soubeyran P, Tilly H, Huijgens PC, Kolstad A, d'Amore F, Gonzalez Diaz M, Petrini M, Sebban C, Zinzani PL, van Oers MH, van Putten W, Bischof-Delaloye A, Rohatiner A, Salles G, Kuhlmann J, Hagenbeek A. Phase III trial of consolidation therapy with yttrium-90-ibritumomab tiuxetan compared with no additional therapy after first remission in advanced follicular lymphoma. *J Clin Oncol.* 2008;26:5156–64.
21. Hainsworth JD, Spigel DR, Markus TM, Shipley D, Thompson D, Rotman R, Dannaher C, Greco FA. Rituximab plus short-duration chemotherapy followed by Yttrium-90 Ibritumomab tiuxetan as first-line treatment for patients with follicular non-Hodgkin lymphoma: a phase II trial of the Sarah Cannon Oncology Research Consortium. *Clin Lymphoma Myeloma.* 2009;9:223–8.
22. Jacobs SA, Swerdlow SH, Kant J, Foon KA, Jankowitz R, Land SR, DeMonaco N, Joyce J, Osborn JL, Evans TL, Schaefer PM, Luong TM. Phase II trial of short-course CHOP-R followed by 90Y-ibritumomab tiuxetan and extended rituximab in previously untreated follicular lymphoma. *Clin Cancer Res.* 2008;14:7088–94.
23. Zinzani PL, Tani M, Pulsoni A, et al. A phase II trial of short course fludarabine, mitoxantrone, rituximab followed by (9)(0)Y-ibritumomab tiuxetan in untreated intermediate/high-risk follicular lymphoma. *Ann Oncol.* 2012;23:415–20.
24. Scholz CW, Pinto A, Linkesch W, Lindén O, Viardot A, Keller U, Hess G, Lastoria S, Lerch K, Frigeri F, Arcamone M, Stroux A, Frericks B, Pott C, Pezzutto A. 90Yttrium-ibritumomab-tiuxetan as first-line treatment for follicular lymphoma: 30 months of follow-up data from an international multicenter phase II clinical trial. *J Clin Oncol.* 2013;31:308–13.
25. Illidge TM, Mayes S, Pettengell R, Bates AT, Bayne M, Radford JA, Ryder WD, Le Gouill S, Jardin F, Tipping J, Zivanovic M, Kraeber-Bodere F, Bardies M, Bodet-Milin C, Malek E, Huglo D, Morschhauser F. Fractionated 90Y-ibritumomab tiuxetan radioimmunotherapy as an initial therapy of follicular lymphoma: an international phase II study in patients requiring treatment according to GELF/BNLI criteria. *J Clin Oncol.* 2014;32:212–8.
26. Mondello P, Cuzzocrea S, Navarra M, Mian M. 90 Y-ibritumomab tiuxetan: a nearly forgotten opportunity. *Oncotarget.* 2016;7:7597–609.
27. Rizzieri D. Zevalin(R) (ibritumomab tiuxetan): after more than a decade of treatment experience, what have we learned? *Crit Rev Oncol Hematol.* 2016;105:5–17.
28. Witzig TE, White CA, Gordon LI, Wiseman GA, Emmanouilides C, Murray JL, Lister J, Multani PS. Safety of yttrium-90 ibritumomab tiuxetan radioimmunotherapy for relapsed low-grade, follicular, or transformed non-hodgkin's lymphoma. *J Clin Oncol.* 2003;21:1263–70.
29. Czuczman MS, Emmanouilides C, Darif M, Witzig TE, Gordon LI, Revell S, Vo K, Molina A. Treatment-related myelodysplastic syndrome and acute myelogenous leukemia in patients treated with ibritumomab tiuxetan radioimmunotherapy. *J Clin Oncol.* 2007;25:4285–92.
30. Witzig TE, Molina A, Gordon LI, Emmanouilides C, Schilder RJ, Flinn IW, Darif M, Macklis R, Vo K, Wiseman GA. Long-term responses in patients with recurring or refractory B-cell non-Hodgkin lymphoma treated with yttrium 90 ibritumomab tiuxetan. *Cancer.* 2007;109:1804–10.
31. Illidge TM, McKenzie HS, Mayes S, Bates A, Davies AJ, Pettengell R, Stanton L, Cozens K, Hampson G, Dive C, Zivanovic M, Tipping J, Gallop-Evans E, Radford JA, Johnson PW. Short duration immunochemotherapy followed by radioimmunotherapy consolidation is effective and well tolerated in relapsed follicular lymphoma: 5-year results from a UK National Cancer Research Institute Lymphoma Group study. *Br J Haematol.* 2016;173:274–82.

32. Decaudin D, Mounier N, Tilly H, Ribrag V, Ghesquière H, Bouabdallah K, Morschhauser F, Coiffier B, Le Gouill S, Bologna S, Delarue R, Huynh A, Bosly A, Brière J, Gisselbrecht C. (90)Y ibritumomab tiuxetan (Zevalin) combined with BEAM (Z -BEAM) conditioning regimen plus autologous stem cell transplantation in relapsed or refractory low-grade CD20-positive B-cell lymphoma. A GELA phase II prospective study. *Clin Lymphoma Myeloma Leuk*. 2011;11:212–8.
33. Philippe L, Helias P, Puyraveau M, Boulahdour H, Deconinck E, Daguindau E. Long-term follow-up of (90)Y-ibritumomab-tiuxetan ((90)YIT) in the conditioning of autologous hematopoietic transplantation for indolent and mantle cell lymphomas in a single French center. *Bone Marrow Transplant*. 2016;51:1140–2.
34. Yang DH, Kim WS, Kim SJ, Kim JS, Kwak JY, Chung JS, Oh SY, Suh C, Lee JJ. Pilot trial of yttrium-90 ibritumomab tiuxetan consolidation following rituximab, cyclophosphamide, doxorubicin, vincristine and prednisolone chemotherapy in patients with limited-stage, bulky diffuse large B-cell lymphoma. *Leuk Lymphoma*. 2012;53:807–11.
35. Briones J, Novelli S, Garcia-Marco JA, Tomás JF, Bernal T, Grande C, Canales MA, Torres A, Moraleda JM, Panizo C, Jarque I, Palmero F, Hernández M, González-Barca E, López D, Caballero D, GELTAMO. Autologous stem cell transplantation after conditioning with yttrium-90 ibritumomab tiuxetan plus BEAM in refractory non-Hodgkin diffuse large B-cell lymphoma: results of a prospective, multicenter, phase II clinical trial. *Haematologica*. 2014;99:505–10.

# Biology and Pathology of B-Cell Lymphoma



Yoichi Tatsumi

**Abstract** Radioimmunotherapy (RIT) is an effective therapeutic option for patients with indolent B-cell non-Hodgkin lymphomas (NHL), for the first-line and the second-line therapies. The target molecule of RIT is CD20, and the clinical outcomes have been demonstrated even in the lack of phase III studies to clearly define the efficacy of RIT. However, the best practice to employ RIT is still controversial. CD20 is an activated-glycosylated phosphoprotein expressed on the surface of all B cells beginning at the pro-B phase (CD45R+, CD117+) and progressively increasing in concentration until maturity. As most of the B-cell lymphomas are derived from the germinal center B-cell stage, they must be potential targets for RIT. For the determination of an appropriate treatment policy of RIT, the background information on the biology and pathology are indispensable. In this chapter, we review the biology and pathology of B-cell lymphoma.

**Keywords** Biology · Radioimmunotherapy · B-cell non-Hodgkin lymphoma · Transforming event · Chromosomal translocations · BCR

## Abbreviations

ATM	Ataxia-telangiectasia mutated serine-threonine kinase
BCR	B-cell receptor
CDKN2A	Cyclin-dependent kinase inhibitor 2A
CLL	Chronic lymphocytic leukemia
FDC	Follicular dendritic cells
GC	Germinal center
MALT	Mucosa-associated lymphoid tissue
REL	REL (related to “reticuloendothelial”) proto-oncogene

---

Y. Tatsumi (✉)  
Department of Hematology and Rheumatology,  
Kindai University Faculty of Medicine, Osaka, Japan  
e-mail: [anzen2@med.kindai.ac.jp](mailto:anzen2@med.kindai.ac.jp)

## 1 Introduction

B cells are lymphocytes that confer efficient and long-lasting adaptive immunity by the generation of high-affinity antibodies against foreign as well as autoantigens. It is estimated that mammalian organisms have the ability to generate on the order of  $10^{11}$  different antibodies [1]. These cells form an essential part of the humoral immune response and play a central role in the immunologic memory. Beyond this, B lymphocytes participate in a broad range of immunological functions, such as antigen presentation, immune regulation, and provision of a cellular and humoral pre-immune repertoire. Their contribution to the immune system is complex and multilayered [2].

Non-Hodgkin lymphoma (NHL) is a collective term for a heterogeneous group of lymphoproliferative malignancies with differing patterns of behavior and responses to treatment [3]. The B-cell lymphomas are types of lymphomas composed of immortalized B cells. The heterogeneity of these B-cell lymphocyte tumors is, in most cases, derived from the normal biological and histological diversity.

The World Health Organization (WHO) classification of neoplasms of the hematopoietic and lymphoid tissues, published in 2001 and updated in 2008, reached consensus on the diagnosis of these tumors, approved for use by pathologists, clinicians, and basic scientists [4].

However, there have been major advances with significant clinical and biologic implications. A major revision was, therefore, being published. In 2016, a revision of the nearly 8-year-old WHO classification of the lymphoid neoplasms and the accompanying monograph has been published. It reflects a consensus among hematopathologists, geneticists, and clinicians regarding both the updates to current entities and the addition of a limited number of new provisional entities [5] (Table 1). In the Western world, about 20 new cases of lymphoma are diagnosed per 100,000 people per year. About 95% of the lymphomas are of B-cell origin; the rest are T-cell malignancies [6]. On the other hand, in the Eastern world especially in Southeast Asia, more T-cell lymphomas are diagnosed without an apparent explanation. This might be surprising, as a similar number of B and T cells exist in the human body, but this result must come from specific factors that influence the pathogenesis of B-cell lymphomas.

Besides T-cell and B-cell differences, the diagnosis of these lymphomas is not only relevant from the pathologic aspects but also extremely important from the aspects of treatment for the lymphoma patients. As the clinical character of each B-cell lymphoma provides different clinical behaviors which basically correlate with the differentiation stage, treatment procedures must be different and depend on the pathological and clinical diagnosis.

In addition, recent evolution of the research on the cellular origin of B-cell lymphomas and on the identification of crucial transforming events was made clear especially of the role of chromosomal translocations in lymphoma pathogenesis. The pathogenesis of B-cell lymphoma depends on exogenous factors that affect normal B-cell differentiation and growth as well as the expansion of malignant B-cell lymphomas. The cellular origin of B-cell lymphomas is thought to be

**Table 1** 2016 WHO classification of mature B-cell neoplasms

Chronic lymphocytic leukemia/small lymphocytic lymphoma	Large B-cell lymphoma with IRF4 rearrangement*
Monoclonal B-cell lymphocytosis*	Primary cutaneous follicle center lymphoma
B-cell prolymphocytic leukemia	Mantle cell lymphoma
Splenic marginal zone lymphoma	In situ mantle cell neoplasia*
Hairy cell leukemia	Diffuse large B-cell lymphoma (DLBCL), NOS
Splenic B-cell lymphoma/leukemia, unclassifiable	Germinal center B-cell type*
Splenic diffuse red pulp small B-cell lymphoma	Activated B-cell type*
Hairy cell leukemia variant	T-cell/histiocyte-rich large B-cell lymphoma
Lymphoplasmacytic lymphoma	Primary DLBCL of the central nervous system (CNS)
Waldenström macroglobulinemia	Primary cutaneous DLBCL, leg type
Monoclonal gammopathy of undetermined significance (MGUS), IgM*	EBV1 DLBCL, NOS*
μ heavy-chain disease	EBV1 mucocutaneous ulcer*
γ heavy-chain disease	DLBCL associated with chronic inflammation
α heavy-chain disease	Lymphomatoid granulomatosis
Monoclonal gammopathy of undetermined significance (MGUS), IgG/A*	Primary mediastinal (thymic) large B-cell lymphoma
Plasma cell myeloma	Intravascular large B-cell lymphoma
Solitary plasmacytoma of bone	ALK1 large B-cell lymphoma
Extraosseous plasmacytoma	Plasmablastic lymphoma
Monoclonal immunoglobulin deposition diseases*	Primary effusion lymphoma
Extranodal marginal zone lymphoma of mucosa-associated lymphoid tissue (MALT lymphoma)	HHV81 DLBCL, NOS*
Nodal marginal zone lymphoma	Burkitt lymphoma
Pediatric nodal marginal zone lymphoma	Burkitt-like lymphoma with 11q aberration*
Follicular lymphoma	High-grade B-cell lymphoma, with MYC and BCL2 and/or BCL6 rearrangements*
In situ follicular neoplasia*	B-cell lymphoma, unclassifiable, with features
Duodenal-type follicular lymphoma*	Intermediate between DLBCL and classical Hodgkin
Pediatric-type follicular lymphoma*	Lymphoma

Adapted from *BLOOD*. 2016;127(20):2376

\*Changes from the 2008 classification

dependent on growth factors, cellular signals derived from B-cell receptors, the microenvironment, etc. [5]. The clinical behavior within each B-cell lymphoma subtype is variable and that may generate the heterogeneous response against targeted antitumor therapy. In order to discuss the resistance of B-cell lymphoma to targeted anticancer therapies, it is important to keep track of the relation between the normal B-cell maturation pathway and the oncogenesis of B-cell malignancies. Therefore, we herein focus on the biology and pathology of B-cell lymphomas.

## 2 Cellular Origin of B-Cell Lymphomas

The differentiation of B cells occurs by a clear mechanism defined specifically for the B-cell receptor (BCR). The BCR is composed of four polypeptides, two identical heavy chains (IgH) and two identical light chains (IgL), which are linked by disulfide bonds. The IgL chains are of either the  $\kappa$  or the  $\lambda$  isotype. All these polypeptides consist of a carboxyterminal constant (C) and an amino terminal variable (V) fragments. The V region includes four framework regions, each separated by hypervariable regions, the complementarity determining regions 1, 2, and 3 (CDRI to CDRIII). Whereas the V H region gene is generated by the recombination of three independent gene segments, the variable (V H), diversity (D H), and joining (J H) segments, the light-chain V region genes are composed of only two segments, namely, the V L and J L segments [7]. Other components of the BCR are the CD79A and CD79B molecules carrying an activation motif based on the cytoplasmic immunoreceptor tyrosine (Fig. 1). When BCRs are cross-linked, these motifs carry signals. Intracellular signaling components activated by BCR cross-linking include several tyrosine kinases. And with activation of other B cell surface receptors that recognize the antigen in response to the differentiation stage of B cells and regulate BCR signaling, B cells are activated, proliferate, and go through a further differentiation stage [8].

Early B-cell development occurring in the bone marrow is concluded that the B-cell precursor successfully rearranged the Ig heavy- and light-chain genes and is equipped with a functional surface antigen receptor (Fig. 2a). And three transcription factors such as early B-cell factor 1 (EBF1), E2A, and PAX5 play a main role for B-cell development [9].

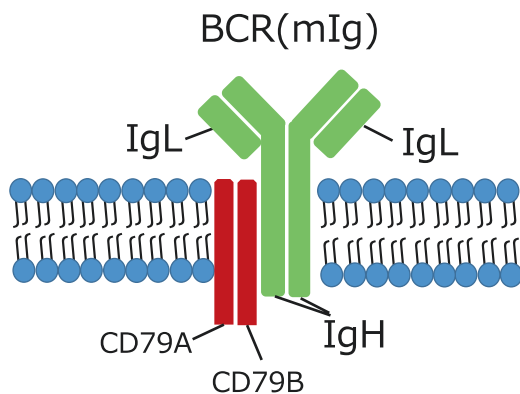


**Fig. 1** The BCR consists of two immunoglobulin (Ig) heavy (IgH) and two Ig light (IgL) chains forming the extracellular, antigen-binding part of the BCR (mIg). The B-cell receptor extends both outside (above the plasma membrane) and inside the cell (below the membrane). These are similar to the secreted antibodies of mature plasma cells and encoded by the same gene loci. The extracellular antigen-recognizing domain is complexed with CD79A and CD79B (Ig $\alpha$  and Ig $\beta$ ) that form the cytoplasmic tail of the BCR

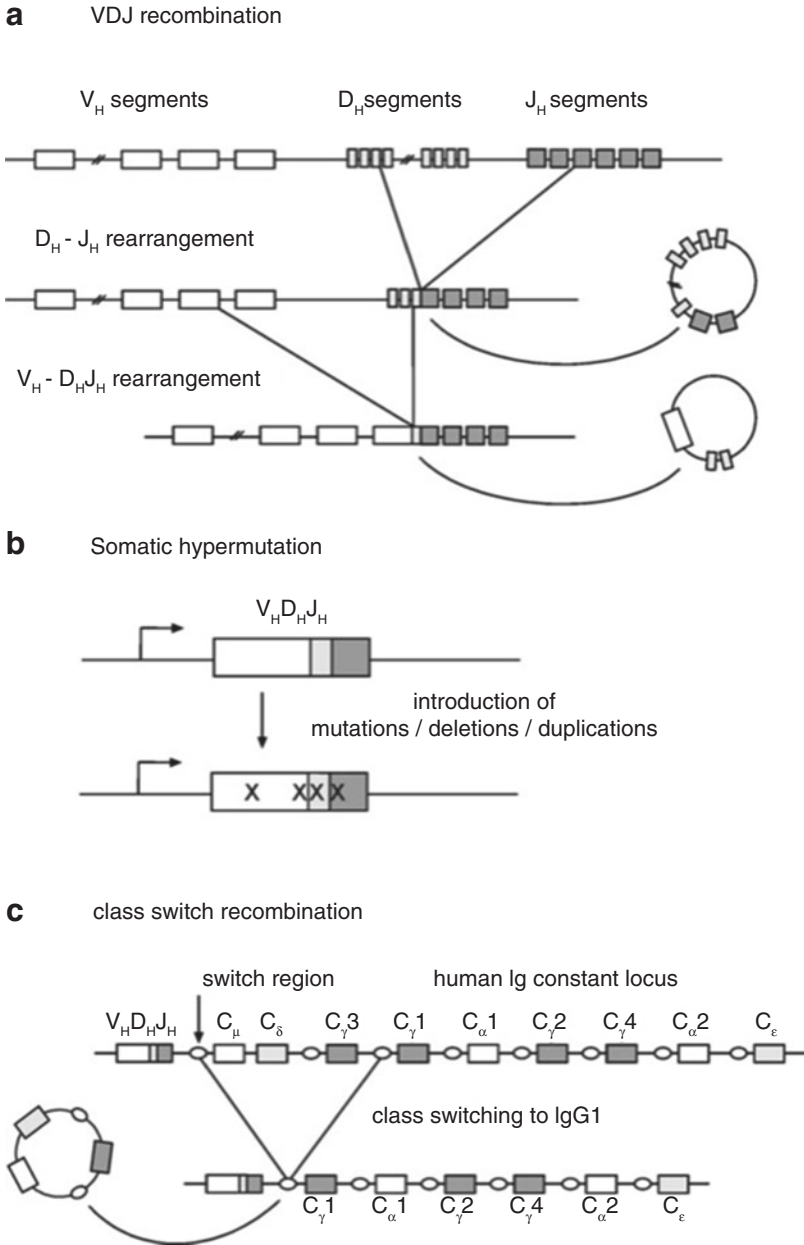


**Fig. 2** Ig gene remodeling processes in B cells. (a) Shown is a schematic presentation of the step-wise rearrangement of V<sub>H</sub>, D<sub>H</sub>, and J<sub>H</sub> segments during B-cell ontogeny. Excision circle by-products are depicted to the right. (b) The introduction of somatic mutations into a transcribed V<sub>H</sub>, D<sub>H</sub>, and J<sub>H</sub> gene by the somatic hypermutation machinery active in GC B lymphocytes. Each “X” denotes an independent mutational event. (c) Schematic presentation of class-switch recombination from C<sub>μ</sub> to C<sub>γ</sub>1 on the human IgH chain constant region locus. An excised switch circle is shown on the left. (Adapted from *Mol Biol.* 2013;971:4)

Cells expressing functional BCRs differentiate into naive B cells for maturation and leave the bone marrow, while B precursor cells not expressing BCR die by undergoing apoptosis [7]. Mature naive B cells are activated by antigen binding the BCR and become involved in the immune response. In the T-cell-dependent immune response, the structure of the Ig genes is changed by antigen-activated B cells by somatic hypermutation and class switching (Fig. 2b, c). It undergoes clonal expansion in a structure called the germinal center (GC).

Upon contact with cognate antigen, mature B cells are activated and migrate into the T-cell zones of secondary lymphatic organs. The interaction with activated T helper cells provides further stimulation to the B lymphocytes and induces proliferation, leading to the formation of primary foci. A fraction of the proliferating B cells differentiates into short-lived plasma cells that secrete antibodies of mostly of the IgM isotype and, hence, provides an initial wave of low-affinity antibodies. Some B cells, however, migrate together with the activated T helper cells into B-cell follicles and initiate a germinal center (GC) reaction [7, 10]. In the GC, actively proliferating GC B cells interact with each other by forming an immunological synapse with follicular T helper cells and follicular dendritic cells (FDC). The mechanisms of these tightly regulated proliferation and cell interactions are characteristics of the histological structure of the GC. FDC, follicular helper T cells, and a slowly related network of GC B cells (centrocytes) form so-called light zones, whereas high-density regions (centroblasts) which rapidly divide B cells are called dark zones. The expanding GC displaces the locally residing, resting B lymphocytes and compacts them into a mantle zone surrounding the GC. The GC B cells circulate mainly within but also between the two zones [7, 8]. In the dark zone, the process of somatic hypermutation (SHM) introduces point mutations as well as small deletions, insertions, or duplications into the rearranged IgV genes [11, 12].

Somatic IgV gene mutations result in changes of the BCR affinity. The mutant acquired centroblasts migrate to the light zone and compete with survival signals from the FDC and T helper cells with other GC B cells. The amount of survival signal correlates with improved or at least retained affinity to the cognate antigen: comparably, low affinity is counterselected by the induction of apoptosis in the corresponding centrocytes. This iterative process gradually improves the affinity of BCR for cognate antigens [13].

Another important DNA recombination process occurs in the centrocytes: the constant region of the antibody heavy chain (CH) can be exchanged by class-switch recombination. The CH region of naive B cells is initially expressed in the IgM and IgD isotypes for alternative splicing. During class switching, the C $\mu$  and C $\delta$  gene segments can be replaced by one of two human C $\alpha$ , one C $\epsilon$ , or four C $\gamma$  gene segments (Fig. 2). The class switch results in improved antibody BCR signaling capacity and changes in effector function [14]. Notably, class switching is not an obligatory feature of GC B cells, as part of the GC B-cell progeny—mostly early descendants leave the GC as non-class-switched lymphocytes [15, 16]. After several cycles of proliferation, mutation, and positive selection, GC B cells differentiate into either secreted plasma cells or resting memory B cells and leave the GC micro-environment [17].



Memory B cells and post-GC plasma cells provide two important B-cell adaptive immune functions. Initially, plasma cells produce potent high-affinity antibodies to invading pathogens. Both cells then provide an enhanced and improved immune response when the pathogen reinvades. These rapid and effective secondary immune responses constitute the humoral immune memory [18].

The stage of B-cell differentiation is characterized by a certain structure of the BCR and an expression pattern of differentiation markers. Since these processes often occur specifically, analysis of these characteristics can determine the origin of various human B-cell lymphomas [19, 20] (Table 2). The classification of such B-cell lymphomas is based on malignant B cells appearing to be frozen at specific differentiation stages reflecting their origin [17, 19, 21]. And it is known that most B-cell lymphomas are derived from GC or post-GC B cells.

When B cells undergo malignant transformation, B cells usually inherit important features of the originating cell of a particular differentiation stage of the lymphoma progenitor cells [22] (Table 2). Therefore, histological and immunohistochemical studies of the lymphomas are very important to classify B-cell malignancies and to determine the cellular induction of these tumors. For example, follicular lymphoma morphologically resembles GC B cells, expresses typical markers of GC B cells, and proliferates in follicular structures that resemble GC and GC T helper cells and FDC having a network [23]. The cellular origin of B-cell lymphoma was further investigated, and new lymphoma subtypes that were not previously recognized were also revealed by gene profiling studies of human B-cell lymphomas and normal B-cell subsets. For example, such studies revealed signs of GC B-cell gene expression associated with a subset of follicular lymphoma, Burkitt's lymphoma, and diffuse large B-cell lymphoma [24].

It became possible to comprehensively study Ig gene rearrangement by polymerase chain reaction (PCR) and sequencing, and V gene analysis complemented histopathological evaluation of lymphomas. For example, follicular lymphoma is thought to be derived from GC B cells if a particular lymphoma cell can retain the somatic mutant Ig V gene characteristic of GC B cells and show symptoms of SHM [25].

The cellular origin of Burkitt's lymphomas could not be clarified based on the histological picture, because Burkitt's lymphomas disrupt the normal lymph node structure and growth in a diffuse pattern. However, the lymphoma cells morphologically resemble centroblasts, they express key GC B-cell markers, and they have somatically mutated Ig V genes with ongoing hypermutation in a fraction of cases. Thus, Burkitt's lymphomas are now considered as derived from GC B cells [17]. These findings indicated that these tumors are of GC B-cell origin. Furthermore, gene expression profiling studies in other lymphomas revealed an unexpected relationship in gene expression patterns.

A breakthrough finding is that the heterogeneous group of diffuse large B-cell lymphomas (DLBCLs) can be subdivided into several subgroups [26, 27]. Two major subgroups were defined by high similarity of lymphoma cells to GC B cells (GCB-DLBCL) or in vitro activated B cells (ABC-DLBCL) [26, 27]. Since GCB-DLBCL often showed ongoing somatic hypermutation, this lymphoma is now

**Table 2** Origin of human mature B-cell lymphomas

Lymphoma	Features	Frequency among lymphomas (%)*	Proposed cellular origin
B-cell chronic lymphocytic leukemia (B-CLL)	Leukemia of small B cells that express the CD5 antigen, involving peripheral blood and bone marrow cells. Common in elderly patients. Called "small lymphocytic lymphoma" when lymph node cells are predominantly involved. Patients with leukemia cells that lack variable (V) region gene mutations have a worse prognosis than patients with mutations in V region genes	7	Memory B cell? Naive B cell? Marginal zone B cell?
Mantle cell lymphoma	Lymphoma arises from cells that populate the mantle zone of follicles, express CD5, and show aberration in cyclin-D1 expression. Nearly all cases are associated with BCL1-IgH translocation	5	CD5+ mantle zone B cell
B-cell prolymphocytic leukemia	Chronic B-cell malignancy related to B-CLL. Over 50% of cancer cells represent prolymphocytes (large lymphocytes with clumped)	<1	Memory B cell
Follicular lymphoma	A nodal lymphoma with a follicular growth pattern. Lymphoma cells morphologically and phenotypically resemble GC B cells. Most cases are associated with BCL2-IgH translocation	20	GC B cell
Hairy-cell leukemia	Chronic B-cell malignancy involving the spleen and bone marrow. Very few circulating leukemia cells. Tumor cells form "hairy" projections	<1	Memory B cell
MALT lymphoma	Extranodal marginal zone B-cell lymphoma. Develops mostly in acquired lymphoid structures	7	Marginal zone B cell
Nodal marginal zone lymphoma	Lymphoma with primary presentation in lymph nodes. Lymphoma cells resemble marginal zone or monocytoid B cells but often have heterogeneous cytology, which ranges from small to large lymphocytes and includes plasma cells	2	Marginal zone B cell? Monocytoid B cell?
Splenic marginal zone lymphoma	Micronodular lymphoid infiltration in the splenic white pulp. Mostly small IgD+ lymphoma cells that replace normal follicles and the marginal zone region. Frequently involves infiltration into the bone marrow and circulation	1	Subset of naive B cells that have partially differentiated into marginal zone B cells?

Burkitt's lymphoma	Fast growing. Mostly extranodal. Characterized by a MYC-Ig translocation. Patients are EBV positive in nearly all cases. Patients with sporadic form are EBV positive in about 30% of cases	2	GC B cell
Diffuse large B-cell lymphoma	Heterogeneous group of lymphomas characterized by large B cells. Several subtypes are recognized. Morphological variants include centroblasts and immunoblasts	30-40	GC or post-GC B cell
Primary mediastinal	Subtype of diffuse large B-cell lymphoma located in the mediastinum. B-cell lymphoma. Tumor cells are large B cells but also show a number of similarities to reed-Sternberg cells of classical Hodgkin lymphoma. Most frequently occurs in young women	2	Thymic B cell
Posttransplant	Mostly of the diffuse large-cell lymphoma type. Lymphomas that arise in patients after organ transplantation. Immunosuppressive treatment confers risk of uncontrolled proliferation of EBV-infected B cells that can develop into lymphomas	<1	GC B cell
Primary effusion lymphoma	Frequently occurs in AIDS or posttransplant patients. Lymphoma cells are found as effusions in serous cavities, such as pleura, pericardium, or peritoneum	<0.5	(post) GC B cell
Lymphoplasmacytic lymphoma	Involves the lymph nodes, bone marrow, and spleen. The tumor-cell population is composed of small B cells, plasmacytoid lymphocytes, and plasma cells. Most patients present with a serum monoclonal protein, usually of the IgM type	1	(post) GC B cell
Multiple myeloma	Neoplastic proliferation of plasma cells in the bone marrow	10	Plasma cell
Classical Hodgkin lymphoma	Characterized by bizarre, large tumor cells. Hodgkin and reed-Sternberg cells account for less than 1% of cells in the tumor and are admixed with various nonneoplastic cell types. Tumor cells show a phenotype not characteristic of any normal hematopoietic cell type	10	Defective GC B cell
Lymphocyte-predominant Hodgkin lymphoma	Rare indolent subtype of Hodgkin lymphoma. Lymphoma cells show a B-cell phenotype, represent a small population in the tissue, and grow in association with follicular dendritic cells and T-helper cells. Good prognosis	0.5	GC B cell

Adapted from *Nat Rev Cancer*. 2005;5:253

AIDS acquired immune deficiency syndrome, *EBV* Epstein-Barr virus, *Ig* immunoglobulin, *MALT* mucosa-associated lymphoid tissue, *GC* germinal center

\*These numbers refer to the frequencies in Europe and North America

considered a kind of GC B-cell lymphoma [28]. On the other hand, ABC-DLBCL has a highly activated phenotype and retains somatic mutation V genes but lacks the most specific features of GC B cells. This lymphoma is most similar to post-GC immunoblasts.

In a case of classical Hodgkin lymphoma, Hodgkin and Reed/Sternberg (HRS) cells, which are tumor cells of classical Hodgkin lymphoma, express little B-cell markers and express multiple markers of various other hematopoietic cell types [29]. However, the B-cell origin of HRS cells was demonstrated by clonally rearranging these cells and having somatic mutated V region genes [30, 31]. Based on this finding, HRS cells were shown to be derived from a pool of pre-apoptotic GC B cells that should originally undergo apoptosis [29].

As a main finding of the numerous studies to reveal the cellular origin of human B-cell lymphomas, it can be concluded that the majority of these lymphomas is derived from GC or post-GC B cells (Fig. 3).

Gene expression profiling studies on other malignant lymphomas also revealed an unexpected relationship in terms of gene expression patterns. For example, B-cell chronic lymphocytic leukemia (B-CLL) cells with mutant Ig variable region (V) region gene, as well as B-CLL cells without mutant Ig V region gene, were shown to be related to memory B cells [32].

It is also possible that the normal B-cell counterpart of some cancer types might not have been identified yet. In the activated B-cell type of diffuse large B-cell lymphoma, the normal counterpart could be a poorly defined, small subset of GC B cells that is undergoing plasmacytoid differentiation or a post-GC immunoblast population [20].

But still there are many unknown mechanisms to introduce malignant transformation. For example, in follicular lymphomas, the prototypic GC B-cell lymphoma, the t(14;18) BCL2/IgH chromosomal translocation, is detected in nearly all cases. And the translocation occurs at the pro-B-cell stage of B-cell development during misguided V gene recombination. This translocation is recognized to be pathogenetically really relevant during B-cell development in GC B cells when BCL2 is normally downregulated [2].

### 3 Transforming Events

In many types of B-cell lymphoma, reciprocal translocation involving one of the Ig loci and a proto-oncogene is recognized (Table 3). As a consequence of such translocation, oncogenes are placed under the control of the active Ig locus and cause deregulated constitutive expression of oncogenes and introduce lymphocytogenesis [33, 34]. These translocations happen as by-products during the processes of V(D)J recombination, SHM, and class switching [33].

Translocation of the proto-oncogene to the Ig locus in B-cell lymphoma deregulates oncogene expression via the associated Ig enhancer, which is highly active

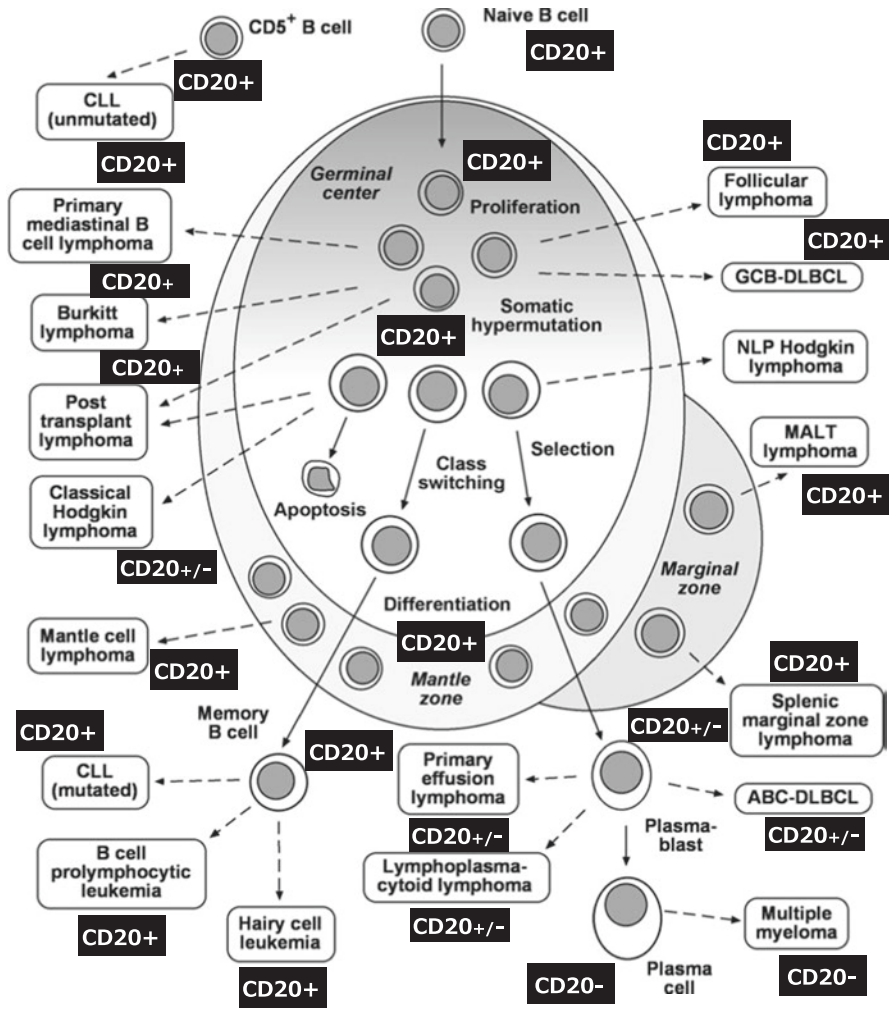


**Fig. 3** Germinal center reaction and cellular origin of human B-cell lymphoma. Most lymphomas are derived from GC B cells or post-GC B cells decisive transformation events that occur in the premalignant GC B-cell precursor of lymphoma. CLL with unmutated IgV gene is derived from CD5+ B cells. Mutated CLL probably originates from a small subset of CD5+ memory B cells, on the other hand. Most mantle cell lymphomas have an unmutated IgV gene, presumably from (CD5+) mantle zone B cells. However, 20–30% of these lymphomas have a mutated V gene, suggesting that they are derived from GC. The primary mediastinal bulky B-cell lymphoma is likely to be a thymus B cell derived from GC. There is a clear marginal zone around the follicle of the spleen. Marginal zone B cells are likely to be the origin of B cells around the spleen, although it is puzzling that normal marginal B cells harbor mutated IgV genes, whereas a considerable fraction of splenic marginal zone B-cell lymphomas has unmutated V genes. Tumor cells of classical Hodgkin lymphomas and some posttransplant lymphomas have a destructive IgV gene mutation, and they might also be derived from GC B cells before apoptosis. The basic CD20 expression level is noted. (Adapted from *Mol Biol.* 2013;971:9)

in B cells. For example, it has been found that in more than 90% of follicular lymphomas, BCL2 translocates to the heavy-chain locus and maintains continuous expression of the BCL2 oncogene even in GC [35, 36].

This BCL2-IgH translocation associated with follicular lymphoma has breakpoints that are directly adjacent to Ig heavy-chain J-region (JH) gene segments or that are adjacent to regions where the Ig heavy-chain D-region (DH) joins the J-region (DHJH) (Fig. 2). As the breakpoints also often show loss of nucleotides at the end of the JH or DH segments and the addition of non-germline-encoded nucleotides—typical features of V(D)J recombination—it is likely that these translocations happen as mistakes during the V(D)J recombination in early B-cell development in the bone marrow [33, 34, 37]. In other translocations, the breakpoints are found within or adjacent to rearranged V(D)J genes, and these V-region genes are always somatically mutated. These and additional features indicate that such translocations occur as by-products of the somatic hypermutation process [10, 31], which is associated with DNA strand breaks [38, 39].

The third type of translocation is characterized by breakpoints in the IgH constant region switch regions, in which DNA breaks are introduced during class switching. This indicates that these events occur during class-switch recombination.

This situation is similar in Burkitt's and mantle cell lymphomas; MYC and CCND1 translocate with the Ig locus in virtually all cases [40–42]. Both MYC and CCND1 cause uncontrolled proliferation in cells with respective translocations. Other lymphomas do not show a single-type translocation pattern like Burkitt's lymphoma or mantle cell lymphoma. A wide variety of translocations have been reported in DLBCL, mucosa-associated lymphoid tissue (MALT) lymphoma, and plasmacytoma/multiple myeloma, but these translocations have not been observed in the majority of cases [43–45] (Table 3). This may suggest that more diverse phenotypes of these kinds of lymphomas can be exhumed. The causes for the generation of DNA strand breaks in the oncogenes involved in Ig-associated translocations are unclear.

The same process mediating translocation to the Ig locus sometimes causes non-Ig translocation. For some of them, the hypothesized effect is deregulation by a mechanism similar to Ig translocation. For example, in DLBCL and lymphocyte-dominant Hodgkin lymphoma, the form of the BCL6 translocation is diverse, resulting in overexpression of these genes [46–48].

In the second class of translocations, fusion genes are formed. They are transcribed as fusion transcripts across breakpoints of translocation and join two separate gene portions. In MALT lymphoma, about one-third of cases leads to the expression of the fusion protein API 2-MALT1 [49]. This protein (the combination of the amino-terminus of API 2 and the carboxyl-terminus of MALT1) acquires the function of noncancerously activating the NF $\kappa$ B pathway by cleaving the NF $\kappa$ B-induced kinase MAP 3 K14 (NIK) into a constitutively active form [49].

The genes encoding BCL6 and CD95/FAS were found to contain mutations in a considerable fraction of normal GC and memory B cells, indicating that these genes are often targeted by the hypermutation machinery in normal B cells and may introduce lymphomagenesis [50–52].

**Table 3** Mechanisms of B-cell lymphoma pathogenesis

Lymphoma	Chromosomal translocations	Tumor suppressor gene mutations	Viruses	Other alterations
Mantle cell lymphoma	CCND1-IgH (95)	ATM (40)		Deletion on 13q14 (50-70)
B-cell chronic lymphocytic leukemia	-	ATM (30), TP53 (15)	-	Deletion on 13q14 (60)
Follicular lymphoma	BCL2-IgH (90)	-	-	-
Diffuse large B-cell lymphoma	BCL6 various (35) BCL2-IgH (15-30) MYC-IgH or MYC-IgL (15)	CD95 (10-20), ATM (15) TP53 (25)	-	Aberrant hypermutation of multiple proto-oncogenes (50)
Primary mediastinal B-cell lymphoma	-	SOC31 (40)	-	Aberrant hypermutation of multiple proto-oncogenes(70)
Burkitt's lymphoma	MYC-IgH or MYC-IgL (100)124,125	TP53 (40) RB2 (20-80)	EBV (endemic, 95; sporadic, 30)	-
Posttransplant lymphomas	-	-	EBV (90)	-
Classical Hodgkin lymphoma	-	IKBA (10-20) IKBE (10) CD95 (<10)	EBV (40)	REL amplifications (50)
Lymphocyte-predominant Hodgkin lymphoma	BCL6 various (48)	-	-	-
Splenic marginal zone lymphoma	-	-	-	Deletion on 7q22-36 (40)

(continued)

Table 3 (continued)

Lymphoma	Chromosomal translocations	Tumor suppressor gene mutations	Viruses	Other alterations
MALT lymphoma	API2-MALT1 (30) BCL10-IgH (5) MALT1-IgH (15–20) FOXPI-IgH (10)	CD95 (5–80)‡	Indirect role of <i>Helicobacter pylori</i> in gastric MALT lymphomas	–
Lymphoplasmacytoid lymphoma	PAX5-IgH (50)	–	–	–
Primary effusion lymphoma	–	– HHV8 (95)	EBV (70)	–
Multiple myeloma	CCND1-IgH (15–20) FGFR3-IgH (10) MAF-IgH (5–10)	CD95 (10)	–	Various MYC alterations (40), RAS mutations (40), deletion on 13q14 (50)*

Numbers in brackets indicate the percentage of cases known to carry mutations in this gene

Also not listed are transforming events that occur in less than 5% of cases of a lymphoma type

API2 apoptosis inhibitor 2, ATM ataxia-telangiectasia mutated, B-CLL B-cell chronic lymphocytic leukemia, CCND1 cyclin D1, EBV Epstein-Barr virus, FGFR3 fibroblast growth factor receptor 3, FOXPI forkhead box P1, HHV8 human herpes virus 8, IKBα inhibitor of nuclear factor-κBα, IKBε inhibitor of nuclear factor-κBε, MALT mucosa-associated lymphoid tissue, MALT1 mucosa-associated lymphoid tissue lymphoma translocation gene 1, PAX5 paired box gene 5; RB2 retinoblastoma-related gene 2, SOCS1 suppressor of cytokine signaling 1

\*The genes relevant for lymphoma pathogenesis affected by these deletions have not yet been identified

‡Different frequencies reported for different subtypes of MALT lymphoma



For example, inactivating mutations of CD95 are found in about 20% of post-GC B-cell lymphomas and can protect lymphoma cells from death induction by CD95 ligand-expressing cells [53]. In the case of the BCL6 gene, the occurrence of hypermutation may cause translocation of this gene to the Ig and non-Ig coding loci. This possibility was demonstrated by the discovery that the 5' region of BCL6, a site of hypermutation, was also found to be a region where chromosomal translocation breakpoints are predominantly found. In diffuse large B-cell lymphomas, abnormal hypermutation of a large number of oncogenes has been reported, which is also an important mechanism of pathogenesis [51, 54].

Two kinds of the molecular processes that could cause chromosome translocations or mutations in non-Ig genes occur exclusively (or at least mainly) in the GC somatic hypermutation and class-switch recombination [55]. This might be a reason that most B-cell lymphomas derive from GC B cells or GC-derived cells. Class switching and somatic hypermutation do not occur in the DNA of T cells. This phenomenon may be a reason why B cells tend to undergo malignant transformation than T cells.

Most B-cell lymphomas are considered to acquire changes during their clonal evolution that allow them to bypass intrinsic or extrinsic signals that normally trigger apoptosis. One of the most important molecules in the apoptosis network is TP53. This gene encodes the tumor suppressor protein p53, a transcription factor influencing the expression of genes that contribute directly or indirectly in apoptosis, senescence, and cell cycle progression [56].

Another important apoptosis-related pathway that is often blocked is the sensing of cellular stress and DNA damage during cell cycle checkpoints. For example, ATM and CDKN2A are often inactivated by mutation, deletion, or epigenetic silencing in lymphoma (Table 3) [57–62].

This allows cell proliferation and proliferation despite accumulation of ongoing DNA damage in the tumor.

Although it is clear that chromosomal translocation involving the Ig locus is a feature of many types of B cell lymphomas, it is not uncommon that mechanisms that do not involve the Ig locus such as mutation of tumor suppressor genes (e.g., genes encoding TP53 and I $\kappa$ B $\alpha$ ), genetic amplification (e.g., REL), and translocation (e.g., API 2 - MALT 1) play an important role in pathogenesis.

## 4 Viruses in B-Cell Lymphomas

In some types of B-cell lymphoma, viruses are involved in their causes. In B-cell lymphocyte formation, two members of the  $\gamma$ -herpesvirus family are mainly known: Epstein-Barr virus (EBV) and human herpesvirus 8 (HHV8) [63, 64]. Most notably, the Epstein-Barr virus (EBV) is found in almost all endemic Burkitt's lymphomas, many of the transplant and primary exudative lymphomas, and about 40% of cases of classic Hodgkin lymphomas [62, 65–67].

HHV8 is found in virtually all cases of primary effusion lymphoma which is a rare lymphoma mainly occurring in acquired immune deficiency syndrome (AIDS) patients [66]. Several viral proteins have been implicated in the pathogenic role of HHV8 in primary exudative lymphomas. Such viral proteins include LNA-1, viral cyclin, and viral FLICE inhibitory proteins [63].

Hepatitis C virus (HCV) does not establish latent infection in B cells but is involved in B-cell lymphocyte formation. In chronic HCV carriers, HCV appears to promote B-cell lymphocyte formation in two routes. On the other hand, HCV may act as an antigen for HCV-specific B cells, which is evidenced by the specificity of BCR of HCV-associated lymphoma [68]. In addition, HCV can upregulate activation-induced cytidine deaminase, which is an important factor of SHM in B cells, and also causes the production of reactive oxygen species, which are a mutagenic factor for B cells [69, 70].

## 5 Microenvironmental Interactions in B-Cell Lymphomas and the Role of the BCR

B cells undergo stringent selection for proper BCR expression. Pre-B cells are selected for pre-BCR (consisting of Ig heavy chain and surrogate light chain); immature B cells need to select non-autoreactive functional BCR. Following these steps, it is possible that GC B cells survive the GC environment and differentiate into memory cells or plasma cells only if the somatic mutation of the V region gene results in the expression of BCR with increased affinity for cognate antigens [7]. Even mature resting B cells result in apoptotic death of BCR-negative B cells under selective pressure to express BCR ablation of BCR expression in mice. Therefore, this BCR dependence seems to be the main determinant of B-cell survival. Whether survival signals supplied by BCR are autonomous signals or initiated by low-level BCR activation by antigen remains to be discussed [71, 72].

Therefore, the interaction of tumor cells with other cells in the microenvironment plays an essential role for the survival and proliferation of the lymphoma cells. In the case of follicular lymphoma, transformed GC B cells proliferate in a follicular structure that closely correlates with FDC and follicular T helper cells and resembles normal GC. The dependence of GC of follicular lymphoma cells on these normal components has been suggested by *in vitro* studies. Malignant cells survive longer when cocultured with CD4+ T cells or stromal cells and under the stimulation of the CD40 receptor, the major viable receptor of GC B cells [73, 74].

There is evidence that sugar-binding receptors (lectins) on the stromal cells always stimulate BCR of lymphoma cells and can replace foreign antigens that are only transiently capable of stimulating GC B cells [75].

CLL, like the case of follicular lymphoma, represents proliferation that mostly takes place in specialized structures in lymph nodes. In these proliferation centers, CD40-expressing CLL cells are in contact with stromal and CD4+ T cells, partly

expressing CD40L [76, 77]. Regarding the relevance of the interaction to the survival of CLL cells, there is an observation that CLL cells survive briefly only when cultured alone, and their survival is significantly improved by stromal cells or coculture with CD40 stimulation [78].

In addition, “resting” CLL B cells are actively engaged and responding to numerous host-derived signals, and some data clearly support a central role for CD154-CD40 interaction in CLL cell survival and induction of NF $\kappa$ B [79]. Moreover, there is now evidence that the BCRs of CLL cells are often polyreactive against autoantigens, including modified components from apoptotic cells. Whether and how such autoantigens are presented in the proliferation centers are currently unclear [80].

Gastric MALT lymphomas are known to associate with chronic immunoinflammatory stimuli, most notably chronic infection by *Helicobacter pylori* (*H. pylori*). This antigenic stimulation initially leads to lymphoid hyperplasia, and sequential acquisition of additional genetic aberrations culminates in the activation of intracellular survival pathways, with disease progression due to proliferation and resistance to apoptosis, and the emergence of a malignant clone. While early-stage gastric MALT lymphoma can frequently regress after the therapeutic reversal of the chronic immune stimulus through antibiotic eradication of *H. pylori* infection, the presence of immortalizing genetic abnormalities, of advanced disease or of eradication refractoriness, requires a more aggressive approach which is, presently, not consensual [81]. The lymphoma cells themselves usually do not recognize these bacteria via their BCR but often express autoreactive surface Ig [82]. However, CD4+ T cells in the MALT lymphoma microenvironment are activated upon interaction with *H. pylori*, and it thus appears that the *H. pylori*-activated T cells stimulate the lymphoma B cells [83]. Interestingly, also in splenic B-cell lymphomas in patients chronically infected with HCV, elimination of the virus by antiviral treatment resulted in regression of the lymphoma [84], representing a further example for chronic antigenic stimulation as critical survival signal for lymphoma cells.

Classical Hodgkin lymphoma is a unique malignant lymphoma that contains a very few number of real tumor cells that usually account for about 1% and surrounded by a majority of various nonmalignant cells, including T cells, B cells, eosinophils, neutrophils, plasma cells, mast cells, and others [85]. For example, HRS cells induce CD4+ T cells by the secretion of large amounts of the cytokine/chemokine TARC (thymus and activation-regulated chemokine), which is normally secreted from dendritic cells [86].

In Hodgkin lymphoma patients, the normal histological structure of the affected lymph nodes is disrupted. CD4+ T helper and regulatory T cells are usually the most frequent cells in the Hodgkin lymphoma microenvironment, and HRS cells are typically directly surrounded by CD4+ T cells. It seems that HRS cells actively attract such cells by secretion of a multitude of chemokines and cytokines [27]. Also, immunosuppression has long been recognized in Hodgkin lymphoma (HL), and unlike PBMCs, Hodgkin lymphoma-infiltrated lymphocytes (HLILs) were anergic to stimulation with mitogen, primary, or recall antigens, mounting no proliferative

responses and only rare T helper 1 (Th1) or Th2 cytokine responses. And HLILs are highly enriched for regulatory T cells, which induce a profoundly immunosuppressive environment and so provide an explanation for the ineffective immune clearance of HRS cells [87].

Other immunosuppressive factors secreted by the HRS cells include TGF- $\beta$  and galectin-1, and HRS cells also express the T-cell-suppressive PD-1 ligand [88–91]. Eosinophils also play a crucial role to an immunosuppressive microenvironment by secretion of TGF- $\beta$ . In addition, the CD30-positive HRS cells are activated through interaction with the CD30 ligand, which is expressed by the eosinophils [27].

## 6 Conclusion

We started to learn about the cellular as well as the molecular biology of B-cell malignancies; all the research that has been carried out on has truly translated into major advances in many kinds of B-cell lymphomas. Our better understanding of the molecular biology will really lead to major shifts in the way we approach these tumor. Focusing on the pathogenesis of B-cell lymphoma, tumor progression not only depends on transforming events, such as chromosomal translocations, but also on survival signals mediated by the expression of a functional BCR and cellular interactions in the lymphoma microenvironment. In many lymphomas, BCR signaling by foreign or autoantigens to induce proliferation might also be involved in lymphomagenesis. Chronic activation of B cells via BCR signaling induces several repertoire of B-cell lymphomas such as follicular lymphoma, MALT lymphoma, B-CLL, and DLBCL. Follicular lymphomas arise and grow in the germinal center, and in some cases, the BCR is autoreactive probably due to the BCR variable domain containing mutations that promote carbohydrate modification. Gastric mucosa-associated lymphoid tissue (MALT) lymphomas are in many cases associated with autoreactive BCR, particularly with rheumatoid factors [92].

B-cell chronic lymphocytic leukemia (CLL) has a restricted variable (V) region gene repertoire, and the BCR is often autoreactive. A BCR specific to human T-cell lymphotropic virus 1 (HTLV-1) has been identified in patients who are infected with this virus [93].

In hepatitis C virus (HCV)-associated lymphomas, HCV specificity of BCR has been reported in some cases [90]. Then, HCV-associated lymphomas usually regress after antiviral therapy. In a case of central nerve system (CNS) B-cell lymphoma, restricted V region gene usage is a hallmark of CNS lymphomas indicating the existence of specific BCR-related chronic activation during the disease process. These results indicate that other than pathogen-derived antigens that cause chronic infections, certain autoantigens can also stimulate reactive B cells. This concept is also supported by the observation that several autoimmune diseases, such as Sjögren's syndrome, rheumatoid arthritis, and autoimmune lymphoproliferative syndrome, are commonly associated with an increased risk of lymphomas [92].

In other aspects of B-cell lymphomas, many B-cell lymphomas carry the character of their normal counterparts at particular stage of differentiation. For example, chromosomal translocations disrupt the normal BCL6 gene function but result in the constitutive expression of this transcription factor, still keeping the GC B cells in a proliferative stage, and prevent their differentiation into a resting stage. And many B-cell lymphomas keep dependency on BCR expression, antigen triggering, and microenvironmental survival signals. The dependency on such factors would select for a tumor phenotype that still resembles normal B cells in many aspects.

Chemotherapy, radiotherapy, immunotherapy, radioimmunotherapy, and hematopoietic stem cell transplantation are available as options for the treatment strategy of B-cell lymphomas. Currently, the treatment plan is decided considering the progress of the disease state and the patient's whole body condition. In the future, we hope that the continuation of innovative research will clarify details of the cell biological background and genetic background of malignant lymphomas, which will be reflected in treatment options, and will improve the prognosis of patients.

## References

1. Nussenzweig MC, Alt FW. Antibody diversity: one enzyme to rule them all. *Nat Med.* 2004;10(12):1304–5.
2. Seifert M, Scholtysik R, Küppers R. Origin and Pathogenesis of B Cell Lymphomas. *Methods Mol Biol (Clifton, NJ).* 2013;971:1–25.
3. Armitage JO. Treatment of non-Hodgkin's lymphoma. *N Engl J Med.* 1993;328(14):1023–30.
4. Swerdlow SH, Campo E, Harris NL, et al. WHO classification of tumours of haematopoietic and lymphoid tissues. Lyon: IARC Press; 2008.
5. Swerdlow SH, Campo E, Pileri SA, Harris NL, Stein H, Siebert R, Advani R, Ghielmini M, Salles GA, Zelenetz AD, Jaffe ES. The 2016 revision of the World Health Organization classification of lymphoid neoplasms. *Blood.* 2016;127:2375–90.
6. Küppers R. Mechanisms of B-cell lymphoma pathogenesis. *Nat Rev Cancer.* 2005;5(4):251–62.
7. Tonegawa S. Somatic generation of antibody diversity. *Nature.* 1983;302:575–81.
8. Rajewsky K. Clonal selection and learning in the antibody system. *Nature.* 1996;381:751–8.
9. Medina KL, Singh H. Genetic networks that regulate B lymphopoiesis. *Curr Opin Hematol.* 2005;12:203–9.
10. MacLennan IC. Germinal centers. *Annu Rev Immunol.* 1994;12:117–39.
11. Küppers R, Zhao M, Hansmann ML, Rajewsky K. Tracing B cell development in human germinal centres by molecular analysis of single cells picked from histological sections. *EMBO J.* 1993;12:4955–67.
12. Goossens T, Klein U, Küppers R. Frequent occurrence of deletions and duplications during somatic hypermutation: implications for oncogene translocations and heavy chain disease. *Proc Natl Acad Sci U S A.* 1998;95:2463–8.
13. Liu YJ, Joshua DE, Williams GT, Smith CA, Gordon J, MacLennan IC. Mechanism of antigen-driven selection in germinal centers. *Nature.* 1989;342:929–31.
14. Manis JP, Tian M, Alt FW. Mechanism and control of class-switch recombination. *Trends Immunol.* 2002;23:31–9.
15. Klein U, Rajewsky K, Küppers R. Human immunoglobulin (Ig)M+IgD+ peripheral blood B cells expressing the CD27 cell surface antigen carry somatically mutated variable region genes: CD27 as a general marker for somatically mutated (memory) B cells. *J Exp Med.* 1998;188:1679–89.

16. Seifert M, Küppers R. Molecular footprints of a germinal center derivation of human IgM+(IgD+)CD27+ B cells and the dynamics of memory B cell generation. *J Exp Med*. 2009;206:2659–69.
17. Klein U, Dalla-Favera R. Germinal centres: role in B-cell physiology and malignancy. *Nat Rev Immunol*. 2008;8:22–33.
18. McHeyzer-Williams M, Okitsu S, Wang N, McHeyzer-Williams L. Molecular programming of B cell memory. *Nat Rev Immunol*. 2012;12:24–34.
19. Küppers R, Klein U, Hansmann M-L, Rajewsky K. Cellular origin of human B-cell lymphomas. *N Engl J Med*. 1999;341:1520–9.
20. Stevenson FK, et al. The occurrence and significance of V gene mutations in B cell-derived human malignancy. *Adv Cancer Res*. 2001;83:81–116; Stevenson FK, et al. The occurrence and significance of V gene mutations in B cell-derived human malignancy. *Adv Cancer Res*. 2001;83:81–116.
21. Shaffer AL, Rosenwald A, Staudt LM. Lymphoid malignancies: the dark side of B-cell differentiation. *Nat Rev Immunol*. 2002;2:920–32.
22. Klein U, Dalla-Favera R. Germinal centres: role in B-cell physiology and malignancy. *Nat Rev Immunol*. 2008;8:22–33; Küppers R. Mechanisms of B-cell lymphoma pathogenesis. *Nat Rev Cancer*. 2005;5:251–62.
23. de Jong D. Molecular pathogenesis of follicular lymphoma: a cross talk of genetic and immunologic factors. *J Clin Oncol*. 2005;23:6358–63.
24. Alizadeh AA, et al. Distinct types of diffuse large B-cell lymphoma identified by gene expression profiling. *Nature*. 2000;403:503–11.
25. Bende RJ, Smit LA, van Noesel CJ. Molecular pathways in follicular lymphoma. *Leukemia*. 2007;21:18–29.
26. Alizadeh AA, Eisen MB, Davis RE, Ma C, Lossos IS, Rosenwald A, Boldrick JC, Sabet H, Tran T, Yu X, Powell JI, Yang L, Marti GE, Moore T, Hudson J Jr, Lu L, Lewis DB, Tibshirani R, Sherlock G, Chan WC, Greiner TC, Weisenburger DD, Armitage JO, Warnke R, Levy R, Wilson W, Grever MR, Byrd JC, Botstein D, Brown PO, Staudt LM. Distinct types of diffuse large B-cell lymphoma identified by gene expression profiling. *Nature*. 2000;403:503–11.
27. Rosenwald A, Wright G, Chan WC, Connors JM, Campo E, Fisher RI, Gascoyne RD, Muller-Hermelink HK, Smeland EB, Giltner JM, Hurt EM, Zhao H, Averett L, Yang L, Wilson WH, Jaffe ES, Simon R, Klausner RD, Powell J, Duffey PL, Longo DL, Greiner TC, Weisenburger DD, Sanger WG, Dave BJ, Lynch JC, Vose J, Armitage JO, Montserrat E, Lopez-Guillermo A, Grogan TM, Miller TP, LeBlanc M, Ott G, Kvaloy S, Delabie J, Holte H, Krajci P, Stokke T, Staudt LM. The use of molecular profiling to predict survival after chemotherapy for diffuse large-B-cell lymphoma. *N Engl J Med*. 2002;346:1937–47. (43, 44).
28. Lossos IS, Alizadeh AA, Eisen MB, Chan WC, Brown PO, Botstein D, Staudt LM, Levy R. Ongoing immunoglobulin somatic mutation in germinal center B cell-like but not in activated B cell-like diffuse large cell lymphomas. *Proc Natl Acad Sci U S A*. 2000;97:10209–113.
29. Küppers R. The biology of Hodgkin's lymphoma. *Nat Rev Cancer*. 2009;9:15–27.
30. Kanzler H, Küppers R, Hansmann ML, Rajewsky K. Hodgkin and Reed-sternberg cells in Hodgkin's disease represent the outgrowth of a dominant tumor clone derived from (crippled) germinal center B cells. *J Exp Med*. 1996;184:1495–505.
31. Küppers R, Rajewsky K, Zhao M, Simons G, Laumann R, Fischer R, Hansmann ML. Hodgkin disease: Hodgkin and reed-sternberg cells picked from histological sections show clonal immunoglobulin gene rearrangements and appear to be derived from B cells at various stages of development. *Proc Natl Acad Sci U S A*. 1994;91:10962–6.
32. Klein U, et al. Gene expression profiling of B cell chronic lymphocytic leukemia reveals a homogeneous phenotype related to memory B cells. *J Exp Med*. 2001;194:1625–38.
33. Küppers R, Dalla-Favera R. Mechanisms of chromosomal translocations in B cell lymphomas. *Oncogene*. 2001;20:5580–94.



34. Willis TG, Dyer MJ. The role of immunoglobulin translocations in the pathogenesis of B-cell malignancies. *Blood*. 2000;96:808–22.
35. Jäger U, Bocskor S, Le T, Mitterbauer G, Bolz I, Chott A, Kneba M, Mannhalter C, Nadel B. Follicular lymphomas' BCL-2/IgH junctions contain templated nucleotide insertions: novel insights into the mechanism of t(14;18) translocation. *Blood*. 2000;95:3520–9.
36. Tsujimoto Y, Gorham J, Cossman J, Jaffe E, Croce CM. The t(14;18) chromosome translocations involved in B-cell neoplasms result from mistakes in VDJ joining. *Science*. 1985;229:1390–3.
37. Tsujimoto Y, Louie E, Bashir MM, Croce CM. The reciprocal partners of both the t(14; 18) and the t(11; 14) translocations involved in B-cell neoplasms are rearranged by the same mechanism. *Oncogene*. 1988;2:347–51.
38. Bross L, et al. DNA double-strand breaks in immunoglobulin genes undergoing somatic hypermutation. *Immunity*. 2000;13:589–97.
39. Papavasiliou FN, Schatz DG. Cell-cycle-regulated DNA double-stranded breaks in somatic hypermutation of immunoglobulin genes. *Nature*. 2000;408:216–21.
40. Re D, et al. Oct-2 and Bob-1 deficiency in Hodgkin and Reed Sternberg cells. *Cancer Res*. 2001;61:2080–4.
41. Stein H, et al. Down-regulation of BOB.1/OBF.1 and Oct2 in classical Hodgkin disease but not in lymphocyte predominant Hodgkin disease correlates with immunoglobulin transcription. *Blood*. 2001;97:496–501.
42. Bräuninger A, et al. Epstein–Barr virus (EBV)-positive lymphoproliferations in posttransplant patients show immunoglobulin V gene mutation patterns suggesting interference of EBV with normal B cell differentiation processes. *Eur J Immunol*. 2003;33:1593–602.
43. Dalla-Favera R, Martinotti S, Gallo RC, Erikson J, Croce CM. Translocation and rearrangements of the c-myc oncogene locus in human undifferentiated B-cell lymphomas. *Science*. 1983;219:963–7.
44. Taub R, Kirsch I, Morton C, Lenoir G, Swan D, Tronick S, Aaronson S, Leder P. Translocation of the c-myc gene into the immunoglobulin heavy chain locus in human Burkitt lymphoma and murine plasmacytoma cells. *Proc Natl Acad Sci U S A*. 1982;79:7837–41.
45. Vaandrager JW, Schuurin E, Zwikstra E, de Boer CJ, Kleiverda KK, van Krieken JH, Kluin-Nelemans HC, van Ommen GJ, Raap AK, Kluin PM. Direct visualization of dispersed 11q13 chromosomal translocations in mantle cell lymphoma by multicolor DNA fiber fluorescence in situ hybridization. *Blood*. 1996;88:1177–82.
46. Baron BW, Nucifora G, McCabe N, Espinosa R 3rd, Le Beau MM, McKeithan TW. Identification of the gene associated with the recurring chromosomal translocations t(3;14)(q27;q32) and t(3;22)(q27;q11) in B-cell lymphomas. *Proc Natl Acad Sci U S A*. 1993;90:5262–6.
47. Wlodarska I, Nooyen P, Maes B, Martin Subero JI, Siebert R, Pauwels P, De Wolf-Peeters C, Hagemeijer A. Frequent occurrence of BCL6 rearrangements in nodular lymphocyte predominance Hodgkin lymphoma but not in classical Hodgkin lymphoma. *Blood*. 2003;101:706–10.
48. Ye BH, Rao PH, Chaganti RS, Dalla-Favera R. Cloning of bcl-6, the locus involved in chromosome translocations affecting band 3q27 in B-cell lymphoma. *Cancer Res*. 1993;53:2732–5.
49. Dierlamm J, Baens M, Wlodarska I, Stefanova-Ouzounova M, Hernandez JM, Hossfeld DK, De Wolf-Peeters C, Hagemeijer A, Van den Berghe H, Marynen P. The apoptosis inhibitor gene API2 and a novel 18q gene, MALT, are recurrently rearranged in the t(11;18)(q21;q21) associated with mucosa associated lymphoid tissue lymphomas. *Blood*. 1999;93:3601–9.
50. Müschen M, et al. Somatic mutation of the CD95 gene in human B cells as a side-effect of the germinal center reaction. *J Exp Med*. 2000;192:1833–40.
51. Pasqualucci L, et al. BCL-6 mutations in normal germinal center B cells: evidence of somatic hypermutation acting outside Ig loci. *Proc Natl Acad Sci U S A*. 1998;95:11816–21.
52. Shen HM, Peters A, Baron B, Zhu X, Storb U. Mutation of BCL-6 gene in normal B cells by the process of somatic hypermutation of Ig genes. *Science*. 1998;280:1750–2.
53. Gronbaek K, et al. Somatic Fas mutations in non-Hodgkin's lymphoma: association with extranodal disease and autoimmunity. *Blood*. 1998;92:3018–24.

54. Pasqualucci L, et al. Hypermutation of multiple proto-oncogenes in B-cell diffuse large-cell lymphomas. *Nature*. 2001;412:341–6.
55. Esser C, Radbruch A. Immunoglobulin class switching: molecular and cellular analysis. *Annu Rev Immunol*. 1990;8:717–35.
56. Gaidano G, et al. p53 mutations in human lymphoid malignancies: association with Burkitt lymphoma and chronic lymphocytic leukemia. *Proc Natl Acad Sci U S A*. 1991;88:5413–7.
57. Vaandrager JW, et al. Direct visualization of dispersed 11q13 chromosomal translocations in mantle cell lymphoma by multicolor DNA fiber fluorescence in situ hybridization. *Blood*. 1996;88:1177–82.
58. Camacho E, et al. ATM gene inactivation in mantle cell lymphoma mainly occurs by truncating mutations and missense mutations involving the phosphatidylinositol-3 kinase domain and is associated with increasing numbers of chromosomal imbalances. *Blood*. 2002;99:238–44.
59. Schaffner C, Idler I, Stilgenbauer S, Döhner H, Lichter P. Mantle cell lymphoma is characterized by inactivation of the ATM gene. *Proc Natl Acad Sci U S A*. 2000;97:2773–8.
60. Cuneo A, et al. 13q14 deletion in non-Hodgkin's lymphoma: correlation with clinicopathologic features. *Haematologica*. 1999;84:589–93.
61. Schaffner C, Stilgenbauer S, Rappold GA, Döhner H, Lichter P. Somatic ATM mutations indicate a pathogenic role of ATM in B-cell chronic lymphocytic leukemia. *Blood*. 1999;94:748–53.
62. Stankovic T, et al. Inactivation of ataxia telangiectasia mutated gene in B-cell chronic lymphocytic leukaemia. *Lancet*. 1999;353:26–9.
63. Carbone A, Ghoghini A. KSHV/HHV8-associated lymphomas. *Br J Haematol*. 2008;140:13–24.
64. Küppers R. B cells under influence: transformation of B cells by Epstein-Barr virus. *Nat Rev Immunol*. 2003;3:801–12.
65. Rickinson AB, Kieff E. Epstein-Barr virus. In: Knipe DM, Howley PM, editors. *Fields Virology*. Philadelphia: Lippincott-Raven; 2001. p. 2575–627.
66. Thorley-Lawson DA, Gross A. Persistence of the Epstein-Barr virus and the origins of associated lymphomas. *N Engl J Med*. 2004;350:1328–37.
67. Young LS, Rickinson AB. Epstein-Barr virus: 40 years on. *Nat Rev Cancer*. 2004;4:757–68.
68. Quinn ER, Chan CH, Hadlock KG, Fountzakis SK, Flint M, Levy S. The B-cell receptor of a hepatitis C virus (HCV)-associated non-Hodgkin lymphoma binds the viral E2 envelope protein, implicating HCV in lymphomagenesis. *Blood*. 2001;98:3745–9.
69. Machida K, Cheng KT, Sung VM, Lee KJ, Levine AM, Lai MM. Hepatitis C virus infection activates the immunologic (type II) isoform of nitric oxide synthase and thereby enhances DNA damage and mutations of cellular genes. *J Virol*. 2004;78:8835–43.
70. Machida K, Cheng KT, Sung VM, Shimodaira S, Lindsay KL, Levine AM, Lai MY, Lai MM. Hepatitis C virus induces a mutator phenotype: enhanced mutations of immunoglobulin and protooncogenes. *Proc Natl Acad Sci U S A*. 2004;101:4262–7.
71. Kraus M, Alimzhanov MB, Rajewsky N, Rajewsky K. Survival of resting mature B lymphocytes depends on BCR signaling via the Ig $\alpha$ / $\beta$  heterodimer. *Cell*. 2004;117:787–800.
72. Lam KP, Kühn R, Rajewsky K. In vivo ablation of surface immunoglobulin on mature B cells by inducible gene targeting results in rapid cell death. *Cell*. 1997;90:1073–83.
73. Johnson PW, Watt SM, Betts DR, Davies D, Jordan S, Norton AJ, Lister TA. Isolated follicular lymphoma cells are resistant to apoptosis and can be grown in vitro in the CD40/stromal cell system. *Blood*. 1993;82:1848–57.
74. Umetsu DT, Esserman L, Donlon TA, DeKruyff RH, Levy R. Induction of proliferation of human follicular (B type) lymphoma cells by cognate interaction with CD4+ T cell clones. *J Immunol*. 1990;144:2550–7.
75. Coelho V, Krysov S, Ghaemmaghami AM, Emará M, Potter KN, Johnson P, Packham G, Martínez-Pomares L, Stevenson FK. Glycosylation of surface Ig creates a functional bridge between human follicular lymphoma and microenvironmental lectins. *Proc Natl Acad Sci U S A*. 2010;107:18587–92.



76. Schmid C, Isaacson PG. Proliferation centres in B-cell malignant lymphoma, lymphocytic (B-CLL): an immunophenotypic study. *Histopathology*. 1994;24:445–51.
77. Ghia P, Strola G, Granziero L, Geuna M, Guida G, Sallusto F, Rufi ng N, Montagna L, Piccoli P, Chilosi M, Caligaris-Cappio F. Chronic lymphocytic leukemia B cells are endowed with the capacity to attract CD4+, CD40L+ T cells by producing CCL22. *Eur J Immunol*. 2002;32:1403–13.
78. Buske C, Gogowski G, Schreiber K, Rave-Frank M, Hiddemann W, Wormann B. Stimulation of B-chronic lymphocytic leukemia cells by murine fibroblasts, IL-4, anti-CD40 antibodies, and the soluble CD40 ligand. *Exp Hematol*. 1997;25:329–37.
79. Schattner EJ. CD40 ligand in CLL pathogenesis and therapy. *Leuk Lymphoma*. 2000;37(5–6):461–72.
80. Herve M, Xu K, Ng YS, Wardemann H, Albesiano E, Messmer BT, Chiorazzi N, Meffre E. Unmutated and mutated chronic lymphocytic leukemias derive from self-reactive B cell precursors despite expressing different antibody reactivity. *J Clin Invest*. 2005;115:1636–43.
81. Pereira M-I, Augusto Medeiros J. Role of *Helicobacter pylori* in gastric mucosa-associated lymphoid tissue lymphomas. *World J Gastroenterol*. 2014;20(3):684–98.
82. Bende RJ, Aarts WM, Riedl RG, de Jong D, Pals ST, van Noesel CJM. Among B cell non-Hodgkin's lymphomas, MALT lymphomas express a unique antibody repertoire with frequent rheumatoid factor reactivity. *J Exp Med*. 2005;201:1229.
83. Hussel T, Isaacson PG, Crabtree JE, Spencer J. *Helicobacter pylori*-specific tumour infiltrating T cells provide contact dependent help for the growth of malignant B cells in low grade gastric lymphoma of mucosa-associated lymphoid tissue. *J Pathol*. 1996;178:122–7.
84. Wotherspoon AC, Doglioni C, Diss TC, Pan L, Moschini A, de Boni M, Isaacson PG. Regression of primary low-grade B-cell gastric lymphoma of mucosa-associated lymphoid tissue after eradication of *Helicobacter pylori*. *Lancet*. 1993;342:575–7.
85. Vardhana S, Younes A. The immune microenvironment in Hodgkin lymphoma: T cells, B cells, and immune checkpoints. *Haematologica*. 2016;101(7):794–802.
86. van den Berg A, Visser L, Poppema S. High expression of the CC chemokine TARC in Reed–Sternberg cells. A possible explanation for the characteristic T-cell infiltration Hodgkin's lymphoma. *Am J Pathol*. 1999;154:1685–91.
87. Marshall NA, Christie LE, Munro LR, Culligan DJ, Johnston PW, Barker RN, Vickers MA. Immunosuppressive regulatory T cells are abundant in the reactive lymphocytes of Hodgkin lymphoma. *Blood*. 2003;103(5):1755–62.
88. Chemnitz JM, Eggle D, Driesen J, Classen S, Riley JL, Debey-Pascher S, Beyer M, Popov A, Zander T, Schultze JL. RNA fingerprints provide direct evidence for the inhibitory role of TGFbeta and PD-1 on CD4+ T cells in Hodgkin lymphoma. *Blood*. 2007;110:3226–33.
89. Gandhi MK, Moll G, Smith C, Dua U, Lambley E, Ramuz O, Gill D, Marlton P, Seymour JF, Khanna R. Galectin-1 mediated suppression of Epstein-Barr virus specific T-cell immunity in classic Hodgkin lymphoma. *Blood*. 2007;110:1326–9.
90. Juszczynski P, Ouyang J, Monti S, Rodig SJ, Takeyama K, Abramson J, Chen W, Kutok JL, Rabinovich GA, Shipp MA. The API1-dependent secretion of galectin-1 by Reed Sternberg cells fosters immune privilege in classical Hodgkin lymphoma. *Proc Natl Acad Sci U S A*. 2007;104:13134–9.
91. Yamamoto R, Nishikori M, Kitawaki T, Sakai T, Hishizawa M, Tashima M, Kondo T, Ohmori K, Kurata M, Hayashi T, Uchiyama T. PD-1–PD-1 ligand interaction contributes to immunosuppressive microenvironment of Hodgkin lymphoma. *Blood*. 2008;111:3220–4.
92. Niemann CU, Wiestner A. Semin B-cell receptor signaling as a driver of lymphoma development and evolution. *Cancer Biol Ther*. 2013;23(6):410–21.
93. Greten TF, Slansky JE, Kubota R, Soldan SS, Jaffee EM, Leist TP, Pardoll DM, Jacobson S, Schneck JP. Direct visualization of antigen-specific T cells: HTLV-1 Tax11-19-specific CD8(+) T cells are activated in peripheral blood and accumulate in cerebrospinal fluid from HAM/TSP patients. *Proc Natl Acad Sci U S A*. 1998;95(13):7568–73.

# Resistance to Y-90 Ibritumomab Tiuxetan Therapy



Koichiro Abe

**Abstract** Y-90 ibritumomab tiuxetan is the first radioimmunotherapy (RIT) agent for patients with relapsed or refractory low-grade CD20-positive B-cell non-Hodgkin's lymphoma. Although accumulated data demonstrate its excellent therapeutic efficiency, there are a certain number of patients that experience disease exacerbation during the post-RIT observation periods. Up to now, advanced disease, bulky mass, poor performance status, a history of frequent chemotherapies before RIT, etc. have been proposed as predictive factors for unfavorable prognosis after RIT. In this chapter, we focus on the bulky disease, the downregulation of the CD20 molecule, the NF- $\kappa$ B activation, and the impaired host immune status as factors presumably related to resistance to Y-90 ibritumomab tiuxetan therapy. We also discuss the mechanisms of the resistance and rational therapeutic approaches. We further illustrate the immunological circumstances in tumor-bearing patients and comment on the immune checkpoint blockade therapy.

**Keywords** Y-90 ibritumomab tiuxetan · Resistance · Bulky mass · Downregulation of CD20 · NF- $\kappa$ B activation · Immunoediting · Abscopal effect · Immunological cell death · Immune checkpoint

## Abbreviations

ABC	Activated B-like diffuse large B-cell lymphoma
ADCC	Antibody-dependent cellular cytotoxicity
Ag	Antigen
APC	Antigen-presenting cell
ATP	Adenosine triphosphate

---

K. Abe (✉)  
Department of Diagnostic Radiology and Nuclear Medicine,  
Tokyo Women's Medical University, Tokyo, Japan  
e-mail: [abe.koichiro@twmu.ac.jp](mailto:abe.koichiro@twmu.ac.jp)

BT	Bulky tumor
CD	Cluster of differentiation
CDC	Complement-dependent cytotoxicity
ODN	Oligodeoxynucleotides
CR	Complete response
CRR	Complete response rate
CRT	Calreticulin
CTLA-4	Cytotoxic T-lymphocyte-associated protein-4
DA-EPOCH-R	Dose-adjusted etoposide, prednisone, vincristine, cyclophosphamide, doxorubicin, and rituximab
DAMP	Damage-associated molecular patterns
DC	Dendritic cell
DLBCL	Diffuse large B-cell lymphoma
EBRT	Extrabeam radiotherapy
EU	European Union
F(ab') <sub>2</sub>	Fab prime 2
Fab	Fragment antigen-binding
Fas-L	Fas-ligand
FcγR	Fcγ receptor
FIT	First-line indolent trial
Flt3-L	Fms-like tyrosine kinase 3 ligand
GCB	Germinal center B cell
GM-CSF	Granulocyte macrophage colony-stimulating factor
HcAb	Heavy-chain antibody
HMGB1	High-mobility group box 1
ICD	Immunological cell death
IFN	Interferon
IL	Interleukin
IPI	International Prognostic Index
mAb	Monoclonal antibody
MCL	Mantle-cell lymphoma
MDSC	Myeloid-derived suppressor cells
MHC	Major histocompatibility complex
MRD	Minimal residual disease
NF-κB	Nuclear factor-κB
ORR	Overall response rate
PD-1	Programmed cell death-1
PD-L1	Programmed cell death ligand 1
PFS	Progression-free survival
P2RX7	Purinergic receptor P2X, ligand gated ion channel, 7
R-CHOP	Rituximab, cyclophosphamide, doxorubicin, vincristine, and prednisone
RIT	Radioimmunotherapy
RN	Radionuclide
scFv	Single-chain variable

TCR	T cell receptor
TGF- $\beta$	Transforming growth factor beta
TLR	Toll-like receptor
TNF $\alpha$	Tumor necrosis factor $\alpha$
Treg	Regulatory T cells
TTP	Time to disease progression
US FDA	US Food and Drug Administration
Y-90	Yttrium-90

## 1 Introduction

Yttrium-90 (Y-90) ibritumomab tiuxetan (Zevalin®) is the first radioimmunotherapy (RIT) agent developed for the treatment of patients with CD20-positive B-cell non-Hodgkin's lymphoma (NHL). This pharmaceutical was approved by the US Food and Drug Administration (US FDA) in 2002 and subsequently within the European Union (EU) in 2004 for the treatment of patients with relapsed or refractory low-grade, follicular, or transformed B-cell NHL and is the only commercially available radioimmunopharmaceutical to date. It was also authorized to be used for consolidation therapy after the induction of remission in first-line chemotherapy within the EU and US in 2008 and 2009, respectively.

The efficacy of Y-90 ibritumomab tiuxetan has been elucidated by numerous clinical trials [1–5] that showed an overall response rate (ORR) of 67–90% in relapsed or refractory low-grade, follicular, or transformed CD20-positive B-cell NHL. Morschhauser et al. demonstrated that Y-90 ibritumomab tiuxetan consolidation significantly prolonged the median 8-year progression-free survival (PFS) with 4.1 years versus 1.1 years for the control ( $p < 0.001$ ) [6]. Long-term follow-up proved that this pharmaceutical was a significantly effective, feasible, and safe therapeutic tool without so much reduction of the quality of life.

Several studies have been conducted in order to address which factors associated with the patient or the disease were positive or negative predictors for attaining a long-term and durable response in this RIT. So far, many researchers suggested that patients with advanced stage [4, 5, 7, 8], having bulky masses [7, 8], and had received multiple regimens of chemotherapy before RIT [4, 5, 8, 9] would not much benefit from the therapy.

Resistance to Y-90 ibritumomab tiuxetan therapy would compromise the following therapeutic strategy and deteriorate patients' prognoses. Although such resistance may deeply be related with the characteristics of the patients and the biological behaviors of tumors, the precise mechanism of this phenomenon is not fully understood as yet. In this chapter, we accumulate the evidences related to the resistance to Y-90 ibritumomab tiuxetan therapy, as well as the resistance to rituximab therapy since these agents bind the exactly same epitope of the CD20 antigen (Ag) on the lymphoma cells. We also discuss the mechanisms of this resistance from the

perspectives of radiological and immunological aspects reported in the published literatures. We also propose future prospects for overcoming the resistance and enhancing the efficacy of Y-90 ibritumomab tiuxetan therapy.

## 2 Bulky Disease

Y-90 is a pure  $\beta$ -emitter that produces high-energy radiation (2.3 MeV) at a long path length (an effective path length, 5.3 mm). The  $\beta$ -ray emitted from Y-90 damages the targeted lymphoma cells and also to the neighbor tumor cells that express less of or no CD20 Ag. This “cross fire” effect is thought to be potentially advantageous in treating bulky, poorly vascularized tumors with heterogeneous Ag expression. However, several studies from the early phase of clinical trials with Y-90 ibritumomab tiuxetan have shown that patients with bulky mass have been considered generally resistant to this treatment [7, 8, 10, 11].

The potential cause of therapeutic inefficiency of this pharmaceutical against bulky tumor might be its decreased permeability into the central part of the tumor. In fact, the early tumor dosimetry study demonstrated that tumors  $\geq 15$  cm<sup>3</sup> received only 1082 cGy of the mean radiation absorbed dose with Y-90 ibritumomab tiuxetan, whereas tumors  $< 15$  cm<sup>3</sup> were delivered 4763 cGy radiation [12]. Witizig et al. conducted the phase I/II trial and reported the excellent therapeutic efficacy of IDEC-Y2B8 (Y-90 ibritumomab tiuxetan) for the treatment of 51 patients with relapsed or refractory CD20-positive B-cell low-grade, intermediate-grade, or mantle-cell lymphomas (MCL) [13]. The authors found that the ORR of this agent for the intent-to-treat patients was 67% and the time to disease progression (TTP) in the responders was 12.91 months. They also analyzed baseline prognostic variables that had correlated with the response to treatment and determined that the response rate in patients with bulky mass ( $\geq 7$  cm) was significantly lower than those with lesions less than 7 cm (41% versus 86%,  $p < 0.002$ ). Their stepwise logistic regression analysis clearly showed that three factors, low-grade/follicular histologic type, absence of bone marrow involvement, and non-bulky disease, were independent predictors of the treatment response. Although several reports have found that the highly beneficial therapeutic effect of Y-90 ibritumomab tiuxetan, even in patients with bulky lesions [3, 14–16], the tumor size seemed to be one of the most important factors for the prediction of the response to the therapy.

Indeed, Y-90 ibritumomab tiuxetan localized at the pericellular membrane of CD20-positive lymphoma cells in an autoradiography study [18], but it does not indicate that the  $\beta$ -ray reaches all parts of the tumor tissue especially if a “bulky” tumor is formed. A recent research using astatine-211 conjugated anti-CD20 monoclonal antibody (mAb) in a mouse lymphoma treatment model simply explained different consequences of the treatment outcome on the bulky and non-bulky diseases. Green et al. analyzed the treatment efficacy of this  $\alpha$ -emitting radiopharmaceutical by comparing a bulky tumor (BT) model, in which a solid tumor mass was formed by subcutaneous injection of tumor cells, with a minimal residual disease

(MRD) model, which was established by intravenous injection of tumor cells [19]. Their mouse experiments clearly showed that, although the prolongation of survival was observed, none of the mice were finally cured in the BT model. By contrast, the MRD model evaluated by the bioluminescence imaging method showed that 70% of the animals eliminated the tumor cells. As the  $\alpha$ -ray emitted from astatine-211 reaches a few cell diameters (effective path length, 50–90  $\mu\text{m}$ ), it would not distribute deeply and diffusely enough in the tumor mass. The modest therapeutic efficacy of the  $\alpha$ -emitting radiopharmaceutical in the BT model comparing with the MRD model would be explicable.

In order to overcome the unfavorable influence of bulky tumors on the antibody penetration into the tumor mass, a combined approach with chemotherapy, surgery, or extrabeam radiotherapy (EBRT) prior to Y-90 ibritumomab tiuxetan therapy would be beneficial. A phase III first-line indolent trial (FIT) clearly demonstrated that RIT was highly effective when it was used as consolidation therapy for patients with advanced follicular lymphoma achieving an initial response to first-line induction treatment [20]. Several different chemotherapy reagents have been combined with Y-90 ibritumomab tiuxetan in the first-line induction therapy. The combination therapy of Y-90 ibritumomab tiuxetan with fludarabine, a potent inhibitor of DNA synthesis, and mitoxantrone, a type II topoisomerase inhibitor, was reported to have achieved high ORR (94%) and CRR (47%) for the patients with recurrent or refractory indolent lymphoma [21]. A phase II FLUMIZ trial that included 32.6% of patients having bulky diseases ( $\geq 10$  cm) employed Y-90 ibritumomab tiuxetan as a consolidation therapy after treatment with the fludarabine plus mitoxantrone regimen. Twelve out of the 14 patients who obtained PR after the initial treatment achieved CR after the consolidation therapy with Y-90 ibritumomab tiuxetan, and CRR in the entire treatment regimen was 96.5% (55 of 57 patients) [22]. Another phase II study was conducted by using Y-90 ibritumomab tiuxetan after three cycles of rituximab, cyclophosphamide, doxorubicin, vincristine, and prednisone (R-CHOP) followed by four additional weekly treatments with rituximab [23]. Although half of the patients in this study had bulky disease ( $\geq 5$  cm), CRR assessed by PET imaging resulted in 96% of the patients completing the protocol therapy. Combined with even a short course of chemoimmunotherapy for debulking and extended rituximab treatment in this regimen, Y-90 ibritumomab tiuxetan achieved a high therapeutic effect. Burdick et al. treated 11 patients with relapsed or refractory bulky ( $\geq 5$  cm) follicular lymphoma with EBRT followed by Y-90 ibritumomab tiuxetan [24]. Although 6 patients relapsed and 2 died during a median 36.1 months follow-up, no patients relapsed within the EBRT field. Considering the fact that relapses often occur in the previous mass forming sites [17], EBRT giving to the bulky lesion prior to Y-90 ibritumomab tiuxetan would enhance its therapeutic efficacy and eventually improve clinical outcomes in patients with such a disease.

As in another approach to make a radiopharmaceutical distribute to the deeper portion of a tumor, several smaller formats of full-length mAb, such as a fragment Ag-binding (Fab), Fab prime 2 (F[ab']<sub>2</sub>), single-chain variable (scFv), minibodies (scFv-CH<sub>3</sub> dimers), heavy-chain antibody (HcAb), etc. could be used as therapeutic agents [25]. Because the interstitial fluid pressure inside the tumor tissue is higher

than that of the surrounding tissue, relatively large molecules like mAb hamper their penetration into the tumor [26]. Interestingly, the smaller molecules are less affected by this pressure gradient and are able to distribute throughout the tumor more homogeneously [27]. One of the promising developments is the nanobody, which consists of the variable domain of the heavy-chain antibody (HcAb) and retains a high binding capacity almost equal to the conventional mAb [28]. A growing number of researchers have applied these Ab constructs for imaging [29, 30] and cancer treatment [31, 32]. The nanobody was also tried for its application to RIT in the recent basic research [33].

A pretargeting system has been also introduced for the similar purpose [34]. In this technique, targeting and delivery of radionuclide (RN) are separated. First, the modified and generally smaller-sized mAb, which is not labeled with RN, is administered into a patient. It distributes throughout the body and binds to a specific target Ag. The unbound mAb to the Ag is designed so that it may be quickly cleared from the background tissue, or a specific scavenger reagent is used to remove the residual mAb from the bloodstream. Subsequently, the radiolabeled pharmaceutical, which is also designed to be washed out after a short time if it is not bound to the first mAb, is administered and, ideally, resulting in the highly specific accumulation of RN into the targeted lesion. In order to bind the second administered RN reagent to the first mAb, there are mainly two kinds of methods extensively studied, namely, the avidin-biotin system and the bispecific mAb binding a specific Ag and a hapten. This system not only enhances the radiopharmaceutical accumulation into the tumor but also reduces the radiation dose of the surrounding tissue. Many previous studies have demonstrated that the pretargeting systems provide less hematologic toxicity and more therapeutic efficacy in both animal [35–37] and human [38, 39] models.

### 3 Downregulation of CD20

CD20 is a four-transmembrane protein with intracellular termini, the N- and C-terminal domains, and two extracellular loops [40]. This molecule is expressed on the surface of normal and most malignant B cells, and is absent on the pro-B cells and plasma cells. As antibody-induced internalization does not happen very often, it has become an attractive target for immunotherapy.

Although the function of the CD20 molecule is not fully elucidated yet, it appears to be involved in transmembrane signaling and calcium influx [41]. Both CD20 and CD19 molecules appear to assemble onto lipid rafts [42], which are liquid-ordered membrane microdomains that are thought to function as platforms for signal transduction and act as calcium channels on the cell membrane [43]. Moreover, CD20 and CD19 aggregate together on lipid rafts and function to compartmentalize and stabilize B-cell receptor (BCR) signaling [44]. The cross-linking of CD20 receptors by a specific mAb activates tyrosine kinase activity and initiates downstream signal transduction resulting in the induction of apoptosis [40].



Various levels of CD20 expression were reported, from higher in follicular lymphoma to relatively lower in chronic lymphocytic leukemia, in different types of lymphoma cells [45–47]. A previous clinical study analyzed 272 patients with diffuse large B-cell lymphoma (DLBCL) and showed that 43 (16%) of the patients had reduced CD20 expression [44]. Of these, 35 (13%) patients who were positive for CD19 had a markedly inferior survival following chemotherapy, which was independent of the International Prognostic Index (IPI) and usage of rituximab. Twenty-eight (81%) of the 35 patients with reduced expression of CD20 also expressed strong Bcl-2 antiapoptotic protein, which might be an explanation of the poor prognosis of this population.

The CD20-specific mAb, rituximab, is known to greatly improve the therapeutic efficiency, and since its approval, this mAb has been used as a standard immunotherapy agent for CD20-positive lymphoma patients. Several studies addressed that complement-dependent cytotoxicity (CDC) and antibody-dependent cellular cytotoxicity (ADCC) of rituximab depend on the CD20 expression level on target lymphoma cells [46, 47], though the cell lysis effect of anti-CD20 mAb would be also subjected to the influence of other factors like complement inhibitors such as CD55 and CD59 [46, 48]. High heterogeneity of CD20 expression levels in different types of cells might be reflected in the clinical result, in which the distribution and the intensity of the accumulation of In-111 ibritumomab tiuixetan did not always correlate with the therapeutic responses in patients with CD20-positive B-cell lymphoma who underwent Y-90 ibritumomab tiuixetan therapy [17, 49].

As the CD20 Ag is the same target of both rituximab and Y-90 ibritumomab tiuixetan therapies, a downregulation of this molecule might be raised as one of the causes that malignant lymphoma acquires resistance against Y-90 ibritumomab tiuixetan therapy. Although there has been no direct evidence that Y-90 ibritumomab tiuixetan affected CD20 expression, several studies using rituximab in combination with other chemotherapy agents have reported decreased expression of CD20 molecule after the treatment [50–54]. Hiraga et al. studied 124 patients with CD20-positive B-cell lymphoma and found 30 (29.0%) of these patients relapsed after combination chemotherapy with rituximab [52]. Of these 30 patients, the CD20 expression status was reanalyzed in 19 patients, and CD20-negative transformation was detected in 5 (26.3%) patients. All these 5 patients died within 1 year in spite of salvage chemotherapies, suggesting that the regulation of CD20 would be correlated with poor prognosis. The same group established a CD20-negative cell line from the patient who changed its CD20 status from positive to negative after repeated chemotherapy with rituximab and analyzed the phenotype of this cell line [55]. They suggested that some epigenetic mechanisms like histone deacetylation would be involved in this phenotypic change.

Several mechanisms of the downregulation of CD20 expression after combined chemotherapy with rituximab have been proposed, such as genomic alterations [53, 56], an abnormal CD20 promoter activity [55], and an impairment of the protein transport from the Golgi to the cell membrane [57]. Indeed, the regulation of CD20 expression would involve various transcriptional and posttranscriptional regulatory mechanisms [58].



Many therapeutic regimens have been proposed to increase CD20 expression on the cell surface. These include cytokines such as interleukin (IL)-4, tumor necrosis factor  $\alpha$  (TNF $\alpha$ ), and granulocyte macrophage colony-stimulating factor (GM-CSF) [59]. Tsai et al. found that IL-4 activated the CD20 promoter, increased the expression of CD20 Ag, and enhanced the response to rituximab treatment [57]. Unmethylated CpG oligodeoxynucleotides (CpG ODNs) also upregulate several surface Ags including CD20 on malignant B cells, which probably enhanced Ag-specific immune responses [60]. CpG ODNs resemble the bacterial or viral DNA sequences and revealed to be recognized by toll-like receptor 9 (TLR9) [61]. CpG ODNs are known to activate predominantly the Th1 immune response and facilitate antitumor immunity [62], which is discussed later. In addition, several anticancer drugs have been demonstrated to upregulate CD20 levels [63, 64]. A recent preclinical research showed that gemcitabine enhanced the treatment efficacy of rituximab by upregulation of the CD20 molecules on the lymphoma cell surface [64]. Although it might promote tumor cell proliferation as discussed below, the authors suggested that nuclear factor- $\kappa$ B (NF- $\kappa$ B) activation by gemcitabine was one of the mechanisms of CD20 upregulation.

CD20 internalization may be one of the mechanisms of resistance to Y-90 ibritumomab tiuxetan therapy. Cragg and his colleagues demonstrated that anti-CD20 mAb would be divided into two types, type I (e.g., rituximab, ofatumumab) and II (e.g., tositumomab, obinutuzumab), according to their modulation capability for CD20 redistribution into lipid rafts on the cell membrane [65, 66]. Type I mAbs, not type II mAbs, have an ability to translocate CD20 into lipid rafts and induce internalization of the mAb:CD20 complexes into lysosomes for degradation [67]. Interestingly, the same group reported that the Fc $\gamma$  receptor (Fc $\gamma$ R)IIb on the target B cell plays a crucial role for the internalization [68], which might explain the heterogeneous sensitivity of B-cell lymphomas to rituximab; polymorphisms of the Fc $\gamma$ R in follicular lymphoma patients were found to correlate with clinical responses to rituximab therapy [69]. Lim et al. proposed that an inhibitor of Fc $\gamma$ RIIb might increase the therapeutic efficacy of rituximab [67]. Tipton et al. suggested the type II mAb, obinutuzumab, as the possible therapeutic agent [66] which could block the membrane fluidity [70] and restore the cell surface expression of the CD20 molecule.

Another mechanism for downregulation of the CD20 molecule was proposed as shaving or trogocytosis by Li et al. They found a phenomenon that infused rituximab rapidly bound CD20 on the tumor cells, being accompanied by activated complement deposition [71]. However, this CD20-rituximab complex was removed from the target cells within 1 h after IV infusion of rituximab, which they called "shaving." Because large amount of human Ig inhibited shaving, Fc $\gamma$ RI on the macrophages would be considered to promote this phenomenon. The same group compared the relative contribution of shaving and internalization mentioned above for the downregulation of CD20 [72]. They demonstrated the shaving occurred more rapidly than internalization and suggested that it would be a more predominant reaction than internalization in the loss of CD20 molecule on the cell surface.

Although the detailed mechanism of the regulation of the CD20 expression is not fully understood, the loss of CD20 expression, which might acquire the resistance against rituximab and Y-90 ibritumomab tiuxetan therapies, would result in the deterioration of the patients' prognosis.

## 4 NF- $\kappa$ B Activation

NF- $\kappa$ B is a protein complex of transcription factors and inactivated by binding with a group of inhibitory cytoplasmic proteins, I $\kappa$ B. Upon various kinds of stimuli such as receptor-ligand ligation, cytokines, chemotherapy, radiation, etc., I $\kappa$ B is rapidly phosphorylated, degraded, and dissociated from NF- $\kappa$ B. Then, NF- $\kappa$ B is translocated from the cytoplasm into the nucleus to regulate effector gene transcription including many stress-responsive genes that encode cell proliferation and survival [73]. On the other hand, constitutive NF- $\kappa$ B activation was found in many human cancers. NF- $\kappa$ B activation not only promotes proliferation and suppresses apoptosis of tumor cells but also promotes angiogenesis and facilitates distant metastasis [74], which would be a factor of the mechanism of acquiring the chemo- and radiation-resistance phenotype [75].

Malignant lymphoma, as with other malignancies, presents NF- $\kappa$ B activation. Alizadeh et al. analyzed the gene expression pattern of DLBCL by using DNA microarrays [76]. They identified two distinct gene expression patterns, a germinal center B-cell (GCB) pattern and an activated B-like DLBCL (ABC) pattern, and could discriminate the patients with the GCB pattern lymphoma as having a significantly better overall survival (OS) from those with the ABC pattern lymphoma even among low clinical risk (IPI 0-2) patients. Wilson et al. reported that patients with the GCB pattern lymphoma treated with dose-adjusted etoposide, prednisone, vincristine, cyclophosphamide, doxorubicin, and rituximab (DA-EPOCH-R) showed more favorable TTP and event-free survival than those with the non-GCB (ABC) pattern lymphoma (100%, 94% vs. 67%, 58%, respectively) [77]. Patients with an activating mutation of NF- $\kappa$ B had worse OS than those without mutations, 3-year OS of 26.1% versus 66.7% ( $p = 0.0337$ ) [78]. Fan et al. reported that pre-exposure of 0.1 Gy irradiation increased NF- $\kappa$ B expression and induced radioresistance in mouse epithelial cells that were subsequently exposed with 2 Gy irradiation [79]. Moreover, one of the therapeutic mechanisms of rituximab was suggested to be an inhibition of NF- $\kappa$ B signaling pathway, resulting in a downregulation of an anti-apoptotic factor, Bcl-X<sub>L</sub> [80]. Although a recent work did not detect significant difference in the expression of NF- $\kappa$ B transcription factors between the ABC and the GCB patterns of DLBCL [81], constitutive NF- $\kappa$ B pathway activation has been demonstrated presumably in the ABC pattern lymphoma [75, 82] and more likely to be correlated with the resistance to chemo- and radiotherapy and an unfavorable outcome of the patients.

Bortezomib (Velcade®) is a proteasome inhibitor, binds to the  $\beta$ -subunits of the core of the proteasome, stabilizes the NF- $\kappa$ B inhibitor, I $\kappa$ B, and inactivates NF- $\kappa$ B. Several

Phase II and Phase III trials showed that the treatments with bortezomib alone [83], combination of bortezomib and rituximab [84], and combination of bortezomib, rituximab, and bendamustine [85] were well tolerable and modestly or highly effective in patients with follicular, small lymphocytic, and marginal zone lymphomas.

The effect of bortezomib on radiation sensitivity was analyzed in a previous pre-clinical study. Russo et al. found that NF- $\kappa$ B was activated when a colorectal cancer cell line, LOVO, was irradiated, and its activation was inhibited when the same cell line was pretreated with bortezomib (PS-341) or transduced with an I $\kappa$ B $\alpha$  super-repressor before irradiation [86]. They also demonstrated that apoptosis of LOVO cells was increased and the cell growth in in vitro culture was decreased by the inhibition of radiation-induced NF- $\kappa$ B activation. Hence, bortezomib inhibits NF- $\kappa$ B activation and its antiapoptotic activity, as a consequence, radiation sensitivity is increased. To date, three phase I clinical trials that analyzed the antitumor effect of bortezomib in combination with RIT have been conducted [87–89]. Twelve patients with relapsed or refractory MCL and low-grade B-cell lymphoma were treated with the combination of bortezomib and Y-90 ibritumomab tiuxetan [87]. Of these, 5 patients achieved complete responses (CRs), and 1 patient had a partial response for ORR of 50%, which did not show the powerful efficacy of this treatment regimen. However, ORR of 80% and CR rate (CRR) of 60% in the patients with MCL were higher than those of each study using bortezomib [90] or Y-90 ibritumomab tiuxetan alone [91]. Another study of bortezomib in combination with Y-90 ibritumomab tiuxetan demonstrated ORR of 89% and CRR of 22% [88], and the other trial with I-131 tositumomab showed ORR of 64% and CRR of 44% [89], without life-threatening complications. In the latter trial, ORR and CRR were achieved 10 (91%) and 9 (82%) patients, respectively, when 11 follicular lymphoma patients were analyzed. Ixazomib is a second-generation small-molecule proteasome inhibitor that has a shorter proteasome dissociation half-life and greater tumor to blood ratio of proteasome inhibition than bortezomib [92]. In vitro experiments showed its improved antitumor activity in a variety of mouse models compared with bortezomib [93]. Recently, the phase I clinical study with single agent of ixazomib was conducted for the patients with relapsed/refractory lymphoma, which demonstrated this treatment was safe and achieved durable responses [94]. Ixazomib might be the next promising candidate for the combination regimen with Y-90 ibritumomab tiuxetan.

## 5 Impaired Host Immune Status

### 5.1 Immunoediting

The circumstance of the host immune system in tumor-bearing patients has been elucidated by recent many energetic researchers. To achieve a long-sustained and a durable protection against tumor recurrence, an efficient stimulation of the host immune system, especially T cell immunity, has been proposed to be a prerequisite [95, 96]. To evoke an effective immune response in patients would be equally essential in the Y-90 ibritumomab tiuxetan therapy.

Currently, many tumor-specific Ags have been discovered even in tumors that have spontaneously developed, and it has been considered that at least a part of the host immune system surely preserves a capability of recognizing these Ags [97]. On the other hand, tumors and their surrounding milieus have many mechanisms that actively evade the host immune systems; an upregulation of death-inducing signals like Fas-ligand (Fas-L) [98] and programmed cell death ligand 1 (PD-L1) [99], a cross presentation without costimulatory signals [100], a secretion of suppressive cytokines like transforming growth factor beta (TGF- $\beta$ ) [101] and IL-10 [102], an upregulation of indoleamine 2,3-dioxygenase [103], a reduction of major histocompatibility complex (MHC) type 1 molecules [104], an induction of regulatory T cells (Treg) [105], myeloid derived suppressor cells (MDSC) [106] and M2 macrophages [107], a formation of large solid mass, etc. Indeed, the immunological status in the tumor-bearing host would be generated when balanced finely and dynamically between host-protective and tumor-promoting conditions. Schreiber et al. termed the concept “immunoediting” whereby the immune system would have opposing dual aspects and tumors would “edit” it for bias toward tumor progression [108].

The immunoediting is composed of three sequential phases: elimination, equilibrium, and escape. In the first step, the elimination phase, the host innate and adaptive immune systems destroy transforming cells and eliminate tumors long before they become clinically apparent, which Burnet called as immunological surveillance in 1970 [109]. However, if a part of the tumor cells sneaks out of the host immunosurveillance, it goes into the next phase, equilibrium, which may span for years [110]. During continuing tumor dormancy, the cancer immunoediting occurs. Constant selective pressure of the host immune systems will make tumor cells acquire genetic or epigenetic changes, resulting in an apparent tumor growth. Finally, the tumor cells enter the escape phase in which they continue their progression despite of the ongoing host immune systems [108].

Tumors generated in immunodeficient mice were regressed in immunocompetent hosts, and tumors from immunocompetent hosts tended to be poorly immunogenic and to evade host immune systems when they were inoculated into immunocompetent hosts [111]. Patients receiving immunosuppressive therapy after organ transplantation tended to generate malignancies in a significantly high rate [112]. These observations clearly support the concept of immunoediting, in which the tumor behavior would be defined by a mutual interaction between the tumors and the state of host immune systems. Several previous clinical studies demonstrated that a significant reduction of the overall or complete survival rate of Y-90 ibritumomab tiuxetan therapy was observed in patients with advanced clinical stage [5, 7] and receiving  $\geq 2$  prior treatment regimens before the RIT [5, 9], who might have been to some extent in an immunosuppressive state.

To make the balance of the host immune systems biased toward a stimulatory state in tumor immunity, various kinds of vaccine adjuvants that help vaccines to evoke and enhance Ag-specific immune responses have been attempted [113]. CpG7909, a synthetic 24mer B-class ODN containing 4 unmethylated CpG motifs, binds to TLR9 expressed on plasmacytoid dendritic cells (DCs), B cells, and most non-Hodgkin’s lymphoma cells [114, 115], is one of the efficient vaccine adjuvants, and has been extensively examined for its effect on malignant B-cell lymphomas [116–119].

After ligation of CpG ODN, TLR signaling could upregulate costimulatory molecules, such as CD20, CD40, CD69, CD80, and CD86, expressed on both the Ag-presenting cells (APCs) and the malignant tumor cells, and produce pro-inflammatory cytokines, such as type 1 interferons (IFNs), TNF $\alpha$ , and IL-6 in the tumor microenvironment [120–123]. Although the detailed mechanisms remain unclear, these pathogen-specific innate immune responses would elicit a stimulation of the Ag-specific adaptive immune responses, resulting in a break of the immunotolerance to tumor-specific Ag and an eventual tumor eradication. Witzig et al. conducted a phase I trial of a combined CpG7909 and Y-90 ibritumomab tiuxetan therapy for patients with relapsed/refractory CD20-positive NHL [119]. Among 27 indolent NHL patients, ORR of 93%, CRR of 63%, and median progression-free survival of 40.5 months were much more favorable than in the previous RIT studies. Significant increases in serum IFN $\gamma$ , IL-12, and IL-1 $\beta$  and decreases in IL-10 and TNF $\alpha$  were found, though no definite change of the biodistribution of In-111 ibritumomab tiuxetan was observed in the response to CpG7909 administrations [119].

## 6 Effect of Ionizing Radiation on the Immune Systems

Ionizing radiation is a common therapeutic tool for patients with malignant neoplasms in combination with surgery and chemotherapy. Radiation is basically immunosuppressive because of its cytotoxic effect not only on tumor cells but also surrounding healthy tissues containing immune cells. However, a recent rapid development of technology has made it possible that extremely a high radiation dose is administered only into the tumor field without harmful dose into surrounding normal tissue which contains a variety of immune cells. Besides the advancement in external radiotherapy equipments, Y-90 ibritumomab tiuxetan therapy has appeared as one of the novel products with advancement of bioengineering technology. This RIT can furthermore limit its radiation field to the intensively narrow range around the target tumor cells with minimal suppressive effect on the immune cells. In these circumstances, many studies have been focusing on the influence of radiotherapy on the immune systems [96, 124–129].

Demaria et al. inoculated s.c. a mammary carcinoma in both flanks of syngeneic mice and irradiated only 1 of the 2 tumors at a single dose of 2 or 6 Gy [124]. After the administration of FMS-like tyrosine kinase 3 ligand (Flt3-L), a stimulant of DC, they found that not only the growth of the irradiated tumor but also that of the nonirradiated tumor outside the radiation fields were suppressed in this therapeutic regimen. It is noteworthy that this antitumor effect was tumor specific because the growth of different lymphoma tumors inoculated in the back of the same mice was not regressed. Moreover, this effect was not observed when nude mice were treated in the same manner. These results suggest that the radiation and a DC growth factor have an ability to evoke an efficient systemic immune response against tumors, resulting in an impairment of tumor growth at distant “out-of-field” location

(abscopal effect), and tumor-specific T cells would play a key role of this effect. The demonstrated therapeutic strategy would be a sort of an *in vivo* tumor vaccine, which is explained by the idea that DCs acquired tumor-specific Ags released from the irradiated tumor cells, presented the Ags to effector T cells, and stimulated them to be activated and to proliferate. As a consequence of the induction of tumor-specific T cell maturation, the eradication of both irradiated and nonirradiated tumors was achieved.

RT and chemotherapy could induce immunological cell death (ICD), a cell death which stimulates an immune response against an Ag derived from the dead cell [130]. Zitvogel and Kroemer elucidated some of the factors that are involved in ICD. Ionizing radiation makes irradiated tumor cells expose calreticulin (CRT) on the cell surface (eat-me signal) and release several damage-associated molecular patterns (DAMP), including adenosine triphosphate (ATP) (find-me signal) and nonhistone chromatin protein high-mobility group box 1 (HMGB1) (danger signal). Through the binding of CRT, ATP, and HMGB1 to CD91, purinergic receptor P2X ligand, gated ion channel, 7 (P2RX7), and TLR4, respectively, DCs are stimulated to mature, engulf tumor-derived Ag, secrete IL-1 $\beta$ , and cross-priming of T cells, resulting in activation and proliferation of tumor-specific effector T cells (Fig. 1).

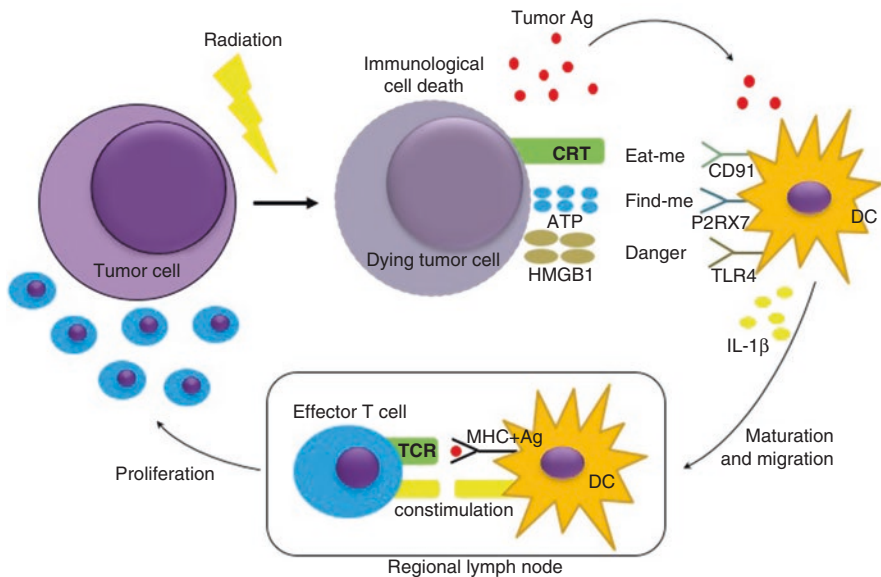


**Fig. 1** When a tumor cell is irradiated, it exposes CRT on the cell surface (eat-me signal) and releases ATP (find-me signal) and HMGB1 (danger signal). CRT, ATP, and HMGB1 bind to CD91, P2RX7, and TLR4 expressed on the DC, respectively. Then, the DC is stimulated to mature, engulfs tumor-derived Ag, secretes IL-1 $\beta$ , and presents tumor-specific Ag to T cells, resulting in activation and proliferation of tumor-specific effector T cells. Ag antigen, CRT calreticulin, ATP adenosine triphosphate, HMGB1 high-mobility group box 1, CD cluster of differentiation, P2RX7 purinergic receptor P2X, ligand gated ion channel, 7, TLR toll-like receptor, DC dendritic cell, IL-1 $\beta$  interleukin-1 beta, MHC major histocompatibility complex, *TCR* T cell receptor



Filatenkov et al. injected s.c. a colon cancer cell line, CT26, in syngeneic mice and analyzed the effect of radiation to the advanced tumor microenvironment [131]. In the nonirradiated tumors, an increased percentage of MDSC (CD11b<sup>+</sup> and Gr-1<sup>hi</sup>) and macrophages (CD11b<sup>+</sup> and Gr-1<sup>lo</sup>), and an increased rate of CD25<sup>+</sup> and Foxp3<sup>+</sup> population of the Treg phenotype in the CD4 T cell population, infiltrated into the tumor tissues, which indicated an immune-suppressed milieu was formed in the tumor microenvironment. After a single dose of 30 Gy local tumor radiation, an intense tumor infiltration of CD8<sup>+</sup> T cells and marked reduction of MDSCs were observed, resulting in disruption of the evasive cell microenvironment and 90% of the mice survived. Experiments using several gene knockout mice and depletion Ab showed this change depended on CD8<sup>+</sup> DCs, secretion of IFN $\gamma$ , and CD4<sup>+</sup> T cells expressing CD40L. A short course of high-dose radiation could transform the tumor microenvironment from an immunosuppressive state into an immunostimulatory one. Intriguingly, an addition of 3 Gy  $\times$  10 days to a single dose of 30 Gy radiation did not only demonstrate restoration of CD8<sup>+</sup> T cells infiltration but also abrogated the therapeutic effect of the first single-dose radiation in this study. Additional daily fractionated radiation decreased CD8<sup>+</sup> T cells and increased MDSCs in the tumor-infiltrated cells [131]. Previous studies showed that radiation might restrain CD8<sup>+</sup> T cells to differentiate into effector cells and infiltrate into the tumor microenvironment [132, 133], and upregulates PD-L1 on tumor cells resulting in the attenuation of antitumor immune responses [134]. It is not clear whether a single high-dose or fractionated radiation brings a more favorable effect on the tumor immunity yet [135]; these results suggest that radiation has a property like a two-edged sword, immunostimulatory and suppressive, in the modulation of tumor immunity.

## 7 Combination of RT and Immune Checkpoint Blockade Therapy

Immune checkpoint molecules have attracted attention over the recent several years. These molecules including programmed cell death-1 (PD-1), PD-L1, cytotoxic T-lymphocyte-associated protein-4 (CTLA-4), etc. are expressed or upregulated on several immune cells including T cells and transduce co-inhibitory signals with each other. It is now generally considered that co-inhibitory and co-stimulatory signals play important roles in the suppression and stimulation of T cell functions, respectively [136]. Co-inhibitory signals physiologically act to suppress T cell function after its activation in order to prevent aberrant or autoreactive T cell overresponses. It has been also elucidated that immune checkpoint molecules presented in tumor tissues are involved in the formation of an immunosuppressive tumor microenvironment [137]. The immune checkpoint blockade might be able to bias the balance of the tumor immune microenvironment and leans toward the immunosuppressive side, toward an immunostimulation dominant state.

There have been robust preclinical data that demonstrated successful antitumor effects of the combination of RT and immune checkpoint blockade therapy. A previous animal experiment showed that local RT, limited within the tumor, alone delayed the tumor growth, though the total survival of the mice was not prolonged compared to that of the control mice [129]. However, mice treated with anti-CTLA-4 mAb after RT demonstrated a statistically significant survival advantage. Moreover, this positive effect on survival seemed to be attributable to the control of lung metastasis formation and the inhibition of metastases that required CD8<sup>+</sup> T cells but not CD4<sup>+</sup> T cells [129]. Another study demonstrated that the administration of anti-CTLA-4 mAb augmented the inhibitory effect of RT not only on the growth of the primary irradiated tumors but also that of the second nonirradiated tumors, which indicated the combination of RT and CTLA-4 blockade is quite efficient on the abscopal effect [138]. Intriguingly, local RT increased tumor-infiltrating T cells in both primary and secondary tumors, while the Treg/effector T cell ratio in both tumors was reversed after CTLA-4 blockade. Several recent reports demonstrated that PDL-1 blockade in combination with RT also enhanced antitumor immunity by decreasing MDSCs [139] and the Treg phenotype [140] and increasing the tumor-specific memory CD8 T cell population. Clinical studies trying to elucidate the efficacy and mechanism of the combination therapy with RT and immune checkpoint blockade on tumor immunity have been examined vigorously [141–145]. Although there have been no published data, for now, the treatment efficacy of the combination of RIT and immune checkpoint blockade therapy would be a highly promising tool for enhancing host antitumor responses.

## 8 Conclusion

Each factor such as bulky disease, downregulation of CD20, or activation of NF- $\kappa$ B, or combination of these discussed above would be, at least partly, a cause of the resistance to Y-90 ibritumomab tiuxetan therapy. However, in order to achieve a prolonged and durable protection against tumor recurrence, an efficient induction of the adaptive immune response, especially T cell immunity, is essential. The balance of host immune responses needs to be biased toward an immunostimulatory state rather than an immunosuppressive one. Ionizing radiation could not only destroy target tumor cells directly but also evoke tumor-specific immune responses in the host immune systems. The immunostimulatory effect of radiation including RIT might be enhanced when combined with several therapeutic approaches. Further studies with the combination of RIT with other reagents are required.

**Acknowledgments** We are indebted to Professors M Harada and K Tamada for their helpful discussions about the immunological cell death and the immune checkpoint blockade therapy.

**Conflict of Interest** No conflict statement: No potential conflicts of interest were disclosed.



## References

1. Witzig TE, White CA, Wiseman GA, Gordon LI, Emmanouilides C, Raubitschek A, Janakiraman N, Gutheil J, Schilder RJ, Spies S, Silverman DH, Parker E, Grillo-López AJ. Phase I/II trial of IDEC-Y2B8 radioimmunotherapy for treatment of relapsed or refractory CD20(+) B-cell non-Hodgkin's lymphoma. *J Clin Oncol.* 1999;17:3793–803.
2. Witzig TE, Flinn IW, Gordon LI, Emmanouilides C, Czuczman MS, Saleh MN, Cripe L, Wiseman G, Olejnik T, Multani PS, White CA. Treatment with ibritumomab tiuxetan radioimmunotherapy in patients with rituximab-refractory follicular non-Hodgkin's lymphoma. *J Clin Oncol.* 2002;20:3262–9.
3. Witzig TE, Gordon LI, Cabanillas F, Czuczman MS, Emmanouilides C, Joyce R, Pohlman BL, Bartlett NL, Wiseman GA, Padre N, Grillo-López AJ, Multani P, White CA. Randomized controlled trial of yttrium-90-labeled ibritumomab tiuxetan radioimmunotherapy versus rituximab immunotherapy for patients with relapsed or refractory low-grade, follicular, or transformed B-cell non-Hodgkin's lymphoma. *J Clin Oncol.* 2002;20:2453–63.
4. Tobinai K, Watanabe T, Ogura M, Morishima Y, Hotta T, Ishizawa K, Itoh K, Okamoto S, Taniwaki M, Tsukamoto N, Okumura H, Terauchi T, Nawano S, Matsusako M, Matsuno Y, Nakamura S, Mori S, Ohashi Y, Hayashi M, Endo K. Japanese phase II study of <sup>90</sup>Y-ibritumomab tiuxetan in patients with relapsed or refractory indolent B-cell lymphoma. *Cancer Sci.* 2009;100:158–64.
5. Uike N, Choi I, Tsuda M, Haji S, Toyoda K, Suehiro Y, Abe Y, Hayashi T, Sawamoto H, Kaneko K, Shimokawa M, Nakagawa M. Factors associated with effects of <sup>90</sup>Y-ibritumomab tiuxetan in patients with relapsed or refractory low-grade B cell non-Hodgkin lymphoma: single-institution experience with 94 Japanese patients in rituximab era. *Int J Hematol.* 2014;100:386–92.
6. Morschhauser F, Radford J, Van Hoof A, Botto B, Rohatiner AZ, Salles G, Soubeyran P, Tilly H, Bischof-Delaloye A, van Putten WL, Klystra JW, Hagenbeek A. <sup>90</sup>Yttrium-ibritumomab tiuxetan consolidation of first remission in advanced-stage follicular non-Hodgkin lymphoma: updated results after a median follow-up of 7.3 years from the International, Randomized, Phase III First-Line Indolent trial. *J Clin Oncol* 2013;31:1977–83.
7. Witzig TE, Molina A, Gordon LI, Emmanouilides C, Schilder RJ, Flinn IW, Darif M, Macklis R, Vo K, Wiseman GA. Long-term responses in patients with recurring or refractory B-cell non-Hodgkin lymphoma treated with yttrium 90 ibritumomab tiuxetan. *Cancer.* 2007;109:1804–10.
8. Fisher RI, Kaminski MS, Wahl RL, Knox SJ, Zelenetz AD, Vose JM, Leonard JP, Kroll S, Goldsmith SJ, Coleman M. Tositumomab and iodine-131 tositumomab produces durable complete remissions in a subset of heavily pretreated patients with low-grade and transformed non-Hodgkin's lymphomas. *J Clin Oncol.* 2005;23:7565–73.
9. Emmanouilides C, Witzig TE, Gordon LI, Vo K, Wiseman GA, Flinn IW, Darif M, Schilder RJ, Molina A. Treatment with yttrium 90 ibritumomab tiuxetan at early relapse is safe and effective in patients with previously treated B-cell non-Hodgkin's lymphoma. *Leuk Lymphoma.* 2006;47:629–36.
10. Rajguru S, Kristinsdottir T, Eickhoff J, Peterson C, Meyer CM, Traynor AM, Kahl BS. Yttrium 90-ibritumomab tiuxetan plus rituximab maintenance as initial therapy for patients with high-tumor-burden follicular lymphoma: a Wisconsin Oncology Network study. *Clin Adv Hematol Oncol.* 2014;12:509–15.
11. Fruchart C, Tilly H, Morschhauser F, Ghesquières H, Bouteloup M, Fermé C, Van Den Neste E, Bordessoule D, Bouabdallah R, Delmer A, Casasnovas RO, Ysebaert L, Ciappuccini R, Briere J, Gisselbrecht C. Upfront consolidation combining yttrium-90 ibritumomab tiuxetan and high-dose therapy with stem cell transplantation in poor-risk patients with diffuse large B cell lymphoma. *Biol Blood Marrow Transplant.* 2014;20:1905–11.

12. Wiseman GA, White CA, Sparks RB, Erwin WD, Podoloff DA, Lamonica D, Bartlett NL, Parker JA, Dunn WL, Spies SM, Belanger R, Witzig TE, Leigh BR. Biodistribution and dosimetry results from a phase III prospectively randomized controlled trial of Zevalin radioimmunotherapy for low-grade, follicular, or transformed B-cell non-Hodgkin's lymphoma. *Crit Rev Oncol Hematol*. 2001;39:181–94.
13. Witzig TE, White CA, Wiseman GA, Gordon LI, Emmanouilides C, Raubitschek A, Janakiraman N, Gutheil J, Schilder RJ, Spies S, Silverman DH, Parker E, Grillo-López AJ. Phase I/II trial of IDEC-Y2B8 radioimmunotherapy for treatment of relapsed or refractory CD20(+) B-cell non-Hodgkin's lymphoma. *J Clinical Oncology*. 1999;17:3793–803.
14. Samaniego F, Berkova Z, Romaguera JE, Fowler N, Fanale MA, Pro B, Shah JJ, McLaughlin P, Sehgal L, Selvaraj V, Braun FK, Mathur R, Feng L, Neelapu SS, Kwak LW. 90Y-ibritumomab tiuxetan radiotherapy as first-line therapy for early stage low-grade B-cell lymphomas, including bulky disease. *Br J Haematol*. 2014;167:207–13.
15. Tamura S, Ikeda T, Kurihara T, Kakuno Y, Nasu H, Nakano Y, Oshima K, Fujimoto T. Bulky pulmonary mucosa-associated lymphoid tissue lymphoma treated with yttrium-90 ibritumomab tiuxetan. *Case Rep Hematol*. 2013;2013:675187. <https://doi.org/10.1155/2013/675187>.
16. Ibatici A, Pica GM, Nati S, Vitolo U, Botto B, Ciochetto C, Petrini M, Galimberti S, Ciabatti E, Orciuolo E, Zinzani PL, Cascavilla N, Guolo F, Fraternali Orcioni G, Carella AM. Safety and efficacy of (90) yttrium-ibritumomab-tiuxetan for untreated follicular lymphoma patients. An Italian cooperative study. *Br J Haematol*. 2014;164:710–6.
17. Gokhale AS, Mayadev J, Pohlman B, Macklis RM. Gamma camera scans and pretreatment tumor volumes as predictors of response and progression after Y-90 anti-CD20 radioimmunotherapy. *Int J Radiat Oncol Biol Phys*. 2005;63:194–201.
18. Jacobs SA, Harrison AM, Swerdlow SH, Foon KA, Avril N, Vidnovic N, Joyce J, DeMonaco N, McCarty KS Jr. Radioisotopic localization of (90)Yttrium-ibritumomab tiuxetan in patients with CD20+ non-Hodgkin's lymphoma. *Mol Imaging Biol*. 2009;11:39–45.
19. Green DJ, Shadman M, Jones JC, Frayo SL, Kenoyer AL, Hylarides MD, Hamlin DK, Wilbur DS, Balkan ER, Lin Y, Miller BW, Frost SH, Gopal AK, Orozco JJ, Gooley TA, Laird KL, Till BG, Bäck T, Sandmaier BM, Pagel JM, Press OW. Astatine-211 conjugated to an anti-CD20 monoclonal antibody eradicates disseminated B-cell lymphoma in a mouse model. *Blood*. 2015;125:2111–9.
20. Morschhauser F, Radford J, Van Hoof A, Vitolo U, Soubeyran P, Tilly H, Huijgens PC, Kolstad A, d'Amore F, Gonzalez Diaz M, Petrini M, Sebban C, Zinzani PL, van Oers MH, van Putten W, Bischof-Delaloye A, Rohatiner A, Salles G, Kuhlmann J, Hagenbeek A. Phase III trial of consolidation therapy with yttrium-90-ibritumomab tiuxetan compared with no additional therapy after first remission in advanced follicular lymphoma. *J Clin Oncol*. 2008;26:5156–64.
21. McLaughlin P, Hagemester FB, Romaguera JE, Sarris AH, Pate O, Younes A, Swan F, Keating M, Cabanillas F. Fludarabine, mitoxantrone, and dexamethasone: an effective new regimen for indolent lymphoma. *J Clin Oncol*. 1996;14:1262–8.
22. Zinzani PL, Tani M, Pulsoni A, Gobbi M, Perotti A, De Luca S, Fabbri A, Zaccaria A, Voso MT, Fattori P, Guardigni L, Ronconi S, Cabras MG, Rigacci L, De Renzo A, Marchi E, Stefoni V, Fina M, Pellegrini C, Musuraca G, Derenzini E, Pileri S, Fanti S, Piccaluga PP, Baccarani M. Fludarabine and mitoxantrone followed by yttrium-90 ibritumomab tiuxetan in previously untreated patients with follicular non-Hodgkin lymphoma trial: a phase II non-randomised trial (FLUMIZ). *Lancet Oncol*. 2008;9:352–8.
23. Jacobs SA, Swerdlow SH, Kant J, Foon KA, Jankowitz R, Land SR, DeMonaco N, Joyce J, Osborn JL, Evans TL, Schaefer PM, Luong TM. Phase II trial of short-course CHOP-R followed by 90Y-ibritumomab tiuxetan and extended rituximab in previously untreated follicular lymphoma. *Clin Cancer Res*. 2008;14:7088–94.

24. Burdick MJ, Neumann D, Pohlman B, Reddy CA, Tendulkar RD, Macklis R. External beam radiotherapy followed by 90Y ibritumomab tiuxetan in relapsed or refractory bulky follicular lymphoma. *Int J Radiat Oncol Biol Phys*. 2011;79:1124–30.
25. Beckman RA, Weiner LM, Davis HM. Antibody constructs in cancer therapy: protein engineering strategies to improve exposure in solid tumors. *Cancer*. 2007;109:170–9.
26. Jain RK, Stylianopoulos T. Delivering nanomedicine to solid tumors. *Nat Rev Clin Oncol*. 2010;7:653–64.
27. Oliveira S, van Dongen GA, Stigter-van Walsum M, Roovers RC, Stam JC, Mali W, van Diest PJ, van Bergen en Henegouwen PM. Rapid visualization of human tumor xenografts through optical imaging with a near-infrared fluorescent anti-epidermal growth factor receptor nanobody. *Mol Imaging*. 2012;11:33–46.
28. Hamers-Casterman C, Atarhouch T, Muyldermans S, Robinson G, Hamers C, Songa EB, Bendahman N, Hamers R. Naturally occurring antibodies devoid of light chains. *Nature*. 1993;363:446–8.
29. Keyaerts M, Xavier C, Heemskerk J, Devoogdt N, Everaert H, Ackaert C, Vanhooij M, Duhoux FP, Gevaert T, Simon P, Schallier D, Fontaine C, Vaneycken I, Vanhove C, De Greve J, Lamote J, Caveliers V, Lahoutte T. Phase I Study of <sup>68</sup>Ga-HER2-Nanobody for PET/CT Assessment of HER2 Expression in Breast Carcinoma. *J Nucl Med*. 2016;57:27–33.
30. Chatalic KL, Veldhoven-Zweistra J, Bolkestein M, Hoeben S, Koning GA, Boerman OC, de Jong M, van Weerden WM. A Novel <sup>111</sup>In-labeled anti-prostate-specific membrane antigen nanobody for targeted SPECT/CT imaging of prostate cancer. *J Nucl Med*. 2015;56:1094–9.
31. Ding L, Tian C, Feng S, Fida G, Zhang C, Ma Y, Ai G, Achilefu S, Gu Y. Small sized EGFR1 and HER2 specific bifunctional antibody for targeted cancer therapy. *Theranostics*. 2015;5:378–98.
32. Kijanka M, Dorresteyn B, Oliveira S, van Bergen en Henegouwen PM. Nanobody-based cancer therapy of solid tumors. *Nanomedicine (Lond)*. 2015;10:161–74.
33. D’Huyvetter M, Vincke C, Xavier C, Aerts A, Impens N, Baatout S, De Raeye H, Muyldermans S, Caveliers V, Devoogdt N, Lahoutte T. Targeted radionuclide therapy with a <sup>177</sup>Lu-labeled anti-HER2 nanobody. *Theranostics*. 2014;4:708–20.
34. Kraeber-Bodéré F, Rousseau C, Bodet-Milin C, Frampas E, Faivre-Chauvet A, Rauscher A, Sharkey RM, Goldenberg DM, Chatal JF, Barbet JA. pretargeting system for tumor PET imaging and radioimmunotherapy. *Front Pharmacol*. 2015 Mar 31;6:54. <https://doi.org/10.3389/fphar.2015.00054>.
35. Axworthy DB, Reno JM, Hylarides MD, Mallett RW, Theodore LJ, Gustavson LM, Su F, Hobson LJ, Beaumier PL, Fritzberg AR. Cure of human carcinoma xenografts by a single dose of pretargeted yttrium-90 with negligible toxicity. *Proc Natl Acad Sci U S A*. 2000;97:1802–7.
36. Pagel JM, Pantelias A, Hedin N, Wilbur S, Saganic L, Lin Y, Axworthy D, Hamlin DK, Wilbur DS, Gopal AK, Press OW. Evaluation of CD20, CD22, and HLA-DR targeting for radioimmunotherapy of B-cell lymphomas. *Cancer Res*. 2007;67:5921–8.
37. Sharkey RM, Karacay H, Litwin S, Rossi EA, McBride WJ, Chang CH, Goldenberg DM. Improved therapeutic results by pretargeted radioimmunotherapy of non-Hodgkin’s lymphoma with a new recombinant, trivalent, anti-CD20, bispecific antibody. *Cancer Res*. 2008;68:5282–90.
38. Chatal JF, Campion L, Kraeber-Bodéré F, Bardet S, Vuillez JP, Charbonnel B, Rohmer V, Chang CH, Sharkey RM, Goldenberg DM, Barbet J, French Endocrine Tumor Group. Survival improvement in patients with medullary thyroid carcinoma who undergo pretargeted anti-carcinoembryonic-antigen radioimmunotherapy: a collaborative study with the French Endocrine Tumor Group. *J Clin Oncol*. 2006;24:1705–11.
39. Salaun PY, Campion L, Bornaud C, Faivre-Chauvet A, Vuillez JP, Taieb D, Ansquer C, Rousseau C, Borson-Chazot F, Bardet S, Oudoux A, Cariou B, Mirallié E, Chang CH, Sharkey RM, Goldenberg DM, Chatal JF, Barbet J, Kraeber-Bodéré F. Phase II trial of anticarcinoembryonic antigen pretargeted radioimmunotherapy in progressive metastatic medullary thyroid carcinoma: biomarker response and survival improvement. *J Nucl Med*. 2012;53:1185–92.

40. Deans JP, Li H, Polyak MJ. CD20-mediated apoptosis: signalling through lipid rafts. *Immunology*. 2002;107:176–82.
41. Li H, Ayer LM, Lytton J, Deans JP. Store-operated cation entry mediated by CD20 in membrane rafts. *J Biol Chem*. 2003;278:42427–34.
42. Brown DA, London E. Structure and function of sphingolipid- and cholesterol-rich membrane rafts. *J Biol Chem*. 2000;275:17221–4.
43. Bubien JK, Zhou LJ, Bell PD, Frizzell RA, Tedder TF. Transfection of the CD20 cell surface molecule into ectopic cell types generates a Ca<sup>2+</sup> conductance found constitutively in B lymphocytes. *J Cell Biol*. 1993;121:1121–32.
44. Johnson NA, Boyle M, Bashashati A, Leach S, Brooks-Wilson A, Sehn LH, Chhanabhai M, Brinkman RR, Connors JM, Weng AP, Gascoyne RD. Diffuse large B-cell lymphoma: reduced CD20 expression is associated with an inferior survival. *Blood*. 2009;113:3773–80.
45. Almasri NM, Duque RE, Iturraspe J, Everett E, Braylan RC. Reduced expression of CD20 antigen as a characteristic marker for chronic lymphocytic leukemia. *Am J Hematol*. 1992;40:259–63.
46. Golay J, Lazzari M, Facchinetti V, Bernasconi S, Borleri G, Barbui T, Rambaldi A, Intronà M. CD20 levels determine the in vitro susceptibility to rituximab and complement of B-cell chronic lymphocytic leukemia: further regulation by CD55 and CD59. *Blood*. 2001;98:3383–9.
47. van Meerten T, van Rijn RS, Hol S, Hagenbeek A, Ebeling SB. Complement-induced cell death by rituximab depends on CD20 expression level and acts complementary to antibody-dependent cellular cytotoxicity. *Clin Cancer Res*. 2006;12:4027–35.
48. Golay J, Zaffaroni L, Vaccari T, Lazzari M, Borleri GM, Bernasconi S, Tedesco F, Rambaldi A, Intronà M. Biologic response of B lymphoma cells to anti-CD20 monoclonal antibody rituximab in vitro: CD55 and CD59 regulate complement-mediated cell lysis. *Blood*. 2000;95:3900–8.
49. Igaru A, Gambhir SS, Goris ML. 90Y-ibrutinomab therapy in refractory non-Hodgkin's lymphoma: observations from 111In-ibrutinomab pretreatment imaging. *J Nucl Med*. 2008;49:1809–12.
50. Davis TA, Czerwinski DK, Levy R. Therapy of B-cell lymphoma with anti-CD20 antibodies can result in the loss of CD20 antigen expression. *Clin Cancer Res*. 1999;5:611–5.
51. Jilani I, O'Brien S, Manshuri T, Thomas DA, Thomazy VA, Imam M, Naem S, Verstovsek S, Kantarjian H, Giles F, Keating M, Albitar M. Transient down-modulation of CD20 by rituximab in patients with chronic lymphocytic leukemia. *Blood*. 2003;102:3514–20.
52. Hiraga J, Tomita A, Sugimoto T, Shimada K, Ito M, Nakamura S, Kiyoi H, Kinoshita T, Naoe T. Down-regulation of CD20 expression in B-cell lymphoma cells after treatment with rituximab-containing combination chemotherapies: its prevalence and clinical significance. *Blood*. 2009;113:4885–93.
53. Nakamaki T, Fukuchi K, Nakashima H, Ariizumi H, Maeda T, Saito B, Yanagisawa K, Tomoyasu S, Homma M, Shiozawa E, Yamochi-Onizuka T, Ota H. CD20 gene deletion causes a CD20-negative relapse in diffuse large B-cell lymphoma. *Eur J Haematol*. 2012;89:350–5.
54. Matsuda I, Hirota S. Bone marrow infiltration of CD20-negative follicular lymphoma after rituximab therapy: a histological mimicker of hematogones and B-cell acute lymphoblastic leukemia/lymphoma. *Int J Clin Exp Pathol*. 2015;8:9737–41.
55. Sugimoto T, Tomita A, Hiraga J, Shimada K, Kiyoi H, Kinoshita T, Naoe T. Escape mechanisms from antibody therapy to lymphoma cells: downregulation of CD20 mRNA by recruitment of the HDAC complex and not by DNA methylation. *Biochem Biophys Res Commun*. 2009;390:48–53.
56. Terui Y, Mishima Y, Sugimura N, Kojima K, Sakurai T, Mishima Y, Kuniyoshi R, Taniyama A, Yokoyama M, Sakajiri S, Takeuchi K, Watanabe C, Takahashi S, Ito Y, Hatake K. Identification of CD20 C-terminal deletion mutations associated with loss of CD20 expression in non-Hodgkin's lymphoma. *Clin Cancer Res*. 2009;15:2523–30.
57. Tsai PC, Hernandez-Ilizaliturri FJ, Bangia N, Olejniczak SH, Czuczman MS. Regulation of CD20 in rituximab-resistant cell lines and B-cell non-Hodgkin lymphoma. *Clin Cancer Res*. 2012;18:1039–50.

58. Czuczman MS, Olejniczak S, Gowda A, Kotowski A, Binder A, Kaur H, Knight J, Starostik P, Deans J, Hernandez-Ilizaliturri FJ. Acquisition of rituximab resistance in lymphoma cell lines is associated with both global CD20 gene and protein down-regulation regulated at the pretranscriptional and posttranscriptional levels. *Clin Cancer Res.* 2008;14:1561–70.
59. Venugopal P, Sivaraman S, Huang XK, Nayini J, Gregory SA, Preisler HD. Effects of cytokines on CD20 antigen expression on tumor cells from patients with chronic lymphocytic leukemia. *Leuk Res.* 2000;24(5):411.
60. Jahrsdörfer B, Hartmann G, Racila E, Jackson W, Mühlhoff L, Meinhardt G, Endres S, Link BK, Krieg AM, Weiner GJ. CpG DNA increases primary malignant B cell expression of costimulatory molecules and target antigens. *J Leukoc Biol.* 2001;69:81–8.
61. Hemmi H, Takeuchi O, Kawai T, Kaisho T, Sato S, Sanjo H, Matsumoto M, Hoshino K, Wagner H, Takeda K, Akira S. A Toll-like receptor recognizes bacterial DNA. *Nature.* 2000;408:740–5.
62. Krieg AM. Development of TLR9 agonists for cancer therapy. *J Clin Invest.* 2007;117:1184–94.
63. Hayashi K, Nagasaki E, Kan S, Ito M, Kamata Y, Homma S, Aiba K. Gemcitabine enhances rituximab-mediated complement-dependent cytotoxicity to B cell lymphoma by CD20 up-regulation. *Cancer Sci.* 2016. <https://doi.org/10.1111/cas.12918>. [Epub ahead of print].
64. Wojciechowski W, Li H, Marshall S, Dell’Agnola C, Espinoza-Delgado I. Enhanced expression of CD20 in human tumor B cells is controlled through ERK-dependent mechanisms. *J Immunol.* 2005;174:7859–68.
65. Cragg MS, Glennie MJ. Antibody specificity controls in vivo effector mechanisms of anti-CD20 reagents. *Blood.* 2004;103:2738–43.
66. Tipton TR, Roghanian A, Oldham RJ, Carter MJ, Cox KL, Mockridge CI, French RR, Dahal LN, Duriez PJ, Hargreaves PG, Cragg MS, Beers SA. Antigenic modulation limits the effector cell mechanisms employed by type I anti-CD20 monoclonal antibodies. *Blood.* 2015;125:1901–9.
67. Lim SH, Vaughan AT, Ashton-Key M, Williams EL, Dixon SV, Chan HT, Beers SA, French RR, Cox KL, Davies AJ, Potter KN, Mockridge CI, Oscier DG, Johnson PW, Cragg MS, Glennie MJ. Fc gamma receptor IIb on target B cells promotes rituximab internalization and reduces clinical efficacy. *Blood.* 2011;118:2530–40.
68. Dransfield I. Inhibitory FcγRIIb and CD20 internalization. *Blood.* 2014;123:606–7.
69. Weng WK, Levy R. Two immunoglobulin G fragment C receptor polymorphisms independently predict response to rituximab in patients with follicular lymphoma. *J Clin Oncol.* 2003;21:3940–7.
70. Lam WA, Rosenbluth MJ, Fletcher DA. Chemotherapy exposure increases leukemia cell stiffness. *Blood.* 2007;109(8):3505.
71. Li Y, Williams ME, Cousar JB, Pawluczko AW, Lindorfer MA, Taylor RP. Rituximab-CD20 complexes are shaved from Z138 mantle cell lymphoma cells in intravenous and subcutaneous SCID mouse models. *J Immunol.* 2007;179:4263–71.
72. Beum PV, Peek EM, Lindorfer MA, Beurskens FJ, Engelberts PJ, Parren PW, van de Winkel JG, Taylor RP. Loss of CD20 and bound CD20 antibody from opsonized B cells occurs more rapidly because of trogocytosis mediated by Fc receptor-expressing effector cells than direct internalization by the B cells. *J Immunol.* 2011;187:3438–47.
73. Wang T, Zhang X, Li JJ. The role of NF-κB in the regulation of cell stress responses. *Int Immunopharmacol.* 2002;2:1509–20.
74. Xia Y, Shen S, Verma IM. NF-κB, an active player in human cancers. *Cancer Immunol Res.* 2014;2:823–30.
75. Turturro F. Constitutive NF-κB activation underlines major mechanism of drug resistance in relapsed refractory diffuse large B cell lymphoma. *Biomed Res Int.* 2015:ID484537.

76. Alizadeh AA, Eisen MB, Davis RE, Ma C, Lossos IS, Rosenwald A, Boldrick JC, Sabet H, Tran T, Yu X, Powell JJ, Yang L, Marti GE, Moore T, Hudson J Jr, Lu L, Lewis DB, Tibshirani R, Sherlock G, Chan WC, Greiner TC, Weisenburger DD, Armitage JO, Warnke R, Levy R, Wilson W, Grever MR, Byrd JC, Botstein D, Brown PO, Staudt LM. Distinct types of diffuse large B-cell lymphoma identified by gene expression profiling. *Nature*. 2000;403:503–11.
77. Wilson WH, Jung SH, Porcu P, Hurd D, Johnson J, Martin SE, Czuczman M, Lai R, Said J, Chadburn A, Jones D, Dunleavy K, Canellos G, Zelenetz AD, Cheson BD, Hsi ED, Cancer Leukemia Group B. A Cancer and Leukemia Group B multi-center study of DA-EPOCH-rituximab in untreated diffuse large B-cell lymphoma with analysis of outcome by molecular subtype. *Haematologica*. 2012;97:758–65.
78. Bohers E, Mareschal S, Bouzeflen A, Marchand V, Ruminy P, Maingonnat C, Ménard AL, Etancelin P, Bertrand P, Dubois S, Alcantara M, Bastard C, Tilly H, Jardin F. Targetable activating mutations are very frequent in GCB and ABC diffuse large B-cell lymphoma. *Genes Chromosomes Cancer*. 2014;53:144–53.
79. Fan M, Ahmed KM, Coleman MC, Spitz DR, Li JJ. Nuclear factor-kappaB and manganese superoxide dismutase mediate adaptive radioresistance in low-dose irradiated mouse skin epithelial cells. *Cancer Res*. 2007;67:3220–8.
80. Jazirehi AR, Huerta-Yepez S, Cheng G, Bonavida B. Rituximab (chimeric anti-CD20 monoclonal antibody) inhibits the constitutive nuclear factor- $\kappa$ B signaling pathway in non-Hodgkin's lymphoma B-cell lines: role in sensitization to chemotherapeutic drug-induced apoptosis. *Cancer Res*. 2005;65:264–76.
81. Odqvist L, Montes-Moreno S, Sánchez-Pacheco RE, Young KH, Martín-Sánchez E, Cereceda L, Sánchez-Verde L, Pajares R, Mollejo M, Fresno MF, Mazorra F, Ruíz-Marcellán C, Sánchez-Beato M, Piris MA. NF $\kappa$ B expression is a feature of both activated B-cell-like and germinal center B-cell-like subtypes of diffuse large B-cell lymphoma. *Mod Pathol*. 2014;27:1331–7.
82. Roschewski M, Staudt LM, Wilson WH. Diffuse large B-cell lymphoma-treatment approaches in the molecular era. *Nat Rev Clin Oncol*. 2014;11:12–23.
83. Di Bella N, Taetle R, Kolibaba K, Boyd T, Raju R, Barrera D, Cochran EW Jr, Dien PY, Lyons R, Schlegel PJ, Vukelja SJ, Boston J, Boehm KA, Wang Y, Asmar L. Results of a phase 2 study of bortezomib in patients with relapsed or refractory indolent lymphoma. *Blood*. 2010;115:475–80.
84. Coiffier B, Osmanov EA, Hong X, Scheliga A, Mayer J, Offner F, Rule S, Teixeira A, Walewski J, de Vos S, Crump M, Shpilberg O, Esseltine DL, Zhu E, Enny C, Theocharous P, van de Velde H, Elsayed YA, Zinzani PL, LYM-3001 Study Investigators. Bortezomib plus rituximab versus rituximab alone in patients with relapsed, rituximab-naïve or rituximab-sensitive, follicular lymphoma: a randomised phase 3 trial. *Lancet Oncol*. 2011;12:773–84.
85. Fowler N, Kahl BS, Lee P, Matous JV, Cashen AF, Jacobs SA, Letzer J, Amin B, Williams ME, Smith S, Saleh A, Rosen P, Shi H, Parasuraman S, Cheson BD. Bortezomib, bendamustine, and rituximab in patients with relapsed or refractory follicular lymphoma: the phase II VERTICAL study. *J Clin Oncol*. 2011;29:3389–95.
86. Russo SM, Tepper JE, Baldwin AS Jr, Liu R, Adams J, Elliott P, Cusack JC Jr. Enhancement of radiosensitivity by proteasome inhibition: implications for a role of NF-kappaB. *Int J Radiat Oncol Biol Phys*. 2001;50:183–93.
87. Beaven AW, Shea TC, Moore DT, Feldman T, Ivanova A, Ferraro M, Ford P, Smith J, Goy A. A phase I study evaluating ibritumomab tiuxetan (Zevalin®) in combination with bortezomib (Velcade®) in relapsed/refractory mantle cell and low grade B-cell non-Hodgkin lymphoma. *Leuk Lymphoma*. 2012;53:254–8.
88. Roy R, Evens AM, Patton D, Gallot L, Larson A, Rademaker A, Cilley J, Spies S, Variakojis D, Gordon LI, Winter JN. Bortezomib may be safely combined with Y-90-ibritumomab tiuxetan in patients with relapsed/refractory follicular non-Hodgkin lymphoma: a phase I trial of combined induction therapy and bortezomib consolidation. *Leuk Lymphoma*. 2013;54:497–502.



89. Elstrom RL, Ruan J, Christos PJ, Martin P, Lebovic D, Osborne J, Goldsmith S, Greenberg J, Furman RR, Avram A, Putman R, Chapman E, Mazumdar M, Griffith K, Coleman M, Leonard JP, Kaminski MS. Phase I study of radiosensitization using bortezomib in patients with relapsed non-Hodgkin lymphoma receiving radioimmunotherapy with 131I-tositumomab. *Leuk Lymphoma*. 2015;56:342–6.
90. Goy A, Bernstein SH, Kahl BS, Djulbegovic B, Robertson MJ, de Vos S, Epner E, Krishnan A, Leonard JP, Lonial S, Nasta S, O'Connor OA, Shi H, Boral AL, Fisher RI. Bortezomib in patients with relapsed or refractory mantle cell lymphoma: updated time-to-event analyses of the multicenter phase 2 PINNACLE study. *Ann Oncol*. 2009;20:520–5.
91. Wang M, Oki Y, Pro B, Romaguera JE, Rodriguez MA, Samaniego F, McLaughlin P, Hagemester F, Neelapu S, Copeland A, Samuels BI, Loyer EM, Ji Y, Younes A. Phase II study of yttrium-90-ibritumomab tiuxetan in patients with relapsed or refractory mantle cell lymphoma. *J Clin Oncol*. 2009;27:5213–8.
92. Kupperman E, Lee EC, Cao Y, Bannerman B, Fitzgerald M, Berger A, Yu J, Yang Y, Hales P, Bruzzese F, Liu J, Blank J, Garcia K, Tsu C, Dick L, Fleming P, Yu L, Manfredi M, Rolfe M, Bolen J. Evaluation of the proteasome inhibitor MLN9708 in preclinical models of human cancer. *Cancer Res*. 2010;70:1970–80.
93. Lee EC, Fitzgerald M, Bannerman B, Donelan J, Bano K, Terkelsen J, Bradley DP, Subakan O, Silva MD, Liu R, Pickard M, Li Z, Tayber O, Li P, Hales P, Carsillo M, Neppalli VT, Berger AJ, Kupperman E, Manfredi M, Bolen JB, Van Ness B, Janz S. Antitumor activity of the investigational proteasome inhibitor MLN9708 in mouse models of B-cell and plasma cell malignancies. *Clin Cancer Res*. 2011;17(23):7313.
94. Assouline SE, Chang J, Cheson BD, Rifkin R, Hamburg S, Reyes R, Hui AM, Yu J, Gupta N, Di Bacco A, Shou Y, Martin P. Phase I dose-escalation study of IV ixazomib, an investigational proteasome inhibitor, in patients with relapsed/refractory lymphoma. *Blood Cancer J*. 2014;4:e251.
95. Crespo J, Sun H, Welling TH, Tian Z, Zou W. T cell anergy, exhaustion, senescence, and stemness in the tumor microenvironment. *Curr Opin Immunol*. 2013;25:214–21.
96. Lee Y, Auh SL, Wang Y, Burnette B, Wang Y, Meng Y, Beckett M, Sharma R, Chin R, Tu T, Weichselbaum RR, Fu YX. Therapeutic effects of ablative radiation on local tumor require CD8+ T cells: changing strategies for cancer treatment. *Blood*. 2009;114:589–95.
97. Sahin U, Türeci O, Schmitt H, Cochlovius B, Johannes T, Schmits R, Stenner F, Luo G, Schobert I, Pfreundschuh M. Human neoplasms elicit multiple specific immune responses in the autologous host. *Proc Natl Acad Sci U S A*. 1995;92:11810–3.
98. Céfal D, Favre L, Wattendorf E, Marti A, Jaggi R, Gimmi CD. Role of Fas ligand expression in promoting escape from immune rejection in a spontaneous tumor model. *Int J Cancer*. 2001;15(91):529–37.
99. Afreen S, Dermime S. The immunoinhibitory B7-H1 molecule as a potential target in cancer: killing many birds with one stone. *Hematol Oncol Stem Cell Ther*. 2014;7:1–17.
100. Gajewski TF, Meng Y, Blank C, Brown I, Kacha A, Kline J, Harlin H. Immune resistance orchestrated by the tumor microenvironment. *Immunol Rev*. 2006;213:131–45.
101. Kim R, Emi M, Tanabe K, Uchida Y, Toge T. The role of Fas ligand and transforming growth factor beta in tumor progression: molecular mechanisms of immune privilege via Fas-mediated apoptosis and potential targets for cancer therapy. *Cancer*. 2004;100:2281–91.
102. Mannino MH, Zhu Z, Xiao H, Bai Q, Wakefield MR, Fang Y. The paradoxical role of IL-10 in immunity and cancer. *Cancer Lett*. 2015;367:103–7.
103. Munn DH, Mellor AL. Indoleamine 2,3 dioxygenase and metabolic control of immune responses. *Trends Immunol*. 2013;34:137–43.
104. Reits EA, Hodge JW, Herbets CA, Groothuis TA, Chakraborty M, Wansley EK, Camphausen K, Luiten RM, de Ru AH, Neijssen J, Griekspoor A, Mesman E, Verreck FA, Spits H, Schlom J, van Veelen P, Neeffjes JJ. Radiation modulates the peptide repertoire, enhances MHC class I expression, and induces successful antitumor immunotherapy. *J Exp Med*. 2006;203:1259–71.

105. Nishikawa H, Sakaguchi S. Regulatory T cells in tumor immunity. *Int J Cancer*. 2010;127:759–67.
106. Marvel D, Gabrilovich DI. Myeloid-derived suppressor cells in the tumor microenvironment: expect the unexpected. *J Clin Invest*. 2015;125:3356–64.
107. Sica A, Schioppa T, Mantovani A, Allavena P. Tumour-associated macrophages are a distinct M2 polarised population promoting tumour progression: potential targets of anti-cancer therapy. *Eur J Cancer*. 2006;42:717–27.
108. Schreiber RD, Old LJ, Smyth MJ. Cancer immunoediting: integrating immunity's roles in cancer suppression and promotion. *Science*. 2011;331:1565–70.
109. Burnet FM. The concept of immunological surveillance. *Prog Exp Tumor Res*. 1970;13:1–27.
110. Swann JB, Smyth MJ. Immune surveillance of tumors. *J Clin Investig*. 2007;117:1137–46.
111. Shankaran V, Ikeda H, Bruce AT, White JM, Swanson PE, Old LJ, Schreiber RD. IFN $\gamma$  and lymphocytes prevent primary tumour development and shape tumour immunogenicity. *Nature*. 2001;410:1107–11.
112. Muenst S, Läubli H, Soysal SD, Zippelius A, Tzankov A, Hoeller S. The immune system and cancer evasion strategies: therapeutic concepts. *J Intern Med*. 2016. <https://doi.org/10.1111/joim.12470>. [Epub ahead of print] *Int Immunol* 2016 Mar 22. pii: dxw015.
113. Temizoz B, Kuroda E, Ishii KJ. Vaccine adjuvants as potential cancer immunotherapeutics. *Int Immunol*. 2016.; pii: dxw015. [Epub ahead of print].
114. Iwasaki A, Medzhitov R. Toll-like receptor control of the adaptive immune responses. *Nat Immunol*. 2004;5:987–95.
115. Bourke E, Bosisio D, Golay J, Polentarutti N, Mantovani A. The toll-like receptor repertoire of human B lymphocytes: inducible and selective expression of TLR9 and TLR10 in normal and transformed cells. *Blood*. 2003;102:956–63.
116. Link BK, Ballas ZK, Weisdorf D, Wooldridge JE, Bossler AD, Shannon M, Rasmussen WL, Krieg AM, Weiner GJ. Oligodeoxynucleotide CpG 7909 delivered as intravenous infusion demonstrates immunologic modulation in patients with previously treated non-Hodgkin lymphoma. *J Immunother*. 2006;29:558–68.
117. Brody JD, Ai WZ, Czerwinski DK, Torchia JA, Levy M, Advani RH, Kim YH, Hoppe RT, Knox SJ, Shin LK, Wapnir I, Tibshirani RJ, Levy R. In situ vaccination with a TLR9 agonist induces systemic lymphoma regression: a phase I/II study. *J Clin Oncol*. 2010;28:4324–32.
118. Zent CS, Smith BJ, Ballas ZK, Wooldridge JE, Link BK, Call TG, Shanafelt TD, Bowen DA, Kay NE, Witzig TE, Weiner GJ. Phase I clinical trial of CpG oligonucleotide 7909 (PF-03512676) in patients with previously treated chronic lymphocytic leukemia. *Leuk Lymphoma*. 2012;53:211–7.
119. Witzig TE, Wiseman GA, Maurer MJ, Habermann TM, Micallef IN, Nowakowski GS, Ansell SM, Colgan JP, Inwards DJ, Porrata LF, Link BK, Zent CS, Johnston PB, Shanafelt TD, Allmer C, Asmann YW, Gupta M, Ballas ZK, Smith BJ, Weiner GJ. A phase I trial of immunostimulatory CpG 7909 oligodeoxynucleotide and 90 yttrium ibritumomab tiuxetan radioimmunotherapy for relapsed B-cell non-Hodgkin lymphoma. *Am J Hematol*. 2013;88:589–93.
120. Jahrsdörfer B, Hartmann G, Racila E, Jackson W, Mühlhoff L, Meinhardt G, Endres S, Link BK, Krieg AM, Weiner GJ. CpG DNA increases primary malignant B cell expression of costimulatory molecules and target antigens. *J Leuk Biol*. 2001;69:81–8.
121. Watts C, West MA, Zaru R. TLR signalling regulated antigen presentation in dendritic cells. *Curr Opin Immunol*. 2010;22:124–30.
122. Iwasaki A, Medzhitov R. Regulation of adaptive immunity by the innate immune system. *Science*. 2010;327:291–5.
123. Decker T, Schneller F, Sparwasser T, Tretter T, Lipford GB, Wagner H, Peschel C. Immunostimulatory CpG-oligonucleotides cause proliferation, cytokine production, and an immunogenic phenotype in chronic lymphocytic leukemia B cells. *Blood*. 2000;95:999–1006.



124. Demaria S, Ng B, Devitt ML, Babb JS, Kawashima N, Liebes L, Formenti SC. Ionizing radiation inhibition of distant untreated tumors (abscopal effect) is immune mediated. *Int J Radiat Oncol Biol Phys.* 2004;58:862–70.
125. Dewan MZ, Galloway AE, Kawashima N, Dewynngaert JK, Babb JS, Formenti SC, Demaria S. Fractionated but not single-dose radiotherapy induces an immune-mediated abscopal effect when combined with anti-CTLA-4 antibody. *Clin Cancer Res.* 2009;15:5379–88.
126. Formenti SC, Demaria S. Combining radiotherapy and cancer immunotherapy: a paradigm shift. *J Natl Cancer Inst.* 2013;105:256–65.
127. Lugade AA, Moran JP, Gerber SA, Rose RC, Frelinger JG, Lord EM. Local radiation therapy of B16 melanoma tumors increases the generation of tumor antigen-specific effector cells that traffic to the tumor. *J Immunol.* 2005;174:7516–23.
128. Gerber SA, Sedlacek AL, Cron KR, Murphy SP, Frelinger JG, Lord EM. IFN- $\gamma$  mediates the antitumor effects of radiation therapy in a murine colon tumor. *Am J Pathol.* 2013;182:2345–54.
129. Demaria S, Kawashima N, Yang AM, Devitt ML, Babb JS, Allison JP, Formenti SC. Immune-mediated inhibition of metastases after treatment with local radiation and CTLA-4 blockade in a mouse model of breast cancer. *Clin Cancer Res.* 2005;11:728–34.
130. Ma Y, Kepp O, Ghiringhelli F, Apetoh L, Aymeric L, Locher C, Tesniere A, Martins I, Ly A, Haynes NM, Smyth MJ, Kroemer G, Zitvogel L. Chemotherapy and radiotherapy: cryptic anticancer vaccines. *Semin Immunol.* 2010;22:113–24.
131. Filatenkov A, Baker J, Mueller AM, Kenkel J, Ahn GO, Dutt S, Zhang N, Kohrt H, Jensen K, Dejbakhsh-Jones S, Shizuru JA, Negrin RN, Engleman EG, Strober S. Ablative tumor radiation can change the tumor immune cell microenvironment to induce durable complete remissions. *Clin Cancer Res.* 2015;21:3727–39.
132. Song CW, Rhee JG, Kim T, Kersey JH, Levitt SH. Effect of x-irradiation on immunocompetency of T-lymphocytes. *Cancer Clin Trials.* 1981;4:331–42.
133. Rosen EM, Fan S, Rockwell S, Goldberg ID. The molecular and cellular basis of radiosensitivity: implications for understanding how normal tissues and tumors respond to therapeutic radiation. *Cancer Investig.* 1999;17:56–72.
134. Dovedi SJ, Adlard AL, Lipowska-Bhalla G, McKenna C, Jones S, Cheadle EJ, Stratford IJ, Poon E, Morrow M, Stewart R, Jones H, Wilkinson RW, Honeychurch J, Illidge TM. Acquired resistance to fractionated radiotherapy can be overcome by concurrent PD-L1 blockade. *Cancer Res.* 2014;74:5458–68.
135. Gandhi SJ, Minn AJ, Vonderheide RH, Wherry EJ, Hahn SM, Maity A. Awakening the immune system with radiation: Optimal dose and fractionation. *Cancer Lett.* 2015;368:185–90.
136. Chen L, Flies DB. Molecular mechanisms of T cell co-stimulation and co-inhibition. *Nat Rev Immunol.* 2013;13:227–42.
137. Shin DS, Ribas A. The evolution of checkpoint blockade as a cancer therapy: what's here, what's next? *Curr Opin Immunol.* 2015;33:23–35.
138. Wu L, Wu MO, De la Maza L, Yun Z, Yu J, Zhao Y, Cho J, de Perrot M. Targeting the inhibitory receptor CTLA-4 on T cells increased abscopal effects in murine mesothelioma model. *Oncotarget.* 2015;6:12468–80.
139. Deng L, Liang H, Burnette B, Beckett M, Darga T, Weichselbaum RR, Fu YX. Irradiation and anti-PD-L1 treatment synergistically promote antitumor immunity in mice. *J Clin Invest.* 2014;124:687–95.
140. Sharabi AB, Nirschl CJ, Kochel CM, Nirschl TR, Francica BJ, Velarde E, Deweese TL, Drake CG. Stereotactic radiation therapy augments antigen-specific PD-1-mediated anti-tumor immune responses via cross-presentation of tumor Antigen. *Cancer Immunol Res.* 2015;3:345–55.
141. Twyman-Saint Victor C, Rech AJ, Maity A, Rengan R, Pauken KE, Stelekati E, Benci JL, Xu B, Dada H, Odorizzi PM, Herati RS, Mansfield KD, Patsch D, Amaravadi RK, Schuchter LM, Ishwaran H, Mick R, Pryma DA, Xu X, Feldman MD, Gangadhar TC, Hahn SM, Wherry EJ, Vonderheide RH, Minn AJ. Radiation and dual checkpoint blockade activate non-redundant immune mechanisms in cancer. *Nature.* 2015;520:373–7.

142. Kwon ED, Drake CG, Scher HI, Fizazi K, Bossi A, van den Eertwegh AJ, Krainer M, Houede N, Santos R, Mahammedi H, Ng S, Maio M, Franke FA, Sundar S, Agarwal N, Bergman AM, Ciuleanu TE, Korbenfeld E, Sengeløv L, Hansen S, Logothetis C, Beer TM, McHenry MB, Gagnier P, Liu D, Gerritsen WR, CA184-043 Investigators. Ipilimumab versus placebo after radiotherapy in patients with metastatic castration-resistant prostate cancer that had progressed after docetaxel chemotherapy (CA184-043): a multicentre, randomised, double-blind, phase 3 trial. *Lancet Oncol.* 2014;15:700–12.
143. Mathew M, Tam M, Ott PA, Pavlick AC, Rush SC, Donahue BR, Golfinos JG, Parker EC, Huang PP, Narayana A. Ipilimumab in melanoma with limited brain metastases treated with stereotactic radiosurgery. *Melanoma Res.* 2013;23:191–5.
144. Alomari AK, Cohen J, Vortmeyer AO, Chiang A, Gettinger S, Goldberg SB, Kluger HM, Chiang VL. Possible interaction of anti-PD-1 therapy with the effects of radiosurgery on brain metastases. *Cancer Immunol Res* 2016. pii: canimm.0238.2015. [Epub ahead of print].
145. Ahmed KA, Stallworth DG, Kim Y, Johnstone PA, Harrison LB, Caudell JJ, Yu HH, Etame AB, Weber JS, Gibney GT. Clinical outcomes of melanoma brain metastases treated with stereotactic radiation and anti-PD-1 therapy. *Ann Oncol.* 2016;27:434–41.

# Features of Ibritumomab as Radionuclide Therapy



**Makoto Hosono**

**Abstract** Ibritumomab tiuxetan labeled with  $^{90}\text{Y}$  is a therapeutic agent for the treatment of patients with relapsed or refractory low-grade, follicular, or transformed B-cell non-Hodgkin's lymphomas. The  $^{111}\text{In}$ -labeled counterpart is used for imaging to verify the biodistribution of ibritumomab tiuxetan prior to therapy by  $^{90}\text{Y}$ -labeled ibritumomab tiuxetan. Ibritumomab tiuxetan has unique features in the application of radioimmunotherapy, which uses antitumor monoclonal antibodies as carrier molecules of radionuclides, and thus involves a potent utilization of monoclonal antibodies to radionuclide therapy. Ibritumomab tiuxetan is one of the limited examples of radioimmunotherapy drugs that have been approved by Food and Drug Administration of the United States and other health authorities of nations. There are advantages of ibritumomab tiuxetan over other radioimmunotherapy drugs that have been studied so far. Theranostic aspects will provide interesting findings on the tumor characteristics and the dosimetry of tumor and normal tissues.

**Keywords** Ibritumomab tiuxetan · Tiuxetan · Zevalin · Radioimmunotherapy · B-cell non-Hodgkin's lymphoma · CD20 · Expected biodistribution · Altered biodistribution · Beta emitter · Theranostic · PET · SPECT

## Abbreviations

$^{90}\text{Y}$	Yttrium-90
DTPA	Diethylenetriaminepentaacetic acid
FDG	18F-fluorodeoxyglucose
Mab	Monoclonal antibody
PET	Positron emission tomography
SPECT	Single-photon emission computed tomography

---

M. Hosono (✉)  
Institute of Advanced Clinical Medicine,  
Kindai University Faculty of Medicine, Osaka, Japan  
e-mail: [hosono@med.kindai.ac.jp](mailto:hosono@med.kindai.ac.jp)

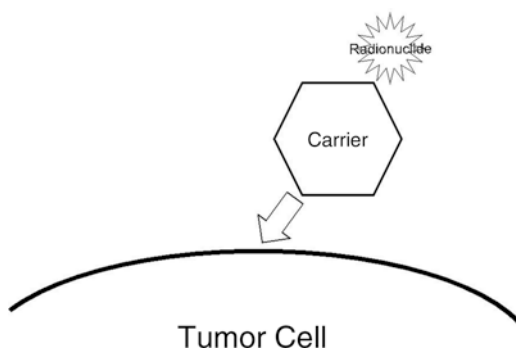
## 1 Introduction

Radionuclide therapy, also referred to nuclear medicine therapy, is based on the use of high-affinity molecules as carriers for the selective delivery of radiation to tumors or target organs [1, 2]. Radiolabeled compounds for radionuclide therapy, or therapeutic radiopharmaceuticals, are usually administered orally, intravenously, intra-arterially, or intracavitarily. Following the administration, such drugs enter the blood and eventually reach their target, that is, a target molecule on the surface of tumor cells or sometimes normal cells, and directly interact with these cells [1, 2]. Some drugs enter inside the cells, and others remain on the surface of the cells. Monoclonal antibodies have been thought to be efficient carrier molecules for the radionuclides to be delivered to the targets.  $^{90}\text{Y}$ -labeled ibritumomab tiuxetan ( $^{90}\text{Y}$ -2B8) is a therapeutic radiopharmaceutical that conjugates an anti-CD20 monoclonal antibody with the beta-emitting radionuclide  $^{90}\text{Y}$  using the well-designed chelating agent tiuxetan. The radionuclide  $^{90}\text{Y}$  is a pure beta emitter with a half-life of 64 h (2.7 days) that decays to  $^{90}\text{Zr}$ . It has high beta energy and an effective path length of 5.3 mm, meaning that 90% of its energy is absorbed within a sphere with a 5.3 mm radius [3]. Ibritumomab tiuxetan was established for the treatment of patients with relapsed or refractory low-grade, follicular, or transformed B-cell non-Hodgkin's lymphomas, including patients with rituximab-refractory follicular lymphoma. Such procedures of radionuclide therapy that utilize antibodies as the carrier molecules of radionuclides are called radioimmunotherapy (Fig. 1).

## 2 Radioimmunotherapy with Ibritumomab

Radionuclide therapy procedures, have long been applied to many neoplasms, and during the course, radioimmunotherapy, which is often shortened as RIT, has been recognized as one of the potent procedures of radionuclide therapy. The main

**Fig. 1** In radionuclide therapy, a radionuclide is delivered to a tumor cell with a carrier, which is an antibody in case of radioimmunotherapy



objective of radionuclide therapy is delivery of radionuclides to cancer cells without any risks for normal tissues, exposure of these cells to highly absorbed doses of ionizing radiation, and their damage. At the present time, the development of novel spatial visualization methods for the assessment of the absorbed dose, both in tumors and normal tissues upon application of TRNT, allows avoiding the side effects and toxicity from excessive irradiation, which leads to personalization of the treatment regimen for every individual patient. This integration of therapy and diagnostics is a fundamental example of the possibilities of a patient [10].

Vast amounts of efforts have been focused on basic and clinical studies for the development of radioimmunotherapy aimed at various neoplasms. So far, indolent B-cell non-Hodgkin's lymphoma is the only neoplasm for which radioimmunotherapy drugs,  $^{90}\text{Y}$ -labeled ibritumomab tiuxetan and  $^{131}\text{I}$ -labeled tositumomab [4], have proved effective and safe enough to be approved by health authorities of nations, [5, 6]. Ibritumomab tiuxetan as well as tositumomab is a CD20-directed radiotherapeutic antibody administered as part of the therapeutic regimen indicated for the treatment of patients with relapsed or refractory, low-grade, or follicular B-cell non-Hodgkin's lymphomas [7].

Studies on radioimmunotherapy against solid tumors have not reached a new drug approval, although antitumor effects were reported as indicated by some investigational endpoints such as response rate, prolonged overall survival or progression-free survival, and improved biomarkers.

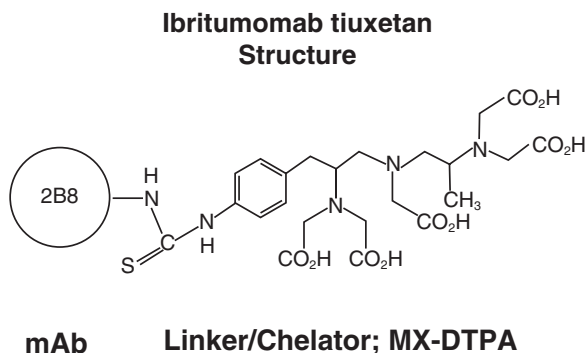
Here, one of the main questions has been to find out ways of extending the success of  $^{90}\text{Y}$ -labeled ibritumomab tiuxetan and  $^{131}\text{I}$ -labeled tositumomab in indolent non-Hodgkin's lymphoma to other types of cancer. Solid tumors are usually more radioresistant than lymphomas, but they may respond to radioimmunotherapy if the lesions are small [8].

For the purpose of reference,  $^{131}\text{I}$ -labeled tositumomab is not supplied into the market any more as of 2016 reportedly due to economic viability on the side of the manufacturer.

One of the key issues, of the development of radioimmunotherapy with ibritumomab is the introduction of the chelating agent tiuxetan [9, 10]. Tiuxetan, [N-[2-bis(carboxymethyl)amino]-3-(p-isothiocyanatophenyl)-propyl]-[N-[2-bis(carboxymethyl)amino]-2-(methyl)-ethyl]glycine, or MX-DTPA is a derivative of diethylenetriaminepentaacetic acid (DTPA) and enables firm binding of antibody and radionuclide as compared to original DTPA (Fig. 2).

There are advantages of monoclonal antibodies as the carrier molecules of radionuclide. They are easily raised against tumor-associated molecules by established methods like the cell fusion/hybridoma method [11]. The monoclonal antibodies, are stable *in vivo* as well as *in vitro*. The conjugation methods of combining monoclonal antibodies and radionuclides are well established. The commercial production of monoclonal antibodies is viable using recombinant techniques and/or proteomics techniques.

**Fig. 2** Structure of the chelating agent tiuxetan and the antibody 2B. (Food and Drug Administration of the United State website; [http://www.fda.gov/ohrms/dockets/ac/01/slides/3782s2\\_01\\_shapiro/sld004.htm](http://www.fda.gov/ohrms/dockets/ac/01/slides/3782s2_01_shapiro/sld004.htm))



### 3 Features of Ibritumomab

Ibritumomab (“2B8”) was raised against the CD20 antigen (Bp35), which is a 35-kDa, cell-surface nonglycosylated, hydrophobic phosphoprotein expressed on normal and malignant B-cells [12–15]. The CD20 antigen does not shed, modulate, or internalize. The CD20 antigen is a transmembrane protein that acts as a calcium channel and plays a key role in cell cycle progression and differentiation of B-cells. One of the advantage of CD20 as a target molecule in the treatment of B-cell lymphoma is that it is reportedly present on approximately 9% of the peripheral blood mononuclear cell fraction and >90% of B-cells from blood and lymphoid organs. Lymphoma cells from >90% of patients with B-cell NHL express this antigen [12–15]. Moreover, CD20 is not expressed on uncommitted hematopoietic precursor stem cells. Studies revealed that when antibodies bind to the CD20 antigen in humans, they induce apoptosis, antibody-dependent cellular cytotoxicity (ADCC), and complement-dependent cytotoxicity (CDC) of lymphoma cells if the antibodies have a human Fc portion of the antibodies that stimulates the immune system of the host. Although CD20 is present on normal B-cells, it appears to be a good tumor target for molecular targeting with antibodies for the treatment of NHL. Ibritumomab was developed as an anti-CD20 MAb and was characterized, and a chimeric 2B8 MAb was constructed and later developed as a US Food and Drug Administration-approved drug, rituximab (unlabeled monoclonal antibody), for NHL therapy. Developed from the same 2B8 mouse hybridoma, ibritumomab is an intact murine IgG1a kappa MAb composed of two murine gamma 1 heavy chains (445 amino acids each) and two kappa light chains (213 amino acids each). With the use of tiuxetan (MX-DTPA) as the linker-chelator,  $^{111}\text{In}$  can be stably linked to ibritumomab for imaging. Alternatively,  $^{90}\text{Y}$ , a pure beta emitter, can be similarly linked to ibritumomab for therapy. MX-DTPA forms a stable covalent urea-type bond with the antibody and chelates the radionuclide via five carboxyl groups and three amino groups. Ibritumomab tiuxetan has an approximate molecular mass of 148 kDa. In the Food and Drug Administration-approved protocol for the  $^{90}\text{Y}$ -ibritumomab tiuxetan therapeutic regimen, 250 mg/m<sup>2</sup> rituximab is given to the patient before the radioactive dose of 185 MBq (5 mCi)/1.6 mg to minimize uptake of  $^{111}\text{In}$ -2B8 by

normal tissues and blood mononuclear cells. An  $^{111}\text{In}$ -2B8 monoclonal antibody scan is performed 48–72 h after administration to detect altered biodistribution of the radiolabeled monoclonal antibody. The commercial kit for the preparation of  $^{111}\text{In}$ -ibritumomab tiuxetan contains 3.2 mg/2 ml ibritumomab tiuxetan in 0.9% sodium chloride solution [3].

## 4 A Model of Theranostic Approach

In some nations and regions, the protocol of clinical application of ibritumomab tiuxetan approved by its health authority includes  $^{111}\text{In}$ -ibritumomab tiuxetan. Therefore, prior to  $^{90}\text{Y}$ -ibritumomab tiuxetan therapy, imaging with  $^{111}\text{In}$ -ibritumomab tiuxetan is performed with the patients according to a therapy protocol implemented there.  $^{111}\text{In}$ -ibritumomab tiuxetan is an immunoconjugate of a murine anti-CD20 monoclonal antibody that is chelated to  $^{111}\text{In}$  for imaging of lymphoid malignancies. It was approved in the United States in 2002 as a required imaging component of the  $^{90}\text{Y}$ -ibritumomab tiuxetan therapeutic regimen for the treatment of patients with relapsed or refractory low-grade, follicular, or transformed B-cell non-Hodgkin's lymphomas, including patients with rituximab-refractory follicular lymphoma.  $^{111}\text{In}$  is a gamma emitter with a physical half-life ( $t(1/2)$ ) of 2.8 days. Thus, in the United States, the therapy protocol did include  $^{111}\text{In}$ -ibritumomab tiuxetan imaging at the time of the approval by the FDA in 2002, but the imaging part "Bioscan" was removed from the protocol requirements. In most parts of Europe, the therapy protocol did not include  $^{111}\text{In}$ -ibritumomab tiuxetan imaging at the time of EU approval in 2004. In some parts of the globe including Japan as of 2016,  $^{111}\text{In}$ -ibritumomab tiuxetan imaging is still a requirement of  $^{90}\text{Y}$ -ibritumomab tiuxetan therapy.

The purpose of  $^{111}\text{In}$ -ibritumomab tiuxetan imaging is to verify the expected biodistribution and exclude patients who show an altered biodistribution, such as the rapid clearance of  $^{111}\text{In}$ -ibritumomab tiuxetan from the blood pool, with prominent liver, spleen, or marrow uptake. Such criteria for expected and altered biodistributions have been proposed and established, based on which the indication of radioimmunotherapy with  $^{90}\text{Y}$ -ibritumomab tiuxetan is assessed.

A high rate of a complete response after  $^{90}\text{Y}$ -ibritumomab tiuxetan therapy has often been observed in patients with negative  $^{111}\text{In}$ -ibritumomab tiuxetan accumulation in lesions [16]. It has been speculated that nonuniformity in the intratumorally absorbed dose plays a significant role in the success or failure of radionuclide therapy. Thus, the association between the tumor response and  $^{111}\text{In}$ -ibritumomab tiuxetan accumulation in lesions should be clarified. For this purpose, single-photon emission computed tomography (SPECT)/CT may have advantages over whole-body planar scans because it provides three-dimensional images by fusing data on function and morphology.  $^{18}\text{F}$ -fluorodeoxyglucose (FDG) positron emission is also important to assess the biological features of tumor.

Another important aspect in the theranostic approaches combining efficiently imaging and therapy in radioimmunotherapy is the application of dosimetry methods which may highlight the assumptions being made in the different dosimetry methodologies.

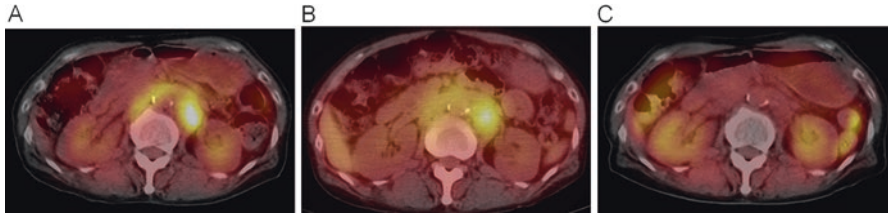


**Fig. 3** A patient with relapsed follicular B-cell non-Hodgkin's lymphoma. (a) Pre-therapy FDG-PET/CT, note the FDG-avid lymphoma lesion (SUVmax, 6.3) around the abdominal aorta. (b) Pre-therapy  $^{111}\text{In}$ -ibritumomab tiuxetan SPECT/CT. High uptake of  $^{111}\text{In}$ -ibritumomab tiuxetan was present. (c) Post-therapy FDG-PET/CT. After  $^{90}\text{Y}$ -ibritumomab tiuxetan complete remission of the para-aortic lesion (SUVmax, 1.4 = background) was achieved

In this context, bremsstrahlung imaging of  $^{90}\text{Y}$ -ibritumomab tiuxetan will be viable to confirm biodistribution and possibly also for the dosimetric calculations (Fig. 3) [17].

## 5 Enhancing Efficacy of Ibritumomab Tiuxetan

For the enhancement of efficacy of ibritumomab tiuxetan as a radioimmunotherapy drug, technologies will progress in two directions [8]. One is the development of pretargeting strategies in which the antibody is not labeled but used to provide binding sites to small molecular weight radioactivity vectors [18–21]. These techniques have been shown to increase tumor to nontarget uptake ratios, and antitumor efficacy has been demonstrated in the clinical studies. This approach is discussed in chapters “Combining RAIT and Immune-Based Therapies to Overcome Resistance in Cancer?” and “Prospects for Enhancing Efficacy of Radioimmunotherapy”. The other approach is the use of various radionuclides adapted to the clinical circumstances. Radionuclides such as lutetium-177 and copper-67 have lower energy of their emission, relatively long half-life and good gamma emission, which may significantly improve efficacy and acceptability. Furthermore, radionuclides emitting particles such as alpha particles or Auger electrons, much more efficient to kill isolated tumor cells, are being tested for radioimmunotherapy [8]. These points are also discussed in chapters “Combining RAIT and Immune-Based Therapies to Overcome Resistance in Cancer?” and “Prospects for Enhancing Efficacy of Radioimmunotherapy”.

## 6 Conclusion

Ibritumomab tiuxetan is one of the most successful radioimmunotherapy agents that achieved drug approvals by health authorities across the globe. The theranostic approach that combines imaging and therapy by considering tumor characterization and dosimetric analysis will enhance the effectiveness and application of the therapy procedure.

**Conflict of Interest** No potential conflicts of interest were disclosed.



## References

1. Chatal JF, Hoefnagel CA. Radionuclide therapy. *Lancet*. 1999;354(9182):931–5.
2. Zukotynski K, Jadvar H, Capala J, Fahey F. Targeted radionuclide therapy: practical applications and future prospects. *Biomark Cancer*. 2016;8(Suppl 2):35–8.
3. Wagner HN Jr, Wiseman GA, Marcus CS, Nabi HA, Nagle CE, Fink-Bennett DM, Lamonica DM, Conti PS. Administration guidelines for radioimmunotherapy of non-Hodgkin's lymphoma with (90)Y-labeled anti-CD20 monoclonal antibody. *J Nucl Med*. 2002;43(2):267–72.
4. Iagaru A, Mitra ES, Ganjoo K, Knox SJ, Goris ML. 131I-Tositumomab (Bexxar) vs. 90Y-Ibritumomab (Zevalin) therapy of low-grade refractory/relapsed non-Hodgkin lymphoma. *Mol Imaging Biol*. 2010;12(2):198–203.
5. Chatal JF, Kraeber-Bodere F, Barbet J. Consolidation radioimmunotherapy of follicular lymphoma: a step towards cure? *Eur J Nucl Med Mol Imaging*. 2008;35(7):1236–9.
6. Kaminski M. Bexxar, iodine I 131 tositumomab, effective in long-term follow-up of non-Hodgkin's lymphoma. *Cancer Biol Ther*. 2007;6(7):996–7.
7. Hanaoka K, Hosono M, Tatsumi Y, Ishii K, Im SW, Tsuchiya N, Sakaguchi K, Matsumura I. Heterogeneity of intratumoral (111)In-ibritumomab tiuxetan and (18)F-FDG distribution in association with therapeutic response in radioimmunotherapy for B-cell non-Hodgkin's lymphoma. *EJNMMI Res*. 2015;5:10.
8. Barbet J, Chatal JF, Kraeber-Bodere F. Radiolabeled antibodies for cancer treatment. *Med Sci (Paris)*. 2009;25(12):1039–45.
9. Jacene HA, Filice R, Kasecamp W, Wahl RL. Comparison of 90Y-ibritumomab tiuxetan and 131I-tositumomab in clinical practice. *J Nucl Med*. 2007;48(11):1767–76.
10. Witzig TE, Molina A, Gordon LI, Emmanouilides C, Schilder RJ, Flinn IW, Darif M, Macklis R, Vo K, Wiseman GA. Long-term responses in patients with recurring or refractory B-cell non-Hodgkin lymphoma treated with yttrium 90 ibritumomab tiuxetan. *Cancer*. 2007;109(9):1804–10.
11. Sands H. Radiolabeled monoclonal antibodies for cancer therapy and diagnosis: is it really a chimera? *J Nucl Med*. 1992;33(1):29–32.
12. Chinn PC, Leonard JE, Rosenberg J, Hanna N, Anderson DR. Preclinical evaluation of 90Y-labeled anti-CD20 monoclonal antibody for treatment of non-Hodgkin's lymphoma. *Int J Oncol*. 1999;15(5):1017–25.
13. Demidem A, Lam T, Alas S, Hariharan K, Hanna N, Bonavida B. Chimeric anti-CD20 (IDEC-C2B8) monoclonal antibody sensitizes a B cell lymphoma cell line to cell killing by cytotoxic drugs. *Cancer Biother Radiopharm*. 1997;12(3):177–86.
14. Grillo-Lopez AJ. Rituximab: an insider's historical perspective. *Semin Oncol*. 2000; 27(6 Suppl 12):9–16.
15. Krasner C, Joyce RM. Zevalin: 90yttrium labeled anti-CD20 (ibritumomab tiuxetan), a new treatment for non-Hodgkin's lymphoma. *Curr Pharm Biotechnol*. 2001;2(4):341–9.
16. Iagaru A, Gambhir SS, Goris ML. 90Y-ibritumomab therapy in refractory non-Hodgkin's lymphoma: observations from 111In-ibritumomab pretreatment imaging. *J Nucl Med*. 2008;49(11):1809–12.
17. Sjogreen-Gleisner K, Dewaraja YK, Chiesa C, Tennvall J, Linden O, Strand SE, Ljungberg M. Dosimetry in patients with B-cell lymphoma treated with [(90)Y]ibritumomab tiuxetan or [(131)I]tositumomab. *Q J Nucl Med Mol Imaging*. 2011;55(2):126–54.
18. Bardies M, Bardet S, Faivre-Chauvet A, Peltier P, Douillard JY, Mahe M, Fiche M, Lisbona A, Giacalone F, Meyer P, et al. Bispecific antibody and iodine-131-labeled bivalent hapten dosimetry in patients with medullary thyroid or small-cell lung cancer. *J Nucl Med*. 1996;37(11):1853–9.
19. Chatal JF, Faivre-Chauvet A, Bardies M, Peltier P, Gautherot E, Barbet J. Bifunctional antibodies for radioimmunotherapy. *Hybridoma*. 1995;14(2):125–8.

20. Hosono M, Hosono MN, Kraeber-Bodere F, Devys A, Thedrez P, Faivre-Chauvet A, Gautherot E, Barbet J, Chatal JF. Two-step targeting and dosimetry for small cell lung cancer xenograft with anti-NCAM/antihistamine bispecific antibody and radioiodinated bivalent hapten. *J Nucl Med.* 1999;40(7):1216–21.
21. Hosono M, Hosono MN, Kraeber-Bodere F, Devys A, Thedrez P, Fiche M, Gautherot E, Barbet J, Chatal JF. Biodistribution and dosimetric study in medullary thyroid cancer xenograft using bispecific antibody and iodine-125-labeled bivalent hapten. *J Nucl Med.* 1998;39(9):1608–13.

# Radiological Evaluation of Response and Resistance of Ibritumomab



Takayoshi Ishimori and Koya Nakatani

**Abstract** Radiolabeled anti-CD20 monoclonal antibody,  $^{90}\text{Y}$ -ibritumomab tiuxetan became available for the treatment of refractory or relapsed low-grade B-cell non-Hodgkin's lymphoma (NHL). Although FDG-PET is widely used for monitoring the response to chemotherapy and radiotherapy, there are limited data for monitoring the response of NHL to radioimmunotherapy (RIT) with FDG-PET.

**Experience in our institute** We retrospectively evaluated our experience using FDG-PET/CT for monitoring the response of NHL to RIT. **Methods** A total of 34 patients received  $^{90}\text{Y}$ -ibritumomab tiuxetan and underwent FDG-PET/CT scans before and at 3 months after RIT. Subsequent scans were performed at 7–12 months and at 12–24 months after RIT. PET/CT scans after additional treatment with clinical evidence of relapse after RIT was excluded from analysis; all patients did not receive additional treatment during the evaluating period. Tumor metabolic activity was assessed before and after RIT visually on PET/CT images and compared with the treatment effect and clinical course. **Results** According to the revised IWC criteria, the maximal response was CR in 22 patients, PR in 5 patients, and PD in 1 patient (1 patient not evaluable). FDG-PET was positive in 10 patients before RIT, 5 patients at 3 months, 5 patients at 7–12 months, and 1 patient at 13 months after RIT. Among 18 patients with negative PET results at 3 months after RIT, only one patient relapsed later. In 2 patients, although PET was positive at 3 months after RIT, abnormal accumulation diminished at 7–9 months after RIT without further treatment.

**Conclusions** FDG-PET/CT is a useful noninvasive imaging modality for monitoring the response of NHL to RIT. Negative PET finding at 3 months after RIT predicts the treatment effects with high probability. However, positive PET results at 3 months after RIT does not warrant immediate additional therapy because the metabolic response to RIT can be gradual, with continued declines of FDG uptake occurring between 7 and 9 months after RIT without additional therapy.

---

T. Ishimori (✉)

Department of Diagnostic Imaging and Nuclear Medicine,  
Kyoto University Graduate School of Medicine, Kyoto, Japan  
e-mail: [ishimori@kuhp.kyoto-u.ac.jp](mailto:ishimori@kuhp.kyoto-u.ac.jp)

K. Nakatani

Department of Diagnostic Radiology, Kurashiki Central Hospital, Kurashiki, Japan

**Keywords** B-cell non-Hodgkin's lymphoma · Follicular lymphoma · Mantle cell lymphoma ·  $^{90}\text{Y}$ -ibritumomab tiuxetan ·  $^{111}\text{In}$ -ibritumomab tiuxetan · Revised IWC criteria · FDG · PET · Metabolic response · Expected biodistribution · Altered biodistribution

## Abbreviations

$^{111}\text{In}$	Indium-111
FDG	18F-fluorodeoxyglucose
MALT	Mucosa-associated lymphoid tissue
PET	Positron emission tomography
RIT	Radioimmunotherapy

## 1 Introduction

Many therapeutic regimens for B-cell lymphomas include the chimeric anti-CD20 monoclonal antibody rituximab, in combination with chemotherapy or alone. Radiolabeled anti-CD20 monoclonal antibody,  $^{90}\text{Y}$ -ibritumomab tiuxetan, as well as  $^{131}\text{I}$ -tositumomab, became available for the treatment of refractory or relapsed low-grade B-cell non-Hodgkin's lymphoma (NHL) as shown in the previous chapters.

FDG-PET is known as a noninvasive imaging modality for disease staging, restaging, and monitoring response of lymphoma to chemotherapy and radiotherapy. Multiple studies have shown that FDG-PET is superior to anatomic imaging for detecting active disease after therapy [1–3].

Although FDG-PET is widely used for monitoring the response to chemotherapy and radiotherapy, there are limited data for monitoring the response of NHL to radioimmunotherapy (RIT) with FDG-PET.

## 2 Evaluation of FDG-PET/CT for Monitoring the Response to RIT

Here we present our experience (in Kurashiki Central Hospital, Kurashiki, Japan) of the evaluation of FDG-PET/CT for monitoring the response of NHL to RIT retrospectively.

A total of 34 clinical patients with relapsed or refractory low-grade B-cell lymphoma who underwent RIT using Y-90-labeled antibody were enrolled in our study (Figs. 1 and 2).

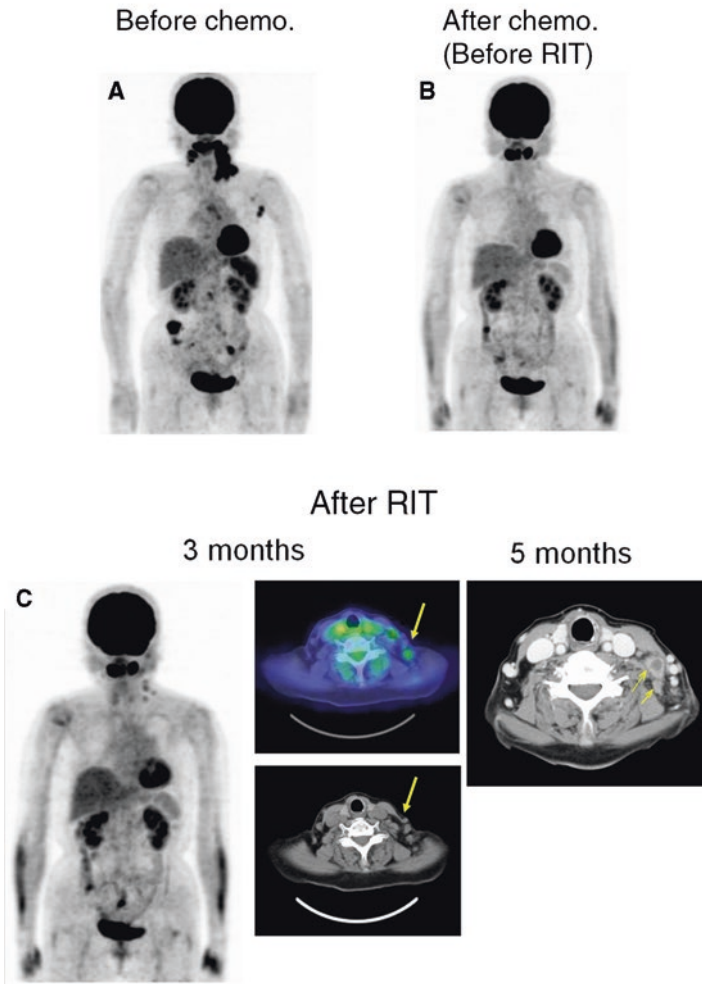


**Fig. 1** (Relapsed case). A 72-year-old female patient with history of follicular lymphoma (grade 3a). She underwent chemotherapy of eight courses of R-THP-COP prior to RIT. FDG-PET images before chemotherapy (**a**) showed multiple FDG-avid nodules in the neck, axilla, spleen, and abdomen before chemotherapy. After chemotherapy (**b**), most of FDG-avid lesions disappeared, while some uptake was still seen in the neck and in the abdomen. At 3 months after RIT (**c**), increased FDG uptake was seen in the neck. At 5 months after RIT, the lymph nodes enlarged and biopsy showed relapse of lymphoma. Afterward she received additional chemotherapy

The patient characteristics are shown in Table 1. Twenty-four patients had follicular lymphoma, while four patients had MALT lymphoma and mantle cell lymphoma. One patient had marginal zone B-cell lymphoma and low-grade B-cell lymphoma not otherwise specified.

All patients received three regimens of chemotherapy before RIT on average (range 1–6).

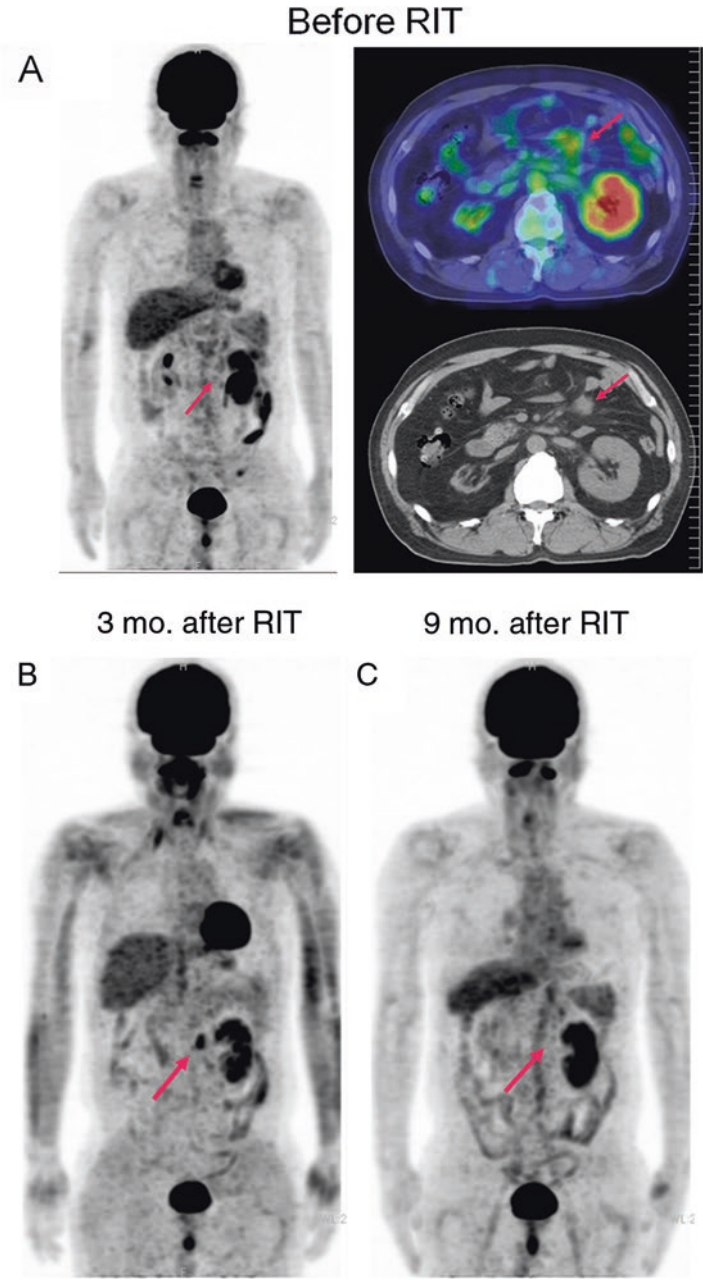


**Fig. 2** (Late responder). A 63-year-old male patient with follicular lymphoma (grade 3). He underwent chemotherapy of R-CHOPx5, DeVICx5, and THP-COPx1 prior to RIT. FDG-PET images before RIT (**a**) (**d**) showed weak FDG accumulation in the mesenteric lymph nodes suggestive of residual lymphoma. At 3 months after RIT (**b**) (**e**), FDG uptake in the abdominal lesion increased. However, the uptake disappeared without additional treatment at 9 months after RIT (**c**) (**f**). The patient achieved CR and did not relapse during the follow-up period, suggestive of transient increase of FDG uptake at 3 months after RIT

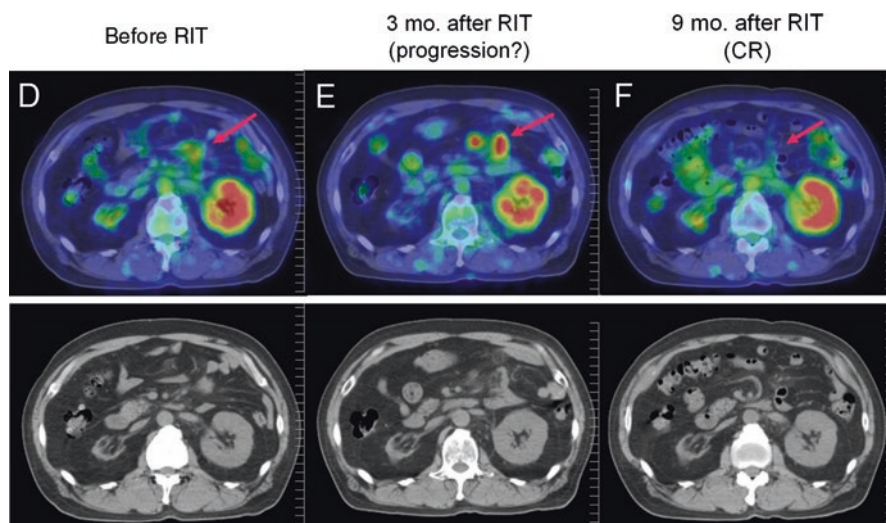


Fig. 2 (continued)

The dose of yttrium-90-labeled antibody for RIT was defined based on the platelet count as follows:

Plt $\geq$ 150,000/ $\mu$ l:	14.8(MBq/kg)	22 patients
Plt 100,000–150,000/ $\mu$ l:	11.1(MBq/kg)	12 patients

Whole-body imaging using indium-labeled antibody was routinely performed 1 week before therapy in all patients to exclude patients with improper distribution of antibody from RIT. However, no patient was excluded from RIT based on the imaging findings.

Yttrium-90-labeled antibody was injected shortly (approx. 1 h) after rituximab pretreatment.

## 2.1 FDG-PET/CT Imaging

A dedicated PET/CT scanner (Aquiduo, Toshiba Medical Systems, Otawara, Japan) was used. After fasting for at least 5 h, each patient received an IV injection of FDG (FDGscan inj., Nihon-Medipysics, Tokyo, Japan). A whole-body PET emission scan was performed 60 min after administration of FDG with our routine protocol. CT images were acquired immediately before the PET scan without the use of contrast media.



**Table 1** Patient characteristics

Total	34 patients
Male	19
Female	15
Age	64.1 ± 10.2 years old (range 43–80 years old)
Histology	
FL <sup>a</sup>	24
MALT <sup>a</sup>	4
Mantle cell	4
MZBCL <sup>a</sup>	1
Others <sup>b</sup>	1
Chemotherapy regimens prior to RIT, 1–6 (mean 3.0)	
Dose of <sup>90</sup> Y-ibritumomab tiuxetan	
14.8(MBq/kg) (Plt ≥ 150,000/μl)	22 pts
11.1(MBq/kg) (Plt 100,000–150,000/μl)	12 pts

<sup>a</sup>*FL* follicular lymphoma, *MALT* mucosa-associated lymphoid tissue lymphoma, *MZBCL* marginal zone B-cell lymphoma

<sup>b</sup>Low-grade B-cell lymphoma not otherwise specified

Tumor metabolic activity was assessed before and after RIT visually on PET/CT images as positive, negative, or inconclusive. PET/CT findings were compared with the treatment effect and clinical course. The maximal treatment response was assessed based on the revised IWC criteria and classified as complete response (CR), partial response (PR), stable disease (SD), and progressive disease (PD) [4].

PET/CT scans after additional treatment with clinical evidence of relapse after RIT were excluded from analysis; all patients did not receive additional treatment during the evaluating period.

### 3 Summary of the Results

The maximal response in all 34 patients during the follow-up period of 91–796 days (median, 420 days) was shown in Table 2. No assessment was available in 1 patient. Four patients relapsed in the study group during the follow-up period.

The overall PET findings before and after RIT are summarized in Table 3. Before RIT, 11 patients were PET positive, while 17 patients were PET negative. After RIT, the number of PET-positive patients decreased by time.

The results of patient subgroups based on PET findings are shown in Tables 4, 5, 6, and 7.



**Table 2** Maximal response

CR	25
PR	7
PD	1
N/A	1
Total	34
Relapsed	4

Follow-up period: 91–796 days (median, 420 days)

**Table 3** Summary of FDG-PET findings before and after RIT

FDG-PET	Before RIT	After RIT		
		3 months	6–12 months	12–24 months
Positive	11	6	5	2
Inconclusive	3	5	3	1
Negative	17	20	8	8
Total	31	31	16	11

**Table 4** PET-positive patients before RIT

FDG-PET	Before RIT			
		3 months	6–12 months	12–24 months
Positive	<b>11</b>	5	3	2
Inconclusive		3	1	1
Negative		3	1	1
N/A			6	7

CR, 5 pts; PR, 5 pts; PD, 1 pt  
Relapsed, 3 pts

Table 4 shows PET-positive results in 11 patients before RIT. After RIT, FDG-PET became negative in three patients, while the other patients became inconclusive or remained PET positive. Although the response rate was high, three patients relapsed during the follow-up period.

Table 5 shows PET-negative results in 17 patients before RIT. Although almost all patients had PET-positive disease initially, these patients became PET-negative after chemotherapy before RIT. After RIT, FDG-PET remained negative in the majority of patients. Sixteen patients achieved CR and no patient relapsed.

Table 6 shows the results of the 6 patients with PET-positive findings at 3 months after RIT. FDG-PET became negative in some patients at subsequent PET scans after 6 months, while some other patients remained PET positive, including 3 relapsed patients.

Table 7 shows PET-negative results in 20 patients at 3 months after RIT. All patients achieved CR and no patient relapsed in this subgroup. In the follow-up PET scans, FDG-PET remained negative in the majority of patients.

**Table 5** PET-negative patients before RIT

FDG-PET	Before RIT	After RIT		
		3 months	6–12 months	12–24 months
Positive		0	0	0
Inconclusive		0	2	0
Negative	<b>17</b>	15	5	5
N/A		2	10	12

CR, 16 pts; N/A, 1 pt

Relapsed, 0 pt

**Table 6** PET-positive patients at 3 months after RIT

FDG-PET	Before RIT	After RIT		
		3 months	6–12 months	12–24 months
Positive	5	<b>6</b>	3	1
Inconclusive				
Negative			2	1
N/A	1		1	4

CR, 2 pts; PR, 3 pts; PD, 1 pt

Relapsed, 3 pts

**Table 7** PET-negative patients 3 months after RIT

FDG-PET	Before RIT	After RIT		
		3 months	6–12 months	12–24 months
Positive	3		0	0
Inconclusive	2		2	0
Negative	15	<b>20</b>	5	7
N/A	0		13	13

CR, 20 pts

Relapsed, 0 pt

## 4 Discussion

FDG-PET/CT is a useful noninvasive imaging technique for monitoring the response of lymphoma to therapy. The response of a tumor to treatment was conventionally evaluated by measuring the tumor size using morphological imaging modalities such as CT and MRI. The determination of treatment response in patients with non-Hodgkin's lymphoma is complicated, and criteria proposed by a National Cancer Institute–sponsored international workshop have been used as a standard system of classification [5]. This system defines categories of complete response, complete response–unconfirmed, partial response, stable disease, and progressive disease. Complete response requires disappearance of all disease at physical examination, normalization of lactate dehydrogenase levels, and CT findings that show that all lymph nodes and nodal masses have regressed to normal size. Partial response requires a greater than 50% decrease in mass size.

However, distinguishing viable residual tumors from fibrotic scars after irradiation is difficult. It is known that FDG-PET can distinguish viable lymphoma from fibrotic change after treatment because most non-Hodgkin's lymphomas are FDG-avid [6–10], and FDG-PET is superior to CT for the assessment of recurrent lymphoma after chemotherapy [11]. Recently, revised criteria for the assessment of lymphoma treatment response were published [4, 12]. We used these criteria for assessment of treatment response of RIT in the present study.

After radioimmunotherapy, Jacene et al. reported FDG uptake in tumors typically dropped significantly and a continued decline in tumor SUVlean max between 12 and 24 weeks without additional therapy can occur, suggesting a need for delayed-response assessment. The information provided by combined 18F-FDG-PET/CT is informative for monitoring the response of lymphoma to radioimmunotherapy [13].

Ulaner et al. reported on 10 patients with refractory or relapsed NHL who underwent 18F-FDG-PET/CT for restaging 4–6 months after <sup>90</sup>Y-ibritumomab tiuxetan, and the results were similar [10]. The use of combined FDG-PET/CT may enable superior assessment of response to <sup>90</sup>Y-ibritumomab tiuxetan treatment than the use of CT alone, at which one may underestimate <sup>90</sup>Y-ibritumomab tiuxetan response by considering inactive residual CT masses to be residual disease.

In another previous report, early assessment of response to RIT by using PET/CT (at 2 months after RIT) might be useful in the identification of patients needing additional therapeutic strategies [14].

Hanaoka et al. reported that a significant difference in pretherapeutic FDG SUVmax was observed between responders and nonresponders and pretherapeutic FDG accumulation was predictive of the tumor response in <sup>90</sup>Y-ibritumomab tiuxetan therapy. The results were consistent with our experience [15].

Quantitative analyses with SUV are not considered necessary to determine PET positivity. We applied IWC-PET criteria in our study to assess response to therapy, although prospective validation of quantitative criteria for determining response may prove helpful in the future, particularly in the setting of residual masses on CT.

The optimal timing to obtain a PET scan after radioimmunotherapy has not been defined. The initial studies evaluating 18F-FDG-PET for monitoring the response of lymphoma were primarily obtained after cytotoxic chemotherapy or radiotherapy. The optimal time to obtain a posttherapy PET is not completely resolved, but a minimum of 10 days after chemotherapy has been recommended, to avoid false-negative and false-positive scan findings due to early treatment effects of stunning and inflammation. Longer and more variable times after external-beam radiation have been suggested. According to our results and literatures, a longer delay to initial response assessment might allow more accurate assessment of a slow responder. Although long delay might not be acceptable in nonresponding patients, the potential benefit from earlier detection of disease and further treatment might not always be critical because the progression of most indolent lymphoma for RIT indication is gradual.

The mechanism of transient increase of FDG accumulation after RIT in our study is not clarified. FDG is not a cancer-specific agent and is known to accumulate in cases of acute inflammation, in granulomatous diseases, and in autoimmune

diseases. Under such conditions, the suggestion is that 18F-FDG is taken up by infiltrating cells such as macrophages, lymphocytes, and granulocytes [16]. In a report of lung cancer patients, FDG is accumulated in the inflammatory tissue of radiation induced pneumonitis and a temporal increase in FDG uptake at 1–2 weeks after stereotactic radiotherapy appeared to reflect the acute reaction of the tumor [17]. The exact mechanism of death of lymphoma cells after RIT is unknown, but it is possible that a combination of a mitotic lymphoma cell death and delayed immunologic effects may contribute to the observed temporal changes of FDG accumulation.

Prior to  $^{90}\text{Y}$ -ibritumomab tiuxetan therapy, imaging with  $^{111}\text{In}$ -ibritumomab tiuxetan may be performed to verify the expected biodistribution and exclude patients who show an altered biodistribution, such as the rapid clearance of  $^{111}\text{In}$ -ibritumomab tiuxetan from the blood pool, with prominent liver, spleen, or marrow uptakes [15]. However, a high rate of a complete response after  $^{90}\text{Y}$ -ibritumomab tiuxetan therapy has often been observed in patients with negative  $^{111}\text{In}$ -ibritumomab tiuxetan accumulation in lesions, and accumulation of  $^{111}\text{In}$ -ibritumomab tiuxetan does not predict treatment effect.

## 5 Conclusions

In conclusion, FDG-PET/CT is a useful noninvasive imaging modality for monitoring the response of NHL to RIT. In our experience, negative PET findings before and at 3 months after RIT predict the treatment effects with high probability. However, positive PET results at 3 months after RIT do not warrant immediate additional therapy because metabolic response to RIT can be gradual, with continued declines of FDG uptake occurring between 7 and 9 months after RIT without additional therapy. The optimal condition of imaging, especially the time interval between the therapy and the FDG-PET/CT scan, is to be established by further prospective studies with a large number of patients.

## References

1. Jerusalem G, Beguin Y, Fassotte MF, et al. Whole-body positron emission tomography using 18F-fluorodeoxyglucose for posttreatment evaluation in Hodgkin's disease and non-Hodgkin's lymphoma has higher diagnostic and prognostic value than classical computed tomography scan imaging. *Blood*. 1999;94:429–33.
2. Naumann R, Vaic A, Beuthien-Baumann B, et al. Prognostic value of positron emission tomography in the evaluation of post-treatment residual mass in patients with Hodgkin's disease and non-Hodgkin's lymphoma. *Br J Haematol*. 2001;115:793–800.
3. Spaepen K, Stroobants S, Dupont P, et al. Prognostic value of positron emission tomography (PET) with fluorine-18 fluorodeoxyglucose ([18F]FDG) after first line chemotherapy in non-Hodgkin's lymphoma: is [18F]FDG-PET a valid alternative to conventional diagnostic methods? *J Clin Oncol*. 2001;19:414–9.

4. Cheson BD, Pfistner B, Juweid ME, et al. Revised response criteria for malignant lymphoma. *J Clin Oncol.* 2007;25:579–86.
5. Cheson BD, Horning SJ, Coiffier B, et al. Report of an international workshop to standardize response criteria for non-Hodgkin's lymphomas. NCI sponsored international working group. *J Clin Oncol.* 1999;17:1244.
6. Conti PS, Lilien DL, Hawley K, Keppler J, Grafton ST, Bading JR. PET and [18F]-FDG in oncology: a clinical update. *Nucl Med Biol.* 1996;23:717–35.
7. Gambhir SS, Czernin J, Schwimmer J, Silverman DH, Coleman RE, Phelps ME. A tabulated summary of the FDG PET literature. *J Nucl Med.* 2001;42(5 Suppl):1S–93S.
8. Joyce JM, Degirmenci B, Jacobs S, McCook B, Avril N. FDG PET CT assessment of treatment response after yttrium-90 ibritumomab tiuxetan radioimmunotherapy. *Clin Nucl Med.* 2005;30:564–8.
9. Torizuka T, Zasadny KR, Kison PV, Rommelfanger SG, Kaminski MS, Wahl RL. Metabolic response of non-Hodgkin's lymphoma to 131I-anti-B1 radioimmunotherapy: evaluation with FDG PET. *J Nucl Med.* 2000;41:999–1005.
10. Ulaner GA, Colletti PM, Conti PS. B-cell non-Hodgkin's lymphoma: PET/CT evaluation after 90Y-ibritumomab tiuxetan radioimmunotherapy: initial experience. *Radiology.* 2008;246:895–902.
11. Hoekstra OS, Ossenkoppele GJ, Golding R, et al. Early treatment response in malignant lymphoma, as determined by planar fluorine-18-fluorodeoxyglucose scintigraphy. *J Nucl Med.* 1993;34:1706–10.
12. Juweid ME, Stroobants S, Hoekstra OS, et al. Use of positron emission tomography for response assessment of lymphoma: consensus of the Imaging Subcommittee of International Harmonization Project in Lymphoma. *J Clin Oncol.* 2007;25:571–8.
13. Jacene HA, et al. FDG PET/CT for monitoring the response of lymphoma to radioimmunotherapy. *J Nucl Med.* 2009;50:8–17.
14. Storto G, et al. Assessment of metabolic response to radioimmunotherapy with 90Y-ibritumomab tiuxetan in patients with relapsed or refractory B-cell non-Hodgkin lymphoma. *Radiology.* 2010;254(1):245–52.
15. Hanaoka K, Hosono M. Et al. Heterogeneity of intratumoral (111)in-ibritumomab tiuxetan and (18)F-FDG distribution in association with therapeutic response in radioimmunotherapy for B-cell non-Hodgkin's lymphoma. *EJNMMI Res.* 2015;5:10. <https://doi.org/10.1186/s13550-015-0093-3>. eCollection 2015.
16. Ishimori T, Saga T, Mamede M, et al. Increased 18F-FDG uptake in a model of inflammation: concanavalin A-mediated lymphocyte activation. *J Nucl Med.* 2002;43:658–63.
17. Ishimori T, Saga T, Nagata Y, et al. 18F-FDG and 11C-methionine PET for evaluation of treatment response of lung cancer after stereotactic radiotherapy. *Ann Nuc Med.* 2004;18:669–74.

# Characteristics of Ibritumomab as Radionuclide Therapy Agent



Hidekazu Kawashima

**Abstract** Ibritumomab tiuxetan was approved by the FDA as the first radiolabeled monoclonal antibody (mAb) for radioimmunotherapy (RIT: a selective internal radiation therapy using radioisotopes conjugated to tumor-directed antibodies or those fragments) in early 2002 and is now widely used for the treatment of B-cell non-Hodgkin's lymphoma (NHL). This pharmaceutical agent consists of the murine anti-CD20 chimeric IgG1 mAb, ibritumomab, which is covalently conjugated with the chelator tiuxetan, permitting stable binding to metal cations. In the clinic, two kinds of radioisotopes can be coupled to ibritumomab tiuxetan, namely  $^{111}\text{In}$  for cancer imaging and  $^{90}\text{Y}$  for the targeted cytotoxic therapy. Dual-label protocols (confirmation of the appropriate mAb distribution using  $^{111}\text{In}$ -ibritumomab tiuxetan, followed by radiotherapy by  $^{90}\text{Y}$ -ibritumomab tiuxetan) can lead to the effective RIT. To better understand how these radiopharmaceuticals achieve “theranostics” (a combination of diagnosis and therapy) against B-cell NHL, the pharmaceutical characteristics of  $^{90}\text{Y}$ -/ $^{111}\text{In}$ -conjugated ibritumomab tiuxetan are outlined in this chapter.

**Keywords** Antigen-antibody reaction · Radioimmunotherapy ·  $\beta^-$ -particle · Cytotoxic radiation ·  $\gamma$  ray · In vivo imaging · Theranostics

## Abbreviations

%ID/g	% injected dose per gram of tissue
$^{111}\text{In}$	Indium-111
$^{90}\text{Y}$	Yttrium-90
ADCC	Antibody-dependent cellular cytotoxicity

---

H. Kawashima (✉)  
Radioisotope Research Center,  
Kyoto Pharmaceutical University, Yamashina-ku, Kyoto, Japan  
e-mail: [kawap@mb.kyoto-phu.ac.jp](mailto:kawap@mb.kyoto-phu.ac.jp)

CDC	Complement-dependent cytotoxicity
DTPA	Diethylenetriaminepentaacetic acid
HAMA	Human antimurine antibody
$K_d$	Dissociation constant
mAb	Monoclonal antibody
MIRD	Medical Internal Radiation Dose
NHL	Non-Hodgkin's lymphoma
PET	Positron emission tomography
RIT	Radioimmunotherapy
SPECT	Single-photon emission computed tomography

## 1 Introduction

Hodgkin's lymphoma (HL) was the first form of lymphoma described and defined by Thomas Hodgkin in 1832 [1]. Histopathological characteristic of this disease is the existence of often multinucleated Hodgkin cells and Reed-Sternberg cells [2]. HL accounts for ~1% of all cancers, and any kind of lymphoma except HL is categorized into NHL. NHL is the most common malignant hematologic disease, and the individual pathological conditions are well characterized by neoplastic transformation of a lymphoid cell that vary significantly in its severity (85% are B-cell derived and 15% are of T-cell origin) [3–5]. Epidemiological survey revealed that the number of new cases of NHL yearly was 19.7 per 100,000 (based on 2008–2012) and the 5-year survival rate was 70% (based on 2005–2011) [6].

mAbs have played an important role in cancer therapy. Among them, anti-CD20 mAbs such as rituximab, ofatumumab, and obinutuzumab are approved for the treatment of B-cell NHL [7–10] (Fig. 1). One of the proposed mechanisms to kill cells by these naked mAbs is attributed to anti-CD20-induced cell-mediated cytotoxicity (antibody-dependent cellular cytotoxicity (ADCC)), complement-dependent cytotoxicity (CDC), and apoptosis [11]. Because NHL is a radiosensitive malignancy, several mAbs conjugated with cytotoxic radioisotopes have been developed in recent years to enhance the therapeutic effect on NHL [12–14].

Ibritumomab tiuxetan (Zevalin®) is a mAb for RIT, which is applied to relapsed or refractory low-grade, follicular, or transformed B-cell NHL and rituximab-refractory B-cell NHL [15]. This antibody preparation is composed of murine anti-CD20 mAb ibritumomab (IDEC-2B8) and amino directed bifunctional chelate tiuxetan (MX-DTPA), to which a radioisotope (either  $^{90}\text{Y}$  for RIT or  $^{111}\text{In}$  for imaging) is coordinated. When  $^{90}\text{Y}$ -ibritumomab tiuxetan binds specifically to the CD20 antigen on the surface of malignant B-cells, ionizing radiation  $\beta$ -particle from the attached isotope will lesion the targeted cells and some neighboring cells (Fig. 2a). The major advantage of RIT is derived from the potential to enhance the cytotoxicity via a radiation “cross-fire effect” [16, 17] (Fig. 2b). Additionally, nonradioactive ibritumomab tiuxetan itself could trigger cell death via anti-CD20-dependent cytotoxic reactions like rituximab.



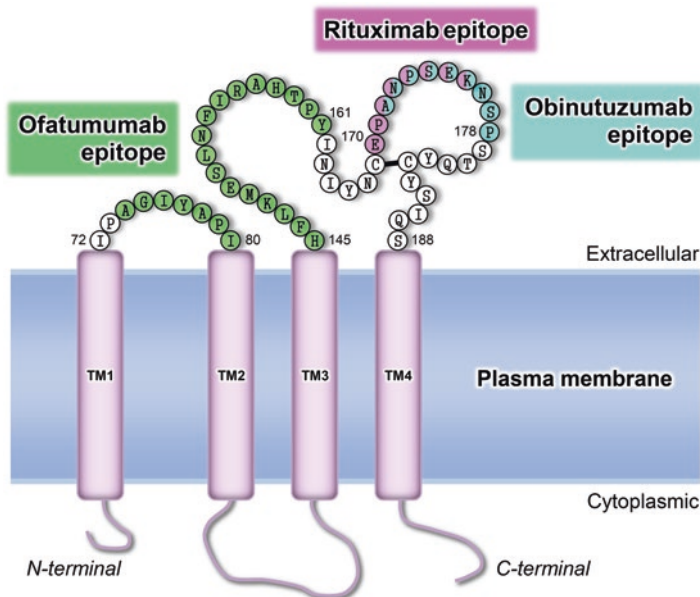


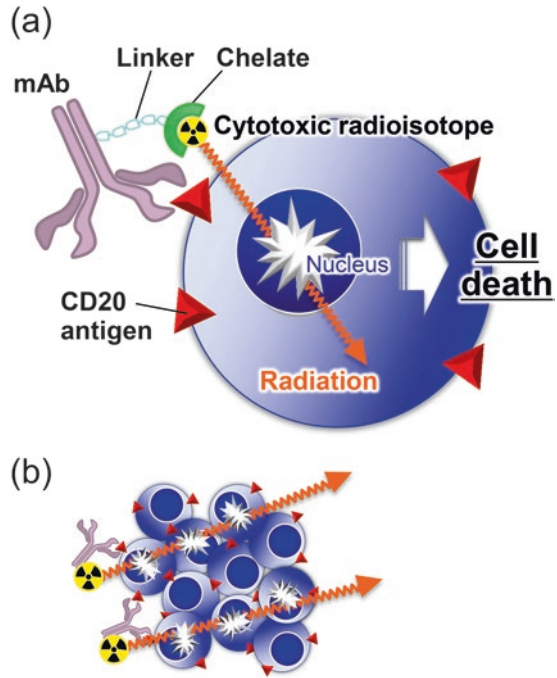
**Fig. 1** The structure of CD20 antigen and the epitopes recognized by rituximab, ofatumumab, and obinutuzumab. The CD20 consists of 297 amino acid residues. This protein possesses intracellular termini and spans the plasma membrane four times. Rituximab and ofatumumab bind to different epitopes, whereas obinutuzumab recognizes partially an overlapping epitope that exists in the large loop between the transmembrane regions TM3 and TM4

Based on the aforementioned background here,  $^{90}\text{Y}/^{111}\text{In}$ -ibritumomab tiuxetan is segmented into its components, and those characteristics are described. Furthermore, this chapter also focuses on clinical protocols (preparation procedure and method for administration) of the radioisotope-conjugated mAb, as well as the preclinical pharmacokinetic observations.

## 2 CD 20: B-Cell Antigen

The CD20 antigen is a 33-kDa (297 amino acids), phosphorylated transmembrane protein. CD20 exists as a tetramer in a heterogeneous complex with other minor components [18] and located not only on the surface of pre-B cells and mature B cells in the bone marrow but also on more than 90% of B-cell NHL tumors [19–23]. CD20 is not expressed on hematopoietic stem cells, and during B-cell maturation, is first expressed in the middle stage of B-lymphoblasts, and is lost toward the final stage to plasma cells. Although native ligand(s) for CD20 remain undiscovered, this protein acts as a  $\text{Ca}^{2+}$  ion channel [24] and is directly involved in the differentiation and proliferation of B-cell during the inactivation [25, 26]. CD20 becomes phosphorylated by ubiquitous kinases after stimulation of the

**Fig. 2** (a) Schematic diagram of RIT for CD20-positive NHL achieved by a radioisotope-conjugated mAb. Irradiated cells absorb high amounts of energy, which promote not only the direct DNA damage but also the generation of cytotoxic radicals. (b) Representation of the “cross-fire effect.” In the internal radiation therapy including RIT, tumor-adjacent cells which do not express the tumor antigens can also be lesioned



B-cell, which is considered to participate in the regulation of intracellular calcium ion level [24, 27, 28]. The binding of mAbs to CD20 induces several intracellular signal transductions which result in (1) serine/threonine and tyrosine phosphorylation of cellular proteins [29], (2) induction of oncogene expression [30], (3) activation of protein tyrosine kinases that induce homotypic adhesion B-cells [31], and (4) expression of other types of major histocompatibility complex (MHC) class II molecules as well as CD antigens [32, 33].

The presence of CD20 on normal B-cells is lower than that of B-cell NHL ( $8 \times 10^3$ – $1.5 \times 10^4$  molecules/cell vs.  $9 \times 10^4$  molecules/cell, respectively) [34]. Moreover, CD20 is not internalized or downregulated after antibody binding [35–37] so that this antigen appears to be a good therapeutic target for most B-cell NHL by using antibodies. Other types of CD molecules such as CD19, CD22, CD30, CD40, and CD80 have also been selected as target candidates for the treatment of NHL [38–44]; however, anti-CD20 mAb is now widely used for the immunotherapy.

### 3 mAb Targeting CD20

mAbs are monospecific antibodies generated by identical immune cells, which are clones of a unique parent cell. In contrast to polyclonal antibodies, mAbs have monovalent affinity and are able to bind to the same epitope. Murine antibodies against tumor cell surface antigens have been generated by virtue of the development of

hybridoma technology. A range of chronic mAbs have been developed against hematologic malignancies as well as solid tumors and hematologic malignancies and entered clinical trials [45].

However, the murine origin of mAbs often produces toxic immunogenic responses in humans [46]. The generation of human antimurine antibodies (HAMAs) induces significantly a reduction to the amount of specific uptake of the mAbs to the tumor site and prevents the use of multiple dosing schedules [47]. To circumvent the limitation of utilizing murine antibodies, chimeric, humanized, or fully human mAbs have been developed [48]. Chimeric mAbs possess the constant domains (Fc domain) of the human IgG combined with the murine variable regions (Fv fragment) by transgenic fusion of the immunoglobulin genes. The chimeric mAbs were produced from engineered hybridomas and Chinese hamster ovary (CHO) cells [48, 49]. The use of chimeric antibodies reduced the HAMA responses to some extent [50, 51].

Rituximab, a chimeric mAb directed against the CD20 antigen, is the first therapeutic antibody preparation approved for the treatment of NHL patients and has already been clinically applied. Rituximab is a type I mAb which binds to the large loop of CD20 [52] (Fig. 1). When antibodies bind to CD20 antigen, the Fc portion of the rituximab binds to the Fc receptors on the surface of cytotoxic T cells or natural killer cells and triggers a lytic reaction leading to cell death or phagocytosis known as ADCC. The antibody also leads to activation of the complement cascade, resulting in cell lysis (CDC) [11, 18].

In a field of RIT, two examples have been extended by  $^{90}\text{Y}$ -ibritumomab tiuxetan and iodine-131-labeled tositumomab ( $^{131}\text{I}$ -tositumomab, Bexxar®), though the latter was discontinued on 2014. Both of them, cytotoxic radioisotopes, are conjugated to murine IgGs (ibritumomab is IgG1  $\kappa$ -mAb, whereas tositumomab is IgG2a  $\lambda$ -mAb) that bind specifically to the CD20 antigen like rituximab [53].

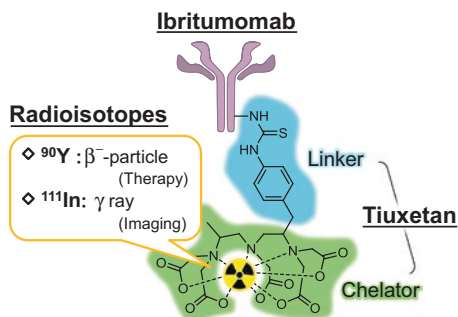
## 4 Ibritumomab Tiuxetan Coupled with Radioisotopes

Ibritumomab, an equivalent of rituximab that targets the same epitope on the CD20 antigen, was developed by IDEC Pharmaceuticals. Radioactive metal ions such as  $^{90}\text{Y}$  or  $^{111}\text{In}$  can be attached to this mAb through a linker metal chelator, called tiuxetan (alias MX-DTPA). Tiuxetan is linked to ibritumomab via a thiourea covalent bond and provides a stable binding site for these radioisotopes (Fig. 3). By using tiuxetan,  $^{111}\text{In}$  can be linked to ibritumomab for imaging of lymphoid malignancies, whereas  $^{90}\text{Y}$  can be similarly linked for the therapy [54–57].

### 4.1 Ibritumomab

Ibritumomab is a murine anti-CD20 chimeric IgG1 mAb [58–62]. 2B8 mAbs (rituximab and ibritumomab) were synthesized based on the hybridoma technique [19, 63]. BALB/c mice were immunized with the human lymphoblastoid cell line

**Fig. 3** Scheme of  $^{90}\text{Y}$ -/ $^{111}\text{In}$ -ibritumomab tiuxetan, which consists of three part: anti CD20 antibody (ibritumomab), radioisotope to perform theranostics ( $^{90}\text{Y}$  or  $^{111}\text{In}$ ), and the linker-chelating unit (tiuxetan)



SB, the spleens were isolated, and the splenocytes were fused with the mouse myeloma SP2/0 [64]. Ibritumomab is a 1316 amino acid IgG1 antibody. It consists of two  $\kappa$ -light chains (213 amino acid each) and two murine  $\gamma_1$ -heavy chains (445 amino acids each). The molecular weight is approximately 144 kDa (non-glycosylated form).

## 4.2 Tiuxetan

2-(*p*-Isothiocyanatobenzyl)-6-methyldiethylenetriaminepentaacetic acid (tiuxetan) is a linker chelator substituting a 4-isothiocyanatobenzyl group and a methyl group onto the carbon backbone of DTPA [54, 65] (Fig. 4). Tiuxetan forms a stable covalent bond with the antibody and chelates the radionuclide through five carboxyl groups and three amino groups [66]. The yttrium-DTPA structure features 9-coordination in monocapped antiprismatic geometry (including an octadentate DTPA and one coordinated water), while indium-DTPA complexes have both 7-coordination and full 8-coordination in distorted pentagonal bipyramidal and square antiprismatic geometries, respectively [67].

## 4.3 Radionuclides

Isotopes used for internal radiation therapy are shown in Table 1. These radionuclides emit cytotoxic  $\beta^-$ -particle. The particulate radiation exposure is predicted to induce significant damage to cancer cells by the direct DNA lesion or via reactive oxygen species (especially hydroxyl radical) generated from radiolysis of water [16]. It is widely accepted that  $\alpha$ -particles and  $\beta^-$ -particles as well as Auger electrons exhibit higher therapeutic effects in comparison with electromagnetic radiations, i.e.,  $\gamma$  ray and X-ray. Providing a comparatively uniform radiation

**Fig. 4** Structure of tiuxetan (MX-DTPA), a preferred derivative of DTPA (a). The isothiocyanate group forms a covalent bond with amino groups such as lysine residues of the protein (b)

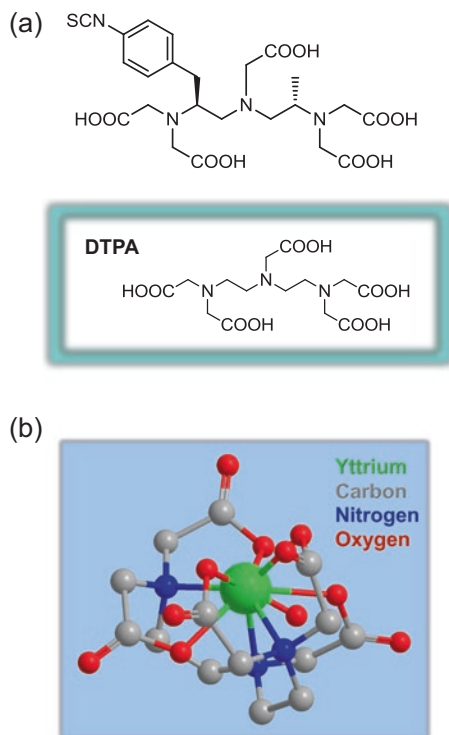


**Table 1**  $\beta^-$ -particle emitters used in RIT

Radioisotope	Energy <sub>max</sub> (MeV)	Range <sub>mean</sub> (mm)	Range <sub>max</sub> (mm)	Half-life
<sup>67</sup> Cu	0.58	0.6 mm	2.1 mm	61.8 h
<sup>89</sup> Sr	1.50	2.4 mm	7.0 mm	50.3 days
<b><sup>90</sup>Y</b>	<b>2.28</b>	<b>2.5 mm</b>	<b>11.1 mm</b>	<b>64.1 h</b>
<sup>131</sup> I	0.61	0.4 mm	2.4 mm	8.02 days
<sup>153</sup> Sm	0.81	0.6 mm	2.5 mm	46.5 h
<sup>177</sup> Lu	0.50	0.3 mm	1.5 mm	6.73 days
<sup>186</sup> Re	1.07	1.1 mm	4.5 mm	90.6 h
<sup>188</sup> Re	2.14	2.7 mm	11.0 mm	17.0 h

dose to the target tissue, RIT by using  $\beta^-$ -particle emitters is appropriate for solid tumors which size is  $\geq 0.5$  cm in diameter. Recently,  $\alpha$ -particle emitters such as <sup>211</sup>At, <sup>213</sup>Bi, <sup>225</sup>Ac, and <sup>227</sup>Th, which release a large amount of energy within a narrow range (50–90  $\mu\text{m}$ , equal to a few cell diameters), have also been applied to RIT for more small-size tumors from the viewpoint of higher relative biological effectiveness (RBE) [68–71].

## 5 Yttrium-90 ( $^{90}\text{Y}$ )

Yttrium is stable in the 3+ oxidation state and coordinates to hard donor atoms such as carboxylate-oxygens and amine-nitrogens. One of the isotopes,  $^{90}\text{Y}$ , can be obtained from its mother nuclide strontium-90 ( $^{90}\text{Sr}$ ) by a generator system based on the secular equilibrium between two radionuclides. The radioactive metal  $^{90}\text{Y}$  is an almost pure high-energy  $\beta^-$ -particle (electron) emitting nuclide [72]. It delivers a maximum particle energy of 2.28 MeV (average energy of 0.94 MeV) and has a half-life of 64.1 h, decaying to zirconium-90 ( $^{90}\text{Zr}$ ) (Fig. 5a).  $^{90}\text{Y}$  also emits a very low abundance of positrons via an internal pair production (branching ratio of  $31.9 \times 10^{-6}$ ) [73], which cannot be detected by positron emission tomography (PET).

The  $\beta^-$ -particle has an effective path length with tissue penetration of 2–10 mm [74, 75], equal to 100–200 cell diameters with low linear energy transfer (LET). When  $^{90}\text{Y}$ -ibritumomab tiuxetan binds to CD20 on the surface of NHL B-cells, this radio-complex evokes a “cross-fire effect” by delivering lethal radiation to not only the cells it binds to but also to nearby cancer cells, which do not express the antigen [76–78].

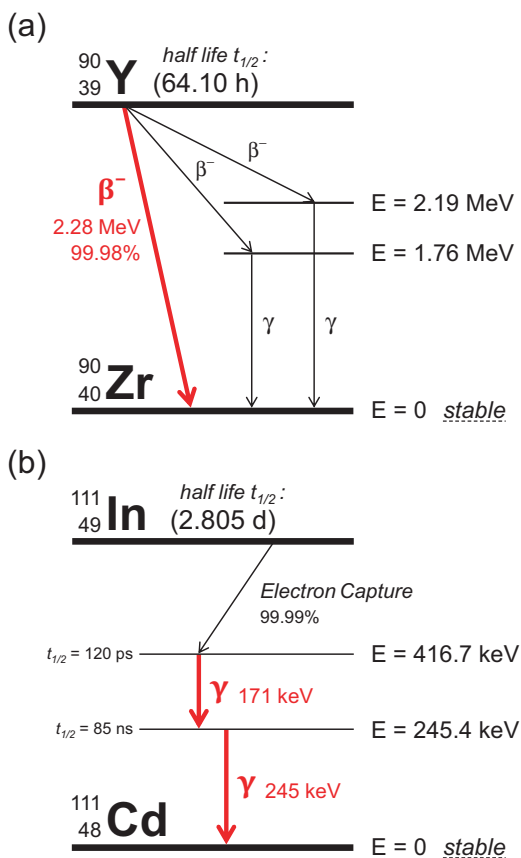
Two radiopharmaceuticals,  $^{90}\text{Y}$ -ibritumomab tiuxetan and  $^{131}\text{I}$ -tositumomab, were clinically used for RIT; however, production of  $^{131}\text{I}$ -tositumomab had been stopped due to the decline in usage as mentioned above. Because the radiation penetration of  $^{90}\text{Y}$  is longer than that of  $^{131}\text{I}$  (about 1 mm),  $^{90}\text{Y}$  provides theoretic advantages in the treatment of bulky and poorly vascularized tumors [79]. This could be one of the reasons why  $^{90}\text{Y}$ -ibritumomab tiuxetan is accepted as a standard radiopharmaceutical for the treatment in NHL.

## 6 Indium-111 ( $^{111}\text{In}$ )

In some cases of tumor treatment, the delivered radiation dose by  $^{90}\text{Y}$  cannot induce a sufficient response on the lesion without considerable toxic effects. Consequently, the analysis of the radiation dose not only on malignant tissues but also on surrounding normal tissues must be calculated. In addition, measurement of radioactivity in the excretory system and the reproductive system is also needed. However, because  $^{90}\text{Y}$  lacks the  $\gamma$ -emission or positron emission required for scintigraphic imaging, quantitative pharmacokinetic information on the post-therapy distribution of  $^{90}\text{Y}$ -ibritumomab tiuxetan is difficult to obtain by itself. Although some approaches for the bremsstrahlung imaging have been attempted, images can be obtained only when an extreme high level of radioactivity was accumulated in the target tissue, which can be realized only by an unreasonable dose in most clinical RIT [72, 80, 81]. Therefore, ibritumomab that incorporates a matched isotope for imaging is necessary to trace *in vivo* kinetics of the mAb and determine the dosimetry [82] (Fig. 5a).

$^{111}\text{In}$  emits two  $\gamma$  rays (171 keV and 245 keV) with a half-life of 2.8 days (67.2 h), which is closer to that of  $^{90}\text{Y}$ , and decay to cadmium-111 ( $^{111}\text{Cd}$ ) (Fig. 5b). Because of its almost ideal physical properties,  $^{111}\text{In}$  has been used as a SPECT imaging surrogate tracer for performing dosimetry with  $^{90}\text{Y}$ -based therapeutics [83, 84]. On the

**Fig. 5** Decay scheme of  $^{90}\text{Y}$  (a) and  $^{111}\text{In}$  (b)



other hand, such surrogate tracers sometimes do not correspond to the in vivo effects by  $^{90}\text{Y}$ -labeled internal radiation agents in some instances, and these discrepancies might cause the unintended toxicities [85–87].

$^{111}\text{In}$  also emits Auger electrons ranging in energy between 0.6 and 25.4 keV with a short tissue penetration range between 0.025 and 12.55  $\mu\text{m}$ , and this radioisotope has been investigated for the usage of radiotherapy [88–91] (Fig. 5b).

## 7 Preclinical Investigation of $^{90}\text{Y}$ -/ $^{111}\text{In}$ -Ibritumomab Tiuxetan

### 7.1 In Vitro Studies

By using flow cytometry, ibritumomab was indicated to bind specifically to B-cells and did not react with other T cells, monocytes, or other types of human tissue [64].

$^{111}\text{In}$ -ibritumomab tiuxetan prepared with a specific activity of 111 MBq/mg



exhibited no apparent loss of immunoreactivity compared to the unlabeled form. An *in vitro* stability study showed that the immunoreactivity was retained for incubation times up to 48 h at 4 °C. The apparent affinity ( $K_d$ ) of ibritumomab tiuxetan for the CD20 antigen was approximately 17 nM.

$^{90}\text{Y}$ -ibritumomab tiuxetan with a specific activity of 700 MBq/mg was also evaluated and showed that the loss of  $^{90}\text{Y}$  was 1% during the 48 h incubation with negligible loss of immunoreactivity. When incubated for up to 96 h at 37 °C in human serum, the loss of  $^{90}\text{Y}$  from the mAb averaged 1% per day [64].

## 7.2 *Ex Vivo/In Vivo Studies*

The biodistribution of  $^{90}\text{Y}$ -ibritumomab tiuxetan was evaluated in BALB/c mice. The levels of blood radioactivity were 39.2% ID/g at 1 h, which was decreased to 15.4% ID/g at 72 h. Radioactivity associated with other organs (liver, kidney, spleen, heart, lung, and gastrointestinal tract) was lower than that of blood throughout the course of the experiment. The radioactivity of the bone was 4.4% ID/g and 3.2% ID/g at 1 h and 72 h after the injection, respectively [64]. In a similar study, the biodistribution of 37 kBq of  $^{111}\text{In}$ -ibritumomab tiuxetan with a specific activity of 111 MBq/mg was determined. The highest radioactivity was measured in the blood (40.3% ID/g), which was decreased to 19.0% ID/g at 72 h. The lung and liver had the next highest levels (lung, 14.2% ID/g and 7.6% ID/g; liver, 10.3% ID/g and 9.9% ID/g at 1 h and 72 h, respectively). Additionally, the localization of  $^{111}\text{In}$ -ibritumomab tiuxetan in athymic mice bearing Ramos B-cell tumors showed that the radioactivity in the tumor increased steadily throughout the course of the experiment (0.5% ID/g at 1 h to 13.4% ID/g at 72 h), and the tumor/muscle ratio increased from 1.5 at 1 h to 20.6 at 72 h. In general, the biodistribution of radioactivity was similar in both radiolabeled mAbs [64].

The accumulation of  $^{90}\text{Y}$ -ibritumomab tiuxetan to the affected tissue was also evaluated by using NOD/SCID mice xenografted with a human mantle cell lymphoma (MCL) cells. When compared with the pathology, the autoradiograms demonstrated that the radioactivity was distributed within the bone marrow heterogeneously, whereas the nonspecific uptake by accessory myeloid cells was observed [92]. Pretreatment with the mouse IgG1 mAb decreased the unexpected background, which provided a clear image of MCL cell infiltration into the bone marrow.

By using the MIRD method, dosimetry of  $^{90}\text{Y}$ -ibritumomab tiuxetan was calculated from the biodistribution data in normal BALB/c mice. The radiation dose was estimated for the total body and selected tissues for the standard human (70 kg weight), based on a 37 MBq input dose for the radiolabeled mAb. Based on these estimates, the spleen and liver were predicted to receive the highest radiation doses for  $^{90}\text{Y}$ -ibritumomab tiuxetan (251 cGy and 240 cGy, respectively). The estimated radiation dose of the red bone marrow was 218 cGy [64].

## 8 Imaging and Therapy Protocol

### 8.1 Preparation of $^{90}\text{Y}$ -Ibritumomab Tiuxetan

Radiopharmaceuticals must be prepared in a manner which satisfies both pharmaceutical quality requirements and radiation safety. Appropriate aseptic manipulations must be taken, complying with the requirements of good manufacturing practice (GMP) of pharmaceuticals.

Zevalin® is supplied as a single dosage kit. Before radiolabeling, the refrigerated cold kit is brought to a room temperature of 25 °C. Outline of the labeling procedure is as follows:

*Step 1: Transfer of sodium acetate solution to the reaction vial*

Sodium acetate solution is transferred to reaction vial. The volume of solution added is equivalent to 1.2 times the volume of yttrium-90 chloride ( $^{90}\text{YCl}_3$ ) to be transferred in step 2.

*Step 2: Transfer of  $^{90}\text{YCl}_3$  to the reaction vial*

1.5 GBq of  $^{90}\text{YCl}_3$  solution was transferred to the reaction vial containing the sodium acetate solution transferred in step 1 and mixed completely. Sterile, pyrogen-free  $^{90}\text{YCl}_3$  must be used for the preparation of  $^{90}\text{Y}$ -ibritumomab tiuxetan.

*Step 3: Transfer of ibritumomab tiuxetan solution to the reaction vial*

1.3 ml of ibritumomab tiuxetan solution is transferred to the reaction vial and mixed completely. The  $^{90}\text{YCl}_3$ /acetate/ibritumomab tiuxetan solution is incubated at room temperature for 5 min.

*Step 4: Addition of the formulation buffer to the reaction vial*

After the 5-min incubation period, formulation buffer that will result in a combined total volume of 10 ml is added to the vial.

*Step 5: Measurement of  $^{90}\text{Y}$ -ibritumomab tiuxetan purity*

Radiochemical purity of the preparation is measured by thin layer chromatography (Tec-Control Chromatography Strips, Biodex, NY, developing solvent: 0.9% saline).  $^{90}\text{Y}$ -ibritumomab tiuxetan will apply to clinical use only if the purity is more than 95%.

### 8.2 Schedule of $^{90}\text{Y}$ -Ibritumomab Tiuxetan Therapy

The “ibritumomab tiuxetan protocol” is performed over 7–9 days. Radiolabeled ibritumomab tiuxetan is dosed on the basis of the patient’s body weight and baseline platelet count [93–96]. An example of the protocol is shown in Fig. 6.

*Day 1:* The patient receives 250 mg/m<sup>2</sup> of rituximab by drip infusion over 2–4 h, followed within 4 h by 185 MBq of  $^{111}\text{In}$ -ibritumomab tiuxetan intravenous injection over 10 min.

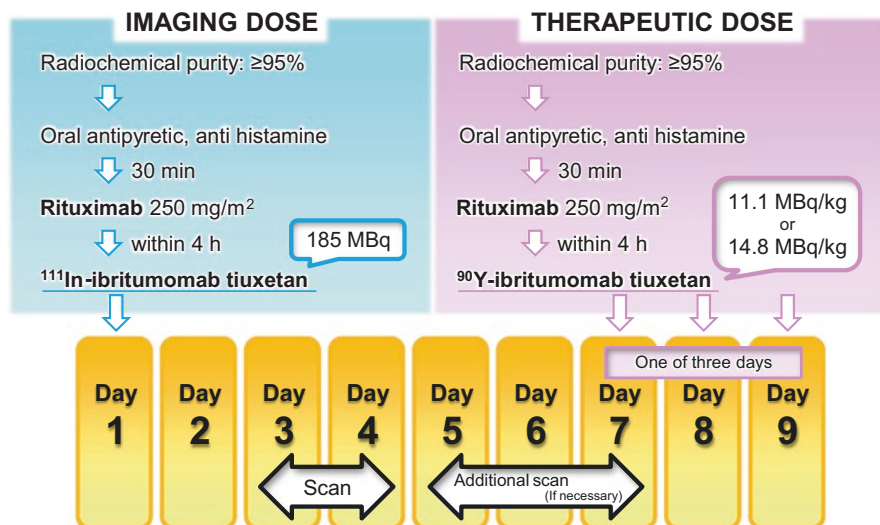


**Fig. 6** An example of the ibrutinomab protocol. One set of imaging and therapeutic medication is performed. The dose of <sup>90</sup>Y-ibrutinomab tiuxetan is determined by measuring the platelet count of the patient

*Day 3 or 4 (48–72 h):* Anterior and posterior whole body images are obtained. If the biodistribution of mAb is satisfactory, therapy treatment using <sup>90</sup>Y-ibrutinomab tiuxetan is continued [97].

*Day 7, 8, or 9:* The patient receives 250 mg/m<sup>2</sup> of rituximab by drip infusion over 2–4 h, followed within 4 h by 14.8 MBq/kg of <sup>90</sup>Y-ibrutinomab tiuxetan (11.1 MBq/kg for patients with platelet counts of  $1.0 \times 10^5/\text{mm}^3$ – $1.5 \times 10^5/\text{mm}^3$ ).

Rituximab pretreatment is necessary to clear circulating B-cells, enabling <sup>90</sup>Y-/<sup>111</sup>In-ibrutinomab tiuxetan to deliver radiation more specifically to the lymphoma B-cells.

The toxic effects of <sup>90</sup>Y-ibrutinomab tiuxetan are primarily hematologic and have been found to be transient and reversible [93]. Treatment with this antibody preparation also leads to temporal depletion of normal CD20-positive B-cells. However, median B-cell count is thought to be within normal range until 9 months after treatment. <sup>90</sup>Y-ibrutinomab tiuxetan is not recommended for use in children and adolescents below 18 years due to a lack of data on safety and efficacy. In elderly patients (aged  $\geq 65$  years old), no overall differences in safety or efficacy were observed compared to younger patients. Moreover, the safety and efficacy have not been verified in patients with hepatic or renal impairment. Therefore, <sup>90</sup>Y-ibrutinomab tiuxetan should be administered with caution to these patients. Details of this section were documented on the website of European Medicine Agency (EMA) [98].

## 9 Perspectives and Conclusion

RIT is a remarkable modality in the treatment of NHL. The combination of targeting-antigen selection, cytotoxic radioisotope, and chemical stability of radioimmunoconjugates is essential to the success of RIT.  $^{90}\text{Y}$ -ibritumomab tiuxetan fulfills these criteria and has shown significant benefits in the clinical field. However, this radiolabeled mAb still has some points for improvement.

One of the problems of RIT is the myelosuppressive adverse effect (anemia, thrombocytopenia, and neutropenia), which is caused by prolonged radiation to the bone marrow. The median biological half-life of  $^{90}\text{Y}$ -ibritumomab tiuxetan in the blood is 48 h [99]. In addition, the median serum effective half-life of radioactivity was 28 h in patients who received drip infusions of 250 mg/m<sup>2</sup> rituximab followed by intravenous injections of 15 MBq/kg of  $^{90}\text{Y}$ -ibritumomab tiuxetan [98]. The half-life of  $^{90}\text{Y}$  fits well to the long biological half-lives of mAbs, which take 2–3 days to fully distribute in tumor tissues. On the other hand, the bone marrow will be exposed to high-energy  $\beta^-$ -particle until circulating  $^{90}\text{Y}$  is excreted through the urinary system after metabolic degradation in the liver.

This hematological toxicity might be avoided by miniaturizing the mAb. Engineered antibody fragments such as Fab', ScFv, minibody, diabody, and scFv can achieve faster delivery to cancer cells and rapid clearance from normal tissues [100–105]. Though the binding affinities of these biomolecules to the antigens are much lower than that of the parent antibody, they might become a new standard of RIT for NHL if high-specific and high-affinity ( $K_d$  of  $<10^{-7}$  M)  $^{90}\text{Y}$ -labeled carriers targeting CD20 are developed.

An alternative approach is pretargeted RIT (PRIT), in which mAbs are injected to patients followed by radioactive effector molecules at a prescribed interval, and they will be conjugated *in vivo* [17, 106]. Issues related to prolonged residence time of antibodies are expected to be circumvented by using this strategy, namely, combination of the high target specificity and affinity provided by mAb and the good pharmacokinetics of a low molecular weight radio-labeled effector. The small size of the effector molecule allows it to distribute easily via the interstitial fluid and then to be eliminated rapidly if tumor-binding mAbs do not exist. Therefore, the overall radiation burden to nontarget tissues such as the bone marrow can be decreased. In preclinical investigation using BALB/c nude mice bearing Ramos human Burkitt lymphoma cells, RRIT indicated better responses with much less hematologic toxicity over the direct RIT with  $^{90}\text{Y}$ -veltuzumab [107, 108].

In this way, the early establishment of the effective treatment protocols for NHL, that is, the development of novel cytotoxic antibody preparations following  $^{90}\text{Y}$ -ibritumomab tiuxetan, which is combined with accurate diagnosis as well as alternative therapeutic drugs, is also desired.

## References

1. Thomas Hodgkin SMJ. Medical immortal and uncompromising idealist. *Proc (Bayl Univ Med Cent)*. 2005;18:368–7.
2. Küppers R, Hansmann ML. The Hodgkin and reed/Sternberg cell. *Int J Biochem Cell Biol*. 2005;37(3):511–7.
3. Bertoni F, Ponzoni M. The cellular origin of mantle cell lymphoma. *Int J Biochem Cell Biol*. 2007;39(10):1747–53.
4. Kridel R, Mottok A, Farinha P, Ben-Neriah S, Ennishi D, Zheng Y, Chavez EA, Shulha HP, Tan K, Chan FC, Boyle M, Meissner B, Telenius A, Sehn LH, Marra MA, Shah SP, Steidl C, Connors JM, Scott DW, Gascoyne RD. Cell of origin of transformed follicular lymphoma. *Blood*. 2015;126(18):2118–27.
5. Ondrejka SL, Hsi ED. T-cell lymphomas: updates in biology and diagnosis. *Surg Pathol Clin*. 2016;9(1):131–41.
6. Stat Fact Sheets SEER. Non-Hodgkin lymphoma, surveillance, epidemiology, and end results program, presented by National Cancer Institute. NIH. <http://seer.cancer.gov/statfacts/html/nhl.html>
7. Coleman M, Lammers PE, Ciceri F, Jacobs IA. Role of rituximab and rituximab biosimilars in diffuse large B-cell lymphoma. *Clin Lymphoma Myeloma Leuk*. 2016;16(4):175–81.
8. Karlin L, Coiffier B. Ofatumumab in the treatment of non-Hodgkin's lymphomas. *Expert Opin Biol Ther*. 2015;15(7):1085–91.
9. Gabellier L, Cartron G. Obinutuzumab for relapsed or refractory indolent non-Hodgkin's lymphomas. *Ther Adv Hematol*. 2016;7(2):85–93.
10. Klein C, Lammens A, Schäfer W, Georges G, Schwaiger M, Mössner E, Hopfner KP, Umaña P, Niederfellner G. Epitope interactions of monoclonal antibodies targeting CD20 and their relationship to functional properties. *MAbs*. 2013;5(1):22–33.
11. Hainsworth JD. Monoclonal antibody therapy in lymphoid malignancies. *Oncologist*. 2000;5(5):376–84.
12. Tomblyn B. Radioimmunotherapy for B-cell non-Hodgkin lymphomas. *Cancer Control*. 2012;19(3):196–203.
13. Read ED, Eu P, Little PJ, Piva TJ. The status of radioimmunotherapy in CD20+ non-Hodgkin's lymphoma. *Target Oncol*. 2015;10(1):15–26.
14. Skarbnik AP, Smith MR. Radioimmunotherapy in mantle cell lymphoma. *Best Pract Res Clin Haematol*. 2012;25(2):201–10.
15. Fink-Bennett DM, Thomas K. <sup>90</sup>Y-ibritumomab tiuxetan in the treatment of relapsed or refractory B-cell non-Hodgkin's lymphoma. *J Nucl Med Technol*. 2003;31(2):61–8.
16. Karagiannis TC. Comparison of different classes of radionuclides for potential use in radioimmunotherapy. *Hell J Nucl Med*. 2007;10(2):82–8.
17. Kawashima H. Radioimmunotherapy: a specific treatment protocol for cancer by cytotoxic radioisotopes conjugated to antibodies. *Sci World J*. 2014;2014:492061.
18. Deans JP, Li H, Polyak MJ. CD20-mediated apoptosis: signalling through lipid rafts. *Immunology*. 2002;107(2):176–82.
19. Stashenko P, Nadler LM, Hardy R, Schlossman SF. Characterization of a human B lymphocyte-specific antigen. *J Immunol*. 1980;125(4):1678–85.
20. Hanto DW, Frizzera G, Gajl-Peczalska KJ, Sakamoto K, Purtilo DT, Balfour HH Jr, Simmons RL, Najarian JS. Epstein-Barr virus-induced B-cell lymphoma after renal transplantation: acyclovir therapy and transition from polyclonal to monoclonal B-cell proliferation. *N Engl J Med*. 1982;306(15):913–8.
21. Anderson KC, Bates MP, Slaughenhaupt BL, Pinkus GS, Schlossman SF, Nadler LM. Expression of human B cell-associated antigens on leukemias and lymphomas: a model of human B cell differentiation. *Blood*. 1984;63(6):1424–33.
22. Hokland P, Ritz J, Schlossman SF, Nadler LM. Orderly expression of B cell antigens during the in vitro differentiation of nonmalignant human pre-B cells. *J Immunol*. 1985;135(3):1746–51.

23. Tedder TF, Disteché CM, Louie E, Adler DA, Croce CM, Schlossman SF, Saito H. The gene that encodes the human CD20 (B1) differentiation antigen is located on chromosome 11 near the t(11;14)(q13;q32) translocation site. *J Immunol.* 1989;142(7):2555–9.
24. Bubien JK, Zhou LJ, Bell PD, Frizzell RA, Tedder TF. Transfection of the CD20 cell surface molecule into ectopic cell types generates a Ca<sup>2+</sup> conductance found constitutively in B lymphocytes. *J Cell Biol.* 1993;121(5):1121–32.
25. Tedder TF, Engel P. CD20: a regulator of cell-cycle progression of B lymphocytes. *Immunol Today.* 1994;15(9):450–4.
26. Uchida J, Lee Y, Hasegawa M, Liang Y, Bradney A, Oliver JA, Bowen K, Steeber DA, Haas KM, Poe JC, Tedder TF. Mouse CD20 expression and function. *Int Immunol.* 2004;16(1):119–29.
27. Valentine MA, Licciardi KA, Clark EA, Krebs EG, Meier KE. Insulin regulates serine/threonine phosphorylation in activated human B lymphocytes. *J Immunol.* 1993;150(1):96–105.
28. Genot EM, Meier KE, Licciardi KA, Ahn NG, Uittenbogaart CH, Wietzerbin J, Clark EA, Valentine MA. Phosphorylation of CD20 in cells from a hairy cell leukemia cell line. Evidence for involvement of calcium/calmodulin-dependent protein kinase II. *J Immunol.* 1993;151(1):71–82.
29. Deans JP, Schieven GL, Shu GL, Valentine MA, Gilliland LA, Aruffo A, Clark EA, Ledbetter JA. Association of tyrosine and serine kinases with the B cell surface antigen CD20. Induction via CD20 of tyrosine phosphorylation and activation of phospholipase C- $\gamma$ 1 and PLC phospholipase C- $\gamma$ 2. *J Immunol.* 1993;151(9):4494–504.
30. Golay J, Cusmano G, Introna M. Independent regulation of *c-myc*, *B-myb*, and *c-myb* gene expression by inducers and inhibitors of proliferation in human B lymphocytes. *J Immunol.* 1992;149(1):300–8.
31. Kansas GS, Tedder TF. Transmembrane signals generated through MHC class II, CD19, CD20, CD39, and CD40 antigens induce LFA-1-dependent and independent adhesion in human B cells through a tyrosine kinase-dependent pathway. *J Immunol.* 1991;147(12):4094–102.
32. Clark EA, Shu G. Activation of human B cell proliferation through surface Bp35 (CD20) polypeptides or immunoglobulin receptors. *J Immunol.* 1987;138(3):720–5.
33. White MW, McConnell F, Shu GL, Morris DR, Clark EA. Activation of dense human tonsillar B cells. Induction of *c-myc* gene expression via two distinct signal transduction pathways. *J Immunol.* 1991;146(3):846–53.
34. Rossmann ED, Lundin J, Lenkei R, Mellstedt H, Osterborg A. Variability in B-cell antigen expression: implications for the treatment of B-cell lymphomas and leukemias with monoclonal antibodies. *Hematol J.* 2001;2(5):300–6.
35. Liu AY, Robinson RR, Murray ED Jr, Ledbetter JA, Hellstrom I, Hellstrom KE. Production of a mouse-human chimeric monoclonal antibody to CD20 with potent Fc-dependent biologic activity. *J Immunol.* 1987;139(10):3521–6.
36. Press OW, Howell-Clark J, Anderson S, Bernstein I. Retention of B-cell-specific monoclonal antibodies by human lymphoma cells. *Blood.* 1994;83(5):1390–7.
37. Press OW, Farr AG, Borroz KI, Anderson SK, Martin PJ. Endocytosis and degradation of monoclonal antibodies targeting human B-cell malignancies. *Cancer Res.* 1989;49(17):4906–12.
38. Sato S, Steeber DA, Jansen PJ, Tedder TF. CD19 expression levels regulate B lymphocyte development: human CD19 restores normal function in mice lacking endogenous CD19. *J Immunol.* 1997;158(10):4662–9.
39. Vlasveld LT, Hekman A, Vyth-Dreese FA, Melief CJ, Sein JJ, Voordouw AC, Dellemijn TA, Rankin EM. Treatment of low-grade non-Hodgkin's lymphoma with continuous infusion of low-dose recombinant interleukin-2 in combination with the B-cell-specific monoclonal antibody CLB CD19. *Cancer Immunol Immunother.* 1995;40(1):37–47.
40. Cesano A, Gayko U. CD22 as a target of passive immunotherapy. *Semin Oncol.* 2003;30(2):253–7.
41. Coleman M, Goldenberg DM, Siegel AB, Ketas JC, Ashe M, Fiore JM, Leonard JP. Epratuzumab: targeting B-cell malignancies through CD22. *Clin Cancer Res.* 2003;9(10):3991s–4s.



42. Delacruz W, Setlik R, Hassantoufighi A, Daya S, Cooper S, Selby D, Brown A. Novel brentuximab vedotin combination therapies show promising activity in highly refractory CD30+ non-Hodgkin lymphoma: a case series and review of the literature. *Case Rep Oncol Med*. 2016;2016:2596423.
43. Advani R, Forero-Torres A, Furman RR, Rosenblatt JD, Younes A, Ren H, Harrop K, Whiting N, Drachman JG. Phase I study of the humanized anti-CD40 monoclonal antibody dacetuzumab in refractory or recurrent non-Hodgkin's lymphoma. *J Clin Oncol*. 2009;27(26):4371–7.
44. Hariharan K, Chu P, Murphy T, Clanton D, Berquist L, Molina A, Ho SN, Vega MI, Bonavida B. Galiximab (anti-CD80)-induced growth inhibition and prolongation of survival *in vivo* of B-NHL tumor xenografts and potentiation by the combination with fludarabine. *Int J Oncol*. 2013;43(2):670–6.
45. Pillay V, Gan HK, Scott AM. Antibodies in oncology. *New Biotechnol*. 2011;28(5):518–29.
46. Kitson SL, Cuccurullo V, Moody TS, Mansi L. Radionuclide antibody-conjugates, a targeted therapy towards cancer. *Curr Radiopharm*. 2013;6(2):57–71.
47. Ross JS, Gray K, Gray GS, Worland PJ, Rolfe M. Anticancer antibodies. *Am J Clin Pathol*. 2003;119(4):472–85.
48. Winter G, Harris WJ. Humanized antibodies. *Trends Pharmacol Sci*. 1993;14(5):139–43.
49. Merluzzi S, Figini M, Colombatti A, Canevari S, Pucillo C. Humanized antibodies as potential drugs for therapeutic use. *Adv Clin Pathol*. 2000;4(2):77–85.
50. Kuus-Reichel K, Grauer LS, Karavodin LM, Knott C, Krusemeier M, Kay NE. Will immunogenicity limit the use, efficacy, and future development of therapeutic monoclonal antibodies? *Clin Diagn Lab Immunol*. 1994;1(14):365–72.
51. Pimm MV. Possible consequences of human antibody responses on the biodistribution of fragments of human, humanized or chimeric monoclonal antibodies: a note of caution. *Life Sci*. 1994;55(2):PL45–9.
52. Teo EC, Chew Y, Phipps C. A review of monoclonal antibody therapies in lymphoma. *Crit Rev Oncol Hematol*. 2016;97:72–84.
53. Davies AJ. Radioimmunotherapy for B-cell lymphoma: Y<sup>90</sup> ibritumomab tiuxetan and I<sup>131</sup> tositumomab. *Oncogene*. 2007;26(25):3614–28.
54. Brechbiel MW, Gansow OA. Backbone-substituted DTPA ligands for <sup>90</sup>Y radioimmunotherapy. *Bioconjug Chem*. 1991;2(3):187–94.
55. Reff ME, Carner K, Chambers KS, Chinn PC, Leonard JE, Raab R, Newman RA, Hanna N, Anderson DR. Depletion of B cells *in vivo* by a chimeric mouse human monoclonal antibody to CD20. *Blood*. 1994;83(2):435–45.
56. Ibritumomab tiuxetan (Zevalin) for non-Hodgkin's lymphoma. *Med Lett Drugs Ther*. 2002;44(1144):101–2.
57. First radiopharmaceutical for non-Hodgkin's lymphoma. *FDA Consum*. 2002;36(3):3.
58. Hagenbeek A, Lewington V. Report of a European consensus workshop to develop recommendations for the optimal use of <sup>90</sup>Y-ibritumomab tiuxetan (Zevalin®) in lymphoma. *Ann Oncol*. 2005;16(5):786–92.
59. Lin FI, Iagaru A. Current concepts and future directions in radioimmunotherapy. *Curr Drug Discov Technol*. 2010;7(4):253–62.
60. Barth M, Raetz E, Cairo MS. The future role of monoclonal antibody therapy in childhood acute leukaemias. *Br J Haematol*. 2012;159(1):3–17.
61. Kattah AG, Fervenza FC. Rituximab: emerging treatment strategies of immune-mediated glomerular disease. *Expert Rev Clin Immunol*. 2012;8(5):413–21.
62. Cang S, Mukhi N, Wang K, Liu D. Novel CD20 monoclonal antibodies for lymphoma therapy. *J Hematol Oncol*. 2012;5:64.
63. Kohler G, Milstein C. Continuous cultures of fused cells secreting antibody of predefined specificity. *Nature*. 1975;256(5517):495–7.
64. Chinn PC, Leonard JE, Rosenberg J, Hanna N, Anderson DR. Preclinical evaluation of <sup>90</sup>Y-labeled anti-CD20 monoclonal antibody for treatment of non-Hodgkin's lymphoma. *Int J Oncol*. 1999;15(5):1017–25.



65. Milenic DE, Brady ED, Brechbiel MW. Antibody-targeted radiation cancer therapy. *Nat Rev Drug Discov.* 2004;3(6):488–99.
66. Wiseman GA, White CA, Sparks RB, Erwin WD, Podoloff DA, Lamonica D, Bartlett NL, Parker JA, Dunn WL, Spies SM, Belanger R, Witzig TE, Leigh BR. Biodistribution and dosimetry results from a phase III prospectively randomized controlled trial of Zevalin radioimmunotherapy for low grade, follicular, or transformed B-cell non-Hodgkin's lymphoma. *Crit Rev Oncol Hematol.* 2001;39(1–2):181–94.
67. Wadas TJ, Wong EH, Weisman GR, Anderson CJ. Coordinating radiometals of copper, gallium, indium, yttrium and zirconium for PET and SPECT imaging of disease. *Chem Rev.* 2010;110(5):2858–902.
68. Andersson H, Cederkrantz E, Bäck T, Divgi C, Elgqvist J, Himmelman J, Horvath G, Jacobsson L, Jensen H, Lindegren S, Palm S, Hultborn R. Intraperitoneal  $\alpha$ -particle radioimmunotherapy of ovarian cancer patients: pharmacokinetics and dosimetry of  $^{211}\text{At}$ -MX35 F(ab')<sub>2</sub>: a phase I study. *J Nucl Med.* 2009;50(7):1153–60.
69. Teiluf K, Seidl C, Blechert B, Gaertner FC, Gilbertz KP, Fernandez V, Bassermann F, Endell J, Boxhammer R, Leclair S, Vallon M, Aichler M, Feuchtinger A, Bruchertseifer F, Morgenstern A, Essler M.  $\alpha$ -Radioimmunotherapy with  $^{213}\text{Bi}$ -anti-CD38 immunconjugates is effective in a mouse model of human multiple myeloma. *Oncotarget.* 2015;6(7):4692–703.
70. Bandekar A, Zhu C, Jindal R, Bruchertseifer F, Morgenstern A, Sofou S. Anti-prostate-specific membrane antigen liposomes loaded with  $^{225}\text{Ac}$  for potential targeted antivascular  $\alpha$ -particle therapy of cancer. *J Nucl Med.* 2014;55(9):1492–8.
71. Abbas N, Heyerdahl H, Bruland OS, Borrebæk J, Nesland J, Dahle J. Experimental  $\alpha$ -particle radioimmunotherapy of breast cancer using  $^{227}\text{Th}$ -labeled p-benzyl-DOTA-trastuzumab. *EJNMMI Res.* 2011;1(1):18.
72. Smith T, Crawley JC, Shawe DJ, Gumpel JMSPECT. Using bremsstrahlung to quantify  $^{90}\text{Y}$  uptake in Baker's cysts: its application in radiation synovectomy of the knee. *Eur J Nucl Med.* 1988;14(9–10):498–503.
73. Selwyn RG, Nickles RJ, Thomadsen BR, DeWerd LA, Micka JA. A new internal pair production branching ratio of  $^{90}\text{Y}$ : the development of a non-destructive assay for  $^{90}\text{Y}$  and  $^{90}\text{Sr}$ . *Appl Radiat Isot.* 2007;65(3):318–27.
74. Minarik D, Sjögren Gleisner K, Ljungberg M. Evaluation of quantitative  $^{90}\text{Y}$  SPECT based on experimental phantom studies. *Phys Med Biol.* 2008;53(20):5689–703.
75. Dancy JE, Shepherd FA, Paul K, Sniderman KW, Houle S, Gabrys J, Hendler AL, Goin JE. Treatment of nonresectable hepatocellular carcinoma with intrahepatic  $^{90}\text{Y}$ -microspheres. *J Nucl Med.* 2000;41(10):1673–81.
76. Press OW. Radiolabeled antibody therapy of B-cell lymphomas. *Semin Oncol.* 1999;26(Suppl 14):58–65.
77. Wiseman GA, White CA, Witzig TE, Gordon LI, Emmanouilides C, Raubitschek A, Janakiraman N, Gutheil J, Schilder RJ, Spies S, Silverman DH, Grillo-López AJ. Radioimmunotherapy of relapsed non-Hodgkin's lymphoma with Zevalin, a  $^{90}\text{Y}$ -labeled anti-CD20 monoclonal antibody. *Clin Cancer Res.* 1999;5(Suppl 10):3281s–6s.
78. Zelenetz AD. Radioimmunotherapy for lymphoma. *Curr Opin Oncol.* 1999;11:375–80.
79. Goldsmith SJ. Radioimmunotherapy of lymphoma: Bexxar and Zevalin. *Semin Nucl Med.* 2010;40(2):122–35.
80. Shen S, DeNardo GL, Yuan A, DeNardo DA, DeNardo SJ. Planar gamma camera imaging and quantitation of yttrium-90 bremsstrahlung. *J Nucl Med.* 1994;35(8):1381–9.
81. Rong X, Frey EC. A collimator optimization method for quantitative imaging: application to Y-90 bremsstrahlung SPECT. *Med Phys.* 2013;40(8):082504.
82. Paganelli G, Bartolomei M, Ferrari M, Cremonesi M, Broggi G, Maira G, Sturiale C, Grana C, Prisco G, Gatti M, Caliceti P, Chinol M. Pre-targeted locoregional radioimmunotherapy with  $^{90}\text{Y}$  biotin in glioma patients: phase I study and preliminary therapeutic results. *Cancer Biother Radiopharm.* 2001;16(3):227–35.

83. van Hemert FJ, Sloof GW, Schimmel KJ, Vervenne WL, van Eck-Smrr BL, Busemann-Sokole E. Radiopharmaceutical management of  $^{90}\text{Y}/^{111}\text{In}$  labeled antibodies: shielding and quantification during preparation and administration. *Ann Nucl Med.* 2006;20(8):575–81.
84. Steiner M, Neri D. Antibody-radionuclide conjugates for cancer therapy: historical considerations and new trends. *Clin Cancer Res.* 2011;17(20):6406–16.
85. de Jong M, Bakker WH, Krenning EP, Breeman WA, van der Pluijm ME, Bernard BF, Visser TJ, Jermann E, Béhé M, Powell P, Mäcke HR. Yttrium-90 and indium-111 labelling, receptor binding and biodistribution of [DOTA<sup>0</sup>,D-Phe<sup>1</sup>,Tyr<sup>3</sup>]octreotide, a promising somatostatin analogue for radionuclide therapy. *Eur J Nucl Med.* 1997;24(4):368–71.
86. Dahle J, Abbas N, Bruland ØS, Larsen RH. Toxicity and relative biological effectiveness of alpha emitting radioimmunoconjugates. *Curr Radiopharm.* 2011;4(4):321–8.
87. Carroll V, Demoin DW, Hoffman TJ, Jurisson SS. Inorganic chemistry in nuclear imaging and radiotherapy: current and future directions. *Radiochim Acta.* 2012;100(8–9):653–67.
88. Silvester DJ, Waters SL. Dosimetry of radiolabelled blood cells. *Int J Nucl Med Biol.* 1983;10(2–3):141–4.
89. Cornelissen B, Waller A, Able S, Vallis KA. Molecular radiotherapy using cleavable radioimmunoconjugates that target EGFR and  $\gamma\text{H2AX}$ . *Mol Cancer Ther.* 2013;12(11):2472–82.
90. Ngo Ndjock Mbong G, Lu Y, Chan C, Cai Z, Liu P, Boyle AJ, Winnik MA, Reilly RM. Trastuzumab labeled to high specific activity with  $^{111}\text{In}$  by site-specific conjugation to a metal-chelating polymer exhibits amplified auger electron-mediated cytotoxicity on HER2-positive breast cancer cells. *Mol Pharm.* 2015;12(6):1951–60.
91. Gao C, Leyton JV, Schimmer AD, Minden M, Reilly RM. Auger electron-emitting  $^{111}\text{In}$ -DTPA-NLS-CSL360 radioimmunoconjugates are cytotoxic to human acute myeloid leukemia (AML) cells displaying the CD123<sup>+</sup>/CD131<sup>-</sup> phenotype of leukemia stem cells. *Appl Radiat Isot.* 2016;110:1–7.
92. Coulot J, Camara-Clayette V, Ricard M, Lavielle F, Velasco V, Drusch F, Bosq J, Schlumberger M, Ribrag V. Imaging of the distribution of  $^{90}\text{Y}$ -ibritumomab tiuxetan in bone marrow and comparison with pathology. *Cancer Biother Radiopharm.* 2007;22(5):665–71.
93. Krasner C, Joyce RM. Zevalin:  $^{90}\text{Y}$ trium labeled anti-CD20 (ibritumomab tiuxetan), a new treatment for non-Hodgkin's lymphoma. *Curr Pharm Biotechnol.* 2001;2(4):341–9.
94. Gordon LI, Witzig TE, Wiseman GA, Flinn IW, Spies SS, Silverman DH, Emmanouilides C, Cripe L, Saleh M, Czuczman MS, Olejnik T, White CA, Grillo-López AJ. Yttrium 90 ibritumomab tiuxetan radioimmunotherapy for relapsed or refractory low-grade non-Hodgkin's lymphoma. *Semin Oncol.* 2002;29(1 Suppl 2):87–92.
95. Wagner HN Jr, Wiseman GA, Marcus CS, Nabi HA, Nagle CE, Fink-Bennett DM, Lamonica DM, Conti PS. Administration guidelines for radioimmunotherapy of non-Hodgkin's lymphoma with  $^{90}\text{Y}$ -labeled anti-CD20 monoclonal antibody. *J Nucl Med.* 2002;43(2):267–72.
96. Juweid ME. Radioimmunotherapy of B-cell non-Hodgkin's lymphoma: from clinical trials to clinical practice. *J Nucl Med.* 2002;43(11):1507–29.
97. Otte A. Diagnostic imaging prior to  $^{90}\text{Y}$ -ibritumomab tiuxetan (Zevalin) treatment in follicular non-Hodgkin's lymphoma. *Hell J Nucl Med.* 2008;11(1):12–5.
98. Annex I Summary of Product Characteristics: Zevalin 1.6 mg/ml kit for radiopharmaceutical preparations for infusion, disclosed by European Medical Agency. [http://www.ema.europa.eu/docs/en\\_GB/document\\_library/EPAR\\_-\\_Product\\_Information/human/000547/WC500049469.pdf](http://www.ema.europa.eu/docs/en_GB/document_library/EPAR_-_Product_Information/human/000547/WC500049469.pdf)
99. Chamarthy MR, Williams SC, Moadel RM. Radioimmunotherapy of non-Hodgkin's lymphoma: from the 'magic bullets' to 'radioactive magic bullets. *Yale J Biol Med.* 2011;84(4):391–407.
100. Boswell CA, Brechbiel MW. Development of radioimmunotherapeutic and diagnostic antibodies: an inside-out view. *Nucl Med Biol.* 2007;34(7):757–78.
101. Peer D, Karp JM, Hong S, Farokhzad OC, Margalit R, Langer R. Nanocarriers as an emerging platform for cancer therapy. *Nat Nanotechnol.* 2007;2(12):751–60.

102. Holliger P, Hudson PJ. Engineered antibody fragments and the rise of single domains. *Nat Biotechnol.* 2005;23(9):1126–36.
103. Schneider DW, Heitner T, Aliche B, Light DR, McLean K, Satozawa N, Parry G, Yoo J, Lewis JS, Parry R. In vivo biodistribution, PET imaging, and tumor accumulation of <sup>86</sup>Y- and <sup>111</sup>In-antimindin/RG-1, engineered antibody fragments in LNCaP tumor-bearing nude mice. *J Nucl Med.* 2009;50(3):435–43.
104. Adams GP, Shaller CC, Dadachova E, Simmons HH, Horak EM, Tesfaye A, Klein-Szanto AJ, Marks JD, Brechbiel MW, Weiner LM. A single treatment of yttrium-90-labeled CHX-A"-C6.5 diabody inhibits the growth of established human tumor xenografts in immunodeficient mice. *Cancer Res.* 2004;64(17):6200–6.
105. Maleki LA, Baradaran B, Majidi J, Mohammadian M, Shahneh FZ. Future prospects of monoclonal antibodies as magic bullets in immunotherapy. *Hum Antibodies.* 2013;22(1–2):9–13.
106. Goldenberg DM, Sharkey RM, Paganelli G, Barbet J, Chatal JF. Antibody pretargeting advances cancer radioimmunodetection and radioimmunotherapy. *J Clin Oncol.* 2006;24(5):823–34.
107. Sharkey RM, Karacay H, Litwin S, Rossi EA, McBride WJ, Chang CH, Goldenberg DM. Improved therapeutic results by pretargeted radioimmunotherapy of non-Hodgkin's lymphoma with a new recombinant, trivalent, anti-CD20, bispecific antibody. *Cancer Res.* 2008;68(13):5282–90.
108. Sharkey RM, Karacay H, Johnson CR, Litwin S, Rossi EA, McBride WJ, Chang CH, Goldenberg DM. Pretargeted versus directly targeted radioimmunotherapy combined with anti-CD20 antibody consolidation therapy of non-Hodgkin lymphoma. *J Nucl Med.* 2009;50(3):444–53.

# Resistance and Heterogeneity of Intratumoral Antibody Distribution



Kohei Hanaoka and Makoto Hosono

**Abstract** Even though ibritumomab tiuxetan provides clinical benefit to follicular lymphoma patients, resistance to ibritumomab tiuxetan develops. Follicular lymphoma shows a remarkable diversity in phenotypic, genetic, and microenvironment intratumoral heterogeneities.

Heterogeneity is one of the most clinically relevant and rapidly evolving fields of cancer research. Despite this growing excitement in the fundamental research, tumor heterogeneity has little practical impact on today's management of cancer patients.

Therefore, understanding the mechanisms for resistance to ibritumomab tiuxetan and developing treatment strategies are important.

**Keywords** Non-Hodgkin's lymphoma · MX-DTPA · Ibritumomab tiuxetan · CD20 · Radiopharmaceuticals · Metal chelator · Radionuclide therapy · MIRD method · Dosimetry

## 1 Introduction

Ibritumomab tiuxetan is a CD20-directed radiotherapeutic antibody administered as part of the therapeutic regimen indicated for the treatment of patients with relapsed or refractory, low-grade, or follicular B-cell non-Hodgkin's lymphoma [1, 2].

Prior to  $^{90}\text{Y}$ -ibritumomab tiuxetan therapy, imaging with  $^{111}\text{In}$ -ibritumomab tiuxetan is performed according to a therapy protocol implemented in certain countries and regions to verify the expected biodistribution and exclude patients who show an altered biodistribution, such as the rapid clearance of  $^{111}\text{In}$ -ibritumomab tiuxetan from the blood pool, with prominent liver, spleen, or marrow uptakes [3, 4]. Such criteria for expected and altered biodistributions have been proposed and established, based on which the indication of radioimmunotherapy with

---

K. Hanaoka · M. Hosono (✉)  
Institute of Advanced Clinical Medicine,  
Kindai University Faculty of Medicine, Osaka, Japan  
e-mail: [hosono@med.kindai.ac.jp](mailto:hosono@med.kindai.ac.jp)

$^{90}\text{Y}$ -ibritumomab tiuxetan is assessed. A high rate of a complete response after  $^{90}\text{Y}$ -ibritumomab tiuxetan therapy has often been observed in patients with negative  $^{111}\text{In}$ -ibritumomab tiuxetan accumulation in lesions [5]. It has been speculated that nonuniformity in the intratumorally absorbed dose plays a significant role in the success or failure of radionuclide therapy [6–9]. Thus, the association between the tumor response and  $^{111}\text{In}$ -ibritumomab tiuxetan accumulation in lesions should be clarified. For this purpose, SPECT/CT may have advantages over whole-body planar scans because it provides three-dimensional images by fusing data on function and morphology. In this study, using SPECT/CT, we measured absolute levels of  $^{111}\text{In}$ -ibritumomab tiuxetan accumulation and assessed the heterogeneity of  $^{111}\text{In}$ -ibritumomab tiuxetan distribution in lesions by calculating the heterogeneity indices.

$^{18}\text{F}$ -Fluorodeoxyglucose (FDG) positron emission tomography (PET) is another imaging modality often used during the course of  $^{90}\text{Y}$ -ibritumomab tiuxetan therapy [10, 11]. This noninvasive, three-dimensional imaging modality has become widely used and essential for the initial staging and evaluation of the response after treatment in patients with malignant lymphoma and has been integrated in the Revised International Workshop criteria for malignant lymphoma [12]. The role of FDG-PET for predicting outcomes after  $^{90}\text{Y}$ -ibritumomab tiuxetan therapy has been reported, and a lower pretherapeutic FDG uptake may correlate with a longer progression-free survival [11].

## 2 SPECT/CT and PET/CT System

The single-photon emission computed tomography/computed tomography (SPECT/CT) system and the positron emission tomography/computed tomography (PET/CT) system have implemented advanced software for acquisition and reconstruction [13–17]. The information associated with images have been consistently and continuously improved (Fig. 1).

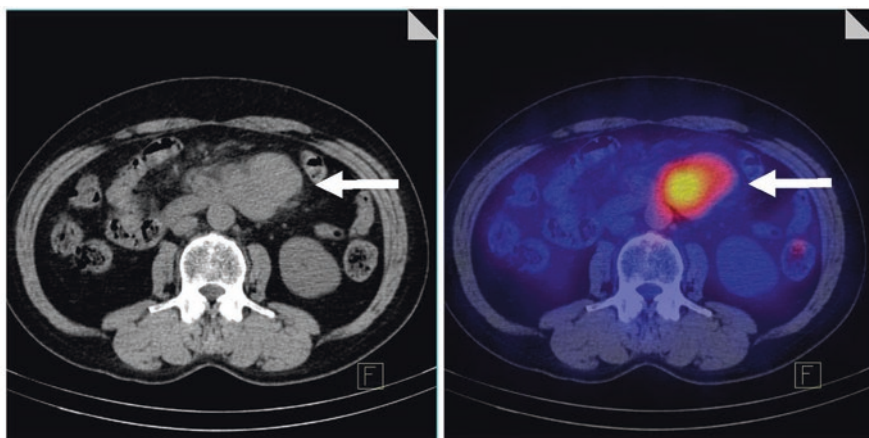


**Fig. 1**  $^{111}\text{In}$ -ibritumomab tiuxetan SPECT/CT fused image (left) and CT image

SPECT/CT or PET/CT deals with only macroscopic lesions due to its spatial resolution, and so microscopic lesions are outside the scope of consideration [18]. In soft tissue, 90% of the energy emitted by the  $^{90}\text{Y}$  radionuclide is absorbed within 5 mm. Also, the spatial resolution of SPECT/CT using the LMEGP collimator is only about 9 mm [19]. Hence, the heterogeneity of  $^{111}\text{In}$ -ibritumomab tiuxetan uptake may be markedly influenced by the tumor size and spatial resolution of SPECT/CT. However, it is clear that SPECT/CT improves the quantification of SPECT alone using techniques such as VOI analysis. In previous  $^{111}\text{In}$ -ibritumomab tiuxetan studies, the tumor characteristics were mostly evaluated on two-dimensional images or even when three-dimensional images were obtained, and only maximum uptake values reflecting a single voxel with the maximum uptake were considered. The three-dimensional analysis of voxels in this study has an advantage over previous studies and provides new findings.

### 3 Statistical Approach Taken to Characterize Lesion's Uptake

There are several methods for measuring the rate and total amount of FDG accumulation in tumors. The maximum standardized uptake value (SUV) is commonly used in clinical practice as a relative measure of FDG uptake [20]. On the pharmacokinetics (metabolism) study, tumor accumulations are expressed as a percentage of the injected dose per gram (%ID/g) [21].

Recently, another statistical approach was considered to characterize the lesion's uptake by quantification of the spatial heterogeneity of voxel-based activities in histograms [22]. The common quantifiers of skewness and kurtosis, describing the asymmetry and extent of symmetrical departure, respectively, were employed [23, 24]. In addition, in order to characterize the heterogeneity of the intratumoral uptake, cumulative SUV histograms (CSH) were sometimes used. In CSH, the percent volume of a tumor was plotted against a threshold value varying from 0% to 100% of SUV<sub>max</sub> of the tumor, and the area under the curve of the cumulative SUV histograms (AUC-CSH) was assessed as a heterogeneity index. A lower AUC-CSH was assumed to correspond to a more heterogeneous distribution [22].

### 4 Resistance and Heterogeneity of Intratumoral Antibody Distribution

Hanaoka et al. investigated 37 patients with histologically confirmed follicular lymphoma underwent  $^{90}\text{Y}$ -ibritumomab tiuxetan therapy [25]. Of these 37 patients, 16 met the following criteria: they underwent (a) pretherapeutic PET/CT, (b) post-therapeutic PET/CT, and (c) pretherapeutic  $^{111}\text{In}$ - ibritumomab tiuxetan SPECT/CT along with whole-body planar scans, and (d) they had at least one lymphoma lesion analyzable on images, that is, 2 cm or more in diameter. The PET/CT and SPECT/CT

examinations of these patients were analyzed based on the tumor response. The institutional review board waived the requirement of the informed consent of patients and approved this retrospective study.

The lesions of the follicular lymphoma patients were classified into responder lesions and non-responder lesions on a lesion-by-lesion basis by referring to CT findings. The long diameter of pretherapeutic lesions was  $15.9 \pm 4.2$  mm and  $17.9 \pm 6.4$  mm for responders and non-responders, respectively. There was a tendency for responders to show a smaller diameter than non-responders, but no significant difference was observed. The pretherapeutic FDG SUV<sub>max</sub> was  $4.8 \pm 2.0$  and  $8.5 \pm 4.7$  ( $p < 0.05$ ) for responders and non-responders, respectively. There was a positive correlation between glucose metabolism and  $^{111}\text{In}$ -ibritumomab tiuxetan accumulation in lesions. On SPECT/CT images, tumor accumulation of  $^{111}\text{In}$ -ibritumomab tiuxetan did not show a significant difference between responders and non-responders.

In SPECT/CT voxel-based histogram analyses of  $^{111}\text{In}$ -ibritumomab tiuxetan uptake, the non-responder group showed a more heterogeneous distribution than the responder group.

## 5 Conclusions and Perspectives

There was a statistically positive correlation between glucose metabolism and  $^{111}\text{In}$ -ibritumomab tiuxetan accumulation in lesions. Pretherapeutic FDG accumulation was predictive of the tumor response to  $^{90}\text{Y}$ -ibritumomab tiuxetan therapy. The heterogeneity of the intratumoral distribution rather than the absolute accumulation level of  $^{111}\text{In}$ -ibritumomab tiuxetan was correlated with the tumor response.

**Conflict of Interest** No conflict statement: No potential conflicts of interest were disclosed.

## References

1. Storto G, De Renzo A, Pellegrino T, Perna F, De Falco T, Erra P, et al. Assessment of metabolic response to radioimmunotherapy with  $^{90}\text{Y}$ -ibritumomab tiuxetan in patients with relapsed or refractory B-cell non-Hodgkin lymphoma. *Radiology*. 2010;254(1):245–52.
2. Witzig TE, Molina A, Gordon LI, Emmanouilides C, Schilder RJ, Flinn IW, et al. Long-term responses in patients with recurring or refractory B-cell non-Hodgkin lymphoma treated with yttrium 90 ibritumomab tiuxetan. *Cancer*. 2007;109(9):1804–10.
3. Conti PS, White C, Pieslor P, Molina A, Aussie J, Foster P. The role of imaging with ( $^{111}\text{In}$ ) In-ibritumomab tiuxetan in the ibritumomab tiuxetan (zevalin) regimen: results from a Zevalin Imaging Registry. *J Nucl Med*. 2005;46(11):1812–8.
4. Jacobs SA, Harrison AM, Swerdlow SH, Foon KA, Avril N, Vidnovic N, et al. Radioisotopic localization of ( $^{90}\text{Y}$ )yttrium-ibritumomab tiuxetan in patients with CD20+ non-Hodgkin's lymphoma. *Mol Imaging Biol*. 2009;11(1):39–45.



5. Iagaru A, Gambhir SS, Goris ML. 90Y-ibritumomab therapy in refractory non-Hodgkin's lymphoma: observations from 111In-ibritumomab pretreatment imaging. *J Nucl Med.* 2008;49(11):1809–12.
6. Amro H, Wilderman SJ, Dewaraja YK, Roberson PL. Methodology to incorporate biologically effective dose and equivalent uniform dose in patient-specific 3-dimensional dosimetry for non-Hodgkin lymphoma patients targeted with 131I-tositumomab therapy. *J Nucl Med.* 2010;51(4):654–9.
7. Hrycushko BA, Ware S, Li S, Bao A. Improved tumour response prediction with equivalent uniform dose in pre-clinical study using direct intratumoural infusion of liposome-encapsulated 186Re radionuclides. *Phys Med Biol.* 2011;56(17):5721–34.
8. O'Donoghue JA. Implications of nonuniform tumor doses for radioimmunotherapy. *J Nucl Med.* 1999;40(8):1337–41.
9. Kalogianni E, Flux GD, Malaroda A. The use of BED and EUD concepts in heterogeneous radioactivity distributions on a multicellular scale for targeted radionuclide therapy. *Cancer Biother Radiopharm.* 2007;22(1):143–50.
10. Jacene HA, Filice R, Kasecamp W, Wahl RL. 18F-FDG PET/CT for monitoring the response of lymphoma to radioimmunotherapy. *J Nucl Med.* 2009;50(1):8–17.
11. Lopci E, Santi I, Derenzini E, Fonti C, Savelli G, Bertagna F, et al. FDG-PET in the assessment of patients with follicular lymphoma treated by ibritumomab tiuxetan Y 90: multicentric study. *Ann Oncol.* 2010;21(9):1877–83.
12. Cheson BD, Pfistner B, Juweid ME, Gascoyne RD, Specht L, Horning SJ, et al. Revised response criteria for malignant lymphoma. *J Clin Oncol.* 2007;25(5):579–86.
13. Assie K, Dieudonne A, Gardin I, Buvat I, Tilly H, Vera P. Comparison between 2D and 3D dosimetry protocols in 90Y-ibritumomab tiuxetan radioimmunotherapy of patients with non-Hodgkin's lymphoma. *Cancer Biother Radiopharm.* 2008;23(1):53–64.
14. Lopci E, Santi I, Tani M, Maffione AM, Montini G, Castellucci P, et al. FDG PET and 90Y ibritumomab tiuxetan in patients with follicular lymphoma. *Q J Nucl Med Mol Imaging.* 2010;54(4):436–41.
15. Dieudonne A, Hobbs RF, Bolch WE, Sgouros G, Gardin I. Fine-resolution voxel S values for constructing absorbed dose distributions at variable voxel size. *J Nucl Med.* 2010;51(10):1600–7.
16. Flux G, Bardies M, Monsieurs M, Savolainen S, Strands SE, Lassmann M. The impact of PET and SPECT on dosimetry for targeted radionuclide therapy. *Z Med Phys.* 2006;16(1):47–59.
17. Jentzen W, Weise R, Kupferschlag J, Freudenberg L, Brandau W, Bares R, et al. Iodine-124 PET dosimetry in differentiated thyroid cancer: recovery coefficient in 2D and 3D modes for PET/(CT) systems. *Eur J Nucl Med Mol Imaging.* 2008;35(3):611–23.
18. Fabbri C, Sarti G, Cremonesi M, Ferrari M, Di Dia A, Agostini M, et al. Quantitative analysis of 90Y bremsstrahlung SPECT-CT images for application to 3D patient-specific dosimetry. *Cancer Biother Radiopharm.* 2009;24(1):145–54.
19. Hughes T, Celler A. A multivendor phantom study comparing the image quality produced from three state-of-the-art SPECT-CT systems. *Nucl Med Commun.* 2012;33(6):663–70.
20. Cazaentre T, Morschhauser F, Vermandel M, Betrouni N, Prangere T, Steinling M, et al. Pre-therapy 18F-FDG PET quantitative parameters help in predicting the response to radioimmunotherapy in non-Hodgkin lymphoma. *Eur J Nucl Med Mol Imaging.* 2010;37(3):494–504.
21. Hanaoka K, Watabe T, Naka S, Kanai Y, Ikeda H, Horisugi G, et al. FBPA PET in boron neutron capture therapy for cancer: prediction of  $(^{10}\text{B})$  concentration in the tumor and normal tissue in a rat xenograft model. *EJNMMI Res.* 2014;4(1):70.
22. Watabe T, Tatsumi M, Watabe H, Isohashi K, Kato H, Yanagawa M, et al. Intratumoral heterogeneity of F-18 FDG uptake differentiates between gastrointestinal stromal tumors and abdominal malignant lymphomas on PET/CT. *Ann Nucl Med.* 2012;26(3):222–7.

23. Vicini P, Bonadonna RC, Utriainen T, Nuutila P, Raitakari M, Yki-Jarvinen H, et al. Estimation of blood flow heterogeneity distribution in human skeletal muscle from positron emission tomography data. *Ann Biomed Eng.* 1997;25(5):906–10.
24. Baek HJ, Kim HS, Kim N, Choi YJ, Kim YJ. Percent change of perfusion skewness and kurtosis: a potential imaging biomarker for early treatment response in patients with newly diagnosed glioblastomas. *Radiology.* 2012;264(3):834–43.
25. Hanaoka K, Hosono M, Tatsumi Y, Ishii K, Im SW, Tsuchiya N, et al. Heterogeneity of intratumoral (111)in-ibritumomab tiuxetan and (18)F-FDG distribution in association with therapeutic response in radioimmunotherapy for B-cell non-Hodgkin's lymphoma. *EJNMMI Res.* 2015;5:10.

# Radiation Dosimetry in Ibritumomab Therapy



Gerhard Glatting

**Abstract** Radioimmunotherapy (RIT) is a special case of targeted radionuclide therapy (TRT) or molecular radiotherapy (MRT) which uses a monoclonal antibody as transporter of the radioactive atoms. The radioactively labelled antibody selectively accumulates in tumour cells and kills or sterilizes the target cells. The treatment effect depends on the absorbed dose; therefore, the absorbed dose must be determined for individual treatment planning. In this chapter the steps for dosimetry-based treatment planning are presented and discussed. These are a prerequisite for adequate determination of the dose-response relationship in clinical trials which in turn is required for optimal individual treatment planning.

**Keywords** Dosimetry · Treatment planning · Molecular radiotherapy (MRT) · Targeted radionuclide therapy (TRT) · Ibritumomab · Radioimmunotherapy

## Abbreviations

BSA	Body surface area
CT	Computed tomography
EU	European Union
NHL	Non-Hodgkin's lymphoma
MIRD	Medical Internal Radiation Dose Committee
MRT	Molecular radiotherapy
OAR	Organ at risk
PET	Positron emission tomography
RIT	Radioimmunotherapy
SPECT	Single-photon emission computed tomography
TAC	Time-activity curve

---

G. Glatting (✉)

Medical Radiation Physics, Department of Nuclear Medicine, Ulm University, Ulm, Germany  
e-mail: [gerhard.glatting@uni-ulm.de](mailto:gerhard.glatting@uni-ulm.de)

TRT	Targeted radionuclide therapy
USA	United States of America
$^{111}\text{In}$	Isotope of Indium with mass number 111 (the radionuclide Indium-111)
$^{90}\text{Y}$	Isotope of Yttrium with mass number 90 (the radionuclide Yttrium-90)

## 1 Introduction

Molecular radiotherapy (MRT) [1, 2] or targeted radionuclide therapy (TRT) [3, 4] is a nuclear medicine treatment modality in which a radionuclide or a radioactively labelled pharmaceutical is administered to the patient. The radioactive substance selectively accumulates in tumour cells and kills or sterilizes the target cells while minimizing adverse effects to other organs (chapter “[Clinical Use and Efficacy of Ibritumomab in B Cell Lymphoma](#)”). Thus, it is a systemic radiotherapy, i.e. after the intravenous injection, the radiolabelled antibody is distributed systemically and accumulates at the target sites due to the specific binding of the transporter molecule to the corresponding antigens. The short range of the emitted particulate radiation, e.g.  $\beta^-$  or  $\alpha$  particles, then ensures high absorbed doses in the accumulating tissues and low absorbed doses in the non-targeted organs at risk.

Radioimmunotherapy is a special case of MRT or TRT in which the radiolabelled drug is an antibody. [ $^{90}\text{Y}$ ]Ibritumomab tiuxetan is a radiolabelled anti-CD20 monoclonal antibody that is used in the treatment of non-Hodgkin’s lymphoma (NHL) and other hematologic malignancies [4–7]. The monoclonal mouse IgG1 antibody ibritumomab is labelled with the  $\beta^-$  emitter  $^{90}\text{Y}$  by the chelator tiuxetan for use in radioimmunotherapy treatment (chapter “[Characteristics of Ibritumomab as Radionuclide Therapy Agent](#)”).

The activity to administer for treatment can be determined in two main ways – either based on activity escalation trials (section “[Activity Escalation Trial and Dose Escalation Trial](#)”) or based on absorbed doses, i.e. on dosimetry (section “[Dosimetry for Molecular Radiotherapy](#)”). [ $^{90}\text{Y}$ ]Ibritumomab tiuxetan dosimetry is presented and discussed in section “[Dosimetry for Ibritumomab Tiuxetan](#)”. An accurate dosimetry is a prerequisite for adequate treatment planning based on a known dose-response relationship [2]. Points to consider in treatment planning, i.e. the determination of the optimal treatment activity, is presented in section “[Treatment Planning for \[ \$^{90}\text{Y}\$ \] Ibritumomab Tiuxetan](#)”. The chapter is completed with a conclusion and an outlook in section “[Conclusion and Outlook](#)”.

## 2 Activity Escalation Trial and Dose Escalation Trial

One method to determine the activity to administer for molecular therapy is analogous to chemotherapy and is often named “dose escalation trial” although in nuclear medicine the more appropriate name is “activity escalation trial”. For this, small groups of patients are treated with a specified (low) activity. This activity may or

may not be adjusted to body weight (BW) or body surface area (BSA). The escalation trial is then performed as follows:

1. Define a (rather low) activity to start with.
2. Treat small groups of patients (3–6 patients).
3. Collect data about occurring adverse effects.
4. Increase activity for each new group step by step, i.e. go back to step 2.
5. If toxicities become severe => lower activity by one step.
6. This activity is defined as the “optimal” activity.

The starting activity in step 1 is defined based on previous knowledge of the biodistribution in patients (and/or animals) and observed effects. The same holds true for the definition of the step size in step 4. Steps 2–4 are then repeated until toxicities become severe (items 5 and 6).

This or similar activity escalation trial algorithms neglect (the often quite large) inter-patient variability, e.g. due to individual differences in the pharmacokinetics or the sensitivity to radiation or the pretreatment. Using a constant activity for all patients, even if it is partially individualized by normalizing to BW or BSA, thus leads to over- and under-treatments for some patients.

From radiation therapy trials, it is well known that the absorbed dose is one main constituent of the effect of tumour cell kill [2]. Therefore, it was expected and already demonstrated [2] that a dose-response relationship exists also for MRT. Thus, to reduce the variability due to different individual pharmacokinetics, an “absorbed dose escalation trial” should be performed instead of the “activity escalation trial” presented above. The algorithm of such a trial could be analogous to the one described above: just instead of a prescribed activity, a prescribed absorbed dose could be used (as in radiation therapy). For this to be possible, a pre-therapeutic dosimetry is needed, to be able to calculate the activity to administer to achieve a prescribed absorbed dose in the target organ, or to stay below a maximum absorbed dose in an organ at risk (OAR). This dosimetry for MRT is described in section “[Dosimetry for Molecular Radiotherapy](#)”.

### 3 Dosimetry for Molecular Radiotherapy

In MRT, the absorbed doses of all the different organs depend on the spatial *and* temporal distributions of the radiolabelled drug. Therefore, the dosimetric approach differs from that used in radiotherapy as described below. A specific methodology was developed by the Medical Internal Radiation Dose Committee (MIRD) and published as a series of “MIRD pamphlets” [8, 9].

In the following sections, the sequence of steps needed to perform nuclear medicine dosimetry for MRT is presented [10–14]. A detailed description of the methodology applied for dosimetry and how to report the obtained results can be found in the (open access) “EANM Dosimetry Committee guidance document: good practice of clinical dosimetry reporting” [11] and specifically for the bone marrow in Ref. [15].

### 3.1 *Quantification of Pharmacokinetics*

Planar gamma camera measurements are still most often performed for imaging of the biodistribution of the radiolabelled drug, although the limitations are well known and not easy to overcome [16, 17]. Besides corrections for attenuation, scatter, dead-time and the geometry (thickness) of the organs, manual region drawing, for example, is hampered by over- and underlying activity of different tissues and is not easy to quantify correctly. Nevertheless, it allows a patient-specific approach for organ absorbed doses, which already is an improvement over methods relying on cohort data without kinetic data of the different organs (e.g. in chemotherapy).

Tomographic modalities, like single-photon emission computed tomography (SPECT)/computed tomography (CT), positron emission tomography (PET)/CT or PET/magnetic resonance imaging (MRI), allow in principle more accurate and precise quantification, provided that attenuation, scatter and dead-time corrections as well as the image reconstruction algorithm are adequately used [18]. In addition, the region drawing step becomes more reproducible in the 3D data set [19].

Hybrid methods based on one tomographic measurement and planar gamma camera measurements are used to reduce the workload [20].

Blood and urine sampling provides additional information on the biokinetics of the investigated drug [21].

### 3.2 *Kinetic Model*

For the calculation of the absorbed doses, one needs to know the number of decays in each accumulating organ. This is calculated from the area under the time-activity curve (TAC). Therefore, it was suggested to use the following multiples of the effective half-life  $T_e$ :  $1/3 T_e$ ,  $2/3 T_e$ ,  $1.5 T_e$ ,  $3 T_e$  and  $5 T_e$  [13, 22]. This suggestion is not easy to follow because the effective half-lives among organs differ. Therefore, the sampling schedule is often based on the rules of thumb [16, 22], e.g. three measurements per exponential. However, there are also standard methods to calculate the optimal sampling schedule based on available population kinetics [23–25]. An increased precision of the calculated areas under the curves for a given number of measurements is then expected.

In the simplest case the measured time points of the patient's biokinetics were fitted simply by sums of exponentials [26, 27]. To determine the "optimal" number of exponential terms, an observer-independent method should be applied, e.g. using the Akaike information criterion [28–30]. To judge the precision of the results, uncertainty measures for the area under the curve must be given [11, 27, 30, 31].

A better approach is the use of physiologically based pharmacokinetic (PBPK) models, as these can integrate previous knowledge about the patients [32–34]. Then, a lower number of parameters needs to be estimated, which yields a more accurate and precise determination of the number of decays in the accumulating organs [35]. In addition, PBPK models enable *in silico* optimization of the biodistribution [36–38].

### 3.3 Prediction of Pharmacokinetics During Therapy

Usually it is assumed that the pre-therapeutic and therapeutic biokinetics are equal. This however has to be demonstrated, as often the activity and amount of drug are changed. For the latter case, it was shown that the amount of (unlabelled) drug influences the biodistribution [39–42].

Fitting the TAC simply by a sum of exponentials (section “Kinetic Model”) clearly does not allow to predict and quantify such changes. This can however be done when using adequate PBPK models [43, 44]. Thus, when using PBPK modelling, active modulation of the biodistribution may allow for individually optimized therapeutic indices [40, 45]. This could be achieved by choosing patient-specific optimal amounts of radiopharmaceuticals and activities independently [43, 44].

In some cases it may even be possible to considerably simplify dosimetry using a PBPK model with prior knowledge and in silico simulations [46, 47].

### 3.4 Absorbed Dose Calculations

For calculation of absorbed doses, the physical properties of the radionuclide, e.g. emitted radiations and energies, are needed together with the geometry in the patients, e.g. mass and locations of organs [22]. For this purpose, whole-body and organ level anthropomorphic phantoms exist [48]. The phantom and radionuclide information is combined into the “S values” [8], which are implemented, for example, in the OLINDA/EXM software [49] to calculate the absorbed doses according to the following equations:

$$D(r_T) = A_0 \cdot \sum_{r_S} \tilde{a}(r_S) \cdot S(r_T \leftarrow r_S) \quad (1)$$

with the administered activity  $A_0$  and the indices S and T denoting source and target. The  $S(r_T \leftarrow r_S)$  value is the dose transmitted to the target organ per decay in the source organ and is calculated as

$$S(r_T \leftarrow r_S) = \sum_i n_i E_i \varphi_i(r_T \leftarrow r_S) / m_T \quad (2)$$

with index  $i$  denominating the different decay modes of the used radionuclide,  $n_i$  the transition probability for mode  $i$ ,  $E_i$  the energy of decay of mode  $i$ , and  $\varphi_i(r_T \leftarrow r_S)$  the absorbed fraction in target organ T for a decay of mode  $i$  in the source organ S.  $m_T$  is the mass of the target organ.

The  $\tilde{a}(r_S)$  value is the time-integrated activity coefficient (TIAC) and is calculated from



$$\bar{a}(r_s) = \frac{1}{A_0} \int_0^\infty A(r_s, t) dt \quad (3)$$

with  $A(r_s, t)$  being the TAC in the source organ. The TIAC is the number of decays in the source organ ( $\Rightarrow$  the integral) per administered activity  $A_0$ . Note that in older literature the TIAC is named “residence time” [9].

Using individual S values instead of the phantom-generated standard S values is a way to improve dosimetry [50], because the patient’s anatomy may vary considerably. Another generalization is possible with respect to the structure of the source and target: Eqs. (1), (2), and (3) are defined for “organs”; however, the generalization to arbitrary “structures” instead of organs is straightforward. Therefore, these structures could also be voxels or cellular level S-factors and, thus, provide further opportunities to improve individualized treatments [48, 51, 52].

The output of the absorbed dose calculations (Eq. (1)) can be transformed to doses per administered activity  $A_0$  for all accumulating or critical organs (by simple division by  $A_0$ ). These doses per administered activity are used in the next step for treatment planning.

### 3.5 Treatment Planning

Standard treatment planning in MRT relies on prescribing a minimum absorbed dose for the target organ and constraining the maximum absorbed doses for the organs at risk [12]. The administered activity is then calculated based on the results of pre-therapeutic dosimetry (section “Absorbed Dose Calculations”) such that the constraints posed by the treating physician are not violated.

The absorbed dose is not the single factor determining the outcome of molecular radiotherapy. Other determinants are, for example, the dose rate and the repair rate [53]. Therefore, the concept of biologically effective dose (BED) [54], which includes radiobiological knowledge [55, 56], showed already promising results in peptide receptor radionuclide therapy (PRRT) [57, 58].

The combination of different radiopharmaceutical therapies could possibly improve the outcome [59]; however, this needs an even better understanding of the complex radiobiological interactions. The same holds true for every other combination therapy.

### 3.6 Treatment and Quality Control Measurements

Verification of the therapeutic dose must be performed. For this, a simple but effective routine quality control methods must still be developed, e.g. quantification of bremsstrahlung imaging for  $^{90}\text{Y}$  or the measurement of serum kinetics during therapy [41, 60].

### 3.7 Conclusion

Dosimetry for MRT is a complex task as seen from the steps described above. The accuracy and precision of the obtained results must be carefully controlled and the obtained results interpreted accordingly. Failure in one of the steps described above can invalidate the results!

## 4 Dosimetry for Ibritumomab Tiuxetan

Ibritumomab is a mouse antibody directed against the CD20 antigen, which is covalently conjugated to the metal chelator tiuxetan. After radiolabelling with the radionuclide  $^{90}\text{Y}$ , it is used for radioimmunotherapy (Zevalin®, Spectrum Pharmaceuticals, Inc., USA and Bayer Schering Pharma AG, Germany).

The radionuclide  $^{90}\text{Y}$  consists of 39 protons and 51 neutrons and decays with a half-life of 64.1 h by  $\beta^-$  emission (99.997%) to the stable  $^{90}\text{Zr}$ ; it is produced by bombardment of  $^{89}\text{Y}$  with neutrons. The emitted  $\beta^-$  particles possess a maximum energy of 2.28 MeV and have an average electron kinetic energy of 0.94 MeV. In tissue, they have a limited penetration with a maximum range of 1.1 cm and a mean range of 3.6 mm. Thus, 90% of the energy is absorbed in a sphere of radius 5.3 mm [61]. A very low electron-positron pair production (0.003%, [62]) can be used for PET imaging [63].

Before therapy with [ $^{90}\text{Y}$ ]Ibritumomab tiuxetan, different preloads with unlabelled antibody are given [6, 7] (chapters “Clinical Use and Efficacy of Ibritumomab in B Cell Lymphoma, Features of Ibritumomab as Radionuclide Therapy, Radiological Evaluation of Response and Resistance of Ibritumomab, and Resistance and Heterogeneity of Intratumoral Antibody Distribution”). This will influence the subsequent biodistribution of radiolabelled antibody and, thus, also the dose distribution. Therefore, it can possibly be used to optimize the individual dose distribution, as was already shown for other antibodies [33, 38, 45].

To confirm a favourable biodistribution, in the USA and Switzerland, pre-therapeutic imaging with [ $^{111}\text{In}$ ]Ibritumomab tiuxetan needs to be performed.  $^{111}\text{In}$ -labelling is used instead of  $^{90}\text{Y}$ , because  $^{90}\text{Y}$  lacks a  $\gamma$  emission and quantitative imaging based on the bremsstrahlung of  $^{90}\text{Y}$  is difficult.

In the EU the biodistribution does not need to be confirmed for use according to the authority approval.

The quantification of the individual pharmacokinetics is one major determinant for obtaining the accurate individual absorbed doses for the target and the organs at risk. Also, it was shown that different measurement protocols will lead to statistically different absorbed doses [20]. As described in section “Quantification of Pharmacokinetics”, tomographic methods are to be preferred over planar methods due to their better accuracy. Nevertheless, even for tomographic methods, accurate quantification is difficult to achieve and must be carefully controlled [7]. A comprehensive overview on the methodologies used and results obtained in different stud-

ies with [ $^{90}\text{Y}$ ]Ibritumomab tiuxetan is given by Sjögreen-Gleisner et al. [7] and in the EANM guideline [6].

[ $^{111}\text{In}$ ]Ibritumomab tiuxetan is administered for pre-therapeutic imaging for dosimetry, whereas for dosimetry during therapy the bremsstrahlung due to the emitted  $\beta^-$  particles of  $^{90}\text{Y}$  is used. Although there is in general a good agreement when using proper corrections [7], it remains, however, unclear if the obtained differences are due to the uncertainties in the (already sophisticated) method of bremsstrahlung quantification or real changes in the biokinetics between both measurements [7].

Changes in the biokinetics could be either due to differences between the radionuclides [21, 64] or due to the time delay between pre-therapeutic and therapeutic measurements, e.g. progress of disease, or due to administering different amounts of antibodies. Differences due to the different radionuclides can be assumed to be small [21, 64]; but, for example, during pre-therapeutic measurement, about 185 MBq of  $^{111}\text{In}$ -labelled ibritumomab tiuxetan are administered, whereas for therapy about 1 GBq of  $^{90}\text{Y}$ -labelled antibody is used. As higher activity needs more antibody molecules to be labelled, also saturation effects [34, 41, 65, 66] or changes in immunoreactivity of the antibodies [65–67] may cause different biokinetics.

Even in case there is no relevant time delay between pre-therapeutic and therapeutic measurements to affect the disease, the measurement protocol for [ $^{90}\text{Y}$ ]Ibritumomab tiuxetan therapy includes already during the pre-therapeutic imaging a drip infusion of 250 mg/m<sup>2</sup> rituximab. This treatment with rituximab has the effect to change the “initial conditions” between the pre-therapeutic imaging and the therapy and, thus, most probably will already change the biokinetics.

The other major determinant for obtaining accurate individual absorbed doses for the target and the organs at risk is the use of adequate S values (section “[Absorbed Dose Calculations](#)”). The true patient-specific S values may differ by a factor of 2 compared to the respective standard S values for the self-irradiation of organs [50]. Only in case that proper mass correction was applied the deviation became less than 26%. An effect of the same magnitude was also shown for the mass dependence of anti-CD66 monoclonal antibodies used for conditioning before blood stem cell transplantation of leukaemia patients [68].

Based on the large biological differences in the biokinetics and the large variety of methodologies, which result in an additional large variability, a large range of results obtained for the absorbed doses per unit administered activity in different studies with [ $^{90}\text{Y}$ ]Ibritumomab tiuxetan is found (Table 1).

**Table 1** Absorbed doses per unit administered activity in different studies with [ $^{90}\text{Y}$ ]Ibritumomab tiuxetan collected by Sjögreen-Gleisner et al. [7]

Organ	Median <sup>a</sup> Gy/GBq	Range Gy/GBq
Total body <sup>b</sup>	≈0.6	0.25–1
Liver	≈4	1–12
Kidneys	≈2.5	0.2–10
Red bone marrow	≈1	0.3–2.7

<sup>a</sup>Estimated median of all included studies in [7]

<sup>b</sup>The agreement between different studies is excellent

## 5 Treatment Planning for [ $^{90}\text{Y}$ ]Ibritumomab Tiuxetan

Treatment planning for molecular radiotherapy with [ $^{90}\text{Y}$ ]Ibritumomab tiuxetan is essentially the determination of the activity to administer, which will yield an optimal safety and efficacy of the treatment. In addition, also the second cancer risk of long survivors could be considered [69].

Due to all the effects discussed in section “[Dosimetry for Ibritumomab Tiuxetan](#)” above, it may be very difficult to implement an individualized treatment planning based on *pre-therapeutic* imaging. Nevertheless, for fractionated treatment the absorbed doses delivered by the first fraction could be shown to predict that delivered by the second fraction [20]. Thus, at least for fractionated treatment, the subsequent absorbed doses could possibly be planned based on the preceding individual therapeutic dosimetry. Therefore, individualization based on biokinetics measurements using quantitative imaging modalities, external counting and blood sampling is reachable to some extent, allowing patient-specific dosimetry to be performed as in radiation therapy. Such an implementation of patient-specific dosimetry – although limited – will help to avoid over- or under-treatment of the patients.

A relatively simple improvement of treatment planning is already achievable by using the individual organ masses, as the use of standard phantom masses for dosimetry is not adequate [68].

A prerequisite for such a treatment planning is a known dose-response relationship [2]. Although a correlation between image-based dosimetry (absorbed dose) and bone marrow toxicity was already shown [20], additional studies are needed.

## 6 Conclusion and Outlook

[ $^{90}\text{Y}$ ]Ibritumomab tiuxetan patient-specific dosimetry for individual treatment planning is possible. This should allow reducing the number of over- and under-treated patients and thus should be preferred. However, further clinical studies with accurately described adequate methodology of the complex dosimetric procedure should be performed. Specifically, the use of a quantitative tomographic imaging modality, i.e. SPECT/CT or PET/CT, is mandatory to obtain reliable data for finding the correct dose-response relationship.

Performing quantitative dosimetry will further allow to develop physiologically-based pharmacokinetic models, which in turn can be used to improve the individual therapy. For example, the patient-specific optimal antibody amounts and activities could possibly be determined based on *in silico* simulations, or *in silico* clinical trials can be performed to prepare an optimal clinical trial.

**Conflict of Interest** No potential conflicts of interest were disclosed.

## References

1. McGowan DR, Guy MJ. Time to demand dosimetry for molecular radiotherapy? *Br J Radiol.* 2015;88(1047):20140720.
2. Strigari L, Konijnenberg M, Chiesa C, Bardies M, Du Y, Gleisner K, et al. The evidence base for the use of internal dosimetry in the clinical practice of molecular radiotherapy. *Eur J Nucl Med Mol Imag.* 2014;41(10):1976–88.
3. Fahey F, Zukotynski K, Jadvar H, Capala J. Proceedings of the second NCI–SNMMI workshop on targeted radionuclide therapy. *J Nucl Med.* 2015;56(7):1119–29.
4. Zukotynski K, Jadvar H, Capala J, Fahey F. Targeted radionuclide therapy: practical applications and future prospects. *Biomarkers Cancer.* 2016 (5629-BIC-Targeted-Radionuclide-Therapy:-Practical-Applications-and-Future-Prosp.pdf):35–8.
5. Wagner HN, Wiseman GA, Marcus CS, Nabi HA, Nagle CE, Fink-Bennett DM, et al. Administration guidelines for radioimmunotherapy of non-Hodgkin's lymphoma with  $^{90}\text{Y}$ -labeled anti-CD20 monoclonal antibody. *J Nucl Med.* 2002;43(2):267–72.
6. Tennvall J, Fischer M, Bischof Delaloye A, Bombardieri E, Bodei L, Giammarile F, et al. EANM procedure guideline for radio-immunotherapy for B-cell lymphoma with  $^{90}\text{Y}$ -radiolabelled ibritumomab tiuxetan (Zevalin). *Eur J Nucl Med Mol Imaging.* 2007;34(4):616–22.
7. Sjögreen-Gleisner K, Dewaraja YK, Chiesa C, Tennvall J, Linden O, Strand SE, et al. Dosimetry in patients with B-cell lymphoma treated with [ $^{90}\text{Y}$ ]ibritumomab tiuxetan or [ $^{131}\text{I}$ ]tositumomab. *Q J Nucl Med Mol Imaging.* 2011;55(2):126–54.
8. Howell RW, Wessels BW, Loevinger R, Watson EE, Bolch WE, Brill AB, et al. The MIRD perspective 1999. Medical internal radiation dose committee. *J Nucl Med.* 1999;40(1):3S–10S.
9. Bolch WE, Eckerman KF, Sgouros G, Thomas SR. MIRD pamphlet no. 21: a generalized schema for radiopharmaceutical dosimetry—standardization of nomenclature. *J Nucl Med.* 2009;50(3):477–84.
10. Konijnenberg M. From imaging to dosimetry and biological effects. *Q J Nucl Med Mol Imaging.* 2011;55(1):44–56.
11. Lassmann M, Chiesa C, Flux G, Bardiès M. EANM dosimetry committee guidance document: good practice of clinical dosimetry reporting. *Eur J Nucl Med Mol Imaging.* 2011;38(1):192–200.
12. Glatting G, Bardiès M, Lassmann M. Treatment planning in molecular radiotherapy. *Z Med Phys.* 2013;23(4):262–9.
13. Glatting G, Lassmann M. Nuclear medicine dosimetry: quantitative imaging and dose calculations. *Z Med Phys.* 2011;21(4):246–7.
14. Sgouros G, Hobbs RF. Dosimetry for radiopharmaceutical therapy. *Semin Nucl Med.* 2014;44(3):172–8.
15. Hindorf C, Glatting G, Chiesa C, Lindén O, Flux G. EANM Dosimetry Committee guidelines for bone marrow and whole-body dosimetry. *Eur J Nucl Med Mol Imaging.* 2010;37(6):1238–50.
16. Siegel JA, Thomas SR, Stubbs JB, Stabin MG, Hays MT, Koral KF, et al. MIRD pamphlet no. 16: techniques for quantitative radiopharmaceutical biodistribution data acquisition and analysis for use in human radiation dose estimates. *J Nucl Med.* 1999;40(2):37S–61S.
17. Frey EC, Humm JL, Ljungberg M. Accuracy and precision of radioactivity quantification in nuclear medicine images. *Semin Nucl Med.* 2012;42(3):208–18.
18. Ljungberg M, Celler A, Konijnenberg MW, Eckerman KF, Dewaraja YK, Sjögreen-Gleisner K. MIRD Pamphlet no. 26: joint EANM/MIRD guidelines for quantitative  $^{177}\text{Lu}$  SPECT applied for dosimetry of radiopharmaceutical therapy. *J Nucl Med.* 2016;57(1):151–62.
19. Flux G, Bardies M, Monsieurs M, Savolainen S, Strand SE, Lassmann M. The impact of PET and SPECT on dosimetry for targeted radionuclide therapy. *Z Med Phys.* 2006;16:47–59.
20. Ferrer L, Malek E, Bodet-Milin C, Legouill S, Prangère T, Robu D, et al. Comparisons of dosimetric approaches for fractionated radioimmunotherapy of non-Hodgkin lymphoma. *Q J Nucl Med Mol Imaging.* 2012;56(6):529–37.

21. Kotzerke J, Glatting G, Seitz U, Rentschler M, Neumaier B, Bunjes D, et al. Radioimmunotherapy for the intensification of conditioning before stem cell transplantation: differences in dosimetry and biokinetics of  $^{188}\text{Re}$ - and  $^{99\text{m}}\text{Tc}$ -labeled anti-NCA-95 MAbs. *J Nucl Med.* 2000;41(3):531–7.
22. Adelstein SJ, Green AJ, Howell RW, Humm JL, Leichner PK, O'donoghue JA, et al. Absorbed-dose specification in nuclear medicine. *J ICRU.* 2002;2(1):1–110.
23. Ogungbenro K, Aarons L. An effective approach for obtaining optimal sampling windows for population pharmacokinetic experiments. *J Biopharm Stat.* 2009;19(1):174–89.
24. Kalicka R, Bochen D. Properties of D-optimal sampling schedule for compartmental models. *Biocybernetics Biomed Eng.* 2005;25(1):23–36.
25. D'Argenio DZ. Optimal sampling times for pharmacokinetic experiments. *J Pharmacokinetic Biopharm.* 1981;9(6):739–56.
26. Strand SE, Zanzonico P, Johnson TK. Pharmacokinetic modeling. *Med Phys.* 1993;20(2 Pt 2):515–27.
27. Glatting G, Landmann M, Kull T, Wunderlich A, Blumstein NM, Buck AK, et al. Internal radionuclide therapy: the UlmDos software for treatment planning. *Med Phys.* 2005;32(7):2399–405.
28. Kletting P, Glatting G. Model selection and inference in pharmacokinetics: the corrected Akaike information criterion and the F-test. *Z Med Phys.* 2009;19(3):200–6.
29. Glatting G, Kletting P, Reske SN, Hohl K, Ring C. Choosing the optimal fit function: comparison of the Akaike information criterion and the F-test. *Med Phys.* 2007;34(11):4285–92.
30. Kletting P, Schimmel S, Kestler HA, Hänscheid H, Luster M, Fernández M, et al. Molecular radiotherapy: the NUKFIT software for calculating the time-integrated activity coefficient. *Med Phys.* 2013;40(10):102504.
31. EURAMED. Common Strategic research agenda for radiation protection in medicine. *Insights Imaging.* 2017;8:183–97.
32. Eger RR, Covell DG, Carrasquillo JA, Abrams PG, Foon KA, Reynolds JC, et al. Kinetic model for the biodistribution of an  $^{111}\text{In}$ -labeled monoclonal antibody in humans. *Cancer Res.* 1987;47(12):3328–36.
33. Kletting P, Bunjes D, Reske SN, Glatting G. Improving anti-CD45 antibody radioimmunotherapy using a physiologically based pharmacokinetic model. *J Nucl Med.* 2009;50(2):296–302.
34. Maaß C, Kletting P, Bunjes D, Mahren B, Beer AJ, Glatting G. Population-based modeling improves treatment planning before  $^{90}\text{Y}$ -labeled anti-CD66 antibody Radioimmunotherapy. *Cancer Biother Radiopharm.* 2015;30(7):285–90.
35. Maaß C, Sachs J, Hardiansyah D, Mottaghy F, Kletting P, Glatting G. Dependence of treatment planning accuracy in peptide receptor radionuclide therapy on the sampling schedule. *EJNMMI Res.* 2016;6(1):30.
36. Kletting P, Reske SN, Glatting G. Dependence of the anti-CD66 antibody biodistribution on the dissociation constant: a simulation study. *Z Med Phys.* 2011;21(4):301–4.
37. Bois FY. Physiologically based modelling and prediction of drug interactions. *Basic Clin Pharmacol Toxicol.* 2010;106(3):154–61.
38. Kletting P, Meyer C, Reske SN, Glatting G. Potential of optimal preloading in anti-CD20 antibody radioimmunotherapy: an investigation based on pharmacokinetic modeling. *Cancer Biother Radiopharm.* 2010;25(3):279–87.
39. Velikyan I, Sundin A, Eriksson B, Lundqvist H, Sorensen J, Bergstrom M, et al. In vivo binding of [ $^{68}\text{Ga}$ ]-DOTATOC to somatostatin receptors in neuroendocrine tumours—impact of peptide mass. *Nucl Med Biol.* 2010;37(3):265–75.
40. Kletting P, Müller B, Erentok B, Schmaljohann J, Behrendt FF, Reske SN, et al. Differences in predicted and actually absorbed doses in peptide receptor radionuclide therapy. *Med Phys.* 2012;39(9):5708–17.
41. Kletting P, Kull T, Bunjes D, Mahren B, Luster M, Reske SN, et al. Radioimmunotherapy with anti-CD66 antibody: improving the biodistribution using a physiologically based pharmacokinetic model. *J Nucl Med.* 2010;51(3):484–91.

42. Glatting G, Müller M, Koop B, Hohl K, Friesen C, Neumaier B, et al. Anti-CD45 monoclonal antibody YAM1568: a promising radioimmunoconjugate for targeted therapy of acute leukemia. *J Nucl Med.* 2006;47(8):1335–41.
43. Kletting P, Schuchardt C, Kulkarni HR, Shahinfar M, Singh A, Glatting G, et al. Investigating the effect of ligand amount and injected therapeutic activity: a simulation study for  $^{177}\text{Lu}$ -labeled PSMA-targeting peptides. *PLoS One.* 2016;11(9):e0162303.
44. Kletting P, Kull T, Maaß C, Malik N, Luster M, Beer AJ, et al. Optimized peptide amount and activity for  $^{90}\text{Y}$ -labeled DOTATATE therapy. *J Nucl Med.* 2016;57(4):503–8.
45. Kletting P, Bunjes D, Luster M, Reske SN, Glatting G. Optimal preloading in radioimmunotherapy with anti-CD45 antibody. *Med Phys.* 2011;38(5):2572–8.
46. Hardiansyah D, Guo W, Kletting P, Mottaghy FM, Glatting G. Time-integrated activity coefficient estimation for radionuclide therapy using PET and a pharmacokinetic model: a simulation study on the effect of sampling schedule and noise. *Med Phys.* 2016;43(9):5145–54.
47. Hardiansyah D, Maass C, Attarwala A, Müller B, Kletting P, Mottaghy F, et al. The role of patient-based treatment planning in peptide receptor radionuclide therapy. *Eur J Nucl Med Mol Imaging.* 2016;43(5):871–80.
48. Stabin M. Nuclear medicine dosimetry. *Phys Med Biol.* 2006;51(13):R187–202.
49. Stabin MG, Sparks RB, Crowe E. OLINDA/EXM: the second-generation personal computer software for internal dose assessment in nuclear medicine. *J Nucl Med.* 2005;46(6):1023–7.
50. Divoli A, Chiavassa S, Ferrer L, Barbet J, Flux GD, Bardiès M. Effect of patient morphology on Dosimetric calculations for internal irradiation as assessed by comparisons of Monte Carlo versus conventional methodologies. *J Nucl Med.* 2009;50(2):316–23.
51. Bouchet LG, Bolch WE, Blanco HP, Wessels BW, Siegel JA, Rajon DA, et al. MIRD pamphlet no. 19: absorbed fractions and radionuclide S values for six age-dependent Multiregion models of the kidney. *J Nucl Med.* 2003;44(7):1113–47.
52. Kletting P, Schimmel S, Hänscheid H, Luster M, Fernández M, Nosske D, et al. The NUKDOS software for treatment planning in molecular radiotherapy. *Z Med Phys.* 2015;25(3):264–74.
53. Dale R. Use of the linear-quadratic radiobiological model for quantifying kidney response in targeted radiotherapy. *Cancer Biother Radiopharm.* 2004;19(3):363–70.
54. Jones B, Dale RG, Deehan C, Hopkins KI, Morgan DAL. The role of biologically effective dose (BED) in clinical oncology. *Clin Oncol.* 2001;13(2):71–81.
55. Deasy JO, Mayo CS, Orton CG. Treatment planning evaluation and optimization should be biologically and not dose/volume based. *Med Phys.* 2015;42(6):2753–6.
56. Pouget J-P, Navarro-Teulon I, Bardies M, Chouin N, Cartron G, Pelegrin A, et al. Clinical radioimmunotherapy - the role of radiobiology. *Nat Rev Clin Oncol.* 2011;8(12):720–34.
57. Barone R, Borson-Chazot F, Valkema R, Walrand S, Chauvin F, Gogou L, et al. Patient-specific dosimetry in predicting renal toxicity with  $^{90}\text{Y}$ -DOTATOC: relevance of kidney volume and dose rate in finding a dose-effect relationship. *J Nucl Med.* 2005;46(Suppl 1):99S–106S.
58. Cremonesi M, Botta F, Di Dia A, Ferrari M, Bodei L, De Cicco C, et al. Dosimetry for treatment with radiolabelled somatostatin analogues. A review. *Q J Nucl Med Mol Imag.* 2010;54(1):37–51.
59. Hobbs RF, Wahl RL, Frey EC, Kasamon Y, Song H, Huang P, et al. Radiobiologic optimization of combination radiopharmaceutical therapy applied to Myeloablative treatment of non-Hodgkin lymphoma. *J Nucl Med.* 2013;54(9):1535–42.
60. Minarik D, Sjögreen-Gleisner K, Linden O, Wingårdh K, Tennvall J, Strand S-E, et al.  $^{90}\text{Y}$  bremsstrahlung imaging for absorbed-dose assessment in high-dose radioimmunotherapy. *J Nucl Med.* 2010;51(12):1974–8.
61. Simpkin DJ, Mackie TR. EGS4 Monte Carlo determination of the beta dose kernel in water. *Med Phys.* 1990;17(2):179–86.
62. Selwyn RG, Nickles RJ, Thomadsen BR, DeWerd LA, Micka JA. A new internal pair production branching ratio of  $^{90}\text{Y}$ : the development of a non-destructive assay for  $^{90}\text{Y}$  and  $^{90}\text{Sr}$ . *Appl Radiat Isot.* 2007;65(3):318–27.



63. Attarwala AA, Molina-Duran F, Busing KA, Schonberg SO, Bailey DL, Willowson K, et al. Quantitative and qualitative assessment of Yttrium-90 PET/CT imaging. *PLoS One*. 2014;9(11):e110401.
64. Carrasquillo JA, White JD, Paik CH, Raubitschek A, Le N, Rotman M, et al. Similarities and differences in  $^{111}\text{In}$ - and  $^{90}\text{Y}$ -labeled 1B4M-DTPA antiTac monoclonal antibody distribution. *J Nucl Med*. 1999;40(2):268–76.
65. Kletting P, Kiryakos H, Reske SN, Glatting G. Analysing saturable antibody binding based on serum data and pharmacokinetic modelling. *Phys Med Biol*. 2011;56(1):73–86.
66. Kletting P, Maaß C, Reske SN, Beer A, Glatting G. Physiologically based pharmacokinetic modeling is essential in  $^{90}\text{Y}$ -labeled anti-CD66 radioimmunotherapy. *PLoS One*. 2015;10(5):e1027934.
67. Glatting G, Reske SN. Determination of the immunoreactivity of radiolabeled monoclonal antibodies: a theoretical analysis. *Cancer Biother Radiopharm*. 2006;21(1):15–21.
68. Kull T, Kletting P, Reske SN, Glatting G. Determination of individual organ masses for  $^{90}\text{Y}$ -anti-CD66 radioimmunotherapy: influence on therapy planning. *Z Med Phys*. 2011;21(4):305–9.
69. Adelstein SJ. Radiation risk in nuclear medicine. *Semin Nucl Med*. 2014;44(3):187–92.

# Combining RAIT and Immune-Based Therapies to Overcome Resistance in Cancer?



Jean-Baptiste Gorin, Jérémie Ménager, Yannick Guilloux,  
Jean-François Chatal, Joëlle Gaschet, and Michel Chérel

**Abstract** Radiation therapy has long been considered as immunosuppressive; therefore its impact on the immune system and other aspects which could be involved in raising efficient antitumor immune responses has been neglected. However, the recent demonstration of the immunogenic properties of ionizing radiation is rapidly modifying the radiation oncology field, and it also opens new and promising perspectives for the development and improvement of radioimmunotherapy. In this chapter, we first review the immunogenic properties of irradiation before discussing available evidence of the benefits of radiation therapy and immunotherapy combinations in the context of lymphoma.

**Keywords** Radioimmunotherapy · Abscopal effect · Immune response · Immunogenic cell death · Ionizing radiation

## Abbreviations

Ab	Antibody
ADCC	Antibody-dependent cellular cytotoxicity

---

J.-B. Gorin · J. Ménager · Y. Guilloux · J. Gaschet (✉)  
CRCNA, UMR 892 Inserm, 6299 CNRS, Université de Nantes, Nantes, France  
e-mail: [Joelle.Gaschet@univ-nantes.fr](mailto:Joelle.Gaschet@univ-nantes.fr)

J.-F. Chatal  
GIP Arronax, Nantes-Saint-Herblain, France

M. Chérel  
ICO-Gauducheau, CRCNA, UMR 892 Inserm, 6299 CNRS,  
Université de Nantes, Nantes, France

APC	Antigen-presenting cells
CAR	Chimeric antigen receptor
CDC	Complement-dependent cytotoxicity
CEA	Carcinoembryonic antigen
CpG	Cytosine-phosphate-guanine motif
CR	Complete response
CRT	Calreticulin
CRu	Unconfirmed complete response
DAMP	Damage-associated molecular pattern
DC	Dendritic cells
Flt3-L	Fms-related tyrosine kinase 3 ligand
G-CSF	Granulocyte-colony stimulating factor
GM-CSF	Granulocyte-macrophage colony-stimulating factor
Gy	Gray
HMGB1	High mobility group box 1
ICAM-1	Intercellular adhesion molecule 1
IFN	Interferon
IgG	Immunoglobulin G
IL	Interleukin
IU	International unit
LFA-3	Lymphocyte function-associated antigen 3
mAb	Monoclonal antibody
MHC	Major histocompatibility complex
MIP1 $\alpha$	Macrophage inflammatory protein 1 $\alpha$
MM	Multiple myeloma
MTD	Maximum tolerated dose
NHL	Non-Hodgkin B-cell lymphoma
NK	Natural killer
NKG2D	Natural killer group 2D receptor
ORR	Overall response rate
PBMCs	Peripheral blood mononuclear cells
PR	Partial response
RAIT	Radioimmunotherapy
SD	Stable disease
TAA	Tumor-associated antigens
TLR	Toll-like receptor
TNF $\alpha$	Tumor necrosis factor $\alpha$
VCAM-1	Vascular cell adhesion molecule-1

## 1 Introduction

The use of ionizing radiation in cancer treatment armamentarium has become predominant as over half of the patients developing a tumor are now treated with irradiation during the course of their treatment [1, 2]. Radioimmunotherapy (RAIT) remains a small fraction of such therapy despite the demonstration of its efficacy and safety in non-Hodgkin B-cell lymphoma (NHL) [3] and the promising results obtained in specific clinical settings of solid tumors [4, 5]. For decades, research into improving RAIT has focused almost entirely on the approach itself, and significant progress has been made in the humanization of monoclonal antibodies, development of new vectors, new radionuclides, more stable chelates, new delivery systems, better dosimetric models, and definition of new target antigens. In parallel, radiobiological studies have addressed the direct and indirect (bystander) effects of ionizing radiation on the tumor cells to some extent, but for long, the complex interactions among the tumor, its microenvironment, inflammation, and the immune system have been ignored by the field.

Among the established hallmarks of cancer are resistance to cell death, evading the immune system, and creation of a tumor microenvironment [6]. Multiple immunosuppressive mechanisms are implemented by tumors to escape immune recognition and destruction which involve the tumor itself and its microenvironment [7]. For long, ionizing radiation and RAIT, often used in combination with chemotherapy, were also considered as immunosuppressive treatments. As a result, studies largely failed to appreciate the effects of ionizing radiation on immunity despite the fact that clinical cases of “abscopal effect” after radiotherapy were reported and that some patients achieved long-term CR after a single dose of RAIT. The elucidation of the mechanisms underlying the off-target effects after irradiation and the demonstration that immunogenic tumor cell death is inducible by ionizing radiation have changed the perception of radiation therapy. And at a time where numerous and promising new immunotherapies are emerging, it also opens a new era of combination therapy options where the immunogenic effects of radionuclides could be a key factor for the success of treatment.

## 2 Ionizing Radiation and Antitumor Immunity

### 2.1 *Abscopal Effect: An Aftermath of Ionizing Radiation Involving the Immune System*

The abscopal effect, originally described by Dr. RH. Mole in 1953 [8], comes from the Latin words “ab” meaning “far” and “scopos” which means “target.” The abscopal effect refers to effects outside the irradiation field of the target, which can result in antitumor responses and the elimination of non-irradiated tumor cells. More generally, the abscopal effect stands for any systemic effect that is observed after a local

treatment. A growing set of preclinical and clinical data point out that the therapeutic potential of ionizing radiation does not reflect only the antiproliferative and cytotoxic activities of X or  $\gamma$  radiation but also implies bystander and systemic (distant) effects [9–11].

The abscopal effect is rarely observed in the clinic; however, it has been documented in patients with hematological malignancies like lymphoma [12, 13] and leukemia [14, 15] and also in patients with a wide variety of solid tumors [16–21]. Investigations of the possible mechanisms underlying the abscopal effect in animal models have demonstrated that it might be possible to favor the development of such an event by modulating the immune system. Chakravarty et al. have shown in a syngeneic and immunocompetent metastatic lung cancer model that combining radiotherapy and injection of Flt3 ligand (Flt3-L), a growth factor for immune cells and especially for dendritic cells (DC) [22], reduced lung metastases, significantly improved survival, and resulted in 56% of disease-free animals. Notably, the abscopal effect was abolished in nude mice lacking T-lymphocytes which demonstrates that this systemic antitumor effect is mediated by the adaptive immune system [23]. In a comparable study using a syngeneic immunocompetent breast carcinoma mouse model, Demaria et al. demonstrated that irradiation of a tumor implanted on the right flank combined with systemic injection of Flt3-L induced regression of a second tumor engrafted on the left flank of the animals. The combined treatment was ineffective if the second tumor was from another cell type than the irradiated breast carcinoma or if the mice were deficient in T-cells [24]. So, in those studies, the abscopal effect was promoted by a tumor-specific response relying upon T-lymphocytes. Another study, combining radiotherapy and injection of ECI301, a recombinant MIP1 $\alpha$  chemokine, showed the involvement of CD4<sup>+</sup> and CD8<sup>+</sup> T-cells or natural killer cells (NK) depending on the tumor type [25]. In addition, in this study, irradiation of healthy tissues did not promote any abscopal effect, which suggests that radiation-induced tumor cell death or damages are mandatory for the development of such antitumor response.

All these above data indicate that ionizing radiation can initiate immune responses involving DC, NK, and T-cells with systemic effects on tumor growth, highlighting the importance of the interactions between ionizing radiation and the immune system to foster an efficient antitumor response. It is, therefore, crucial to understand how irradiation acts on the tumor, its microenvironment, and on the immune system.

## ***2.2 Immunological Effects of Ionizing Radiation***

Cancer development is strongly influenced by inflammation, innate and adaptive immunity, and the very complex interrelationships and modulations between those different components can either lead to tumor growth or to tumor regression. Although ionizing radiation has been mainly used to treat cancer through its direct cytotoxicity, there is now evidence that irradiation also modulates inflammation and

the immune system at multiple levels including the production of reactive oxidative species, the generation of danger signals, the release of cytokines and other soluble factors, the activation of immune cells, and the induction of various types of cell death. Depending on the low or high dose of irradiation, the generation of acute or chronic inflammation, these underlying mechanisms can have immunosuppressive or immunostimulatory effects [26–30]. It is, therefore, important to understand the links between ionizing radiation and the immune response to cancer to try and develop treatments that could limit the immunosuppressive effects of radiation while boosting antitumor immunity. In the present chapter, we will focus on the studies that have shown the various mechanisms by which radiotherapy and chelated radionuclides might boost the immune system.

### 2.3 *Modulation of Tumor Cell Immunogenicity*

Although radiation therapy has been used traditionally to kill tumor cells, the dose received by a number of cells within a given tumor mass is too low to cause their death (event which is further emphasized in hypoxic areas). Several preclinical studies have shown, however, that such low radiation doses are capable of inducing phenotypic changes in neoplastic cells, which help their recognition and elimination by the immune system. The molecules described to be upregulated at the surface of tumor cells by such ionizing radiation doses are tumor-associated antigen (TAA), MHC class I molecules, the death receptor Fas (CD95), NKG2D ligands, the costimulatory molecule B7–1 (CD80), and adhesion molecules including LFA-3 (CD58 or lymphocyte function-associated antigen 3) and ICAM-1 (intercellular adhesion molecule 1) [31–37]; Fas, MHC class I molecules, ICAM-1, and TAA such as CEA (carcinoembryonic antigen) and the mucin glycosylated phosphoprotein Muc-1 have also been shown to be upregulated on tumor cells after irradiation with  $\beta$ -particle emitters  $^{153}\text{Sm}$  [38] and  $^{90}\text{Y}$  [39]. Interestingly, the B7–1 costimulatory molecule is also upregulated in B-cell lymphoma following irradiation [40]. All these molecules are known to play a role in tumor destruction by cytotoxic CD8<sup>+</sup> T-cells and the development of an antitumor immune response.

One of the major consequences induced by tumor destruction after irradiation is the exposure of a large amount of TAA to the immune system. The delivery of tumor antigens is done because of tumor cell necrosis, apoptosis, or the release of cell fragments [41, 42]. The increased availability of those TAA allows circulating DCs to capture and present those antigens to induce a specific T-cell response against the tumor. One study demonstrated that irradiated tumors expressing low levels of antigen, as MHC-peptide complex, provide a sufficient amount of TAA to allow the destruction of tumor cells by cytotoxic CD8<sup>+</sup> T-cells [43].

Additionally, cell death induced by irradiation may allow the release of new TAA that will be captured by the DCs in the tumor microenvironment and lymph nodes. Reits et al. have demonstrated that radiotherapy increases, within tumor cells, the repertoire of peptides available for MHC class I molecules presentation to

cytotoxic CD8<sup>+</sup> T-cells. This broader repertoire does not only result from an increased degradation of the existing proteins, but also in the activation of the mTOR pathway, which leads to increased protein translation and, thus, the creation of a new peptide repertoire [36].

## 2.4 Immunogenic Cell Death

All cell deaths do not promote an immune response. The immune system is able to distinguish between an immunogenic death and a non-immunogenic death which results either in the activation of adaptive immunity or in the persistence of tolerance. Tumor cell death induced by ionizing radiation can be quite immunogenic and potentiates the presentation of TAA by DCs to activate T-cells and the development of an immune response [44, 45]. Several molecular danger signals, DAMP (danger-associated molecular pattern), have been identified among the main features of an immunogenic cell death.

1. The translocation of calreticulin (CRT), an endoplasmic reticulum chaperone protein, to the outer face of the plasma membrane of the cells undergoing apoptosis is an important “eat-me” signal for the professional antigen-presenting cells (APCs) such as DCs [46–49].
2. The release of HMGB1 (high mobility group box 1, a nonhistone protein associated to the chromatin and in the cell nucleus) by dying cells will transmit proinflammatory signals after binding to TLR4 (Toll-like receptor 4) [50–52]. Those DAMPs, CRT, and/or HMGB1 are induced following exposure of tumors cells to external irradiation [46, 53] but also to  $\alpha$ -particle emitters like <sup>213</sup>Bi [54].
3. The third signal is the release of ATP from the cells undergoing apoptosis. ATP functions both as a “find-me” signal to professional APCs and as a potent proinflammatory signal through binding to the P2X7 purinergic receptor, thereby triggering inflammasome activation [55–60]. Its release has not been demonstrated following irradiation yet. But, since autophagy is necessary for the release of ATP [61] and ionizing radiation can promote autophagy [62–64], the third signal may be generated by ionizing radiation when autophagy precedes cell death.
4. Heat-shock proteins, especially HSP70, are expressed at the cell surface but also released during tumor cell stress or cell death after exposure to ionizing radiation like X-rays [65, 66] or  $\alpha$ -particles [54] and stimulate innate and adaptive immune responses mediated by NK, DC cells, and T-cells through antigen cross presentation [67].

All these experimental data support the idea that tumor cell stress and death resulting from ionizing radiation are sensed by the immune system as “danger” signals which in turn can stimulate an immune response.



## **2.5 Secretion of Cytokines**

Radiotherapy also modifies the tumor microenvironment by generating a proinflammatory environment [29, 68]. For example, CXCL9, CXCL10, and CXCL16 chemokines promote the recruitment of CD8<sup>+</sup> effector T-cells, and Th1 helper CD4<sup>+</sup> T-cells are induced following ionizing radiation in various types of tumors [69–71]. Irradiation also promotes the production of proinflammatory cytokines such as IL-1 $\beta$ , type I and type II IFN (IFN- $\alpha$ , IFN- $\beta$ , IFN- $\omega$ , and IFN- $\gamma$ ), and TNF $\alpha$ , involved in the cytotoxic and cytostatic effects on cancer cells after irradiation, including tumor regression, inhibition of proliferation, tumor cell death, and immune cell recruitment [68, 69, 72–75]. Such an inflammatory context after radiotherapy may facilitate the initiation and amplification of an antitumor immune response.

## **2.6 Blood Vessels**

After antigen activation, T-lymphocytes must reach and infiltrate tumors. Ionizing radiation can promote this process in many ways. For example, the radiation-induced remodeling of abnormal tumor vessels results in an effective tumor infiltration by antitumor T-cells following adoptive transfer in a transgenic mouse model of insulinoma [76]. In an experimental model of melanoma, increased expression of VCAM-1 adhesion molecule (vascular cell adhesion molecule-1) induced by ionizing radiation boosts T-cell infiltration of the tumor [77].

Overall, these data demonstrate that ionizing radiation can drive an immune response to cancer in a number of ways; it is therefore important to consider these beneficial effects while designing cancer treatments. This also constitutes a strong rationale for combining radiation therapy with immunotherapy in order to improve current therapies.

# **3 Combining Ionizing Radiation and Immunotherapy**

## **3.1 Preclinical Evidence in Hematopoietic Cancer Models**

### **3.1.1 Radiotherapy and Immunotherapy**

By taking advantage of the immunogenic properties of ionizing radiation described in the previous sections, numerous preclinical studies have successfully combined radiotherapy with immunotherapies in solid tumors to obtain impressive responses (reviewed in [68, 78]). Here, we will focus on the available data for radiotherapy and immunotherapy combinations in preclinical models of lymphoma.

In 1997, the group of Batterman in Utrecht assessed the efficacy of supplementing local radiotherapy with locoregional low-dose injection of interleukin-2 (IL-2) in a subcutaneous model using the spontaneously arisen SL2 T-lymphoma [79, 80]. IL-2 is a potent T-cell activator, which has proved its efficacy and safety in the SL2 preclinical model [81, 82] as well as in human patients with Hodgkin's and non-Hodgkin's lymphomas [83–85]. In their SL2 model, they demonstrated that the combination of local radiation therapy (20Gy) followed by two cycles of 4-day injection of IL-2 (7000 IU/day) peri-tumorally led to 93% of long-term disease-free survival compared to 17% with radiation alone ( $p < 0.0001$ ). Additionally, in a setting where they inoculated mice with two subcutaneous tumors (one on each thigh), they showed that treatment of one tumor with irradiation and IL-2 led to antitumor effects in the second, untreated tumor in 80% of mice and local response was increased to 100%. When the second, non-irradiated tumor was also treated with peritumoral IL-2, both local and distant responses increased to 100%, and disease-free survival reached 70%. Interestingly, in an attempt to reproduce more closely the radiotherapy scheduled applied in the clinic, they reproduced the experiments with a fractionated regimen of radiotherapy (2.5Gy/day for 10 days). Fractionated therapy was far less efficient than single-dose regimen and led to only 12% local response and no disease-free survival. However, even in these settings, combination with IL-2 therapy improved treatment outcome up to 90% local response and 10% disease-free survival. The authors postulated that the selected fractionation schedule was not optimal for the SL2 model, possibly because it is a highly aggressive tumor that metastasizes quickly and, therefore, needs a rapid rather than prolonged treatment. They did not observe any toxicity related to IL-2 and, therefore, showed that IL-2 therapy was both safe and efficient in improving both local and systemic responses to radiotherapy. This study was the first to demonstrate the potential of radiotherapeutic association with immunotherapy in a lymphoma model.

In 2003, the group of Illidge in Manchester tested the combination of total body irradiation with an agonistic anti-CD40 antibody on the murine A31 and BCL<sub>1</sub> B-lymphoma models [86]. CD40 is a costimulatory protein expressed on APCs such as DCs, B-cells, monocytes, and macrophages and participates to their activation. Interestingly, CD40 is also expressed on various tumors, in particular B-cell lymphomas. Therapeutic treatment of lymphoma using agonistic antibodies targeted to CD40 can have multiple complementary antitumor effects. Indeed, activated APCs are able to generate antigen-specific T-cell responses, while the targeting of CD40<sup>+</sup> tumor cells can have a direct tumoricidal effect by inducing apoptosis [87]. Interestingly, it has also been shown that anti-CD40 agonists can sensitize multiple myeloma (MM) and B-lymphoma cell lines to  $\gamma$ -radiation in vitro [88]. Anti-CD40 antibodies are the object of several ongoing clinical trials in leukemia, MM, and NHL [89]. Recently, a phase II trial using an agonistic anti-CD40 as a monotherapy on patients with relapsed diffuse large B-cell lymphoma demonstrated low toxicity but only modest efficacy [90], suggesting that these therapies need combination with other cancer treatment modalities to reach their full potential. In this study, Honeychurch et al. showed that radiotherapy (5Gy)

with anti-CD40 (1 mg) led to an impressive long-term disease-free survival of 100% of treated mice as opposed to 0% for single-agent treatments in both orthotopic models of lymphoma (A31 and BCL<sub>1</sub>). Mice treated with a single treatment survived slightly longer than untreated controls, but eventually all succumbed to their lymphoma. The effect of the combination treatment was not due to combined cytotoxicities as the anti-CD40 Ab did not induce cell death of lymphoma cell lines nor did it sensitize the tumor cells to radiation. Instead, the effect was mediated by a strong specific CD8<sup>+</sup> T-cell response which was long-lasting, as demonstrated by protection against later a tumor challenge (therefore suggesting the onset of immune memory), and transferable to naive recipients. Interestingly, they observed that the combined therapy was less efficient on smaller tumor loads, indicating that radiation cytotoxicity needs to liberate a critical amount of TAA to allow anti-CD40 activated APCs to mount an efficient immune response. This study, therefore, brought to light mechanisms by which radiation therapy can synergize with immunotherapy by simultaneously reducing tumor load and providing antigens for an optimal immune response against lymphoma.

More recently, the same group published a study testing the association of local radiotherapy with the TLR7 agonist R848 in subcutaneous B-cell (A20) and T-cell (EL4, EG7) lymphoma models [91]. TLR7 is a pattern recognition receptor that is expressed on the endosomal membranes of DC (mainly plasmacytoid DC) and B-cells [92]. It has been shown to induce DC, B-cell, and T-cell activation in vivo and lead to an effective antitumor cytotoxic T-cell response when combined with doxorubicin in a murine T-lymphoma model [93]. Studies also demonstrated that ex vivo stimulation of cutaneous T-cell lymphoma patients' PBMCs with TLR7 agonists induced the secretion of IFN- $\alpha$  and IFN- $\gamma$  and led to NK cell and T-cell activations in vitro [94, 95]. A phase II clinical trial also showed that treatment with the TLR7 agonist 825A was well tolerated in patients with refractory hematological malignancies and associated with evidence of immune activation [96]. Finally, treatment with TLR7 agonists has also been shown to potentiate the efficacy of radiotherapy in preclinical models of solid tumors [97, 98]. In their study, Dovedi et al. first demonstrated that systemic injection of R848 appeared well tolerated and led to increased levels of IL-6, IFN- $\gamma$ , TNF- $\alpha$ , and IL-5 and activation of B- and T-lymphocytes in EG7 tumor-bearing mice. They then showed that the combination of local radiotherapy (10 Gy) and intravenous injection of R848 (3 mg/kg) could lead up to 75% of long-term survival as compared to only 25% with either monotherapy. This improved outcome was not due to combined cytotoxicities as R848 did not sensitize EG7 tumor cells to radiation. Instead the effect was mediated by a specific CD8<sup>+</sup> T-cell response and led to the generation of long-lived specific memory T-cells. Depletion of B-cells with anti-CD20 Ab also showed that the efficacy of treatment combination in the T-lymphoma model was independent on B-lymphocytes. Interestingly, they showed that although radiotherapy alone induced the release of HMGB1 by tumor cells and led to their phagocytosis by DCs, it was not sufficient to trigger DC activation. The addition of R848 was required to induce upregulation of CD80 and CD86 after irradiation of tumor cells, suggesting that both radiation and TLR7 stimulation were required

to mount an efficient T-cell response. Finally, they showed that using fractionated radiation regimen (5x2 Gy) led to better responses in both EL4 T-lymphoma and A20 B-lymphoma models, leading to 100% of long-term survival. Interestingly, weekly injections of R848 for 5 weeks were more efficient than a single dose, suggesting that repeated irradiation and immune stimulation could act as immune boosters for antitumor immunity and prevent the reestablishment of a suppressive tumor environment.

Although one could question the use of immune adjuvants in diseases originating from immune cells and hypothesize that stimulation with IL-2 in a T-cell malignancy could sustain tumor growth or that CD40 and TLR agonists could promote B-lymphoma cell survival, those three studies above demonstrate no such effect. On the contrary, the immunostimulants tested in these hematological malignancies all improve survival outcome with no apparent induced toxicity. These studies also clearly demonstrate that combining the immunogenic properties of ionizing radiation associated to tumor antigen release with immune stimulation can lead to efficient antitumor immunity. This immunity seems mainly driven by DC activation of specific cytotoxic CD8<sup>+</sup> response, leading to the establishment of long-lasting immune memory. B-cells do not seem to participate in the observed antitumor responses, but other immune populations could potentially be involved and further investigations should address this possibility. Altogether, those findings warrant further trials of various immune-modulatory molecules and radiotherapy schedules in order to find the best combinations for the treatment of lymphomas.

### 3.1.2 Radioimmunotherapy and Immunotherapy

To date, very few studies have investigated combination therapy of RAIT and immunotherapy in preclinical tumor models. To our knowledge, Chakraborty et al. have been the first to report such a combination in a study where RAIT was combined with cancer vaccination to treat human CEA expressing murine carcinoma in CEA transgenic mice [39]. This group had previously demonstrated that tumor cells were more susceptible to T-cell killing after exposure to non-lytic doses of external radiation therapy [34]. They, thus, hypothesized that delivering RAIT to a tumor mass might have the same effect. To this end, they used a <sup>90</sup>Y-labeled anti-CEA mAb and a recombinant vaccine containing the *CEA*, *B7-1*, *ICAM-1*, and *LFA-3 genes*. They observed that survival of the tumor engrafted mice was significantly increased after a single dose of RAIT in combination with vaccine compared to vaccine or radiolabeled mAb alone. Analysis of the immune response showed that in mice receiving the combination therapy, the amount of CEA-specific CD8<sup>+</sup> T-cells infiltrating the tumor was significantly increased over vaccine alone. Interestingly, the animals cured after treatment with the combination therapy demonstrated a broadening in the antitumor immune response, since in addition to CD4<sup>+</sup> and CD8<sup>+</sup> T-cell responses against CEA which was encoded by the vaccine, they also observed T-cell responses against other TAA [39].

More recently, our group investigated the possibilities to promote an efficient and long-lasting antitumor response by combining  $\alpha$ -RAIT and adoptive transfer of tumor-specific T-lymphocytes in a multiple myeloma murine model expressing the TAA CD138 and ovalbumin (OVA) [99]. The therapeutic efficacy was evaluated by treatment with a  $^{213}\text{Bi}$ -labeled anti-CD138, followed by an adoptive transfer of OT-I cells, which are OVA-specific  $\text{CD8}^+$  T-cells. We observed a significant tumor growth control and an improved survival in the animals treated with the combined treatment over radiolabeled mAb or OT-I cell transfer alone. Both studies demonstrate that not only radiotherapy but also RAIT in combination with immunotherapy promotes an effective antitumor response, which may have implications in the design of future clinical trials.

## 3.2 Clinical Evidence

### 3.2.1 Radiotherapy and Immunotherapy

The occurrence of abscopal effects after radiotherapy without concurrent immune stimulation is a rare event in the clinic. Although this may be due, in part, to underreporting, it is likely a consequence of tumor-derived immunosuppression and suggests that the threshold for antitumor immune activation is high in clinical settings. Notably, most of the reported cases of the abscopal effect occurred in renal cell carcinoma, melanoma, and lymphoma [100], indicating that these cancers are the most likely to benefit from the combination with immunotherapy. Clinical trials have assessed the efficacy of various immunotherapies in combination with radiotherapy [101], and many trials are still ongoing [102], but most of the work has been performed on patients with solid non-hematopoietic tumors, in particular melanoma [103].

The Stanford group is currently investigating the potency of combined treatments in patients with lymphoma in three trials testing the efficacy of radiotherapy associated with the TLR9 agonist SD-101 (NCT02266147, NCT01745354) and the anti-CTLA4 mAb ipilimumab (NCT02254772). They also already published one study on the subject [104]. In this study, 15 patients with recurrent stage III or IV low-grade B-cell lymphoma were treated with local radiotherapy combined with intratumoral TLR9 agonist (CpG PF-3512676) injection at one site only, while distant tumor sites were evaluated for response. There was no treatment limiting adverse event, and all patients completed the full course of therapy. They obtained 27% of overall objective response rate at the distant untreated sites with 1 CR lasting 61 weeks, 3 PR lasting 20, 64 and over 111 weeks and 8 SD. Tumor-reactive  $\text{CD8}^+$  T-cells were detected in the peripheral blood of several responding patients, but no significant correlation between T-cell immunity and clinical response was found. Interestingly, some patients' tumors were able to induce a T-reg phenotype in autologous  $\text{CD4}^+$  T-cells in vitro, and those patients had significantly shorter progression-free survival. This suggests that tumor-derived immunosuppression

may be the main obstacle to treatment efficacy. These preliminary results warrant confirmation; nevertheless, this is the first study to demonstrate that the association of radiotherapy with intratumoral injection of an immunostimulant can be safe and trigger efficient systemic responses in patients with lymphoma.

### 3.2.2 Radioimmunotherapy and Immunotherapy

Only one trial tested the combination of RAIT with an immune stimulant so far [105], and the same team also recently completed a trial in which they tested the association of  $^{90}\text{Y}$ -ibritumomab tiuxetan with rituximab, G-CSF, and IL-11 (NCT00012298), but the results have not been published at the time this manuscript was produced. In the former study, 30 patients with relapsed or refractory CD20<sup>+</sup> B-cell NHL have been treated with  $^{90}\text{Y}$ -ibritumomab tiuxetan (0.4 mCi/kg) in association with rituximab (250 mg/kg) and CpG 7909, a TLR9 agonist. Four doses of CpG 7909 have been tested (0.08, 0.16, 0.32, and 0.48 mg/kg) without reaching the MTD, demonstrating the safety of treatment. They obtained an impressive ORR of 93%, with 63% CR/CRu and 30% PR, and responses were durable with a median time to progression of 42.7 months. T-cell responses have not been evaluated in this study, but analysis of serum cytokines showed a statistically significant decrease in IL-10 and TNF $\alpha$  and increase in IL-1 $\beta$ , consistent with the development of an immune response. It is important to note that IgG themselves can trigger immune responses. In particular, chimeric IgG such as rituximab have been shown to trigger CDC and ADCC in vitro. However the extent to which these phenomena participate in rituximab efficacy in vivo is still unclear [106]. In this trial, measurement of ADCC induced by rituximab was very variable between subjects and did not show any statistically significant difference between groups. Although they warrant confirmation, these phase I results are extremely encouraging. Nevertheless, further studies should assess the mechanisms and importance of the immune response in the efficacy of this treatment combination.

Based in part on the observations that Ab treatments could induce antitumor responses through the induction of CDC and ADCC but also through Ab-targeted tumor antigen cross presentation [107], it has been postulated that RAIT combined with maintenance anti-CD20 Ab treatment may trigger protective T-cell responses in lymphoma patients [108]. There have been several studies testing the efficacy of  $^{90}\text{Y}$ -ibritumomab tiuxetan after treatment with rituximab and chemotherapy [109–111], and all obtained a very good response rate. However, only Jacobs et al. used rituximab as a maintenance treatment after RAIT, and none of these trials assessed the presence of an antitumor immune response. Besides, chemotherapies used in those studies, such as fludarabine, cyclophosphamide, and prednisone, can induce important immunosuppression and lymphopenia and may, therefore, limit the induction of an effective immune response against lymphoma.

Overall, the results obtained from the combination of RAIT and immune-related treatments in patients with lymphoma are very encouraging. However, there are still very little data available on the implication of the immune system in patient

responses to these treatments. Notably, it will be of prime importance in the future to assess the effect of vectors on the immune response to tumors in RAIT.

## 4 Conclusions and Perspectives

Within the past two decades, important advances have been done in our knowledge of the complex interplay among ionizing radiation, inflammation, and the immune system. The immunogenic properties of irradiation are now clearly demonstrated, and, even though most of the data come from external radiation therapy, the few reports using radionuclides and RAIT strongly support that  $\alpha$ - and  $\beta$ -particle emitters can also drive an antitumor immune response. More importantly, these immunogenic aspects have opened a new era of research in radiation oncology by the initiation of clinical trials combining ionizing radiation and immune-based therapy. Notably, preliminary results in patients with lymphoma are very encouraging. Combination therapies appeared safe, and, to date, neither limiting adverse effects nor cumulative or overlapping toxicity was observed in any of the trials. These trials are initial investigations, and there are still a lot of parameters to optimize in order to overcome tolerance and maximize the synergy of combined therapies toward tumor cell destruction. In that aspect, RAIT may be of great interest in the treatment of disseminated and poor prognostic metastatic solid cancer as this approach will generate locally but at hundred tumor sites: high dose to the tumor and cell death, production of ROS, release of TAA, acute inflammation, and other immunogenic effects which should represent an ideal springboard for the combined immune-based therapy. In order to develop a systemic antitumor response, and to ultimately achieve an immune memory and long-term protection, future directions will have to address which radionuclide, treatment schedule (single vs fractionation), and dose to use for different pathologies and different patients. Some clinical studies have already been completed, but several more are about to start exploring radiation therapy in combination with immunotherapies using growth factors like Flt3 ligand or GM-CSF [112] or checkpoint inhibitors such as anti-CTLA4 (ipilimumab), anti-PD-1 (nivolumab) [102], or anti-PD-L1 (atezolizumab) mAbs. On July 2016, searching the [clinicaltrials.gov](http://clinicaltrials.gov) website for checkpoint inhibitor mAb + radiation gives 41 results: 2 trials for ipilimumab, 35 trials for nivolumab, and 4 trials for atezolizumab. Among these 41 clinical trials, all but one use external radiation therapy; the remaining one will use  $^{90}\text{Y}$  glass microspheres in hepatocellular carcinoma (NCT02837029). Despite the limited use of radionuclides so far, RAIT in combination with cytokines or immune checkpoint blockers do represent an exciting option. Several other attractive combination opportunities come from the development of adoptive T-cell therapies and chimeric antigen receptors (CAR) (for review [113, 114]) and other classes of small molecules designed for immuno-oncology treatments (for review [115]). This multitude of options implies to define biomarkers to identify patients who are the most likely to benefit from such combined treatments and especially from the immune-based therapy.



**Acknowledgments** This work has been supported by a grant from the French National Agency for Research titled “Investissements d’Avenir” Labex IRON (n° ANR-11-LABX-0018-01), Labex IGO (n° ANR-11-LABX-0016-01), and ArronaxPlus Equipex (n° ANR-11-EQPX-0004) and also by grants from La Ligue Contre le Cancer and from the Pays de la Loire Council “Nucléaire pour la Santé” (NucSan).

**Conflict of Interest** No conflict statement: No potential conflicts of interest were disclosed

## References

1. Begg AC, Stewart FA, Vens C. Strategies to improve radiotherapy with targeted drugs. *Nat Rev Cancer*. 2011;11:239–53.
2. Delaney G, Jacob S, Featherstone C, Barton M. The role of radiotherapy in cancer treatment: estimating optimal utilization from a review of evidence-based clinical guidelines. *Cancer*. 2005;104:1129–37.
3. Tomblyn M. Radioimmunotherapy for B-cell non-hodgkin lymphomas. *Cancer Control*. 2012;19:196–203.
4. Kraeber-Bodéré F, Salaun P-Y, Oudoux A, Goldenberg DM, Chatal J-F, Barbet J. Pretargeted radioimmunotherapy in rapidly progressing, metastatic, medullary thyroid cancer. *Cancer*. 2010;116:1118–25.
5. Tomblyn MB, Katin MJ, Wallner PE. The new golden era for radioimmunotherapy: not just for lymphomas anymore. *Cancer Control*. 2013;20:60–71.
6. Hanahan D, Weinberg RA. Hallmarks of cancer: the next generation. *Cell*. 2011;144:646–74.
7. Munn DH, Bronte V. Immune suppressive mechanisms in the tumor microenvironment. *Curr Opin Immunol*. 2016;39:1–6.
8. Mole RH. Whole body irradiation—radiobiology or medicine? *Br J Radiol*. 1953;26:234–41.
9. Mothersill C, Seymour CB. Radiation-induced bystander effects – implications for cancer. *Nat Rev Cancer*. 2004;4:158–64.
10. Prise KM, O’Sullivan JM. Radiation-induced bystander signalling in cancer therapy. *Nat Rev Cancer*. 2009;9:351–60.
11. Kroemer G, Zitvogel L. Abscopal but desirable: the contribution of immune responses to the efficacy of radiotherapy. *Oncoimmunology*. 2012;1:407–8.
12. Rees GJ. Abscopal regression in lymphoma: a mechanism in common with total body irradiation? *Clin Radiol*. 1981;32:475–80.
13. Antoniadis J, Brady LW, Lightfoot DA. Lymphangiographic demonstration of the abscopal effect in patients with malignant lymphomas. *Int J Radiat Oncol Biol Phys*. 1977;2:141–7.
14. Sham RL. The abscopal effect and chronic lymphocytic leukemia. *Am J Med*. 1995;98:307–8.
15. Aalbers AM, Aarts MJ, Krol ADG, Marijnen CAM, Posthuma EFM. The beneficial local and abscopal effect of splenic irradiation in frail patients with chronic lymphocytic leukaemia. *Neth J Med*. 2016;74:122–9.
16. Stamell EF, Wolchok JD, Gnjatic S, Lee NY, Brownell I. The abscopal effect associated with a systemic anti-melanoma immune response. *Int J Radiat Oncol Biol Phys*. 2013;85:293–5.
17. Grimaldi AM, Simeone E, Giannarelli D, Muto P, Falivene S, Borzillo V, et al. Abscopal effects of radiotherapy on advanced melanoma patients who progressed after ipilimumab immunotherapy. *Oncoimmunology*. 2014;3:e28780.
18. Cotter SE, Dunn GP, Collins KM, Sahni D, Zukotynski KA, Hansen JL, et al. Abscopal effect in a patient with metastatic Merkel cell carcinoma following radiation therapy: potential role of induced antitumor immunity. *Arch Dermatol*. 2011;147:870–2.
19. Ohba K, Omagari K, Nakamura T, Ikuno N, Saeki S, Matsuo I, et al. Abscopal regression of hepatocellular carcinoma after radiotherapy for bone metastasis. *Gut*. 1998;43:575–7.

20. Ishiyama H, Teh BS, Ren H, Chiang S, Tann A, Blanco AI, et al. Spontaneous regression of thoracic metastases while progression of brain metastases after stereotactic radiosurgery and stereotactic body radiotherapy for metastatic renal cell carcinoma: abscopal effect prevented by the blood-brain barrier? *Clin Genitourin Cancer*. 2012;10:196–8.
21. Takaya M, Niibe Y, Tsunoda S, Jobo T, Imai M, Kotani S, et al. Abscopal effect of radiation on toruliform para-aortic lymph node metastases of advanced uterine cervical carcinoma – a case report. *Anticancer Res*. 2007;27:499–503.
22. O'Neill DW, Adams S, Bhardwaj N. Manipulating dendritic cell biology for the active immunotherapy of cancer. *Blood*. 2004;104:2235–46.
23. Chakravarty PK, Alfieri A, Thomas EK, Beri V, Tanaka KE, Vikram B, et al. Flt3-ligand administration after radiation therapy prolongs survival in a murine model of metastatic lung cancer. *Cancer Res*. 1999;59:6028–32.
24. Demaria S, Ng B, Devitt ML, Babb JS, Kawashima N, Liebes L, et al. Ionizing radiation inhibition of distant untreated tumors (abscopal effect) is immune mediated. *Int J Radiat Oncol Biol Phys*. 2004;58:862–70.
25. Shiraishi K, Ishiwata Y, Nakagawa K, Yokochi S, Taruki C, Akuta T, et al. Enhancement of antitumor radiation efficacy and consistent induction of the abscopal effect in mice by ECI301, an active variant of macrophage inflammatory protein-1alpha. *Clin. Cancer Res*. 2008;14:1159–66.
26. Formenti SC, Demaria S. Systemic effects of local radiotherapy. *Lancet Oncol*. 2009;10:718–26.
27. Golden EB, Formenti SC. Is tumor (R)ejection by the immune system the “5th R” of radiobiology? *Oncoimmunology*. 2014;3:e28133.
28. Frey B, Hehlhans S, Rödel F, Gaipf US. Modulation of inflammation by low and high doses of ionizing radiation: implications for benign and malign diseases. *Cancer Lett*. 2015;368:230–7.
29. Lumniczky K, Safrany G. The impact of radiation therapy on the antitumor immunity: local effects and systemic consequences. *Cancer Lett*. 2015;356:114–25.
30. Hekim N, Cetin Z, Nikitaki Z, Cort A, Saygili EI. Radiation triggering immune response and inflammation. *Cancer Lett*. 2015;368:156–63.
31. Ifeadi V, Garnett-Benson C. Sub-lethal irradiation of human colorectal tumor cells imparts enhanced and sustained susceptibility to multiple death receptor signaling pathways. *PLoS One*. 2012;7:e31762.
32. Kim J-Y, Son Y-O, Park S-W, Bae J-H, Chung JS, Kim HH, et al. Increase of NKG2D ligands and sensitivity to NK cell-mediated cytotoxicity of tumor cells by heat shock and ionizing radiation. *Exp Mol Med*. 2006;38:474–84.
33. Vondráček J, Sheard MA, Krejčí P, Minksová K, Hofmanová J, Kozubík A. Modulation of death receptor-mediated apoptosis in differentiating human myeloid leukemia HL-60 cells. *J Leukoc Biol*. 2001;69:794–802.
34. Chakraborty M, Abrams SI, Camphausen K, Liu K, Scott T, Coleman CN, et al. Irradiation of tumor cells up-regulates Fas and enhances CTL lytic activity and CTL adoptive immunotherapy. *J Immunol*. 2003;170:6338–47.
35. Garnett CT, Palena C, Chakraborty M, Chakraborty M, Tsang K-Y, Schlom J, et al. Sublethal irradiation of human tumor cells modulates phenotype resulting in enhanced killing by cytotoxic T lymphocytes. *Cancer Res*. 2004;64:7985–94.
36. Reits EA, Hodge JW, Herberts CA, Groothuis TA, Chakraborty M, Wansley EK, et al. Radiation modulates the peptide repertoire, enhances MHC class I expression, and induces successful antitumor immunotherapy. *J Exp Med*. 2006;203:1259–71.
37. Vereecque R, Buffenoir G, Gonzalez R, Cambier N, Hetuin D, Bauters F, et al. Gamma-ray irradiation induces B7.1 expression in myeloid leukaemic cells. *Br J Haematol*. 2000;108:825–31.
38. Chakraborty M, Wansley EK, Carrasquillo JA, Yu S, Paik CH, Camphausen K, et al. The use of chelated radionuclide (samarium-153-ethylenediaminetetramethylenephosphonate) to modulate phenotype of tumor cells and enhance T cell-mediated killing. *Clin Cancer Res*. 2008;14:4241–9.

39. Chakraborty M, Gelbard A, Carrasquillo JA, Yu S, Mamede M, Paik CH, et al. Use of radiolabeled monoclonal antibody to enhance vaccine-mediated antitumor effects. *Cancer Immunol Immunother.* 2008;57:1173–83.
40. Seo A, Ishikawa F, Nakano H, Nakazaki H, Kobayashi K, Kakiuchi T. Enhancement of B7-1 (CD80) expression on B-lymphoma cells by irradiation. *Immunology.* 1999;96:642–8.
41. Chen Z, Moyana T, Saxena A, Warrington R, Jia Z, Xiang J. Efficient antitumor immunity derived from maturation of dendritic cells that had phagocytosed apoptotic/necrotic tumor cells. *Int J Cancer.* 2001;93:539–48.
42. Kotera Y, Shimizu K, Mulé JJ. Comparative analysis of necrotic and apoptotic tumor cells as a source of antigen(s) in dendritic cell-based immunization. *Cancer Res.* 2001;61:8105–9.
43. Zhang M, Yao Z, Patel H, Garmestani K, Zhang Z, Talanov VS, et al. Effective therapy of murine models of human leukemia and lymphoma with radiolabeled anti-CD30 antibody, HeFi-1. *Proc Natl Acad Sci U S A.* 2007;104:8444–8.
44. Ma Y, Kepp O, Ghiringhelli F, Apetoh L, Aymeric L, Locher C, et al. Chemotherapy and radiotherapy: cryptic anticancer vaccines. *Semin Immunol.* 2010;22:113–24.
45. Zitvogel L, Kepp O, Kroemer G. Decoding cell death signals in inflammation and immunity. *Cell.* 2010;140:798–804.
46. Obeid M, Tesniere A, Ghiringhelli F, Fimia GM, Apetoh L, Perfettini J-L, et al. Calreticulin exposure dictates the immunogenicity of cancer cell death. *Nat Med.* 2007;13:54–61.
47. Panaretakis T, Kepp O, Brockmeier U, Tesniere A, Bjorklund A-C, Chapman DC, et al. Mechanisms of pre-apoptotic calreticulin exposure in immunogenic cell death. *EMBO J.* 2009;28:578–90.
48. Panaretakis T, Joza N, Modjtahedi N, Tesniere A, Vitale I, Durchschlag M, et al. The co-translocation of ERp57 and calreticulin determines the immunogenicity of cell death. *Cell Death Differ.* 2008;15:1499–509.
49. Sukkurwala AQ, Martins I, Wang Y, Schlemmer F, Ruckenstein C, Durchschlag M, et al. Immunogenic calreticulin exposure occurs through a phylogenetically conserved stress pathway involving the chemokine CXCL8. *Cell Death Differ.* 2014;21:59–68.
50. Yamazaki T, Hannani D, Poirier-Colame V, Ladoire S, Locher C, Sistigu A, et al. Defective immunogenic cell death of HMGB1-deficient tumors: compensatory therapy with TLR4 agonists. *Cell Death Differ.* 2014;21:69–78.
51. Scaffidi P, Misteli T, Bianchi ME. Release of chromatin protein HMGB1 by necrotic cells triggers inflammation. *Nature.* 2002;418:191–5.
52. Tang D, Loze MT, Zeh HJ, Kang R. The redox protein HMGB1 regulates cell death and survival in cancer treatment. *Autophagy.* 2010;6:1181–3.
53. Apetoh L, Ghiringhelli F, Tesniere A, Obeid M, Ortiz C, Criollo A, et al. Toll-like receptor 4-dependent contribution of the immune system to anticancer chemotherapy and radiotherapy. *Nat Med.* 2007;13(9):1050.
54. Gorin J-B, Ménager J, Gouard S, Maurel C, Guilloux Y, Faivre-Chauvet A, et al. Antitumor immunity induced after  $\alpha$  irradiation. *Neoplasia.* 2014;16:319–28.
55. Martins I, Tesniere A, Kepp O, Michaud M, Schlemmer F, Senovilla L, et al. Chemotherapy induces ATP release from tumor cells. *Cell Cycle.* 2009;8:3723–8.
56. Elliott MR, Chekeni FB, Trampont PC, Lazarowski ER, Kadl A, Walk SF, et al. Nucleotides released by apoptotic cells act as a find-me signal to promote phagocytic clearance. *Nature.* 2009;461:282–6.
57. Ghiringhelli F, Apetoh L, Tesniere A, Aymeric L, Ma Y, Ortiz C, et al. Activation of the NLRP3 inflammasome in dendritic cells induces IL-1 $\beta$ -dependent adaptive immunity against tumors. *Nat Med.* 2009;15:1170–8.
58. Aymeric L, Apetoh L, Ghiringhelli F, Tesniere A, Martins I, Kroemer G, et al. Tumor cell death and ATP release prime dendritic cells and efficient anticancer immunity. *Cancer Res.* 2010;70:855–8.
59. Martins I, Wang Y, Michaud M, Ma Y, Sukkurwala AQ, Shen S, et al. Molecular mechanisms of ATP secretion during immunogenic cell death. *Cell Death Differ.* 2014;21:79–91.

60. Chekeni FB, Elliott MR, Sandilos JK, Walk SF, Kinchen JM, Lazarowski ER, et al. Pannexin 1 channels mediate “find-me” signal release and membrane permeability during apoptosis. *Nature*. 2010;467:863–7.
61. Michaud M, Martins I, Sukkurwala AQ, Adjemian S, Ma Y, Pellegatti P, et al. Autophagy-dependent anticancer immune responses induced by chemotherapeutic agents in mice. *Science*. 2011;334:1573–7.
62. Gorin J-B, Gouard S, Ménager J, Morgenstern A, Bruchertseifer F, Faivre-Chauvet A, et al. Alpha particles induce autophagy in multiple myeloma cells. *Front Med (Lausanne)*. 2015;2:74.
63. Rieber M, Rieber MS. Sensitization to radiation-induced DNA damage accelerates loss of bcl-2 and increases apoptosis and autophagy. *Cancer Biol Ther*. 2008;7:1561–6.
64. Rodriguez-Rocha H, Garcia-Garcia A, Panayiotidis MI, Franco RDNA. Damage and autophagy. *Mutat Res*. 2011;711:158–66.
65. Schildkopf P, Frey B, Ott OJ, Rubner Y, Multhoff G, Sauer R, et al. Radiation combined with hyperthermia induces HSP70-dependent maturation of dendritic cells and release of pro-inflammatory cytokines by dendritic cells and macrophages. *Radiother Oncol*. 2011;101:109–15.
66. Rubner Y, Muth C, Strnad A, Derer A, Sieber R, Buslei R, et al. Fractionated radiotherapy is the main stimulus for the induction of cell death and of Hsp70 release of p53 mutated glioblastoma cell lines. *Radiat Oncol*. 2014;9:89.
67. Multhoff G, Pockley AG, Schmid TE, Schilling D. The role of heat shock protein 70 (Hsp70) in radiation-induced immunomodulation. *Cancer Lett*. 2015;368:179–84.
68. Formenti SC, Demaria S. Combining radiotherapy and cancer immunotherapy: a paradigm shift. *J Natl Cancer Inst*. 2013;105:256–65.
69. Lugade AA, Sorensen EW, Gerber SA, Moran JP, Frelinger JG, Lord EM. Radiation-induced IFN-gamma production within the tumor microenvironment influences antitumor immunity. *J Immunol*. 2008;180:3132–9.
70. Matsumura S, Demaria S. Up-regulation of the pro-inflammatory chemokine CXCL16 is a common response of tumor cells to ionizing radiation. *Radiat Res*. 2010;173:418–25.
71. Matsumura S, Wang B, Kawashima N, Braunstein S, Badura M, Cameron TO, et al. Radiation-induced CXCL16 release by breast cancer cells attracts effector T cells. *J Immunol*. 2008;181:3099–107.
72. Ishihara H, Tsuneoka K, Dimchev AB, Shikita M. Induction of the expression of the interleukin-1 beta gene in mouse spleen by ionizing radiation. *Radiat Res*. 1993;133:321–6.
73. Burnette BC, Liang H, Lee Y, Chlewicki L, Khodarev NN, Weichselbaum RR, et al. The efficacy of radiotherapy relies upon induction of type I interferon-dependent innate and adaptive immunity. *Cancer Res*. 2011;71:2488–96.
74. Burnette B, Weichselbaum RR. Radiation as an immune modulator. *Semin Radiat Oncol*. 2013;23:273–80.
75. Ozsoy HZ, Sivasubramanian N, Wieder ED, Pedersen S, Mann DL. Oxidative stress promotes ligand-independent and enhanced ligand-dependent tumor necrosis factor receptor signaling. *J Biol Chem*. 2008;283:23419–28.
76. Ganss R, Ryschich E, Klar E, Arnold B, Hämmerling GJ. Combination of T-cell therapy and trigger of inflammation induces remodeling of the vasculature and tumor eradication. *Cancer Res*. 2002;62:1462–70.
77. Lugade AA, Moran JP, Gerber SA, Rose RC, Frelinger JG, Lord EM. Local radiation therapy of B16 melanoma tumors increases the generation of tumor antigen-specific effector cells that traffic to the tumor. *J Immunol*. 2005;174:7516–23.
78. Reynders K, Illidge TM, Siva S, Chang JY, De Ruyscher D. The abscopal effect of local radiotherapy: using immunotherapy to make a rare event clinically relevant. *Cancer Treat Rev*. 2015;41:503–10.
79. Everse LA, Renes IB, Jürgenliemk-Schulz IM, Rutgers DH, Bernsen MR, Dullens HF, et al. Local low-dose interleukin-2 induces systemic immunity when combined with radiotherapy of cancer. A pre-clinical study. *Int J Cancer*. 1997;72:1003–7.

80. Jürgenliemk-Schulz IM, Renes IB, Rutgers DH, Everse LA, Bernsen MR, Otter Den W, et al. Anti-tumor effects of local irradiation in combination with peritumoral administration of low doses of recombinant interleukin-2 (rIL-2). *Radiat Oncol Investig.* 1997;5:54–61.
81. Maas RA, Dullens HF, De Jong WH, Otter Den W. Immunotherapy of mice with a large burden of disseminated lymphoma with low-dose interleukin 2. *Cancer Res.* 1989;49:7037–40.
82. Masztalerz A, Everse LA, Otter WD. Presence of cytotoxic B220+CD3+CD4-CD8- cells correlates with the therapeutic efficacy of lymphoma treatment with IL-2 and/or IL-12. *J Immunother.* 2004;27:107–15.
83. Poiré X, Kline J, Grinblatt D, Zimmerman T, Conner K, Muhs C, et al. Phase II study of immunomodulation with granulocyte-macrophage colony-stimulating factor, interleukin-2, and rituximab following autologous stem cell transplant in patients with relapsed or refractory lymphomas. *Leuk Lymphoma.* 2010;51:1241–50.
84. Nagler A, Berger R, Ackerstein A, Czyz JA, Diez-Martin JL, Naparstek E, et al. A randomized controlled multicenter study comparing recombinant interleukin 2 (rIL-2) in conjunction with recombinant interferon alpha (IFN-alpha) versus no immunotherapy for patients with malignant lymphoma postautologous stem cell transplantation. *J Immunother.* 2010;33:326–33.
85. Lum LG, Thakur A, Pray C, Koultab N, Abedi M, Deol A, et al. Multiple infusions of CD20-targeted T cells and low-dose IL-2 after SCT for high-risk non-Hodgkin's lymphoma: a pilot study. *Bone Marrow Transplant.* 2014;49:73–9.
86. Honeychurch J, Glennie MJ, Johnson PWM, Illidge TM. Anti-CD40 monoclonal antibody therapy in combination with irradiation results in a CD8 T-cell-dependent immunity to B-cell lymphoma. *Blood.* 2003;102:1449–57.
87. Khong A, Nelson DJ, Nowak AK, Lake RA, Robinson BWS. The use of agonistic anti-CD40 therapy in treatments for cancer. *Int Rev Immunol.* 2012;31:246–66.
88. Zhou Z-H, Shi Q, Wang J-F, Chen Y-J, Zhuang Y-M, Pan J-Z, et al. Sensitization of multiple myeloma and B lymphoma lines to dexamethasone and gamma-radiation-induced apoptosis by CD40 activation. *Apoptosis.* 2005;10:123–34.
89. Hassan SB, Sørensen JF, Olsen BN, Pedersen AE. Anti-CD40-mediated cancer immunotherapy: an update of recent and ongoing clinical trials. *Immunopharmacol Immunotoxicol.* 2014;36:96–104.
90. de Vos S, Forero-Torres A, Ansell SM, Kahl B, Cheson BD, Bartlett NL, et al. A phase II study of dacetuzumab (SGN-40) in patients with relapsed diffuse large B-cell lymphoma (DLBCL) and correlative analyses of patient-specific factors. *J Hematol Oncol.* 2014;7:44.
91. Dovedi SJ, Melis MHM, Wilkinson RW, Adlard AL, Stratford IJ, Honeychurch J, et al. Systemic delivery of a TLR7 agonist in combination with radiation primes durable antitumor immune responses in mouse models of lymphoma. *Blood.* 2013;121:251–9.
92. Kobold S, Wiedemann G, Rothenfuß S, Endres S. Modes of action of TLR7 agonists in cancer therapy. *Immunotherapy.* 2014;6:1085–95.
93. Zhu J, He S, Du J, Wang Z, Li W, Chen X, et al. Local administration of a novel Toll-like receptor 7 agonist in combination with doxorubicin induces durable tumouricidal effects in a murine model of T cell lymphoma. *J Hematol Oncol.* 2015;8:21.
94. Wysocka M, Newton S, Benoit BM, Introcaso C, Hancock AS, Chehimi J, et al. Synthetic imidazoquinolines potently and broadly activate the cellular immune response of patients with cutaneous T-cell lymphoma: synergy with interferon-gamma enhances production of interleukin-12. *Clin Lymphoma Myeloma Leuk.* 2007;7:524–34.
95. Wysocka M, Dawany N, Benoit B, Kossenkov AV, Troxel AB, Gelfand JM, et al. Synergistic enhancement of cellular immune responses by the novel toll receptor 7/8 agonist 3M-007 and interferon- $\gamma$ : implications for therapy of cutaneous T-cell lymphoma. *Leuk Lymphoma.* 2011;52:1970–9.
96. Weigel BJ, Cooley S, DeFor T, Weisdorf DJ, Panoskaltsis-Mortari A, Chen W, et al. Prolonged subcutaneous administration of 852A, a novel systemic toll-like receptor 7 agonist, to activate innate immune responses in patients with advanced hematologic malignancies. *Am J Hematol.* 2012;87:953–6.

97. Dewan MZ, Vanpouille-Box C, Kawashima N, DiNapoli S, Babb JS, Formenti SC, et al. Synergy of topical toll-like receptor 7 agonist with radiation and low-dose cyclophosphamide in a mouse model of cutaneous breast cancer. *Clin Cancer Res.* 2012;18:6668–78.
98. Adlard AL, Dovedi SJ, Telfer BA, Koga-Yamakawa E, Pollard C, Honeychurch J, et al. A novel systemically administered toll-like receptor 7 agonist potentiates the effect of ionizing radiation in murine solid tumor models. *Int J Cancer.* 2014;135:820–9.
99. Ménager J, Gorin J-B, Maurel C, Drujont L, Gouard S, Louvet C, et al. Combining  $\alpha$ -radioimmunotherapy and adoptive T cell therapy to potentiate tumor destruction. *PLoS One.* 2015;10:e0130249.
100. Abuodeh Y, Venkat P, Kim S. Systematic review of case reports on the abscopal effect. *Curr Probl Cancer.* 2016;40:25–37.
101. Seyedin SN, Schoenhals JE, Lee DA, Cortez MA, Wang X, Niknam S, et al. Strategies for combining immunotherapy with radiation for anticancer therapy. *Immunotherapy.* 2015;7:967–80.
102. Crittenden M, Kohrt H, Levy R, Jones J, Camphausen K, Dicker A, et al. Current clinical trials testing combinations of immunotherapy and radiation. *Semin Radiat Oncol.* 2015;25:54–64.
103. Barker CA, Postow MA. Combinations of radiation therapy and immunotherapy for melanoma: a review of clinical outcomes. *Int J Radiat Oncol Biol Phys.* 2014;88:986–97.
104. Brody JD, Ai WZ, Czerwinski DK, Torchia JA, Levy M, Advani RH, et al. In situ vaccination with a TLR9 agonist induces systemic lymphoma regression: a phase I/II study. *J Clin Oncol.* 2010;28:4324–32.
105. Witzig TE, Wiseman GA, Maurer MJ, Habermann TM, Micallef INM, Nowakowski GS, et al. A phase I trial of immunostimulatory CpG 7909 oligodeoxynucleotide and 90 yttrium ibritumomab tiuxetan radioimmunotherapy for relapsed B-cell non-Hodgkin lymphoma. *Am J Hematol.* 2013;88:589–93.
106. Abulayha A, Bredan A, Enshasy El H, Daniels I. Rituximab: modes of action, remaining dispute and future perspective. *Future Oncol.* 2014;10:2481–92.
107. Weiner LM, Dhodapkar MV, Ferrone S. Monoclonal antibodies for cancer immunotherapy. *Lancet.* 2009;373:1033–40.
108. Buchegger F, Larson SM, Mach J-P, Chalandon Y, Dietrich P-Y, Cairoli A, et al. Radioimmunotherapy combined with maintenance anti-CD20 antibody may trigger long-term protective T cell immunity in follicular lymphoma patients. *Clin Dev Immunol.* 2013;2013:875343.
109. Jacobs SA, Swerdlow SH, Kant J, Foon KA, Jankowitz R, Land SR, et al. Phase II trial of short-course CHOP-R followed by 90Y-ibritumomab tiuxetan and extended rituximab in previously untreated follicular lymphoma. *Clin Cancer Res.* 2008;14:7088–94.
110. Pisani F, Sciuto R, Dessanti ML, Giannarelli D, Kayal R, Rea S, et al. Long term efficacy and safety of fludarabine, cyclophosphamide and rituximab regimen followed by (90) Y-ibritumomab tiuxetan consolidation for the treatment of relapsed grades 1 and 2 follicular lymphoma. *Exp Hematol Oncol.* 2015;4:17.
111. Witzig TE, Hong F, Micallef IN, Gascoyne RD, Dogan A, Wagner H, et al. A phase II trial of RCHOP followed by radioimmunotherapy for early stage (stages I/II) diffuse large B-cell non-Hodgkin lymphoma: ECOG3402. *Br J Haematol.* 2015;170:679–86.
112. Golden EB, Chhabra A, Chachoua A, Adams S, Donach M, Fenton-Kerimian M, et al. Local radiotherapy and granulocyte-macrophage colony-stimulating factor to generate abscopal responses in patients with metastatic solid tumours: a proof-of-principle trial. *Lancet Oncol.* 2015;16:795–803.
113. Davila ML, Sadelain M. Biology and clinical application of CAR T cells for B cell malignancies. *Int J Hematol.* 2016;104:6–17.
114. Morris EC, Stauss HJ. Optimizing T-cell receptor gene therapy for hematologic malignancies. *Blood.* 2016;127:3305–11.
115. Adams JL, Smothers J, Srinivasan R, Hoos A. Big opportunities for small molecules in immuno-oncology. *Nat Rev Drug Discov.* 2015;14:603–22.



# Prospects for Enhancing Efficacy of Radioimmunotherapy



Clément Bailly, Caroline Bodet-Milin, François Guérard, Caroline Rousseau, Michel Chérel, Françoise Kraeber-Bodéré, and Jean-François Chatal

**Abstract** Radioimmunotherapy has been in use for more than 20 years and has progressed significantly since its efficacy has first been demonstrated in hematology. Yet it still has limitations that prevent its large-scale clinical use. This chapter reviews recent developments to overcome these limitations including new antibody specificities, pretargeting methods, fractionated injections, and the use of alpha emitters. Immuno-PET is also likely to assist in selecting patients for radioimmunotherapy, optimizing injected activities, and noninvasively monitoring therapy efficacy.

**Keywords** Radioimmunotherapy · Fractionation · Pretargeting · Alpha-RIT · Theranostic

## Abbreviations

ADC	Antibody drug conjugate
AML	Acute myeloid leukemia
ARC	Antibody radionuclide conjugate

---

C. Bailly · C. Bodet-Milin  
CHU, CRCNA, UMR 892 Inserm, 6299 CNRS, Université de Nantes, Nantes, France

F. Guérard  
CRCNA, UMR 892 Inserm, 6299 CNRS, Université de Nantes, Nantes, France

C. Rousseau · M. Chérel  
ICO-Gauducheau, CRCNA, UMR 892 Inserm, 6299 CNRS,  
Université de Nantes, Nantes, France

F. Kraeber-Bodéré  
CHU, ICO-Gauducheau, CRCNA, UMR 892 Inserm, 6299 CNRS,  
Université de Nantes, Nantes, France

J.-F. Chatal (✉)  
GIP Arronax, Nantes-Saint-Herblain, France  
e-mail: [chatal@arronax-nantes.fr](mailto:chatal@arronax-nantes.fr)



BsMAb	Bispecific monoclonal antibody
CEA	Carcinoembryonic antigen
EGFR	Epidermal growth factor receptor
HSG	Histamine-succinyl-glutamine
LET	Linear energy transfer
MRD	Minimal residual disease
MTD	Maximum tolerated dose
NHL	Non-Hodgkin B-cell lymphoma
PSMA	Prostate-specific membrane antigen
RIT	Radioimmunotherapy
SPECT	Single-photon emission computed tomography
PET	Positron emission tomography

## 1 Introduction

Clinical development of radioimmunotherapy (RIT) started in the 1980s and progressed rapidly due to advancements in recombinant humanized or human antibodies and in the development of radiolabeling methods and/or superior chelating agents. The first clinical application was for non-Hodgkin B-cell lymphoma (NHL) because the radiosensitivity of this type of cancer allows good efficacy for a relatively moderate tumor dose delivery. Two radioimmunoconjugates targeting the CD20 antigen have been approved:  $^{131}\text{I}$ -tositumomab (Bexxar; GlaxoSmithKline) which was subsequently discontinued and  $^{90}\text{Y}$ -ibritumomab tiuxetan (Zevalin; Spectrum Pharmaceuticals) which continues to be used both in the US and in Europe. While most clinicians agree that this last radioimmunoconjugate has demonstrated clinical efficacy, it has not been successfully adopted by the hematologist community.

For more radioresistant solid tumors, the clinical efficacy of RIT remains limited, and up to now, no radioimmunoconjugate has been yet approved.

In parallel with the clinical development of radioimmunoconjugates, also termed antibody radionuclide conjugates (ARCs), some pharmaceutical companies have developed antibody drug conjugates (ADCs) for treatment of several types of cancer [1]. A recent review summarized the results of 11 studies including 598 patients treated with 6 ADCs and 9 studies including 377 patients treated with 5 ARCs [1]. While it was obviously not possible to statistically compare the results of both modalities, the objective was to roughly estimate their respective toxicity and clinical efficacy. Toxicity was generally less frequent with ADCs (less than 20%) than with ARCs but led to more uncomfortable side effects. Hematologic toxicity was higher with ARCs than with ADCs. Clinical efficacy was roughly comparable.

There is no doubt that RIT still has limitations preventing its large-scale clinical use. These limitations can be partially overcome by using fractionation of the injected activities and combination therapy with nonradioactive drugs that have non-overlapping toxicity and synergistic effects. Finally, the use of alpha-emitting

radionuclides could dramatically improve the clinical efficacy for microscopic tumors or clusters of malignant cells disseminated throughout the body.

## 2 Current Limitations of RIT

The current limitations of RIT are technical, logistical, and societal. Until now the majority of clinical studies have used a single injection for treatment of the most common large bulk tumors. Under these conditions tumor uptake was low or very low resulting from an inefficient weak dose. However, it has been clearly documented that dose delivery to tumors increases with decreasing tumor mass [2, 3]. For treatment of medullary thyroid cancer using a pretargeting technique, a tumor dose as high as 174 cGy/mCi (4.7 cGy/MBq) has been calculated for a small resected tumor of 1.8 g. By extrapolating this value to an injected activity of 100 mCi (3700 MBq) comparable to the activity of  $^{131}\text{I}$  administered for treatment of metastases of differentiated thyroid carcinoma, a tumoricidal absorbed tumor dose of 174 Gy would have been obtained. Moreover, a serious problem for macroscopic tumors is the accessibility of circulating antibody to cells of the inner hypoxic areas [4]. Thus there is a consensus that the best situation for an efficient RIT would be a dissemination of small-size tumors or some clusters of malignant cells in the body.

Another serious limitation of RIT is the need for a reliable supply chain for the radionuclide. Big pharma companies do not have such a supply chain and are generally not familiar with coupling radionuclides to antibody molecules. That is probably why they prefer the use of chemotherapeutic drugs which they control very well for antibody drug conjugates. Changing from chemotherapeutic drugs to radionuclides would require them to secure radionuclide supply in the event of a very efficient RIT, for example, with an overall survival gain of 6 months to 1 year, which is longer than that generally observed for many chemotherapeutic drugs.

Finally, RIT may cause concern among patients due to the use of radioactivity and may require secondary myelodysplasia/acute/leukemia risk management by oncologists, even though such a risk is limited to heavily pretreated patients.

## 3 Prospects to Improve RIT

### 3.1 Fractionation of Injections

The rationale for using fractionated instead of single-dose RIT was reported in 2002 by DeNardo et al. [5]. The main advantage of injected activity fractionation is to reduce hematologic toxicity as a consequence of faster and more efficient bone marrow repair than tumor cell repair. Several preclinical studies over many years have tended to validate this concept [6]. The number of clinical studies is more limited. Two in particular, using well-known radioimmunoconjugates in a substantial number

**Table 1** Clinical studies with single or fractionated injected activities

	<sup>90</sup> Y-Ibritumomab tiuxetan		<sup>177</sup> Lu-hJ591 (ATL101)	
	Single1	Fractionated2	Single3	Fractionated4
Number of patients	59	74	47	44
Injected activity	15 MBq/m <sup>2</sup> up to max 1200 MBq	11.1 MBq/m <sup>2</sup> × 2 up to max 888 × 2	65–70 mCi/m <sup>2</sup>	40–45 mCi/m <sup>2</sup> × 2
Interval time between two injections	NA	8–12 w	NA	2 w
Thrombocytopenia Gr 3/4	48%	56.4%	65.7%	Global hematol tox (plts+neutro):73.5%
Neutropenia Gr 3/4	32%	36.4%	65.6%	
ORR	87%	94.4%	NA	NA
CR/CRu	56%	58.3%	NA	NA
PFS	26 m	40.2 m	NK	NK
OS	Median OS not reached	Median OS not reached	21.8 m	42.9 m

NA Not applicable, ORR Overall response rate, NK Not known, CR/CRU Complete/unconfirmed complete response, PFS Progression-free survival, OS Overall survival

of patients, have provided important information for future applications (Table 1). The first study used the approved <sup>90</sup>Y-ibritumomab tiuxetan (Zevalin®) radioimmunoconjugate in 74 patients as an initial therapy for follicular lymphoma [7]. The patients were sequentially injected twice with an activity of 11.1 MBq/m<sup>2</sup> (not exceeding twice 888 MBq) 2–12 weeks apart. Another study used the same radioimmunoconjugate in 59 patients, again as an initial treatment for follicular lymphoma, with a single activity of 15 MBq/m<sup>2</sup> (not exceeding 1200 MBq) [8]. The fractionated radioimmunotherapy therefore used a cumulative activity 48% higher than in the single-dose radioimmunotherapy. The hematologic toxicity was roughly comparable between the single and fractionated studies with grade 3/4 thrombocytopenia and neutropenia of 48 and 56% and 32 and 36%, respectively. The clinical efficacy was clearly improved with fractionation, with an overall response rate of 94 vs 87% with single-dose therapy and more impressively a progression-free survival of 40 vs 26 months. These studies using <sup>90</sup>Y-ibritumomab tiuxetan illustrate a clear advantage of activity fractionation compared to single-dose activity and allow the overall injected activity to be significantly increased while maintaining the same level of toxicity.

A second study used the <sup>177</sup>Lu-J591 (ATL101) DOTA radioimmunoconjugate in 44 patients with metastatic prostate cancer [9]. The patients were sequentially injected twice with an activity of 1480–1665 MBq/m<sup>2</sup> 2 weeks apart. Another study used the same radioimmunoconjugate in 47 patients in the same indication of metastatic prostate cancer with a single activity of 2405–2590 MBq/m<sup>2</sup> [10]. The fractionated radioimmunotherapy used a cumulative activity 26% higher than in the single-dose radioimmunotherapy.

The hematologic toxicity was difficult to compare between the two approaches because with fractionation only global toxicity was evaluated with 73.5% grade 3/4. However, compared to 66% of grade 3/4 thrombocytopenia and neutropenia with single-dose activity, a clear higher toxicity with fractionation does not appear significant.

However, the clinical efficacy was clearly improved with fractionation showing an overall survival of 43 vs 22 months with the single-dose activity. The predominant bone metastases in prostate cancer did not allow evaluation of overall response rate. It is obviously not possible to statistically compare the results of both single and fractionated studies in these two clinical indications using these two methodological approaches. Only a rough estimate of efficacy and toxicity can be drawn. It appears that fractionation is clearly preferable to single activity, allowing the injected activity to be substantially increased and consequently improving clinical efficacy without impairing hematologic toxicity. However, fractionation needs to be optimized for each radioimmunoconjugate. Two parameters should be taken into consideration, namely, the level of fractionated activity and the time interval between two sequential injections. It is well known that following irradiation, bone marrow repair is faster and more efficient than tumor repair. Consequently, it is logical to wait for 6–8 weeks, i.e., the time required for hematologic recovery, before reinjection. Determining the level of injected activity is more difficult, and the choice is somewhat empirical. In preclinical studies it is easy to test a range of injected activities; however extrapolating these results to the clinical situation is questionable. In clinical studies, testing a selected activity requires months to years to accrue sufficient patient numbers to estimate the toxicity and clinical efficacy. This is why the choice of the level of activity is relatively empirical.

### ***3.2 Combinations with Other Therapeutic Agents***

The rationale for combining RIT with other systemic therapies, especially chemotherapy, is to take advantage of potentially radiation-enhancing drugs and the non-overlapping drug-limiting toxicity of each agent. It is well established that for a large tumor burden, the tumor dose delivered by RIT does not exceed 15–40 Gy, which is not sufficient for an efficient tumor-killing effect. The situation is different for small or microscopic tumors for which much higher tumor doses can be delivered. One way to increase RIT efficacy is to combine it with systemic drugs with a different and if possible synergistic tumor-killing effect. Many preclinical animal studies using human cancer xenograft models in nude mice have clearly shown a significant benefit of such a combination in terms of tumor shrinkage and survival time [11]. However, the extrapolation of these results to clinical studies in predicting efficacy should be made with caution. Hence the only way to assess the real benefit of combining RIT and chemotherapy is to refer to clinical studies performed with specific radioimmunoconjugates, chemotherapeutic drugs, and clinical situations. Only a limited number of RIT +/- combined therapy studies have been performed.

Phase I clinical trials assessing three radioimmunoconjugates, combined or not, with three chemotherapeutic drugs have been performed (Table 2). In patients treated with a maximum tolerated dose (MTD) of 614 MBq/m<sup>2</sup> of an anti-carcinoembryonic antigen antibody labeled with yttrium-90 (T84–66), combined or not with 5-fluorouracil in, respectively, 21 and 22 patients with metastatic CEA-producing

**Table 2** Clinical studies with combined or RIT alone

	<sup>90</sup> Yttrium-anti-CEA chimeric T84.66		<sup>90</sup> Yttrium-clivatuzumab		<sup>177</sup> Lu-J591	
	RIT alone	RIT+ 5-FU	RIT alone	Fract RIT + gemcitabine	RIT alone	Fract RIT docetaxel
Number of patients	22	21	9	17	12	15
Injected MTD	614–814 MBq/m <sup>2</sup>	614 MBq/m <sup>2</sup>	740 MBq/m <sup>2</sup>	444 × 3 MBq/m <sup>2</sup>	2220–2775 MBq/m <sup>2</sup>	
Thrombocytopenia Gr 3/4	10%	24%	55%	74%	75%	
Neutropenia Gr 3/4	20%	19%	44%		67%	
Overall response rate	0	0	22%	16%	11%	73.3%
Stabilization and mixed response	32%	57%	ND	42%	≥50% PSA decline 46% PSA Stabilization	≥50% PSA decline
Overall survival	ND	ND	4.3 m	8 m	ND	ND

malignancies, thrombocytopenia was slightly higher for combination therapy (24 vs 10%), while neutropenia was the same (19% and 20%) [12, 13]. There was no objective response in either situation and a slightly higher mixed or stable response with combination treatment (57% vs 32%).

A second radioimmunoconjugate, clivatuzumab, is an anti-PAM4 reactive mucin antibody labeled with yttrium-90. Treatment of pancreatic carcinoma patients with clivatuzumab alone or combined with gemcitabine (17 and 9 patients, respectively) at the MTD in a fractionated mode (444 MBq x3) showed that the hematologic toxicity was roughly comparable, even though the interpretation of this parameter is difficult to assess because the combination study of thrombocytopenia and neutropenia results was merged [14, 15]. There was no real difference in the response rate but a tendency toward a longer overall survival with the fractionated and combined study (8 vs 4.4 months).

Finally, an anti-PSMA antibody, labeled with lutetium-177 (J591) at the MTD, was compared against combined therapy with docetaxel (15 and 12 patients, respectively) for the treatment of prostate cancer [16, 17]. While these results should be treated with caution due to the small number of patients, combination therapy resulted in a trend toward improved clinical efficacy without altered toxicity. Promotion to phase II trials will require a substantial increase in patient numbers and data and most likely a number of years.

### **3.3 Pretargeting Using Bispecific Antibodies**

Pretargeting may be achieved by a primary injection of an unlabeled bispecific monoclonal antibody (BsMAb), followed by a second injection of a radiolabeled bivalent hapten-peptide [18, 19]. Using this strategy, the radiolabeled bivalent peptide binds more avidly to the BsMAb attached to the antigen expressed at the tumor cell surface, whereas nontargeted hapten-peptide in the circulation clears rapidly through the kidneys. After the promising phase I/II studies, encouraging clinical results have been obtained using an anti-CEA chimeric hMN-14x734 BsMAb and <sup>131</sup>I-di-DTPA peptide in a prospective multicentric phase II study performed in 45 patients with progressive metastatic medullary thyroid carcinoma (MTC) [20]. This study demonstrated a disease control rate of 76.2% (durable stabilization plus objective response) according to RECIST, with 1 case of durable complete response of at least 40 months (2.4%) and 31 durable stable disease cases of  $\geq 6$  months (73.8%). After RIT, 21 of 37 assessed patients (56.7%) showed a  $\geq 100\%$  increase in serum biomarker concentration doubling time or prolonged decrease in serum biomarker concentration. As expected for these patients with a high frequency of diffuse bone marrow involvement, high-grade 3 and 4 hematologic toxicity was observed in 54.7% of patients and myelodysplastic syndrome reported in two cases, including one treated heavily previously.

New-generation recombinant humanized trivalent BsMAb and bivalent histamine-succinyl-glutamine (HSG) peptides have been produced. These can be

labeled with a variety of radionuclides, including yttrium-90 and lutetium-177 for therapeutic purposes [21–23]. This new-generation pretargeting system using anti-CEA  $\times$  anti-HSG BsMAb TF2 and  $^{177}\text{Lu}$ -IMP288 has been performed and optimized in two clinical trials in patients with metastatic colorectal carcinoma and lung carcinoma [24, 25]. Different schedules were studied to define the optimal molar doses of TF2 and IMP-288 and the optimal delay between the two infusions.

Three cohorts of three patients were included in the first part of a phase I/II clinical trial designed to optimize and assess anti-CEA  $\times$  anti-HSG BsMAb TF2 in CEA-expressing lung cancer patients. Patients underwent a pre-therapeutic imaging session S1 (44 or 88 nmol/m<sup>2</sup> of TF2 followed by 4.4 nmol/m<sup>2</sup> and 185 MBq of  $^{111}\text{In}$ -IMP288) and, 1–2 weeks later, a therapy session S2 (240 or 480 nmol/m<sup>2</sup> of TF2 followed by 24 nmol/m<sup>2</sup>, 1.1 GBq/m<sup>2</sup>,  $^{177}\text{Lu}$ -IMP288). The pretargeting delay was 24 or 48 h. According to the pharmacokinetic and imaging analysis, the best dosing parameters corresponded to the shorter pretargeting delay (24 h) and to the highest TF2 molar doses. While toxicity was quite limited in the eight patients evaluated, treatment efficacy was minimal in this optimization part of the study, with only two cases of disease stabilization for only short periods of time [25]. Thus, to improve treatment efficacy, the injected activity should be increased for the second part of the study, which is planned with an activity escalation. Overall, it was not expected that a single therapy cycle would be sufficient to deliver antitumor therapeutic doses and the use of shorter half-life and higher intrinsic toxicity radionuclides, such as yttrium-90, could be preferable to that of lutetium-177. Taking into account these data, a prospective phase I study is ongoing, to assess fractionated injection of  $^{90}\text{Y}$ -IMP288 in metastatic colorectal carcinoma patients.

### 3.4 Alpha-Emitting Radionuclides

Due to their high linear energy transfer (LET),  $\alpha$ -particles deliver a high fraction of their energy inside the targeted cells leading to highly efficient killing, making them particularly suited for targeting of isolated tumor cells and minimal residual disease (MRD). Moreover,  $\alpha$ -particle cytotoxicity is considered to be independent of the dose rate and oxygenation [26]. Among the large number of identified  $\alpha$ -emitting radionuclides, only few of them exhibit physical characteristics adapted for RIT.  $^{213}\text{Bi}$  is available through a  $^{225}\text{Ac}/^{213}\text{Bi}$  generator, but its short half-life (T<sub>1/2</sub>) of 45.6 min makes it difficult to use. While  $^{225}\text{Ac}$  (T<sub>1/2</sub> = 10 days) appears clinically more suitable, its decay produces a series of alpha-emitting daughter nucleons that are released from the chelating agent which then increase irradiation of normal tissues. With an intermediate half-life of 7.2 h and 100% of decays leading to the emission of an  $\alpha$ -particle,  $^{211}\text{At}$ , which is available from cyclotron production, may be a better candidate, although its availability and chemistry remain to be improved [27].

The first clinical report of alpha-RIT was performed using an anti-CD33 monoclonal antibody labeled with  $^{213}\text{Bi}$ . The CD33 antigen is a 67 kDa glycoprotein expressed on most myeloid leukemias and clonogenic leukemia progenitors but not



on normal stem cells. Anti-CD33 RIT has been developed using the murine M195 and the HuM195 (lintuzumab) humanized antibodies by the Scheinberg group at the Memorial Sloan-Kettering Institute. A phase I dose-escalation study assessing  $^{213}\text{Bi}$ -lintuzumab was conducted in 18 patients with relapsed and refractory acute myeloid leukemia (AML) or chronic myelomonocytic leukemia treated with 10.36–37.0 MBq/kg  $^{213}\text{Bi}$ -RIT [28]. No significant non-hematologic toxicity was observed. Dose-limiting toxicity, defined as grade 4 leukopenia for more than 35 days from the beginning of therapy, was observed in one patient treated at the 37 MBq/kg dose level following relapse after allogeneic transplantation.  $^{213}\text{Bi}$ -HuM195 was retained in areas of leukemic involvement (bone marrow, liver, and spleen). The estimated total absorbed dose to the marrow, and therefore to CD33<sup>+</sup> target cells, ranged from 6.6 to 73 Sv, whereas the total dose to the liver, spleen, and blood ranged from 2.4 to 23.5 Sv, 2.9 to 36.8 Sv, and 1.1 to 11 Sv, respectively. Absorbed dose ratios between the bone marrow, liver, spleen, and the whole body were approximately 1000 times higher for  $^{213}\text{Bi}$ -HuM195 than those for the  $\beta$ -emitting immunoconjugates. An antileukemic effect was observed: 15/18 patients had leukemic blasts in the blood before treatment, and 14 of them showed reductions in circulating blasts after  $\alpha$ -RIT. Even at the lowest activity level, patients showed elimination of more than 99% of peripheral blasts. Up to three logs of circulating leukemia cells were killed, and four patients (27%) had complete eradication of peripheral leukemia cells. Fourteen of the 18 patients (78%) experienced reductions in the percentage of bone marrow leukemia cells 7–10 days after  $\alpha$ -RIT. Among the four patients with complete elimination of peripheral blood blasts, three also experienced reductions in bone marrow blasts (Table 3).

The major obstacles to the widespread clinical use of  $^{213}\text{Bi}$ -lintuzumab are the short half-life of  $^{213}\text{Bi}$  and the requirement of an on-site  $^{225}\text{Ac}/^{213}\text{Bi}$  generator. On the other hand, the much longer-lived  $^{225}\text{Ac}$  ( $T_{1/2} = 10$  days) can serve as an in vivo generator (atomic nanogenerator) of four  $\alpha$ -particles. A phase I trial evaluating  $^{225}\text{Ac}$ -lintuzumab was conducted on 18 patients with relapsed or refractory AML [29]. Patients were treated with a single infusion of 0.5–4  $\mu\text{Ci}/\text{kg}$  (18.5–150 kBq/kg) of  $^{225}\text{Ac}$ -lintuzumab. The MTD was determined to be 3  $\mu\text{Ci}/\text{kg}$  (110 kBq/kg). Serious non-hematologic toxicity was observed in three patients (transient grade 3 liver function abnormalities), but there was no evidence of radiation-induced nephrotoxicity. Peripheral blasts were eliminated in 10 of 16 evaluable patients (63%) but only at doses of 1  $\mu\text{Ci}/\text{kg}$  (37 kBq/kg) or more. Bone marrow blast reductions were observed in 10 of 15 evaluable patients (67%) 4 weeks after treatment.

Alpha-RIT using a  $^{212}\text{Pb}/^{212}\text{Bi}$  generator has also been assessed in a phase I trial using an anti-HER2 radiolabeled mAb intraperitoneally injected in patients with HER2-positive peritoneal carcinomatosis for which no standard therapy is available [30].  $^{212}\text{Pb}$ -TCMC-trastuzumab was delivered intraperitoneally within less than 4 h after administration of trastuzumab (4 mg/kg intravenously). The five activity levels assessed in this study (7.4, 9.6, 12.6, 16.3, and 21.1 MBq/m<sup>2</sup>) showed minimal toxicity. The lack of substantial toxicity was consistent with the dosimetry results (mean equivalent dose to the marrow, 0.18 mSv/MBq). Further studies are required to assess  $^{212}\text{Pb}$ -TCMC-trastuzumab efficacy.

**Table 3** Clinical studies with alpha particle emitting radionuclides

	<sup>213</sup> Bi		<sup>225</sup> Ac	<sup>211</sup> At		<sup>212</sup> Pb
	Anti-CD33	Anti-chondroitin sulfate proteoglycan	Anti-CD33	Anti-tenascin (IC)	Anti-NaPi2B (IP)	Trastuzumab (IP)
Type of cancer	Myeloid leukemia	Metastatic melanoma	Myeloid leukemia	Brain tumor	Ovarian cancer	Ovarian cancer
Number of patients	18	38	18	18	9	16
Thrombocytopenia gr 3/4	NA	0	Gr 4 in one patient	0	0	0
Non-hematologic toxicity	0	0	Gr3 liver in three patients	22% (seizures)	0	0
Response rate	Bone marrow blasts reduction in 78%	Partial response: 10% Stable: 40%	Bone marrow blasts reduction in 67%	NK	NK	No objective response
MTD	Not reached	Not reached	110 kBq/kg	NK	NK	Not reached

*IC* Intracavitary, *IP* Intraperitoneal, *MTD* Maximum tolerated dose, *NK* Not known

Astatine-211, an  $\alpha$ -emitting radionuclide with a physical half-life of 7.2 h, also appears relevant for RIT. Preclinical studies recently showed that anti-CD45 <sup>211</sup>At-RIT and bone marrow transplantation prolonged survival in a disseminated acute myeloid leukemia murine model [31]. Biodistribution studies showed excellent localization of the <sup>211</sup>At-anti-murine CD45 mAb 30F11 to the marrow and spleen within 24 h. In syngeneic hematopoietic stem cell transplantation studies, <sup>211</sup>At-RIT improved the median survival of leukemic mice in a dose-dependent fashion with minimal toxicity. <sup>211</sup>At-RIT feasibility was reported in two clinical trials. The first study assessed anti-tenascin <sup>211</sup>At-RIT followed by chemotherapy in patients with glioblastoma [32]. The radioimmunoconjugate was injected into the resection cavity with a maximum activity of 347 MBq (9.4 mCi). Six patients out of 18 experienced reversible grade 2 neurotoxicity but no grade 3–4 toxicities were observed. Maximum tolerated activity was not reached, and observed median survival favorably compared with that of historical control groups. In the second study, <sup>211</sup>At-MX35 F(ab')<sub>2</sub> was assessed in women in complete response after a second-line chemotherapy for recurrent ovarian carcinoma in a phase I study [33]. MX35 F(ab')<sub>2</sub> was labeled with <sup>211</sup>At via the *N*-succinimidyl 3-(trimethylstannyl)-benzoate reagent. Nine patients underwent laparoscopy 2–5 days before <sup>211</sup>At-RIT. Before RIT infusion, the abdominal cavity was inspected to exclude the presence of macroscopic tumor growth or major adhesions. Patients were infused with <sup>211</sup>At-MX35 (22.4–101 MBq/L) in the dialysis solution via the peritoneal catheter. The estimated absorbed dose was

$15.6 \pm 1.0$  mGy/MBq/L to the peritoneum,  $0.14 \pm 0.04$  mGy/MBq/L to the red bone marrow, and  $24.7 \pm 11.1$  mGy/MBq/L to the unblocked thyroid. This dose decreased when the thyroid was blocked ( $1.4 \pm 1.6$  mGy/MBq/L). No adverse effects were reported.

These first clinical results of alpha-RIT appear very promising, and larger phase II clinical trials have been performed in patients with minimal residual disease to fully demonstrate efficacy. However, large clinical trials will require access to higher production levels of alpha-emitting radionuclides.

### ***3.5 Theranostic Approaches: Imaging of Radiolabeled Antibodies to Improve RIT Procedures***

For more than two decades, mAbs have been labeled with  $\gamma$ -emitting radionuclides, such as  $^{131}\text{I}$ ,  $^{177}\text{Lu}$ , or  $^{111}\text{In}$ , and subsequently used in planar or single-photon emission computed tomography (SPECT) imaging procedures to try and improve RIT using dosimetry procedures. Indeed, optimization studies performed using new-generation pretargeting systems in both colorectal carcinoma and lung carcinoma patients [24, 25] assessed the potential of  $^{111}\text{In}$ -IMP288 imaging to predict  $^{177}\text{Lu}$ -IMP288 dosimetry. In an optimization PRIT study using anti-CEA  $\times$  anti-HSG BsMAb TF2 in 20 patients with colorectal carcinoma, Schoffelen et al. reported that individual high-activity doses in PRIT could be safely administered by predicting the radiation dose to the red marrow and kidneys, based on dosimetric imaging obtained with a test dose of TF2 and  $^{111}\text{In}$ -IMP288 [24]. These results were confirmed by the phase I/II clinical trial using the same pretargeting system in CEA-expressing lung cancer patients showing that a pre-therapeutic imaging session using  $^{111}\text{In}$ -IMP288 accurately predicted pharmacokinetics as well as absorbed doses of the therapeutic session using  $^{177}\text{Lu}$ -IMP288, potentially allowing for patient selection and dose optimization [25].

While providing reliable information, this modality suffers from several drawbacks including poor sensitivity, poor spatial resolution, and complex scatter correction due to the collimator. Accurate quantitative information could be better achieved using positron emission tomography (PET) for mAb imaging. The improved spatial resolution of PET makes the delineation of tumors and organs better than with SPECT. Additionally, exact attenuation correction, precise scatter correction, and, last but not the least, high sensitivity combined with the possibility of performing true whole body imaging in a reasonable time constitute additional key factors for the superiority of PET over SPECT or planar imaging. As for therapeutic emitters, marrying mAbs and PET emitters requires an appropriate match between the biologic half-life of the protein and the physical half-life of the isotope [34].  $^{89}\text{Zr}$  and  $^{124}\text{I}$  with their long half-life of 78 and 100 h are well suited to the labeling of larger molecules such as intact immunoglobulins.  $^{64}\text{Cu}$  with an intermediate half-life of

12.7 h can also be used for labeling of a large number of molecules of different sizes. Within the scope of a “theranostic” approach, pairs of beta+/beta-emitting radionuclides ( $^{124}\text{I}/^{131}\text{I}$ ,  $^{86}\text{Y}/^{90}\text{Y}$ ,  $^{64}\text{Cu}/^{67}\text{Cu}$ ,  $^{44}\text{Sc}/^{47}\text{Sc}$ ) are very promising because the same distribution is expected both for dosimetry imaging and therapy with the same elements. Animal studies showed that immuno-PET could be useful for visualizing CD138-expressing tumors with  $^{124}\text{I}$ -B-B4 in the context of treatment of metastatic triple-negative breast cancer that cannot benefit from hormone therapy or anti-Her2/neu immunotherapy [35]. PET distribution of the  $^{124}\text{I}$ -B-B4 radiolabeled mAb correlated well with the biodistribution data analyzed on sacrificed animals. Moreover, it has been recently demonstrated that  $^{64}\text{Cu}$ -cetuximab immuno-PET represented EGFR expression levels in an esophageal squamous cell carcinoma model,  $^{177}\text{Lu}$ -cetuximab RIT effectively inhibited tumor growth, and that  $^{64}\text{Cu}$ -/ $^{177}\text{Lu}$ -PCTA-cetuximab may be useful as a diagnostic tool in patient selection and a potent RIT agent for EGFR-positive tumors [36]. Similarly, Rizvi et al. conducted a prospective clinical study to evaluate the biodistribution and radiation dosimetry of  $^{90}\text{Y}$ -ibritumomab tiuxetan (Zevalin®) using  $^{89}\text{Zr}$ -ibritumomab tiuxetan [37]. Patients with relapsed or refractory aggressive B-cell (CD20-positive) NHL underwent a PET scan at 1, 72, and 144 h after injection of 70 MBq  $^{89}\text{Zr}$ -ibritumomab tiuxetan and again 2 weeks later after coinjection of 15 MBq/kg or 30 MBq/kg of  $^{90}\text{Y}$ -ibritumomab tiuxetan. Biodistribution of  $^{89}\text{Zr}$ -ibritumomab tiuxetan was not influenced by simultaneous therapy with  $^{90}\text{Y}$ -ibritumomab tiuxetan, and the correlation between predicted pre-therapy and absorbed therapy organ doses as based on  $^{89}\text{Zr}$ -ibritumomab tiuxetan images was high. These results are similar to previous data presented by Perk et al. [38] and confirm the potential value of pre-therapy  $^{89}\text{Zr}$ -immuno-PET to enable individualized treatment by optimizing RIT dose schedules and limit unnecessary toxicity for patients.

## 4 Conclusion

While radiolabeled mAbs have demonstrated encouraging results in the treatment of hemopathies and several solid tumors, randomized clinical trials in stratified patients need to be performed to confirm efficacy. Treatment of solid tumors by RIT should be developed in combination with several other drugs and in repeated courses of treatment, just as chemotherapy is used. Combinations of all possible new developments, including new antibody specificities, pretargeting methods, fractionated injections, and the use of alpha emitters, are needed to improve RIT efficacy in radioresistant solid tumors. Immuno-PET is likely to assist in selecting patients for RIT, optimizing injected activities, and noninvasively monitoring therapy efficacy.

**Acknowledgments** This work has been supported in part by grants from the French National Agency for Research called “Investissements d’Avenir” Labex IRON n°ANR-11-LABX-0018-01 and Equipex Arronax-Plus n°ANR-11-EQPX-0004.

## References

1. Chatal JF, Kraber-Bodere F, Bodet-Milin C, Rousseau C. Therapeutic immunoconjugates. Which cytotoxic payload: chemotherapeutic (ADC) or radionuclide (ARC) ? *Curr Cancer Therapy Rev.* 2016;12:54.
2. Siegel JA, Pawlyk DA, Lee RE, Sasso NL, Horowitz JA, Sharkey RM, et al. Tumor, red marrow, and organ dosimetry for <sup>131</sup>I-labeled anti-carcinoembryonic antigen monoclonal antibody. *Cancer Res.* 1990;50:1039s–42s.
3. Bardiès M, Bardet S, Faivre-Chauvet A, Peltier P, Douillard JY, Mahé M, et al. Bispecific antibody and iodine-131-labeled bivalent hapten dosimetry in patients with medullary thyroid or small-cell lung cancer. *J Nucl Med.* 1996;37:1853–9.
4. Zanzonico P. Radioimmunotherapy of micrometastases: a continuing evolution. *J Nucl Med.* 1992;33:2180–3.
5. DeNardo GL, Schlom J, Buchsbaum DJ, Meredith RF, O'Donoghue JA, Sgouros G, et al. Rationales, evidence, and design considerations for fractionated radioimmunotherapy. *Cancer.* 2002;94:1332–48.
6. Schlom J, Molinolo A, Simpson JF, Siler K, Roselli M, Hinkle G, et al. Advantage of dose fractionation in monoclonal antibody-targeted radioimmunotherapy. *J Natl Cancer Inst.* 1990;82:763–71.
7. Illidge TM, Mayes S, Pettengell R, Bates AT, Bayne M, Radford JA, et al. Fractionated <sup>90</sup>Y-ibritumomab tiuxetan radioimmunotherapy as an initial therapy of follicular lymphoma: an international phase II study in patients requiring treatment according to GELF/BNLI criteria. *J Clin Oncol.* 2014;32:212–8.
8. Scholz CW, Pinto A, Linkesch W, Lindén O, Viardot A, Keller U, et al. (90)Yttrium-ibritumomab-tiuxetan as first-line treatment for follicular lymphoma: 30 months of follow-up data from an international multicenter phase II clinical trial. *J Clin Oncol.* 2013;31:308–13.
9. Batra JS, Karir BS, Vallabhajosula S, Christos PJ, Hodes G, Date PR, et al. Fractionated dose radiolabeled antiprostata specific membrane antigen (PSMA) radioimmunotherapy (<sup>177</sup>Lu-J591) with or without docetaxel for metastatic castration-resistant prostate cancer (mCRPC). *ASCO Meeting Abstr.* 2015;33:194.
10. Tagawa ST, Milowsky MI, Morris M, Vallabhajosula S, Christos P, Akhtar NH, et al. Phase II study of Lutetium-177-labeled anti-prostate-specific membrane antigen monoclonal antibody J591 for metastatic castration-resistant prostate cancer. *Clin Cancer Res.* 2013;19:5182–91.
11. Tschmelitsch J, Barendsward E, Williams C, Yao TJ, Cohen AM, Old LJ, et al. Enhanced antitumor activity of combination radioimmunotherapy (<sup>131</sup>I-labeled monoclonal antibody A33) with chemotherapy (fluorouracil). *Cancer Res.* 1997;57:2181–6.
12. Wong JYC, Chu DZ, Yamauchi DM, Williams LE, Liu A, Wilczynski S, et al. A phase I radioimmunotherapy trial evaluating <sup>90</sup>yttrium-labeled anti-carcinoembryonic antigen (CEA) chimeric T84.66 in patients with metastatic CEA-producing malignancies. *Clin Cancer Res.* 2000;6:3855–63.
13. Wong JYC, Shibata S, Williams LE, Kwok CS, Liu A, Chu DZ, et al. A phase I trial of <sup>90</sup>Y-anti-carcinoembryonic antigen chimeric T84.66 radioimmunotherapy with 5-fluorouracil in patients with metastatic colorectal cancer. *Clin Cancer Res.* 2003;9:5842–52.
14. Gulec SA, Cohen SJ, Pennington KL, Zuckier LS, Hauke RJ, Horne H, et al. Treatment of advanced pancreatic carcinoma with <sup>90</sup>Y-Clivatuzumab Tetraxetan: a phase I single-dose escalation trial. *Clin Cancer Res.* 2011;17:4091–100.
15. Ocean AJ, Pennington KL, Guarino MJ, Sheikh A, Bekaii-Saab T, Serafini AN, et al. Fractionated radioimmunotherapy with (90) Y-clivatuzumab tetraxetan and low-dose gemcitabine is active in advanced pancreatic cancer: a phase I trial. *Cancer.* 2012;118:5497–506.
16. Bander NH, Milowsky MI, Nanus DM, Kostakoglu L, Vallabhajosula S, Goldsmith SJ. Phase I trial of <sup>177</sup>lutetium-labeled J591, a monoclonal antibody to prostate-specific membrane antigen, in patients with androgen-independent prostate cancer. *J Clin Oncol.* 2005;23:4591–601.

17. Tagawa ST, Whang YE, Kaur G, Vallabhajosula S, Christos PJ, Nikolopoulou A, et al. Phase I trial of docetaxel/prednisone plus fractionated dose radiolabeled anti-prostate-specific membrane antigen (PSMA) monoclonal antibody 177Lu-J591 in patients with metastatic, castration-resistant prostate cancer (mCRPC). ASCO Meeting Abstr. 2014;32:5064.
18. Barbet J, Peltier P, Bardet S, Vuillez JP, Bachelot I, Denet S, et al. Radioimmunodetection of medullary thyroid carcinoma using indium-111 bivalent hapten and anti-CEA x anti-DTPA-indium bispecific antibody. *J Nucl Med.* 1998;39:1172–8.
19. Kraeber-Bodéré F, Rousseau C, Bodet-Milin C, Mathieu C, Guérard F, Frampas E, et al. Tumor immunotargeting using innovative radionuclides. *Int J Mol Sci.* 2015;16:3932–54.
20. Salaun P-Y, Campion L, Bournaud C, Faivre-Chauvet A, Vuillez J-P, Taieb D, et al. Phase II trial of anticarcinoembryonic antigen pretargeted radioimmunotherapy in progressive metastatic medullary thyroid carcinoma: biomarker response and survival improvement. *J Nucl Med.* 2012;53:1185–92.
21. Rossi EA, Goldenberg DM, Cardillo TM, McBride WJ, Sharkey RM, Chang C-H. Stably tethered multifunctional structures of defined composition made by the dock and lock method for use in cancer targeting. *Proc Natl Acad Sci U S A.* 2006;103:6841–6.
22. Sharkey RM, McBride WJ, Karacay H, Chang K, Griffiths GL, Hansen HJ, et al. A universal pretargeting system for cancer detection and therapy using bispecific antibody. *Cancer Res.* 2003;63:354–63.
23. Schoffelen R, van der Graaf WTA, Franssen G, Sharkey RM, Goldenberg DM, McBride WJ, et al. Pretargeted 177Lu radioimmunotherapy of carcinoembryonic antigen-expressing human colonic tumors in mice. *J Nucl Med.* 2010;51:1780–7.
24. Schoffelen R, Woliner-van der Weg W, Visser EP, Goldenberg DM, Sharkey RM, McBride WJ, et al. Predictive patient-specific dosimetry and individualized dosing of pretargeted radioimmunotherapy in patients with advanced colorectal cancer. *Eur J Nucl Med Mol Imaging.* 2014;41:1593–602.
25. Bodet-Milin C, Ferrer L, Rauscher A, Masson D, Rbah-Vidal L, Faivre-Chauvet A, et al. Pharmacokinetics and dosimetry studies for optimization of Pretargeted Radioimmunotherapy in CEA-expressing advanced lung Cancer patients. *Front Med (Lausanne).* 2015;2:84.
26. Chatal J-F, Davodeau F, Cherel M, Barbet J. Different ways to improve the clinical effectiveness of radioimmunotherapy in solid tumors. *J Cancer Res Ther.* 2009;5(Suppl 1):S36–40.
27. Guérard F, Gestin J-F, Brechbiel MW. Production of [(211)At]-astatinated radiopharmaceuticals and applications in targeted  $\alpha$ -particle therapy. *Cancer Biother Radiopharm.* 2013;28:1–20.
28. Jurcic JG, Larson SM, Sgouros G, McDevitt MR, Finn RD, Divgi CR, et al. Targeted alpha particle immunotherapy for myeloid leukemia. *Blood.* 2002;100:1233–9.
29. Jurcic JG, Rosenblat TL. Targeted alpha-particle immunotherapy for acute myeloid leukemia. *Am Soc Clin Oncol Educ Book.* 2014:e126–31.
30. Meredith R, Torgue J, Shen S, Fisher DR, Banaga E, Bunch P, et al. Dose escalation and dosimetry of first-in-human  $\alpha$  radioimmunotherapy with 212Pb-TCMC-trastuzumab. *J Nucl Med.* 2014;55:1636–42.
31. Orozco JJ, Bäck T, Kenoyer A, Balkin ER, Hamlin DK, Wilbur DS, et al. Anti-CD45 radioimmunotherapy using (211)At with bone marrow transplantation prolongs survival in a disseminated murine leukemia model. *Blood.* 2013;121:3759–67.
32. Zalutsky MR, Reardon DA, Akabani G, Coleman RE, Friedman AH, Friedman HS, et al. Clinical experience with alpha-particle emitting 211At: treatment of recurrent brain tumor patients with 211At-labeled chimeric antitenascin monoclonal antibody 81C6. *J Nucl Med.* 2008;49:30–8.
33. Andersson H, Cederkrantz E, Bäck T, Divgi C, Elgqvist J, Himmelman J, et al. Intraperitoneal alpha-particle radioimmunotherapy of ovarian cancer patients: pharmacokinetics and dosimetry of (211)At-MX35 F(ab')<sub>2</sub> – a phase I study. *J Nucl Med.* 2009;50:1153–60.
34. Kraeber-Bodéré F, Bodet-Milin C, Rousseau C, Eugène T, Pallardy A, Frampas E, et al. Radioimmunoconjugates for the treatment of cancer. *Semin Oncol.* 2014;41:613–22.

35. Rousseau C, Ruellan AL, Bernardeau K, Kraeber-Bodéré F, Gouard S, Loussouarn D, et al. Syndecan-1 antigen, a promising new target for triple-negative breast cancer immuno-PET and radioimmunotherapy. A preclinical study on MDA-MB-468 xenograft tumors. *EJNMMI Res.* 2011;1:20.
36. Song IH, Lee TS, Park YS, Lee JS, Lee BC, Moon BS, et al. Immuno-PET imaging and radioimmunotherapy of  $^{64}\text{Cu}$ -/ $^{177}\text{Lu}$ -labeled anti-EGFR antibody in esophageal squamous cell carcinoma model. *J Nucl Med.* 2016;57:1105.
37. Rizvi SNF, Visser OJ, Vosjan MJWD, van Lingen A, Hoekstra OS, Zijlstra JM, et al. Biodistribution, radiation dosimetry and scouting of  $^{90}\text{Y}$ -ibritumomab tiuxetan therapy in patients with relapsed B-cell non-Hodgkin's lymphoma using  $^{89}\text{Zr}$ -ibritumomab tiuxetan and PET. *Eur J Nucl Med Mol Imaging.* 2012;39:512–20.
38. Perk LR, Visser OJ, Stigter-van Walsum M, Vosjan MJWD, Visser GWM, Zijlstra JM, et al. Preparation and evaluation of  $(^{89}\text{Zr})$ -Zevalin for monitoring of  $(^{90}\text{Y})$ -Zevalin biodistribution with positron emission tomography. *Eur J Nucl Med Mol Imaging.* 2006;33:1337–45.



# Index

## A

Abscopal effect, 44, 47, 121–122  
Acute myeloid leukemia (AML), 147  
Ag-presenting cells (APCs), 44  
Akaike information criterion, 108  
Alpha particle emitting radionuclides, 148  
Altered biodistribution, 63, 76, 99  
Antibody drug conjugates (ADCs), 140  
Antibody radionuclide conjugates (ARCs), 140  
Antibody-dependent cellular cytotoxicity (ADCC), 39, 80, 83  
Antigen-presenting cells (APCs), 124  
Antitumor immune response, 131  
Apoptosis, 80  
Area under the curve of the cumulative SUV histograms (AUC-CSH), 101  
Atezolizumab, 131

## B

B-cell chronic lymphocytic leukemia (B-CLL) cells, 18  
B-cell lymphoma, 12, 14, 15, 18, 68, 69  
  adaptive immunity, 10  
  BCR signaling, 12  
  bone marrow, 12  
  Burkitt's lymphomas, 15  
  cognate antigen, 14  
  expression pattern, 14, 15  
  GC B cells, 14  
  gene recombination, 18  
  human B-cell lymphomas, 18  
  IgM and IgD isotypes, 14  
  memory B cells, 15

  progenitor cells, 15  
  somatic IgV gene mutations, 14  
  V region, 12  
  clinical and biologic implications, 10  
  evolution, 10  
  microenvironmental interactions, 24–26  
  origin  
  reciprocal translocation, 18, 20, 23  
  vs. T-cell, 10  
  viruses, 23, 24  
B-cell non-Hodgkin's lymphoma (NHL), 35, 68, 99  
B-cell receptor (BCR), 12, 15, 24–26  
B-cells, 81–82  
Beta emitter, 60, 62  
<sup>213</sup>Bi-lintuzumab, 147  
Biokinetics, 112  
Biologically effective dose (BED), 110  
Bispecific monoclonal antibody (BsMAb), 145  
Blockade therapy, 46, 47  
Body surface area (BSA), 107  
Body weight (BW), 107  
Bortezomib, 41, 42  
Bulky disease, 36–38  
Bulky tumor (BT) model, 36  
Burkitt's lymphomas, 15  
Bystander effect, 2

## C

Calreticulin (CRT), 124  
Carcinoembryonic antigen (CEA), 123  
CD20 antigen, 2, 3, 5, 38–41, 81–82, 99  
Chemotherapeutic drugs, 141

- Chemotherapy, 27
- Chimeric antigen receptors (CAR), 131
- Chinese hamster ovary (CHO), 83
- Chromosomal translocations, 10, 18, 23, 27
- Chronic lymphocytic leukemia (CLL), 26
- Complement-dependent cytotoxicity (CDC), 39, 80
- Complete response rate (CR), 3
- Conditioning therapy, 5
- Consolidation therapy, 5
- Cross-fire effect, 2, 80, 82
- Cumulative SUV histograms (CSH), 101
- Cyclophosphamide, 130
- Cytotoxic radiation, 80
- Cytotoxic T-lymphocyte-associated protein-4 (CTLA-4), 46
- D**
- Damage-associated molecular patterns (DAMP), 45, 124
- Decay scheme, 87
- Dendritic cells (DCs), 43, 122
- Diffuse large B-cell lymphomas (DLBCLs), 15
- DNA recombination process, 14
- Dosimetry, 108
- MRT (*see* Molecular radiotherapy (MRT))
- radioactive substance, 106
- radioimmunotherapy, 106
- <sup>90</sup>Y-ibritumomab tiuxetan, 111–113
- Downregulation of CD20, 38–41
- E**
- Epitopes, 81
- Epstein-Barr virus (EBV), 23, 24
- European Medical Agency (EMA), 90
- Expected biodistribution, 63, 76, 99
- Extrabeam radiotherapy (EBRT), 37
- F**
- Fab prime 2 (F[ab']<sub>2</sub>), 37
- Fcγ receptor (FcγR), 40
- First-line indolent trial (FIT), 37
- Flt3 ligand (Flt3-L), 122
- Fludarabine, 37, 130
- <sup>18</sup>F-fluorodeoxyglucose (FDG), 63, 100
- Fluorodeoxyglucose-positron emission tomography (FDG-PET)
- biodistribution, 76
- chemotherapy and radiotherapy, 68, 73
- CT imaging, 71–72
- external-beam radiation, 75
- fibrotic scars, 75
- granulomatous diseases, 75
- indium-labeled antibody, 71
- inflammatory tissue, 76
- <sup>111</sup>In-ibritumomab tiuxetan, 76
- maximal response, 73
- negative patients
- after RIT, 74
- before RIT, 74
- non-Hodgkin's lymphoma, 74
- noninvasive imaging, 68, 74
- patient characteristics, 69, 72
- patient subgroups, 72
- positive patients
- after RIT, 74
- before RIT, 73
- quantitative analyses, 75
- revised IWC criteria, 72
- RIT, 72
- <sup>90</sup>Y-ibritumomab tiuxetan, 75, 76
- Follicular dendritic cells (FDC), 14
- Follicular lymphoma, 69, 70
- Frontline therapy, 3, 4
- G**
- Germinal center (GC), 14, 19
- Good manufacturing practice (GMP), 89
- Granulocyte macrophage colony-stimulating factor (GM-CSF), 40
- H**
- Heat-shock proteins, 124
- Heavy-chain antibody (HcAb), 38
- Hematological toxicity, 91
- Hematopoietic cancer models
- radioimmunotherapy and immunotherapy, 128–129
- radiotherapy and immunotherapy, 125–128
- Hepatitis C virus (HCV), 24, 26
- Hepatocellular carcinoma, 131
- High-mobility group box 1 (HMGB1), 45, 124
- Histamine-succinyl-L-glutamine (HSG), 145
- Hodgkin and reed/Sternberg (HRS), 18
- Hodgkin's lymphoma (HL), 18, 80
- Human antimurine antibodies (HAMAs), 83
- Human mature B-cell lymphomas, 17, 22
- Hybridoma technology, 83

**I**

- Ibritumomab tiuxetan, 64, 80, 83–84, 99
- Ig gene remodeling processes, 13
- Immune checkpoint molecules, 46, 47
- Immunoediting, 42–44
- Immunological cell death (ICD), 45
- Immunosuppressive/immunostimulatory effects, 123
- Immunosurveillance, 43
- Immunotherapy, 27
  - See also* Ionizing radiation
- Indium-111 (<sup>111</sup>In), 86–87
- Intercellular adhesion molecule 1 (ICAM-1), 123
- Interleukin-4 (IL)-4, 40
- Interleukin-2 (IL-2), 126
- Intratumoral antibody distribution
  - FDG-PET, 100
  - PET/CT, 100–101
  - radionuclide therapy, 100
  - resistance and heterogeneity, 101–102
  - SPECT/CT, 100–101
- Ionizing radiation, 44–46, 125–129
  - abscopal effect, 121–122
  - blood vessels, 125
  - cytokines, 125
  - hematopoietic cancer (*see* Hematopoietic cancer models)
  - immunogenic cell death, 124
  - immunological effects, 122–123
  - immunotherapy
    - radioimmunotherapy and, 130–131
    - radiotherapy, 129–130
  - monoclonal antibodies, 121
  - RAIT, 121
  - tumor cell immunogenicity, 123–124
  - tumor microenvironment, 121
- Ipilimumab, 131
- Isothiocyanate group, 85

**L**

- Light zones, 14
- Linear energy transfer (LET), 86, 146
- LMEGP collimator, 101
- Low-grade B cell non-Hodgkin's lymphoma (NHL), 2
- Lymphocyte function-associated antigen 3, 123

**M**

- Major histocompatibility complex (MHC), 43, 82
- Mantle-cell lymphomas (MCL), 36, 69, 88
- Maximum tolerated dose (MTD), 143

- Medical Internal Radiation Dose Committee (MIRD), 107
- Medullary thyroid carcinoma (MTC), 141, 145
- Metabolic response, 76
- Microenvironmental interactions, 24–26
- Minimal residual disease (MRD) model, 36–37, 146
- Mitoxantrone, 37
- Molecular radiotherapy (MRT), 106, 108, 109
  - absorbed dose calculations, 109–110, 112
  - kinetic model, 108
  - organs, 107, 108
  - pharmacokinetics
    - prediction, 109
    - quantification, 108
  - physiologically based pharmacokinetic (PBPK) models, 108
  - treatment and quality control measurements, 110
  - treatment planning, 106, 110
- Monoclonal antibodies (mAbs), 80, 82, 83
- Multiple myeloma (MM), 126
- Myeloid derived suppressor cells (MDSC), 43
- Myelosuppressive adverse effect, 91

**N**

- Nivolumab, 131
- Non-Hodgkin B-cell lymphoma (NHL), 2, 10, 140
- Nuclear factor- $\kappa$  (NF- $\kappa$ ) activation, 40–42
- Nuclear medicine therapy, 60

**O**

- OLINDA/EXM software, 109
- Organ at risk (OAR), 107
- Ovalbumin (OVA), 129
- Overall response rate (ORR), 3, 35

**P**

- Partial response (PR), 3
- Peptide receptor radionuclide therapy (PRRT), 110
- Polymerase chain reaction (PCR), 15
- Positron emission tomography/computed tomography (PET/CT), 86, 100, 101, 149
- Prednisone, 130
- Pretargeted RIT (PRIT), 91
- Programed cell death ligand 1 (PD-L1), 43
- Programmed cell death-1 (PD-1), 46
- Progression-free survival (PFS), 35

**R**

- Radioimmunotherapy (RIT), 27, 35, 60, 61
  - ADCs and ARCs, 140
  - alpha-emitting radionuclides, 140–141, 146–149
  - CD20 antigen, 140
  - fractionation of injections, 141–143
  - hematologic toxicity, 140
  - human antibodies, 140
  - limitations, 141
  - pretargeting, bispecific antibodies, 145–146
  - radioresistant solid tumors, 140
  - theranostic approaches, 149, 150
  - therapeutic agents, 143–145
- Radioisotope-conjugated mAb, 82
- Radionuclide (RN) therapy, 38, 84–86, 100
  - carrier molecules, 60
  - ibritumomab tiuxetan, 62–64
  - radioimmunotherapy, 60, 61
  - radiolabeled compounds, 60
  - theranostic approach, 63–64
  - <sup>90</sup>Y, 60
- Radiotherapy, 27
- Relative biological effectiveness (RBE), 85
- Resistance, 35, 40, 41
- Rituximab, 83

**S**

- Safety profile, 4
- Shaving, 40
- Single-chain variable (scFv), 37
- Single-photon emission computed tomography/computed tomography (SPECT/CT), 63, 100, 101, 149
- Small lymphocytic lymphoma, 16
- Somatic hypermutation (SHM), 14
- Somatic IgV gene mutations, 14
- Standardized uptake value (SUV), 101
- Syngeneic mice, 44

**T**

- Targeted radionuclide therapy (TRT), 106
- T-cell, 10
- Theranostic approach, 63–64, 84
- Time to disease progression (TTP), 36
- Time-activity curve (TAC), 108

- Time-integrated activity coefficient (TIAC), 109
- Tiuxetan, 83, 84
- Toll-like receptor 4 (TLR4), 124
- Toll-like receptor 9 (TLR9), 40
- Toxicities, 4
- Transforming event, 18, 20, 23
- Tumor necrosis factor  $\alpha$  (TNF $\alpha$ ), 40
- Tumor-associated antigen (TAA), 123

**U**

- US Food and Drug Administration (US FDA), 35

**V**

- Vascular cell adhesion molecule-1 (VCAM-1), 125
- Viruses, 23, 24

**W**

- World Health Organization (WHO), 10

**Y**

- <sup>90</sup>Y-/<sup>111</sup>In-ibritumomab tiuxetan, 2, 86
  - bulky disease, 36–38
  - CD20 downregulation, 38–41
  - clinical trials, 35
  - ex vivo/in vivo studies, 88
  - factors, 35
  - NF- $\kappa$ B activation, 41–42
  - preparation, 89
  - schedule, 89–90
  - therapy, 35, 36
  - tumor cell, 45

**Z**

- Zevalin<sup>®</sup>, 89
  - characteristics, 2
  - dosage, 2, 3
  - factors, 5
  - frontline therapy, 3, 4
  - refractory patients, 3
  - relapse, 3
  - toxicity, 4
  - treatment schedule, 2, 3